Intertidal Morphodynamics of the Avon River Estuary

Photo by C. Banks, 1968

Final report submitted to the
Nova Scotia Department of Transportation and Public Works (NSTPW)

Prepared by
Dr. Danika van Proosdij, Department of Geography, Saint Mary's University
& Greg Baker, MP_SpARC, Saint Mary's University
923 Robie, St. Halifax, N.S., B3H 3C3

September 30, 2007

TABLE of CONTENTS

EXECUTIVE SUMMARY

The purpose of this research was to investigate the spatial and temporal variability in intertidal morphodynamics of the Avon River Estuary, and assess the resilience of the system to the influence of tidal barrier construction. The research was conducted on the Avon River Estuary in the Minas Basin from the head of the estuary to the lighthouse at Horton Bluff approximately 16 km downstream of the existing causeway.   Contemporary bathymetric surveys (December 2005, June & August 2006) were compared with historical surveys conducted by the Maritime Marshland Rehabilitation Administration (MMRA) in the late 1960s and early 1970s, as well as bathymetric surveys from the Canadian Hydrographic Service (CHS) in 1969 and 1976, and an 1858 bathymetric chart from the archives of the United Kingdom Hydrographic Office in the United Kingdom.   In addition, changes in salt marsh habitat and the position of intertidal features were quantified using historical charts, aerial photo mosaics and satellite imagery in ArcGIS 9.1 from 1858 to 2003.

In recent years, attention has shifted from the construction of large tidal barrages to the potential removal of large tidal barriers, such as the Petitcodiac Causeway in New Brunswick, or smaller barriers and dykes through salt marsh restoration projects. In addition, there has been a resurgence of interest in tidal power, although this would be generated most likely using underwater turbines rather than the large scale barrage scheme proposed in the 1970s. All of these activities could result in changes to the hydrodynamic and sedimentary regime, and the consequences of such alterations cannot be predicted with confidence at the present time. It is not a question of whether or not intertidal ecosystems will be impacted. Rather, it is the magnitude and extent, both spatially and temporally, of these impacts on new or altered equilibrium states, that has to be determined.

However, discerning the impacts of these large scale structures from natural ecosystem changes (e.g. storm frequency, sea level, sediment sources) or non point impacts (e.g. historical dyking) can be a challenge. Cycles of sedimentation and erosion have been documented on numerous marsh and mudflat systems in macrotidal estuaries around the world. These cycles have been linked to changes in sea level and to the tidal prism due to human activities such as tidal barrier construction, dyke construction or dredging and changes in natural processes such as changes in wind/wave climate, sediment supply, cliff morphology, intertidal sedimentation, river discharge, and changes in the location of the major tidal channel. Many of these studies also indicate the difficulty of discerning changes based on limited field data of a historical or contemporary nature.

As previous research has indicated, the intertidal geomorphology of the Avon River Estuary has been impacted by the construction of the Windsor causeway. However, the spatial extent and magnitude of this impact is less than originally postulated in the 1970s. Many of the changes might also be associated with natural fluctuations in the position of the main tidal channel thalweg. Expanding the temporal scope of the research to include almost a 150 year period has revealed that, despite significant changes in anthropogenic modifications to the estuary, the Avon River Estuary is a resilient system which may be considered to be in an equilibrium state over most of its reach. This equilibrium state, however, is not necessarily the same one which existed in 1858.

Overall, there has been a significant decrease in the intertidal cross section (e.g. sedimentation) since the construction of the causeway within the first 1500 m downstream. This decrease in cross sectional area ranged from 75% to 54% from 1970 to 2006 as a layer of sediment between 5.8 to 6.5 m deep accumulated downstream of the causeway. These changes can likely be directly attributed to the construction of the causeway in 1969. However, this significant accumulation of sediment has occurred at the site of an intertidal bar which was present before the construction of the Windsor causeway, and evidence suggests that it was also present in 1858.

The extensive salt marsh which has evolved adjacent to the causeway marsh and mudflat surface is now near the limit of the Higher High Water Mean Tides level, and rates of sedimentation on the marsh surface will decrease due to decreased innundation frequency. An increase in the high marsh (*Spartina patens*) community is anticipated. As a result of the decreased frequency of innundation and sequestration of sediment, more sediment will be available for deposition elsewhere such as the main tidal channel parallel to the causeway and newly developing salt marsh on the Newport bar or along the western shore close to the tide gate.

Beyond this point, changes in cross section have been minimal or have significantly increased (e.g. deepened) until 3 km downstream. Although there has been another significant decrease in cross sectional area between 3 and 4.5 km downstream of the causeway, this decrease is more likely associated with the natural migration of the main tidal channel than the causeway. In addition, evidence is presented to support seasonal cycles of changes in bed elevation by as much as 2 m, which exceed the differences recorded between 1858-1969 and 2005/2006 in some locations. Seasonality and meteorological conditions (e.g. rainfall and runoff) can exert a strong influence on the interpretation and comparison of survey data. In addition, the resolution of sampling points and employing spatial

interpolation techniques can influence the interpretation of change in the tidal prism. For the remaining 11 km or so downstream, there have been negligiable changes in intertidal cross sectional since 1858. Any changes in bed elevation can be linked to changes in the position of major sand intertidal bodies. Any areas of sedimentation along the shoreline are compensated by either deepening of the main tidal channel or bank erosion along the opposite shore.

The tidal prism (the volume of water passing through a particular cross section) decrease of 7.3% from 1858 to 1969 is likely associated with dyking, and an additional 7.2% from construction of the causeway. Despite this decrease in the tidal prism, the Avon River estuary appears to have adjusted to a new equilibrium state through channel deepening, particularly in the St. Croix and Kennetcook Rivers. In addition, the Avon River is joined by the St. Croix and then further downstream by the Kennetcook which likely play key roles in flushing the system and preserving a predominantly sandy base level.

Cycles of erosion and accretion of mudflat and salt marsh habitat were shown to be strongly influenced by the position of the thalweg of the main tidal channel. While the eroded material does have the potential to subsequently 'feed' any new bar formation, this has yet to be empricaly tested. However, this cyclicity in marsh habitat is similar in rate and pattern to studies elsewhere (e.g. UK and Cumberland Basin, NB). In general, there is an overall decrease in salt marsh area from 1858 to 1964 with the exception of 1955. Over the following decade, the percentage of salt marsh area (as a proportion of the tidal prism) remains constant at around 11 % and begins to increase slightly in 1992. By September 2007, the proportion of the Avon River study area covered by salt marsh vegetation had exceeded 1955 levels, though it did not exceed the 1858 levels. Overall there was an 87% loss of salt marsh from 1858 to 1955 (including upstream of the causeway) and an additional 14% loss from 1955 to 1964. It is estimated that 11% of salt marsh loss was due to 'natural causes' and 89% was due to dyking. However, this value should be interpreted with caution due to the poor reliability of the 1858 upstream data. The proportion of marsh lost between 1955 and the construction of the causeway has been more than compensated for by the growth of new marsh downstream of the causeway and along the western shore and new growth starting on the 'Newport' bar.

The Avon river estuary is a classic example of a resilient intertidal system which has responded to significant anthropogenic impacts (e.g. dyking and causeway construction) very effectively since 1858. Although there have been some very marked and visible changes in the system, namely the

development of an extensive salt marsh and mudflat ecosystem downstream of the causeway, the direct impacts of the causeway have been very localized. Any changes beyond 1.5 km downstream are more likely associated with natural processes such as the migration of the main tidal channel. This research demonstrates clearly that the Avon River is not simply another Petitcodiac. This is due to differences in hydrology (chiefly presence of 2 rivers draining into it), position of the causeway within the broader estuary, size and length of the estuary, sediments and associated sediment dynamics. The river has likely now achieved a new equilibrium state and any modifications to the system (e.g. construction or modification of tidal barriers) will likely disrupt this equilibrium with no guarantee as to how the system might respond. The risk to the causeway from storm surges or wave effects is low due to the presence of the salt marsh which acts as a natural form of coastal defense.   However, with the approach of the Saros Tides in 2012-2013, the risk will increase and should be assessed further. Additionally, there is a greater risk to the causeway from freshwater flooding, depending on the timing of the storm relative to the tide.   Additional research and high resolution data, particularly lidar and high resolution satellite imagery as well as modern measures of the sediment dynamics of the system will be required before any predictions can be made regarding impacts of modifying the existing causeway structure and identifying specific areas at risk from flooding.

ACKNOWLEDGEMENTS & FUNDING SOURCES

available through MP_SpARC at Saint Mary's University. This centre was funded by the Canada Foundation for Innovation, Nova Scotia Innovation Trust Fund and various industrial partnerships (e.g. ESRI, Leica).

LIST of FIGURES

LIST of TABLES

Intertidal Morphodynamics of the Avon River Estuary

1.0 INTRODUCTION

In a 'natural' world, salt marshes and mudflats represent systems delicately balanced between hydrodynamic forces and ecological, sedimentological, and morphological responses. However, this balance may be changed as a result of anthropogenic activities such as construction of engineering structures (e.g. causeways, culverts, shore protection), dredging, or altering landuse activities. Over the last century, the majority of rivers entering the Bay of Fundy have been modified through the construction of tidal barriers such as causeways and culverts (Figure 1.1). The construction of these barriers has resulted in either partial or total obstruction of tidal flow in many areas around the Bay. Tidal barriers decrease turbulent energy in the tidal system which causes sediment and other particles to drop from suspension and accumulate as deposits of mud, sand, and silt. Ecosystems such as mudflats and salt marshes are some of the first environments to feel the effects of coastal modification.
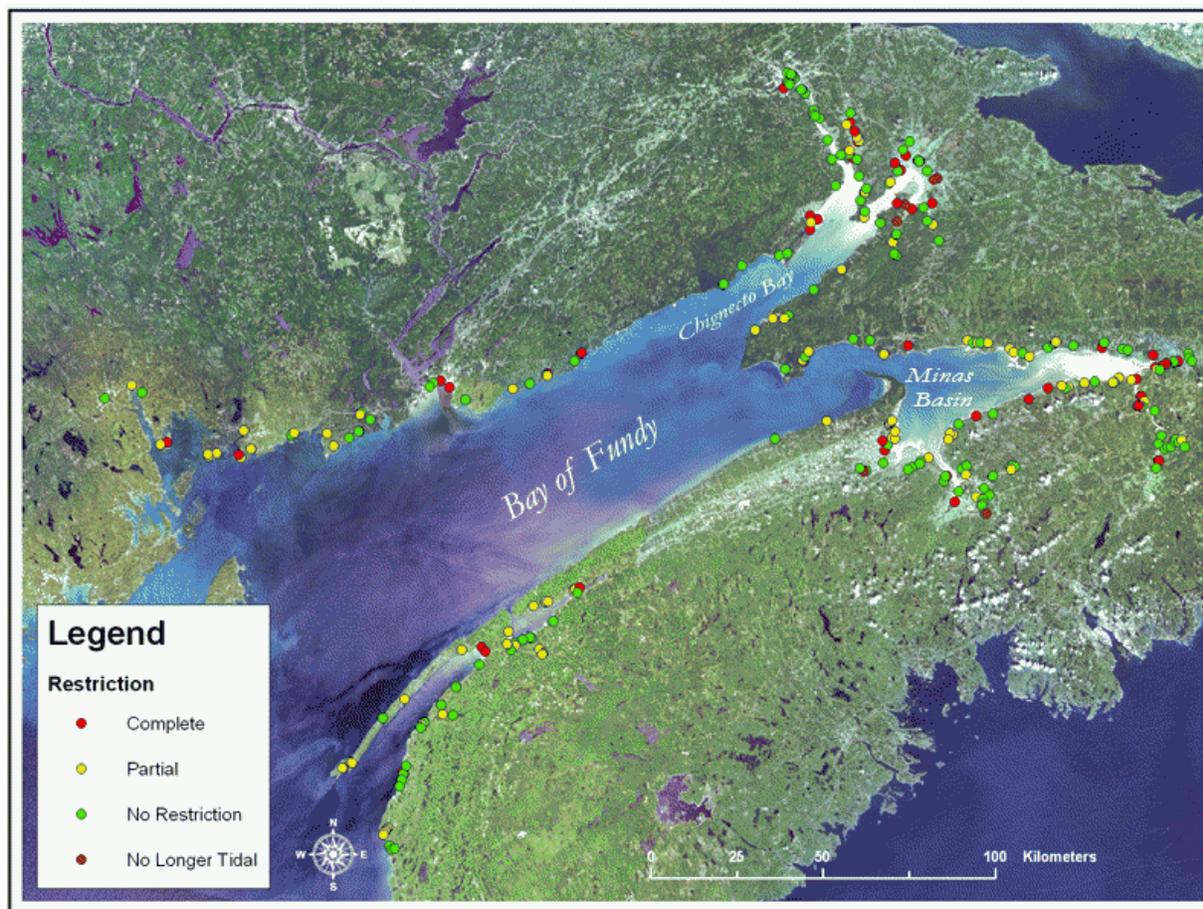
Figure 1.1: Location and categories of tidal barriers in the Bay of Fundy derived from the tidal barrier audits conducted by the Ecology Action Center and the Conservation Council of New Brunwick (van Proosdij & Dobek, 2005).

The construction of barriers across tidal rivers and estuaries has a long history of altering the sediment dynamics and ecosystem processes in the surrounding area. The degree of alteration to the system depends in part on structure design, surrounding geology, sediment characteristics, tidal range, and basin morphology. Tidal barriers can cause changes in sedimentation patterns within the estuary that may, over time, alter the cross sectional area of the channels and the overall capacity of the system to distribute tidal waters. Rapid sedimentation and subsequent colonization by halophytic vegetation can be recorded downstream of the tidal barrier as can be seen downstream of the Windsor causeway, Nova Scotia (e.g. Amos 1977; Turk et al., 1980; van Proosdij and Townsend, 2006; Daborn et al., 2003a;b; van Proosdij et al., 2004). Restriction of flow can increase the risk of flooding from both upstream (e.g. tide gate will not be able to 'flush' or discharge water due to high amounts of sedimentation) and downstream (e.g. storm surge and perigeen spring tides) sources. The potential for flooding will continue to increase with rising sea levels, placing infrastructure at risk. In other areas, localized erosion may be initiated either directly upstream or downstream of a partially restrictive barrier (Bowron and Fitzpatrick, 2001).

Research on the impacts of these structures is generally stimulated in the initial scoping phase of the project (e.g. Fundy tidal power or Storm surge barriers in the Netherlands) or after the effects on ecosystems become noticeable (e.g. Petitcodiac, Netherlands land reclamation project, Australian Ord River Estuary). In most cases excessive siltation is reported in the years following closure of the estuary with extensive changes to the intertidal geomorphology (eg. Wolanski et al., 2001 in Ord River Estuary, Australia; Bray et al., 1982 in the Petitcodiac River, Canada; Tonis et al., 2002 in Haringvliet Estuary, Netherlands), in the composition of intertidal sediments (e.g. Turk et al., 1980 on the Windsor mudflats), in ecosystem processes and composition (e.g. Locke et al., 2003 in the Petitcodiac River; Smaal and Nienhuis, 1992 in the Eastern Scheldt, Netherlands), and altered hydrodynamics and decreased tidal prism (e.g. Amos, 1976 in the Avon River; Owen and Odd, 1972 on the Thames Estuary, UK). Over the last three decades there has been considerable interest in macrotidal estuarine processes and the impacts of tidal barriers on these ecosytems. In the Bay of Fundy, as in other areas of the world, much of the research in the 1970s and 1980s was spawned as a result of potential large scale tidal power projects (e.g. Pelletier & McMullen, 1972; Amos, 1976; Yeo & Risk, 1980; Daborn, 1987), and causeways at Annapolis Royal, Moncton, and Windsor were viewed as useful models for assessing the environmental implications of large tidal barriers (Daborn et al., 2003). The primary concerns at that time were the potential effects on tidal energy and amplitudes, and on sediment distribution, with secondary concerns related to biological productivity (Daborn, 1977).

The ecological impacts of tidal barriers have been extensively documented (e.g. Locke et al., 2003 in the Petitcodiac River; Smaal and Nienhuis, 1992 in the Eastern Scheldt, Netherlands; Wells, 1999; Niles, 2001, Bay of Fundy) and range from changes in intertidal habitat and nutrient cycling to interference with the movement of fish or invertebrates (Issacman, 2005). In some cases fish passage is completely obstructed, in other cases fish passage is available only during limited periods during a tidal cycle. Impacts of tidal barriers are both negative (e.g. decrease fish passage) and positive (e.g. new growth of intertidal habitat), and it is often difficult to discern natural versus anthropogenic impacts. Unfortunately, many studies are limited by the lack of accurate and reliable historical data.

'Ecomorphodynamics' refers to the study of the interactions and feedbacks that occur between topography, biota (e.g. vegetation and invertebrates), hydrodynamic (e.g. waves and currents) and sedimentary (e.g. suspended sediment concentration, deposition, erosion) processes, and the resultant adjustments of morphology. These feedbacks are clearly evident within the vast intertidal ecosystems located in the Bay of Fundy. For example, changes in marsh or mudflat surface elevation within the tidal frame or changes in edge morphology will in turn induce changes in tidal prism (volume of water that must pass through a particular cross section to raise the water level from low water to high water), hydrodynamic forces, vegetation community structure, rates of sedimentation, and dissipation (marsh platform) or amplification (cliff) of wave energy. The rate of these changes can be significantly influenced by human development such as the construction of tidal barriers or installation of shore protection such as dykes or rip rap.

In recent years, attention has shifted from the construction of large tidal barrages to the potential removal of large tidal barriers, such as the Petitcodiac Causeway in New Brunswick, or smaller barriers and dykes through salt marsh restoration projects. In addition, there has been a resurgence of interest in tidal power, although this would most likely be generated using underwater turbines rather than the large scale barrage scheme proposed in the 1970s. All of these activities could result in changes to the hydrodynamic and sedimentary regime, and the consequences of such alterations cannot be predicted with confidence at the present time. It is not a question of whether or not intertidal ecosystems will be impacted. Rather, it is the magnitude and extent, both spatially and temporally, of these impacts on new or altered equilibrium states, that has to be determined.

Discerning the impacts of these large scale structures from natural ecosystem changes (e.g. storm frequency, sea level, sediment sources) or non point impacts (e.g. historical dyking) can be a challenge.

Cycles of progradation and retreat have been documented on a number of marsh and intertidal systems (e.g. Ollerhead et al. in press: Baker and van Proosdij, 2004; van der Wal and Pye, 2004; Cox et al., 2003; Pringle, 1995). These cycles have been linked to changes in sea level (van der Wal and Pye, 2004; French and Burningham, 2003; van der wal and Pye, 2003; Vos and van Kesteren, 2000; Allen, 2000; Allen, 1989) and to the tidal prism due to human activities such as tidal barrier construction (Allen, 2000), dyke construction (e.g. Hood, 2004; Wilkens & Mayerle, 2005) or dredging (French and Burningham, 2003; Cox et al., 2003), changes in wind/wave climate (van der Wal and Pye, 2004; Cox et al., 2003; Allen and Duffy, 1998; Pye, 1995; Allen, 1989), sediment supply (Allen, 2000; Gordon et al, 1985), cliff morphology (Moller and Spencer, 2002; Pringle, 1995; Pye, 1995), intertidal sedimentation (Schwimmaer and Pizzuto, 2000; Shi et al., 1995), river discharge (Allen et al., 1976), and changes in the location of the major tidal channel (Allen, 1996; Pringle, 1995; Pye, 1995; Shi et al., 1995). Many of these studies indicate the difficulty of discerning changes based on limited field data of a historical or contemporary nature.

Technological advances in digital image processing and GIS have provided a significant advantage to modern researchers examining the long term changes in large intertidal estuarine environments (e.g. Uncles, 2002). One of the most effective ways of documenting these changes is through the analysis of rectified aerial photographs, satellite imagery, and bathymetric charts within a GIS system. This is the preliminary stage that is required before any serious questions regarding the 'why' of these changes can be addressed, and before the future vulnerability of the area to flooding can be assessed. This information can then serve as the basis for future hydrodynamic modeling exercises.

This project represents a continuation of the work initiated in 2005 investigating the spatial and temporal variations in the intertidal geomorphology of the Avon River Estuary. In an undisturbed system, salt marshes and mudflats represent a delicate balance between hydrodynamic forces and ecological, sedimentological, and morphological responses. However, this balance may be upset as a result of anthropogenic forcing functions such as construction of engineering structures, dredging, or altering landuse activities. van Proosdij et al. 2006 concluded that the direct impacts of the Windsor causeway were limited to the first kilometre or so downstream due to the influence of the St. Croix and the Kennetcook Rivers (van Proosdij *et al.*, 2006) based on two sets of survey data (1969-1971 and 2005). Changes in channel form and cross sectional area below this point were variable and were likely associated with changes in the location of the thalweg of the Avon River. Seasonal variability in channel bed elevations were recorded for the 1960-1970s surveys which support the visual

observations in the field and limited field data from other areas (Crewe, 2004). However, conflicting results from earlier studies (e.g. Amos 1976) call for additional investigation, and one of the goals of this report is to examine those earlier results in a broader spatial and temporal context.

Over time, changes in sedimentation patterns within the estuary will alter the cross sectional area of the channels and the overall capacity of the system to distribute tidal waters. This may in turn increase the risk of flooding, particularly from freshwater runoff, when aboiteau structures are not able to release this runoff. Accordingly, it is critical to understand the rates and processes of change in intertidal geomorphology over time. This will permit an accurate assessment of the vulnerability of the causeway infrastructure to the impacts of climate change. The results of this assessment can then be incorporated into the planning and construction processes associated with twinning Highway 101 across the Avon River Estuary at Windsor.

The purpose of this research was to expand the temporal scale of the original investigation of the intertidal morphodynamics of the Avon River estuary initiated in 2005, and to provide a synthesis and assessment of the long term resilience and stability of this system within the study area (Figure 1.2), including impacts from both dyking and causeway construction. Specific objectives addressed in this report include a:

1. Review of relevant scientific literature on the intertidal morphodynamics of estuarine systems, and the impacts of tidal barrier construction.

2. Detailed examination of the position of intertidal geomorphological features (e.g. salt marshes and mudflats) including the location of major tidal channels, mudflats and marsh habitats, and shoreline position from 1860 to the present.

3. Integration of available bathymetric data into ArcGIS including datum conversions, marsh elevations, and generation of digital elevation models for tidal prism calculations.

4. Summary of tidal and meteorological conditions (where available) pre and post causeway construction.

5. Evaluation of the overall stability and evolution of intertidal environments within the study area, including seasonal variability in bed elevation.

6. Assessment of the vulnerability of the Windsor causeway to climate change and recommendations for effective coastal zone management.
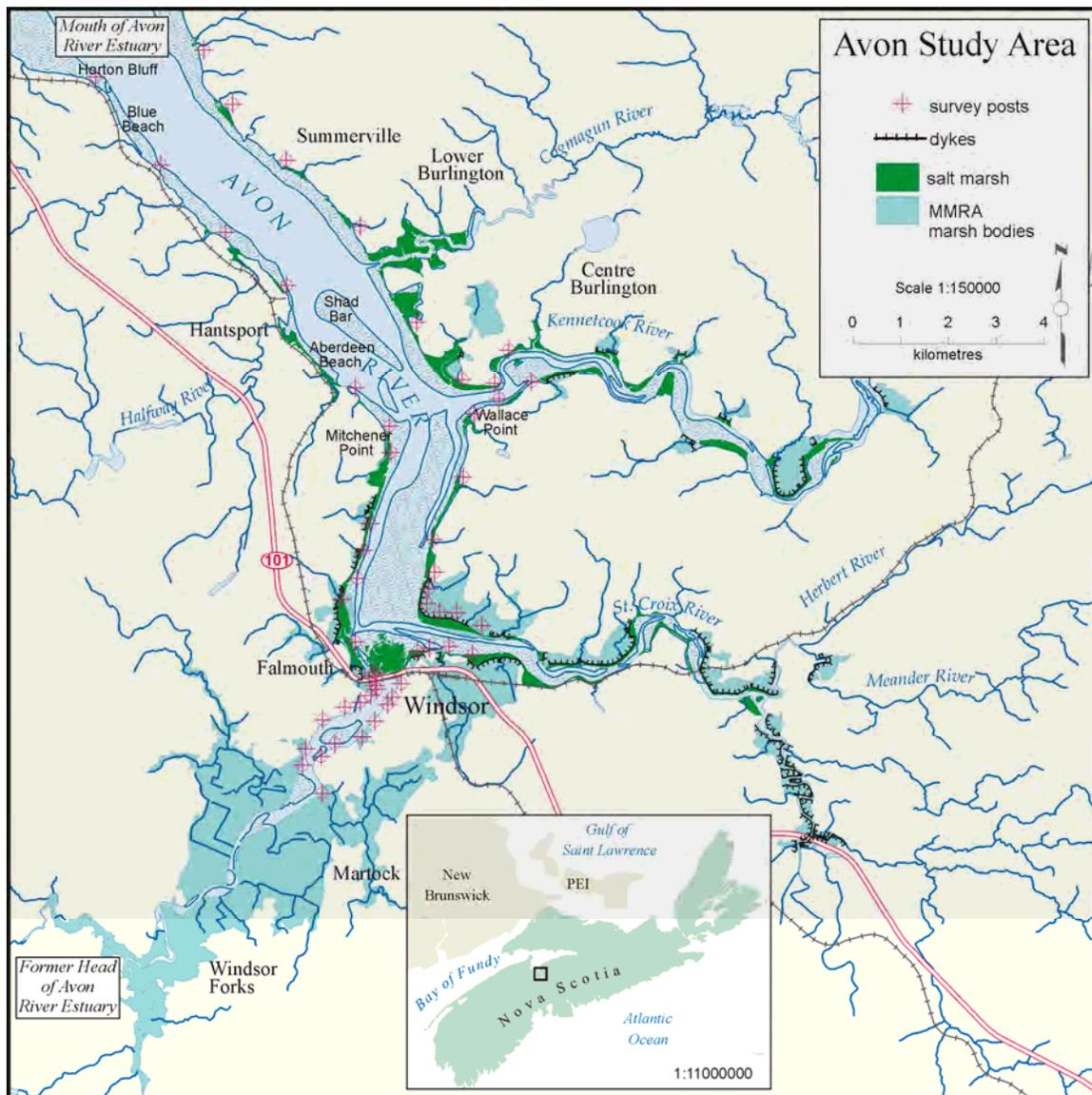
Figure 1.2: Location of the Avon study area. MMRA marsh bodies represent areas of former salt marsh that are now primarily agricultural land that is protected by dykes. Figure created by C. Prostak, 2007.

2.0   STUDY AREA

2.1   Geographical and Environmental Setting

The upper Bay of Fundy is a macro tidal estuary characterized by a semi-diurnal tidal regime with a maximum tidal range of 16 m, high suspended sediment concentrations and the presence of ice and snow for at least three months of the year. This research project was conducted on a section of the Avon River estuary in the Minas Basin extending from the historic head of the tide approximately 8 km upstream from the causeway near Windsor Forks, through the town of Windsor, to a lighthouse at Horton Bluff approximately 16 km downstream, incorporating sections of both Hants and Kings Counties (Figure 1.2). Three major rivers, the Avon, the St. Croix, and the Kennetcook discharge into the study area. However, since 1970 the discharge from the Avon has been controlled by a sluice gate within the causeway.   The Avon and the St. Croix also have hydroelectric and water storage dams in their upper reaches. The three rivers account for 1694 km^2 of the total 1836 km^2 drainage basin system (NS Department of Environment and Labour).   The Cogmagon and Halfway rivers as well as miscellaneous small creeks contribute the remainder (Table 2.1).   The reach of the Avon River is approximately 2 km wide and the study area (Figure 1.2) increases in width to around 2.5 km near at the northern end near Horton Bluff.   It then expands in width to roughly 6 km beyond that point (Lambiase, 1980).

	Total	Avon	St. Croix	Kennetcook	Cogmagon & small streams
Drainage area (km^2)	1836	447	742	506	142
% of total area	100	24	40	28	8

Table 2.1: Secondary watershed statistics for the Avon River System watershed. Source: NS Department of Environment and Labour Watershed GIS datatbase

The Avon River can be classified as a well mixed estuary by Pritchard's (1967) definition, however Lambiase (1980) noted a slight stratification in the salinity profiles that he performed. His study found a vertical salinity difference of 0.3 ppt near the estuary head which decreased in the offshore direction, and a longitudinal difference of 2 ppt. Salinities are 28.5 ppt near the head of the estuary and 30.5 ppt near the mouth (Lambiase, 1980). Salinities between 25.6 and 28.0 ppt were also recorded in 2002 in the tide gate channel at Windsor (Daborn et al., 2002).

2.1.1   Climate & Meterological Conditions

A comprehensive description of the estuary and surrounding region, as well as a summary of previous research in the area can be found in Daborn et al., 2003. The mean annual temperature (1913-2006) at

the nearby Kentville meteorological station was 6.8 ^{0}C with a mean total annual precipitation of 92 mm (Figure 2.1). Dominant winds are from the WSW and SW with the strongest winds during the winter months (Figure 2.2). In 2004 a meteorogical station was installed near the Windsor Tide Gate to provide local measures of temperature, precipitation, barometric pressure, and wind speed and direction. Comparison of wind speed and direction data with Kentville over the same time period suggests that strong NNE winds do occur at the Windsor site during the winter months

Figure 2.1: Climatograph for Kentville, NS, based on data from 1913-2006

(Figure 2.2). This has implications for wave hindcast modelling, and it could potentially cause some water set-up within the estuary, as this time frame coincides with the dominant fetch (distance 6.5 km) for the southern reach.
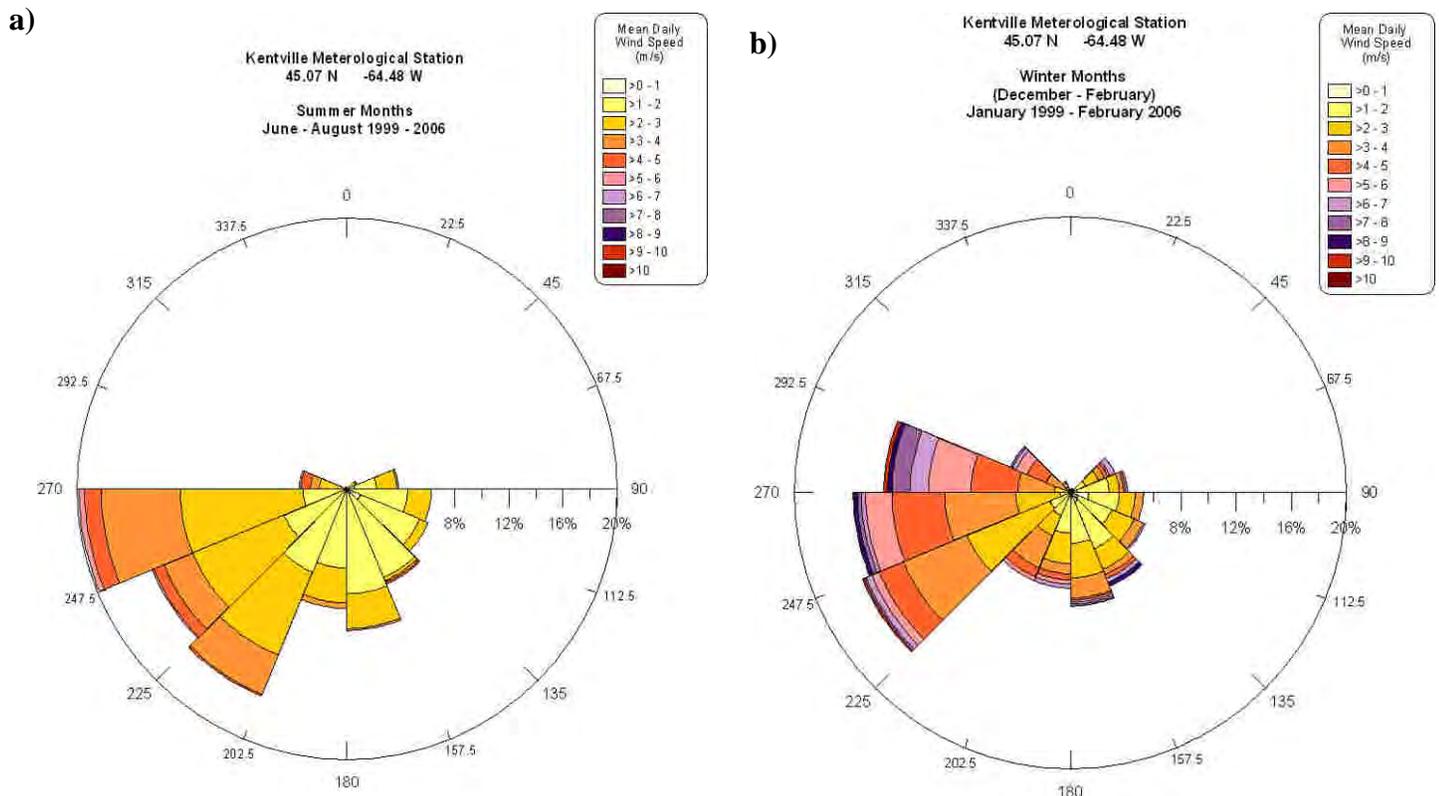
Figure 2.2: Wind rose diagrams derived from available wind speed and direction data from the Kentville meteorological station from 1996 to 2006 . Data are divided into a) summer and b) winter months.
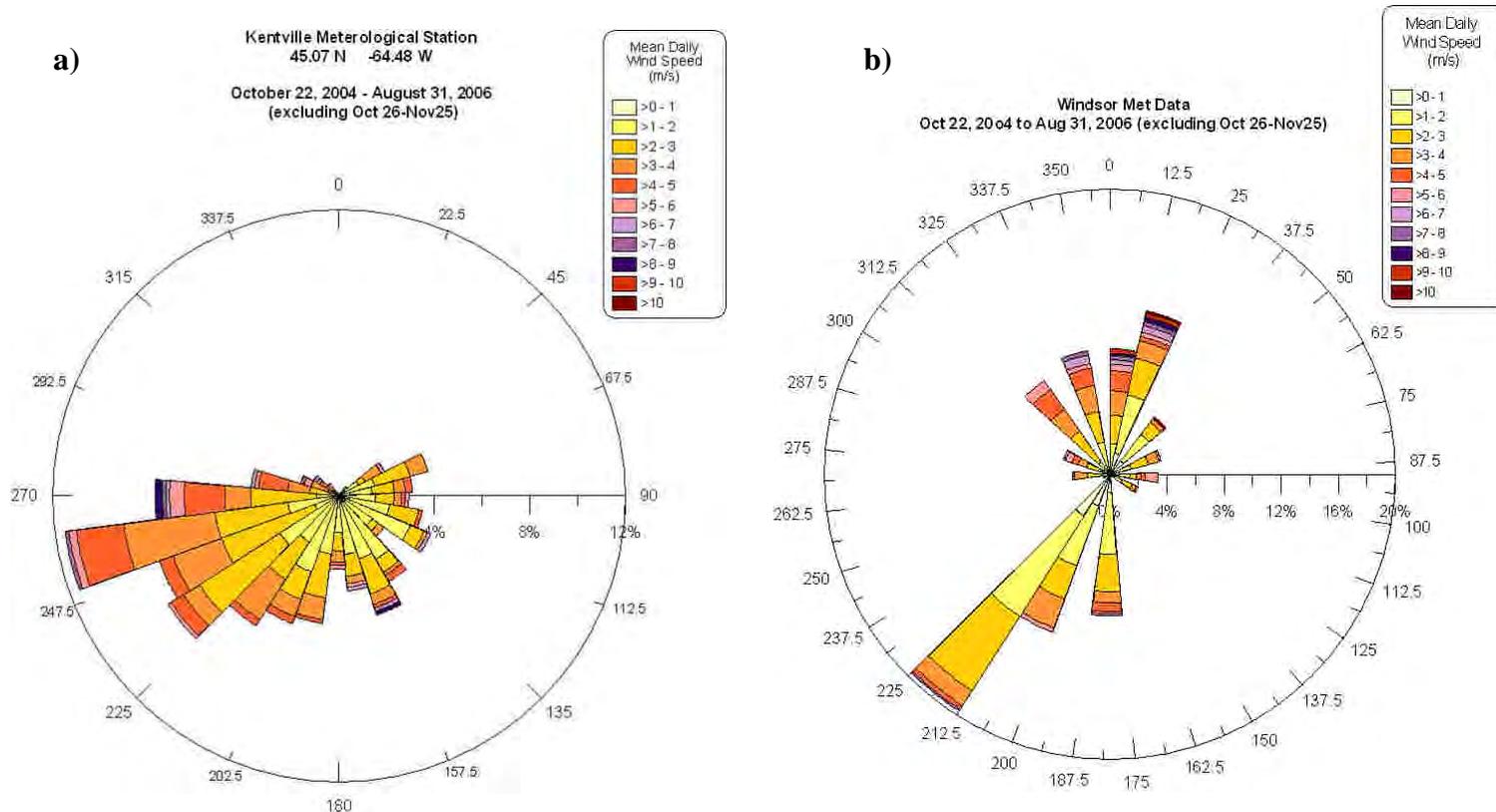
Figure 2.3: Comparison of wind speed and direction between a) the Kentville meteorological station (45.07N, -64.48W) from Oct 22, 2004 to August 31, 2006 and b) Windsor for the same time period recorded at a Weatherhawk^{tm} meterological station (44.99 N, -64.15 W). Data from Oct 26 to Nov 25, 2005 are not available.

2.1.2 Tides

The Bay of Fundy is renowned for its large tidal range, which reaches a maximum of 16.3 m at Burntcoat Head in the Minas Basin. Tidal range in the Avon River estuary varies from 8.2 m Chart Datum at neap tide and 15.6 m CD at lunar perigee spring tide (CHS 1976, predictions for Hantsport). Tides are strongly semidiurnal with a diurnal inequality that is almost always less than 0.6 m (Lambiase, 1980).

Tides produce strong currents which are the main agents of transportation and deposition of sedimentary material in the Bay, effectively transporting, creating, and remolding surface and geological features. A recent publication by Desplanque and Mossman (2004) provides a comprehensive overview of the mechanics and impacts of Fundy tidal processes on the geology of the region. Due to the relatively shallow nature of the Avon River Estuary, the rising limb of the tide will be compacted within a shorter period, whereas the period of the falling tide will increase (Carter 1998). However, this process will vary depending on the lunar cycle. At neap tide, the tidal curve is generally symmetrical with both the ebb and the flood flow lasting around 6.5 hours. In contrast, the tidal curve

for spring tides is slightly assymetric at the mouth of the estuary with ebb flows lasting 0.5 hours longer than flood. This asymetry increases as one travels up the estuary, where there can be as much as 8.5 h of ebb flow with only 4 h of flood flow (Lambiase, 1980). This can result in the formation of a tidal bore during large spring tides which can attain an amplitude of 0.15 m and advances upstream at nearly 1 m·s^{-1} (Lambiase, 1980). Such tidal bores are observed regularly at the tide gate at the Windsor Causeway (Figure 2.4).

Figure 2.4.   Tidal bore at Windsor Tide Gate at 12:36 pm on June 17, 2003 (photo by K. Carroll, 2003)

As mentioned previously, the tidal prism is the volume of water flowing in and out of the estuary with the rise and fall of the tide. Because tides are variable in strength, the tidal volume and tidal prism are variable, as is the wetted cross sectional area. In addition, during low water, sections of the estuary south of Hantsport are completely drained since bottom elevations are higher than the lower tidal limit.

Cycle	Period	~ Tidal range
Diurnal cycle due to relation of moon to earth	0.517 days (12 hr 25 min)	11.0 m
Spring/neap cycle	14.77 days	13.5 m
Perigee (high) / apogee (low)	27.55 days	14.5 m
206 day cycle due to spring/neap and perigee/apogee cycles	206 days	15.5 m
Saros cycle (last peaked in 1994-95 predicted peak in 2012-2013 AD)	18.03 years	16.0 m

Table 2.2: Summary of characteristics of major constituents of tidal cycles in upper sections of the Bay of Fundy (Desplanque & Mossman, 2004).

In general, higher water levels are recorded during spring tides and lower water levels are recorded during neap tides although, due to the tidal assymetry in the Bay of Fundy, this is not always the case. In addition, the absolute elevation of the tide will vary depending on the relative position of the sun and the moon and orbital cycles (Table 2.2). The most favorable combination of factors to produce strong tides in the Bay of Fundy occurs when the perigee coincides with a spring tide and other cycles

to produce Saros tides every 18.03 years (Desplanque & Mossman, 2004). Based on Desplanque & Mossman's (2004) calculations, the peaks of the Saros cycles within the last century occurred in 1904-1905, 1922-1923, 1940-1941, 1958-1959, 1976-1977, 1994-1995, and the next will occur in 2012-2013. In addition, detailed tidal records over several decades show that there will be slightly higher maximum monthly high water marks in a 4.5 cycle year, examples being the peaks in 1998 and 2002 (Desplanque & Mossman, 2004).

The only permanent tide gauge operated by CHS is located in St. John, New Brunswick, therefore one must depend on predicted tides at Hantsport for most historical calculations. Table 2.3 summarizes the results of an archive CHS tide records search of the Marine Environmental Data Service (MEDS) (http://www.meds-sdmm.dfo-mpo.gc.ca/meds/Home_e.htm) managed by the Integrated Science Management Branch of DFO. Data were located for both Windor and Hantsport stations for limited two month time periods. The majority of the data (exception 1975) were stored as microfilm and were not analyzed as part of this report. However, detailed tide records have been maintained by Maritime Marshland Rehabilitation Administration (MMRA) and Department of Agriculture personnel at the Windsor Tide gate from the mid 1980s. Earlier records are in the form of strip charts and since 2002 tide levels have been recorded digititally every few minutes from a pressure transducer. Although those data do not capture the lower portion of the tide, they do provide a valuable long term record of high tides in the area.
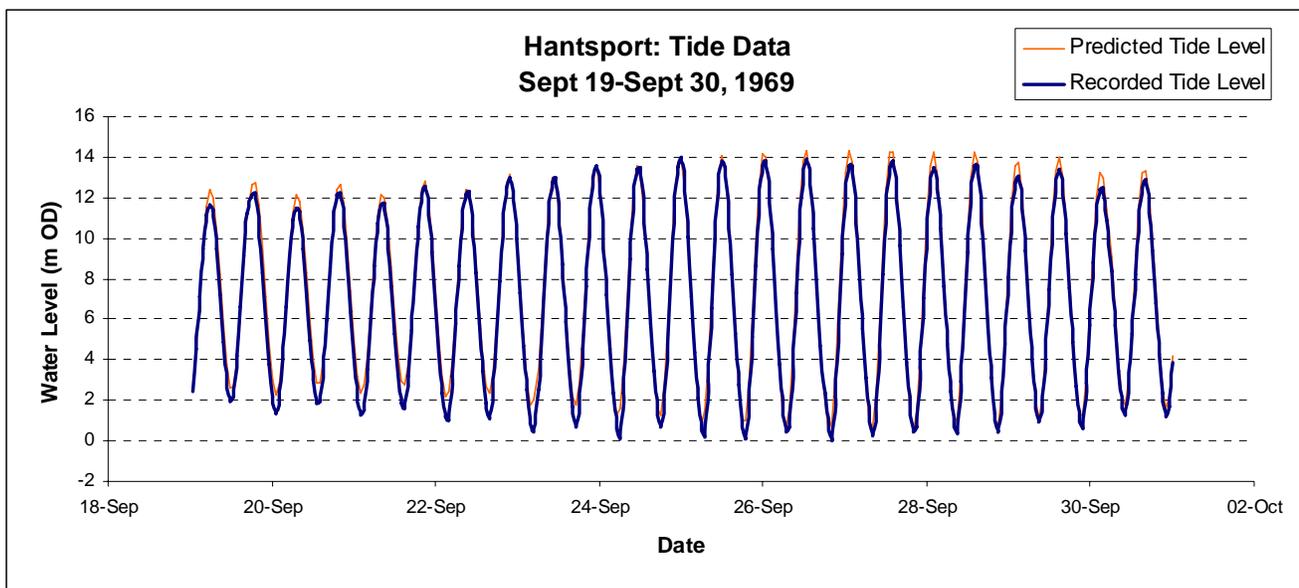
Figure 2.5: Tide data recorded by CHS at Hantsport (station 282) in 1969 and predicted tides for the same location.

Location (station ID)	Year	Dates	Format	File or Film #
Hantsport (Station 282)	1960	July 14 – Oct 15	microfilm	63F6-19
	1969	Sept 19 - Oct 31	digital	1969-22
Windsor (Station 280)	1898	Aug – Oct	microfilm	618-4
	1919	Aug - Nov	microfilm	618-21

Table 2.3: Historical CHS tide records available for the Avon River through MEDS.

In addition, MMRA and NSDA personnel routinely recorded tides at select marsh bodies throughout the region for short time periods. These data provide an idea of the difference in water level elevations between different marsh bodies. For example, a large tide on April 4, 1958 was recorded as 8.23 m CGVD28 (26.96 ft) at the Windsor bridge and 8.18 m at Burlington marsh (across from Hantsport), but 8.23 m at Herbert River and Chambers. Fortunately, the MMRA had recently increased the height of dykes in the region but this had not received extensive support at the time.

> *"The highest tide recorded by the MMRA at the Windsor Bridge was 26.96 geodetic on April 4th, 1958, when the tide height predicted (tide table) for Saint John, New Brunswick was 29.1 low water datum. Note that this was the highest predicted tide for the region at least since 1932. The actual height reached at Saint John on this occasion was 29.0. The tide in the upper end of the Falmouth Great Dyke, above the Windsor Bridge, reached 26.85 geodetic, approximately one-tenth of a foot lower than the Windsor bridge peak.*
>
> *Many of the dykes constructed by this Administration around the inner perimeter of the Bay of Fundy were overtopped in sections by this tide which was sufficiently above our predictions to puzzle us. There were meteorological conditions favouring this particular occurrence and subsequent tides of the same predicted magnitude verified this as having been unusually severe.*
>
> *These tides, of 1958 and 1959, as peaks of the very definite cycle of approximately 18 years proved to us the adequacy of our dyke construction grades. It may be of interest to note that marshland owners at Falmouth were of the opinion dyke grades were too high when construction was in progress. It is believed that this 18 year cycle is not generally realized and that past occurrences are attributed to other factors or are forgotten."*
>
> Portion of letter from J.D. Conlon, Chief Engineer, Dept of Agriculture, MMRA to
> Mr. J.A. Brown, District Engineer, Habours & Rivers Engineering Branch,
> Department of Public Works on Oct 12, 1961in response to file No. 1411-11
> re Windsor Tidal Flooding.

To date, the highest tides recorded at the causeway tide gate were 8.87 m (29.1 ft) (pers com. K. Carroll, 2007) and 8.6 m CGVD28 (28.2 ft) on January 10,1997. These tide levels reflect the Saros cycle or the 4.5 yr cycle mentioned previously. Examining the digital record between April 2002 and September. 2006, a total of 121 tides exceeded the HHWLT elevation (7.57 m CGVD28). Eleven of

these dates were greater than 8.0 m (Table 2.4) with the highest recorded tide on February 1, 2006 (8.2 m) which overtopped dykes in many areas (Figure 2.6).

Date	Recorded Tide Height (m CGVD28)
Feb 1, 2006	8.211
Nov 25, 2003	8.206
Feb 09. 2005	8.170
Feb 10, 2005	8.129
Feb 11, 2005	8.129
Dec 25, 2003	8.082
Dec 13, 2004	8.046
Dec 24, 2003	8.040
Dec 12, 2002	8.004
Aug 21, 2005	8.004
Feb 28, 2006	8.004

Table 2.4: Record of tides greater than 8 m geodetic at the Windsor tide gate between April 2002 and Sept. 2006.

2.1.3   Waves & Storms

Due to the large tidal range, the time period during which waves can exert a significant influence is limited. Lambiase (1980) reports that waves are not an important hydraulic process on intertidal sand bodies in the Avon River estuary since waves tend to be small due to the limited fetch. These waves are believed to be the cause of small-scale slumps observed on sand bodies in the Avon and Cobequid bay (Darlrymple, 1979). Observed wave heights did not exceed 1.3 m in Lambiase's (1980) study and most ranged between 0.3 and 0.6 m. However, during high water the foreshore is covered with a significant amount of water, and a much larger percentage of wave energy reaches the shoreline than when the tide is at low water. Waves can exert a significant influence in exposed areas on the edges of marsh cliffs and foreshore, causing erosion and local re-suspension of sedimentary material. This has been observed in other marshes in the Upper Bay (e.g. van Proosdij et al., 2006). Once waves travel over the marsh surface however, their energy is rapidly dissipated (e.g. Möller & Spencer, 2002). Therefore, the extensive marsh which has developed downstream of the Windsor causeway offers a natural form of shore protection for the causeway, although limited protection is provided in the tide gate channel itself.   In other areas, strong tidal currents will be the primary forces causing foreshore and marsh erosion.

Figure 2.6: Storm impacts on Feb 1, 2006 at the Avonport Dyke. a) storm waves battering marsh; b) storm surge reached upper limits of dyke and dyke overtopped. Photo by T. Hamilton, 2006.

Storm surges are a large rise in water level which can accompany a coastal storm, and are caused by strong winds and low atmospheric pressure. Conversely, a negative storm tide can result from higher atmospheric pressure producing lower water levels than predicted. Compared to the Atlantic coast, storm surges exert less of an influence on the intertidal zone in the Upper Bay of Fundy due to the large tidal range. For example, a hurricaine in July 1975 (recorded speeds of 130 km/h) only generated waves around 1.25 m in height and caused minimal changes to the morphology of sand waves in the Avon River Estuary (Lambiase, 1980). However, when a storm tide coincides with an exceptionally high astronomical (e.g. perigeen or Saros tide) tide the results can be signficant, causing extensive coastal flooding and damage to infrastructure. The heavy rainfall accompanying such an event can also cause extensive overland, freshwater flooding since the numerous aboiteaux and tide gates cannot discharge water at high tide. This has been seen in Truro, Nova Scotia on a number of occasions.

Historically, a number of significant storm events have occurred in the Bay of Fundy. Desplanque and Mossman (2004) provide a detailed account of the events surrounding them. One of the most notable storms was the Saxby Gale (or "Saxby Tide") which occurred on October 4th, 1869. Severe coastal flooding and wind damage occurred all along the North American seaboard. By 1:00 am on October 5th, the Saxby tide overtopped dykes by at least 0.9 m. In the Cumberland Basin, the tides were such that two fishing vessels were lifted over the dykes boardering the Tantramar marshes and deposited 5 km from the shoreline. At Moncton, the water level rose about 2 m higher than the next highest tide on record (Desplanque & Mossman, 2004). While damage in the Minas Basin was less severe, dykes were breached throughout the region, cattle and sheep drowned, and in many areas travel become impossible since the transportation lines (e.g. rail and road) were washed away. Desplanque and Mossman (2004) estimate that the Saxby Tide was at least 1.5 m higher than astronomically caused high tides.

The 'Groundhog's Day' storm (February 2nd, 1976) is a classic example of the difference in impact due to timing with tide levels. Signifant damage and coastal flooding were reported in Maine where water levels rose more than 2.5 m above the predicted level, heavily eroding the shoreline (Desplanque & Mossman, 2004). The strong SSE winds which had been blowing for five to six hours over the open water resulted in a storm surge up Penobscott Bay, and much of Bangor, Maine was flooded. Water levels rose to 3.2 m above predicted tides in fifteen minutes (Desplanque & Mossman, 2004). Fortunately for those in the Bay of Fundy, the tide was an apogean (e.g. lower) spring tide, therefore, although there was a recorded surge of 1.46 m, the damage was limited. If the storm had occurred

during the perigeen spring (sixteen days later on February 18th), the damage would have been significant (Desplanque & Mossman, 2004). It is estimated that if the Goundhog's Day storm had occurred on April 16th, 1976 it would have had the potential of "*causing calamity on the scale of the Saxby Tide*" (Desplanque & Mossman, 2004 p. 102).

If such an event were to occur in the present day it would result in billions of dollars of damaged infrastructure and potentially loss of life, given the amount of development which has occurred behind the dykes (Shaw et al., 1994). Desplanque & Mossman (2004) suggest that the probability that a 'Saros' tide would coincide with an astronomically high spring tide is about 3%. However, postglacial sea-level rise significantly influences this probability.   With every repeat of the 'Saros', an increase of the high tide mark of at least 3.6 cm (2 mm/yr for 18 yrs) can be expected (Desplanque & Mossman, 2004).

> *"Since the Saxby Tide more than seven 'Saros' ago, sea level has risen eustatically nearly 25 cm. Added to the minimum 1.5 m by which the Saxby Tide exceeded high astronomical tides, a height is calculated that that is more than sufficient to overtop the present dyke system"*
>
> (Desplanque & Mossman, 2004)

2.2　Sedimentary Dynamics

2.2.1　Surficial Geology and Geomorphology

The channel of the Avon River Estuary consists of a rock bound, wave-cut shelf, no deeper than 10 m below lower low water (LLW). This platform is incised by a paleo-drainage system that is graded to approximately 50 m below LLW. Elongate tidal sand bars have the form of ebb-tidal deltas and are covered by active sand waves. Megaripples are also found in this channel (Pelletier & McMullen, 1972; Lambiase, 1980) (Figure 2.7). The vast majority of the sand in the Minas Basin is supplied by erosion of the Triassic sandstone cliffs that border the Basin (Amos, 1976; Amos & Tee, 1989). Most of the sand that is released is either trapped in Cobequid Bay to the east, or moves westwards along the south shore of the Minas Basin and enters the Avon River Estuary. Supratidal shorelines range from low-lying salt marshes to cliffs up 22 m in height, although much of the original salt marsh has been dyked. Both lower and upper intertidal facies are recognized. In most cases, the higher intertidal facies consist of gravel with a veneer of mud (Figure 2.8) that is on average less than 0.1 m thick. In a few areas there is a small beach of sand or shingle (Lambiase, 1980).

Grain size analyses on sediments within the Avon River estuary were performed by both Pelletier & McMullen (1972) and Lambiase (1980). Both studies concur that the dominant material is sand, found primarily in the central portion of the estuary in the form of six major sand bodies (Figure 2.8). Mean size decreases from the estuary mouth, where most of the mean grain sizes are coarser than 250 μm (medium sand) to the estuary head, where most are between 250 μm and 63 μm (very fine sand to coarse silt) (Pelletier & McMullen, 1972). Sediments at the mouth are more poorly sorted than those in the head (Lambiase, 1980). However, neither study extensively sampled the rapidly developing mudflat immediately downstream of the Windsor causeway.
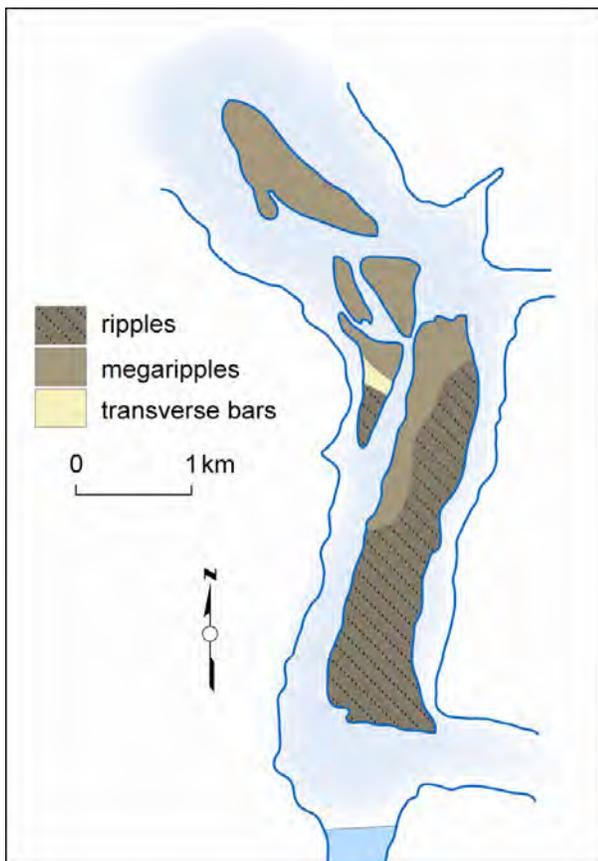
Figure 2.7: Bedform distribution at the head of the Avon River estuary. Modified from Lambiase, 1980.
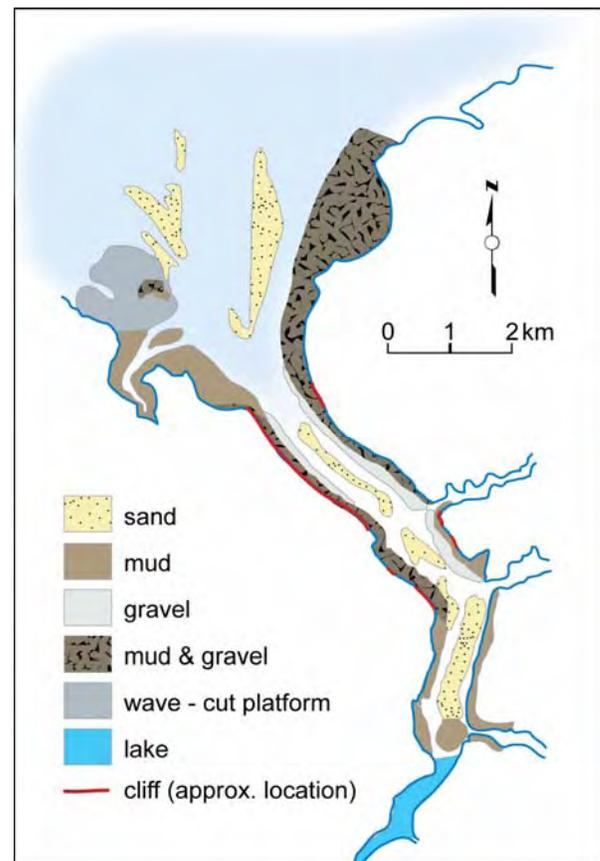
Figure 2.8: Intertidal facies of the Avon River estuary Modified from Lambiase, 1980.

2.2.2   Suspended Sediment Concentration and Deposition

Turk et al. (1980) sampled the mudflat during the summer months from 1976 to 1979 to determine the effects of rapid sedimentation on the sedimentological and biological characteristics of the intertidal mudflats when compared to other 'natural' flats in the region. When compared to other mudflats in the Minas Basin, the Windsor flat had high water content (50% vs 30% wet weight), small grain sizes (20 μm – medium silt in 1976 to 3 μm – clay - in 1979), and elevated organic carbon content (0.82% vs 0.24 % dry weight). Suspended sediment concentrations recorded on the Windsor Mudflat in the early

1980s ranged from 26.3 to 93.5 mg·l^{-1} (Amos & Mosher, 1985). Sediments are characterised in that study as silty clay. Sediment samples analyzed on the same flat in 2002 (Daborn et al., 2002) indicate that the sediments of the Windsor tidal flats were predominantly well sorted, fine silts (~68%) with a substantial clay fraction (~23%) with a mean grain size of 23-30 μm. Size distribution was commonly unimodal or slightly bimodal with principal mode(s) in the range of 9-30 microns (Daborn et al., 2002). Water contents were comparable to the values reported over 20 years earlier despite consolidation of sediment and extensive growth of the salt marsh vegetation *Spartina alterniflora*. In 2001-2002, thirteen boreholes were analyzed by Jacques, Whitford & Associates. The majority of these were taken directly adjacent to or on the existing causeway and along the proposed re-alignment. One of the cores that was directly on the marsh surface also recorded high water contents (53-71%) (Jacques, Whitford & Associates, 2002) and the material was classified as organic clay and clay. Two additional cores were located along the toe of the existing causeway. Depths of the organic clay layer ranged from 3.6 to 7.3 m and were underlain in all cases by dense silts, sands and gravels. Depths to bedrock along all boreholes ranged from 22 to 24 m (Jacques, Whitford & Associates, 2002). A detailed technical report is provided in Jacques, Whitford & Associates (2002).

Ambient suspended sediment concentrations in flood waters in the channels and over the marsh ranged from 100 mg·l^{-1} to 1,700 mg·l^{-1} in the bore or the wave front of the advancing tide (Daborn et al.,2002). No fluid mud was observed in that study nor from interpretation of dual frequency echo soundings from bathymetric surveys along the Avon in 2005 and 2006. Over the marsh surface the highest recorded concentrations were ~500 mg·l^{-1} in unvegetated areas. On average, 7.8 g·cm^{-2} settled out during each flood tide which is slightly higher than studies in the Cumberland Basin (van Proosdij, 2001; Davidson-Arnott et al., 2002). This translates to roughly 0.32 cm per month. Additional sediment accretion studies along transects perpendicular to the causeway recorded a mean of 0.5 cm per month (van Proosdij, 2005). As anticipated, the rate of sediment deposition is decreasing as the marsh is rising higher within the tidal frame. Almost twenty years previously, direct measurements were made of the rate of sediment accretion on the mudflat, and values ranging from 1.0 to > 14 cm per month (average 5 cm per month) were recorded (Amos, 1976). Deposition on the marsh is a combined function of the frequency of tidal flooding, below ground organic matter production, and ice rafting of sediment. A detailed accounting of ice processes are presented in van Proosdij (2005).

2.2.3 Currents

Lambiase (1980) measured current velocities at 29 stations with a direct reading current meter and a vertical velocity profile was recorded each half hour for a complete tidal cycle at each station. Tidal currents ranged from 0.6 and 1.7 m·s^{-1} with lower velocities (< 1 m·s^{-1}) at the estuary mouth and velocities greater than 1 m·s^{-1} at the head. Maximum current speeds occur on both flood and ebb tides while the flow is channelized between intertidal sand bodies (Lambiase, 1980). There appears to be distinct ebb and flood dominant zones in the estuary, forming elliptical transport cells (Lambiase, 1980). The boundaries of these zones are usually sand body crests. These cells are similar to those reported in other areas of the Minas Basin (e.g. Darylmple et al., 1975; Darylmple et al. 1990).

2.3 Intertidal Ecosystems

Due to its macrotidal nature, the upper Bay of Fundy has an extensive intertidal zone which primarily contains sand or mudflat and salt marsh ecosystems. These ecosystems form an important component of the estuarine food web contributing nutrients and organic matter (e.g. Daborn et al., 2003; Gordon and Cranford, 1994; Gordon et al., 1985; Van Zoost, 1969). Salt marshes may be categorized as either high marsh (e.g. *Spartina patens*) or low marsh (e.g. *Spartina alterniflora*) species (Figure 2.9). In general, high marsh occurs above the mean high water level while the low marsh occupies the zone between mean high water and the high water level of neap tides (Daborn et al., 2003a).

Figure 2.9: Spartina alterniflora on Windsor salt marsh August, 2001.

Figure 2.10: Ice blocks stranded on the Windsor saltmarsh close to the Windsor Tourist Bureau on Feb 17, 2007. Photo by D. van Proosdij, 2007
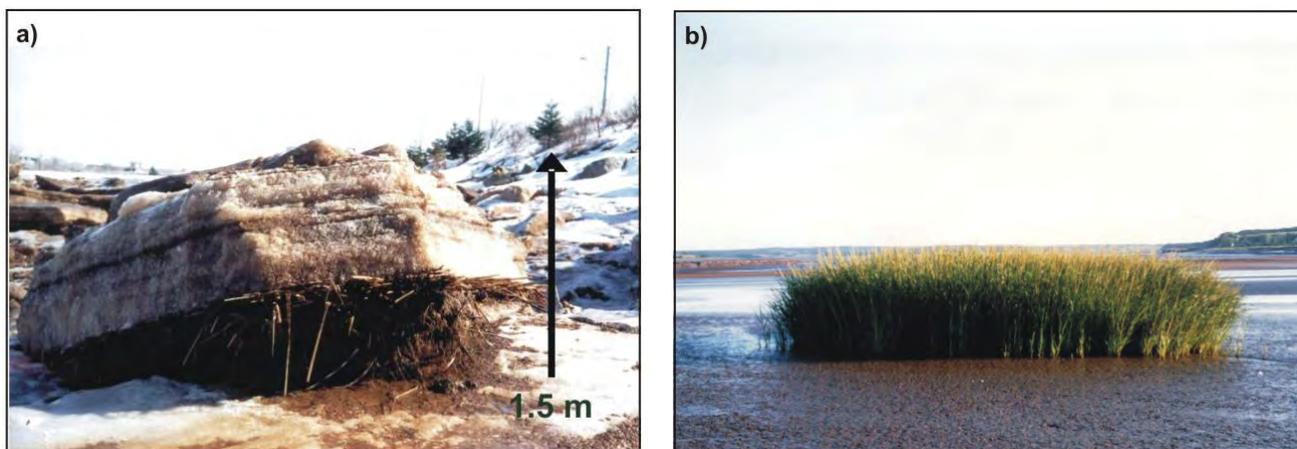
Figure 2.11: a) Rafted ice block (Feb, 2002) adjacent to the Windsor Causeway and b) Spartina alterniflora colony on the north-east edge of the Windsor marsh/mudflat ecosystem (Aug, 2003).

During the winter months, intertidal areas are covered with snow and ice that is rafted in with the tides and stranded on the marsh surface and within the tidal creek channels (Figures 2.10 and 2.11-a). This ice is quite ephemeral in nature, and can appear and disappear within only a few tides (van Proosdij, 2005). However, it can also build up within the tidal creeks, altering patterns of flow and erosion/deposition of sediments (Figure 2.12). These ice blocks contain high concentrations of both sediment and plant rhizome material which are important inputs to the salt marsh system (Ollerhead et al., 1999; van Proosdij et al., 2006). This material, including very coarse sediments, can be deposited on the marsh surface in the Spring. Standing vegetation in the Spring is quite sparse, having been sheared off in most years by ice and wave action. Significant amounts of marsh wrack material will then accumulate along the edge of the causeway and dykes. This material will be exported into the estuary in areas exposed to wave action (e.g. Windsor mudflats). Marshes in more sheltered areas will retain more of their dead material and it will decompose *in situ* (Gordon and Cranford, 1994). This is also evident at the Windsor site with dead *Spartina alterniflora* lying flat on the marsh surface in more sheltered areas (Figure 2.13).

Figure 2.12: Approximately 2.5 m high by 4 m block of ice blocking creek channel near southeast corner of marsh adjacent to causeway. Metre stick for scale. Photo by D. van Proosdij, Feb 25, 2005.

Figure 2.13: Sediment deposited on spartina alterniflora in sheltered areas on the Windsor marsh. Over time, the vegetation will decompose and be incorporated within the soil matrix. Photo by D. van Proosdij on Feb 25, 2005

2.4   History of Dyking and Construction of the Windsor Causeway

Settlers around the Bay of Fundy, primarily of Acadian stock, have constructed dykes and aboiteaux for over 350 years in order to farm the fertile tidal marshes of the Bay of Fundy. Marshland in the province was privately dyked until 1948 when the federal government set up the Maritime Marshland Reclamation act to rebuild the dykes in the Maritimes. Under the act, the federal government was responsible to provide the main protective works (where economically sound), while the provinces ensured proper use of the protected land (MMRA, 1966). From 1948, the Maritime Marshland Rehabilitation Administration (MMRA) has been applying modern engineering techniques to the traditional problems of dykeland construction and maintenance (MMRA, 1966).

The protection of marshlands from the tides is normally accomplished by the construction of dykes. Tidal gate structures, known as aboiteaux, are incorporated at major stream crossings where fresh water runoff is discharged and salt water is prevented from entering. River bank control and foreshore protection works are installed where required. The MMRA ensured the protection of 18,000 hectares of tidal farmland in Nova Scotia and 13,500 hectares in New Brunswick, building over 370 km of dyke in the two provinces (NSDAM, 1987). In 1966, the Federal Government turned over the responsibility of maintenance for the dykes to the province. The construction trend at the time was directed by economic feasibility studies focused towards protecting areas in groups, using a single large aboiteaux or dam instead of miles of dyke and large numbers of small aboiteaux (MMRA, 1966). In addition, multipurpose projects (e.g. creating or improving transportation corridors) were encouraged. This

resulted in a number of major tidal dams (.e.g Annapolis, Petitcodiac, Windsor, Memramcook) being constructed in the 1960s and 1970s. Today the NS Department of Agriculture (NSDA), Resource Stewardship Division, Land Protection Section is responsible for tidal dyke maintenance along a total of 241 km of dyke with 260 aboiteaux structures (NSDAM, 1987).

Interest in the construction of a causeway across the Avon River in the Town of Windor was formally initiated sometime around 1966 in collaboration with the Nova Scotia Department of Highways and the Dominion Atlantic Railway (MMRA, 1966, Figure 2.14). During that same year, construction was started on a major multipurpose dam on the Petitcodiac River in New Brunswick immediately adjacent to the City of Moncton with a similar goal of providing protection for upstream marshlands and a highway crossing (MMRA, 1966). Percy (in press) provides a detailed accounting of the historical, political, social, and environmental issues associated with "crossing Avon". This report will focus more on the sedimentological issues associated with the construction process.

Figure 2.14: Extensive intertidal flats evident at low tide on the Avon River near the Town of Windsor during the Winter of 1963. This aerial photo demonstrates evidence of natural bar formation in the location of the future causeway. Photo by C.A. Banks, 1968.

The construction of the Windsor Causeway was conducted in phases. In September 1968, rock fill was extended from the western edge for a distance of 300 ft from the new tide gate structure (K. Carroll, per com. and Figure 2.15 and 2.16). This new gate structure would be completed 'on land' (Figure 2.17) cutting through old marshland and channels, and then dug to allow water to pass through the

gates (Figure 2.17, 2.18, 2.19). In November 1968, infilling began from the east side. By July 30th, 1969 33% of the project had been completed, increasing to 54% by November 28th, 1969. By January 20th, 1970 (K. Carroll, pers com.) a gap of only 1000 ft remained for water exchange (Figure 2.16). The causeway was closed completely in July 1970 and the gates were opened.
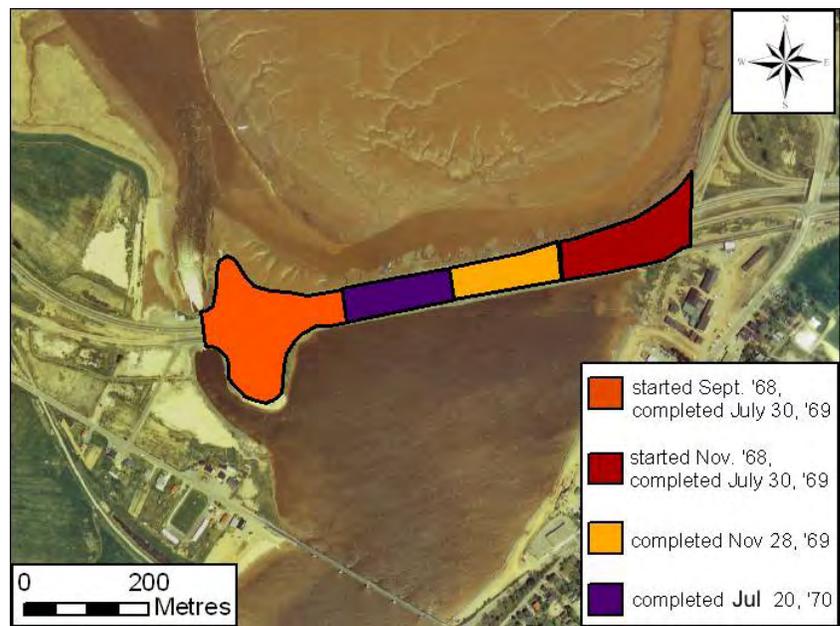
Figure 2.15: Sequence of closure during the construction of the Windsor Causeway superimposed on 1973 aerial photo mosaic. Data obtained from MMRA architectural drawing of proposed causeway, 1967.
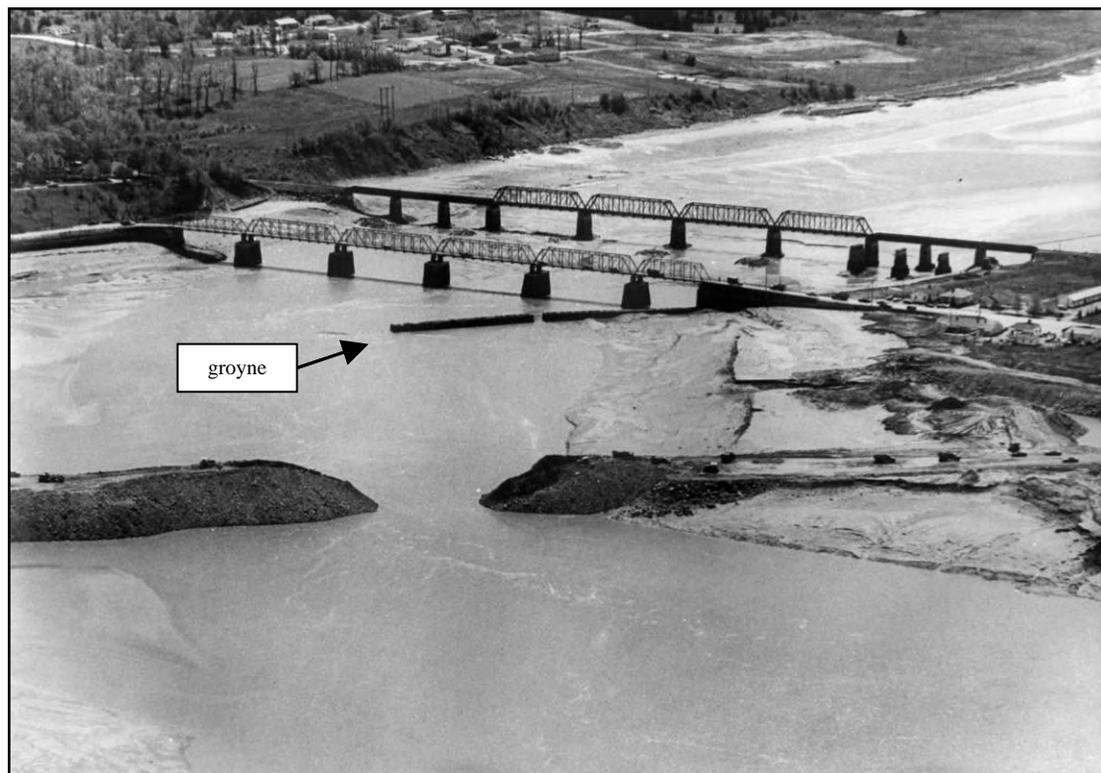
Figure 2.16: Final phase of the construction of the Windsor Causeway, around November, 1969. Photo from NSDA archives. Note the presence of a groyne seaward of the bridge. This groyne is indicative of earlier efforts by Public Works to keep sediment from accumulating and closing the shipping channel near the Wharf at Windsor.
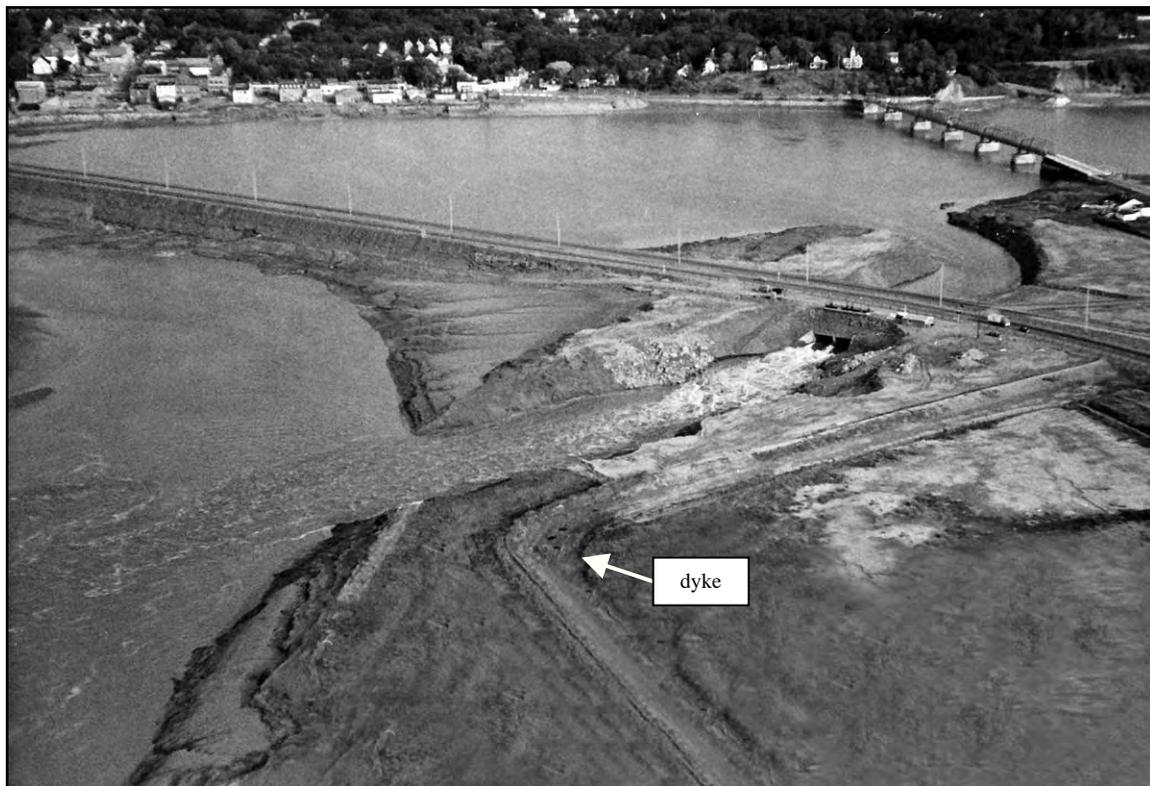
Figure 2.17: Location of the new tide gate constructed on old salt marsh. Note presence of dyke and strength of downstream flow (photo from MMRA Archives Aug 1971).
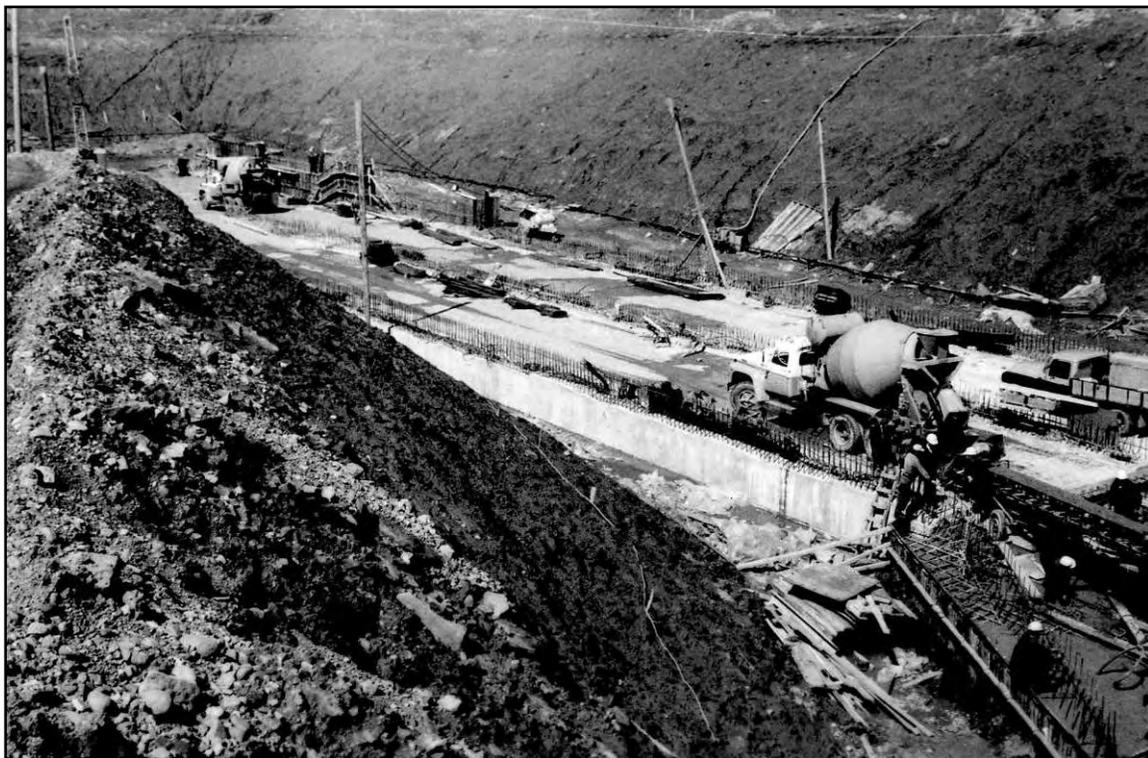
Figure 2.18: Construction of the floor of the new tide gate channel in late 1969 (photo from MMRA Archives 1969).
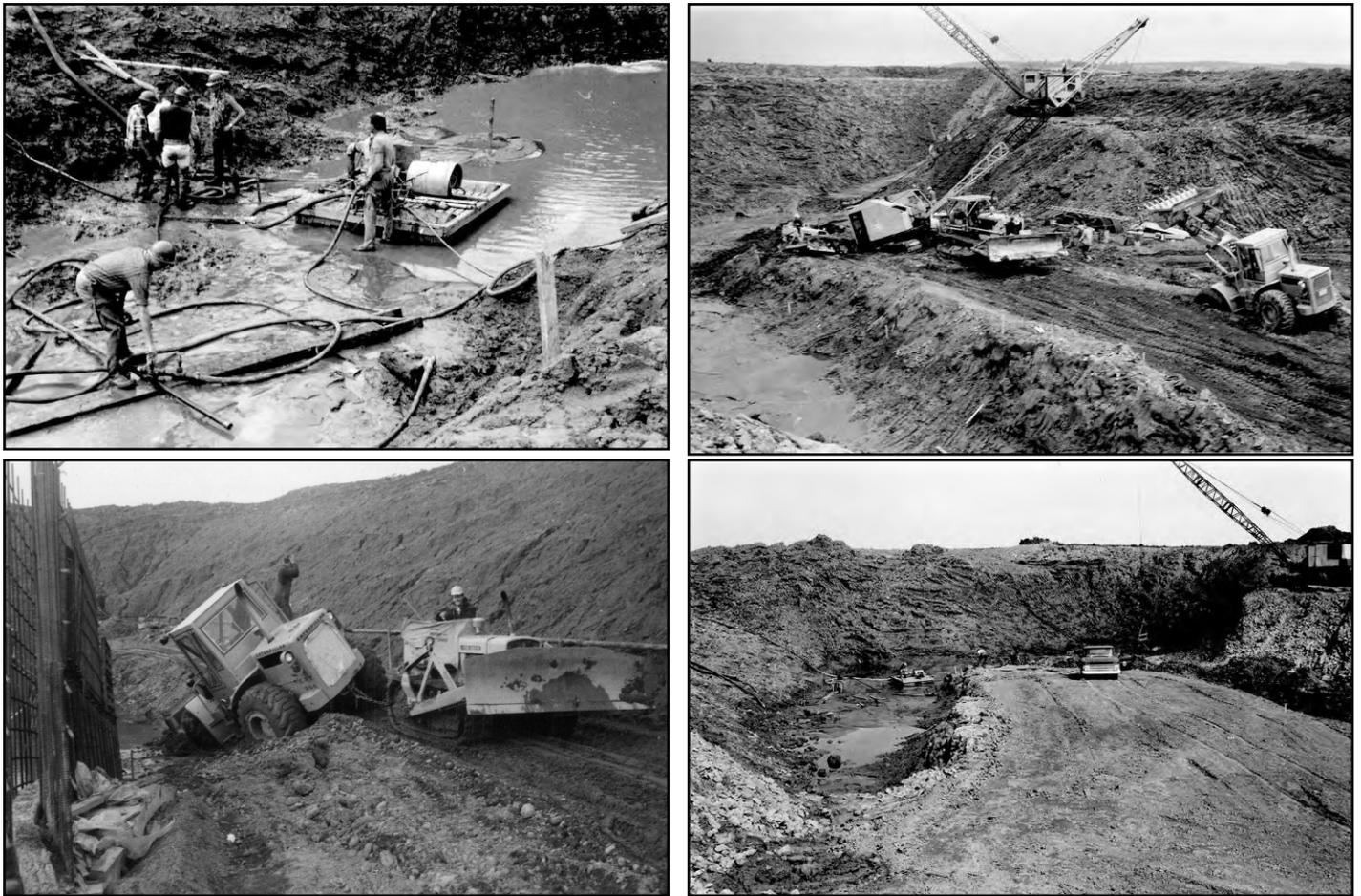
Figure 2.19: Soft sediments caused numerous challenges during the construction of the tide gate channel.
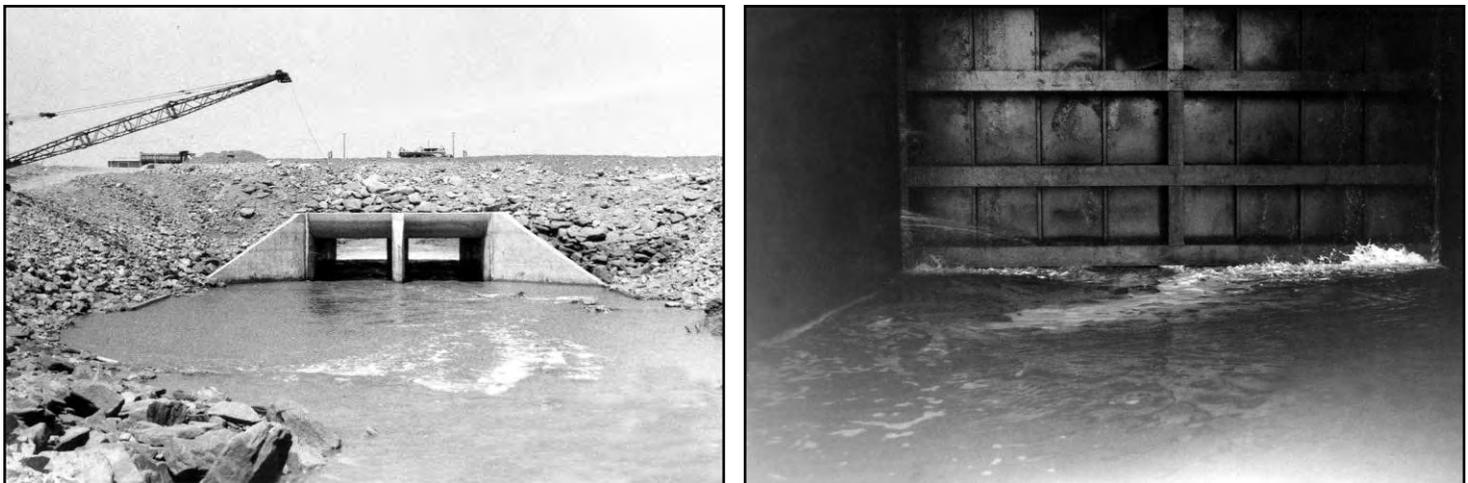
Figure 2.20: Completion of the sluice gates and opening of gates (MMRA archives Aug 1970).

Once the causeway was closed, freshwater continued to seep through the causeway fill for at least one year until it was gradually plugged with sediment (Figure 2.21).

Initiation of tidal creek channel
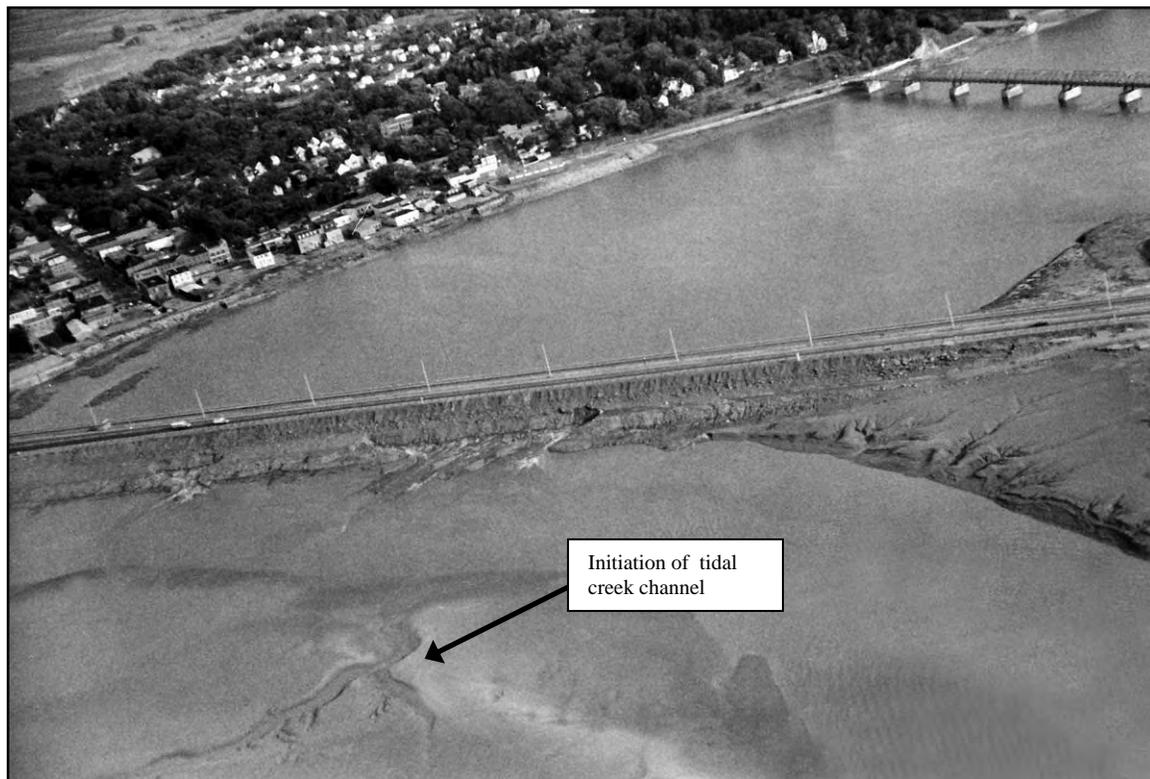
Figure 2.21: Once the causeway was completed, freshwater contined to seep through the structure almost one year later (MMRA archives Aug 1971). Note formation of tidal creek at southern section of the photo. This will become one of the main drainge channels for the new marsh.

Approximate location of future causeway
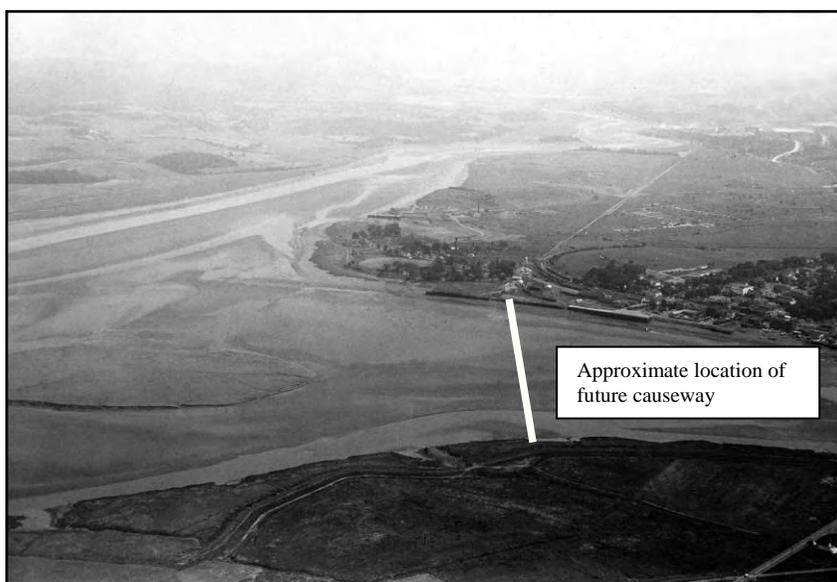
Figure 2.22: Aerial view of intertidal zone near future causeway in July 1963, prior to the construction of the causeway (MMRA, 1963)

Sediment began accumulating rapidly in the vicinity of an existing mud/sand bar (Figure 2.15; 2.22; 2.25). This mud/sand bar appears to have been present since 1858. Sedimentation rates measured in 1975 and 1976 ranged from 1 to > 14 cm·mth^{-1} with an average value of 5 cm·mth^{-1} (Amos, 1977). This early material was unconsolidated and contained high water contents, small grain sizes, and elevated organic carbon content (Amos, 1977; Turk et al., 1980). By the early 1980s, the max mudflat surface elevation was 4.75 m above geodetic datum (Amos & Mosher, 1985).

Figure 2.23: Rapid accumulation of unconsolidated sediment close to the causeway. a) Development of what appears to be a mud point bar in Oct 1970 near eastern end of causeway, 3 months after the construction was completed and b) infilling of channel parallel to the causeway in Nov 1970. The future 'causeway' channel is likely the one visible in photo 'a' top left (photos from MMRA, 1970).

Figure 2.24: View downstream from tide gate at the Windsor causeway in a) July 1970 when construction was completed (photo from MMRA, 1970) and in November 2002 following heavy rainfall (photo by K. Carroll, 2002).
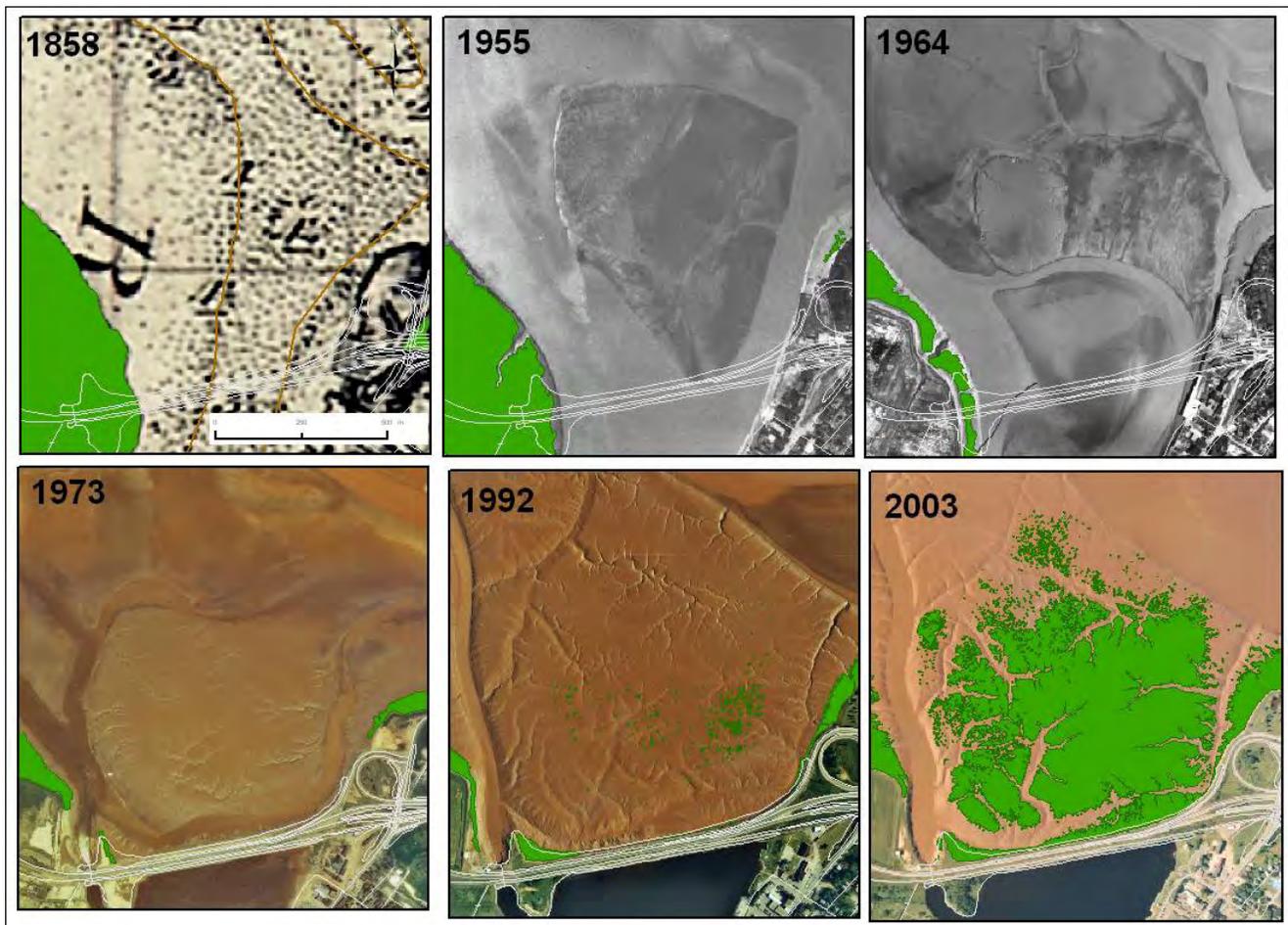
Figure 2.25: Sequence of evolution of the Windsor mudflat from 1858 to 2003. Position of the future causeway is provided on each aerial photograph used in the GIS analysis. Salt marsh areas indicated in green.

Salt marsh vegetation began to appear on the exposed mudflat surface around 1981, likely introduced by rafted ice (van Proosdij and Townsend, 2006). After 1992 the rate of colonization by *Spartina alterniflora* increased exponentially as the vegetation became firmly established on the mudflat surface, expanding in size from ~41,000 m^2 to >390,000 m^2 by 2001 (Figure 2.25). By the summer of 2005 almost the entire suitable mudflat surface had been colonized (Figure 2.26). Colonies of marsh vegetation are now appearing on the Newport Bar (Daborn and Brylinsky, 2004), downstream of the Windsor marsh/mudflat (Figure 2.27). The northeast edge of the Windsor marsh/mudflat is being eroded by tens of meters per year by the main channel of the St. Croix river (Figure 2.28).

Figure 2.26: View towards Falmouth exit from dyke adjacent to the tourist bureau in August 2006. Note the development of Spartina patens, a high marsh species adjacent to the causeway and complete coverage by Spartina alterniflora in the remainder of the original mudflat area (photo by D. van Proosdij, 2006).

Figure 2.27: View towards the Newport bar and colonies of spartina alterniflora that were established on it in August 2006 (photo by D. van Proosdij, 2006).

Figure 2.28: Erosion of north eastern edge of Windsor mudflat/saltmarsh by the main St. Croix channel currents in August 2006 (photo by D. van Proosdij, 2006).

3.0   METHODS

3.1   General Research Approach

The research presented here represents a component of a larger study examining the ecomorphodynamics of intertidal ecosystems in the upper Bay of Fundy being conducted as a collaborative exercise between Saint Mary's University, Nova Scotia Department of Agriculture (Resource Stewardship, Land Protection Section) and Nova Scotia Department of Transportation. Of specific interest is the impact of the many tidal barriers within the region on the evolution of intertidal geomorphology, and the resulting influence on contemporary sediment dynamics, and ecosystem response to climate change.   However, before any direct cause and effect relationships can be determined or the future response of the system can be predicted, it is important to understand quantitatively what has changed and to what degree these changes have occurred.   Therefore the general approach of this component of the research program was to utilize all available bathymetric and topographic surveys from 1858 to the present, combined with available aerial photography and satellite imagery within ArcGIS 9.1 to quantify changes in the intertidal geomorphology of the Avon River Estuary in response to engineering activities.   This report represents an extension of the research reported in van Proosdij et al., 2006. Methods presented and data analyzed within that report will be incorporated here for consistency.

3.2   Bathymetric and Topographic Data

3.2.1   Historical Bathymetry

The archives of both the Canadian Hydrogaphic Service and the United Kingdom Hydrographic office (UKHO) were searched to locate historical bathymetric surveys conducted within the Avon River Estuary.   Original charts and field logs from the British Admiralty (BA) were examined at the UKHO Archives in Taunton, UK, and appropriate charts were scanned at 500 dpi by UKHO personnel in 2005-2006 (Figure 3.1). Charts were chosen based on legibility, presence of potential georeferencing control points for rectification, and availability of chart datum information (Table 3.1).   A similar process was undergone at the Canadian Hydrographic Service (CHS) at the Bedford Institute of Oceanography and two mylar charts were secured (Table 3.1); one from a regular CHS survey in 1969 and the other from a research cruise lead by Dr. Carl Amos in 1976. Neither of the CHS surveys

however contained data points within the Avon, upstream of the Kennetcook river (Figure 3.2). Both agencies provided permission for these charts to be digitized for research purposes and presented here.

Source	Year	Scale	Horizontal datum	Type of data	Vertical datum	Adjustment to modern chart datum (CD)*	Collection method
United Kingdon Hydrographic Office Archives Surveyed by the British Admiralty	1858-59	*"1 inch to 1 statute mile in Latitude 45"*	Lat/long GCS_ Clarke1866	FS D4801	MLWS	-1.8 ft (+3 ft)	Lead line
	1860			Chart 353-B19	MLWS	-1.8 ft (+3 ft)	
Canadian Hydrographic Service (Atlantic)	1969	1:10000	UTM 20 NAD27	FS 4254 A	47.96 ft below BM1-1969	-2.4 ft	MS 26B Echo sounder
	1976	1:20000		FS 4654		-2.4 ft	Raytheon 719 dual frequency echo sounder
Maritime Marshland Rehabilitation Administration	1969-1971		UTM 20 NAD83 CSRS98**	paper strip chart recording	CGVD28	NA	Echosounding & traditional survey (level with stadia rod)
Hughes Surveys & Consultants Inc.	2005-06		UTM 20 NAD83 CSRS98	GPS xyz points	CGVD28	NA	Knudsen 320 B/P Dual Frequency Digital Echo Sounder & Differential GPS
Maritime Provinces Spatial Analysis Research Center (Saint Mary's University)	2003-06		UTM 20 NAD83 CSRS98	GPS xyz points	CGVD28	NA	Differential GPS (Leica GS50) & total station (Leica TS

*adjustment provided by Canadian Hydrographic Service (Atlantic). Adjustment to drying heights in brackets.
** converted to NAD83 during digitization process.

Table 3.1: Source of bathymetric and topographic survey data used for analysis. FS= field sheet; MLWS = mean low water spring

The raster 1858 BA field sheet (Table 3.1, Figure 3.1) was georeferenced in ArcGIS 9.1 to a grid of points (x,y) representing lat/long coordinates indicated on the paper chart. A new, rectified image of the map was created with this georeferencing information. This image represents the map in lat/long in the 1858 datum. Shoreline, mudlfat contours, salt marsh, roads, soundings, and drying heights were digitized on-screen. The features were added to a UTM 20, NAD83 dataframe and projected 'on-the-fly' because of the unknown horizontal datum for 1858. Upon analysis, significant differences in position were detected. A link table was created linking features in the 1858 datum to the current 1:10,000 map data in UTM Zone 20, NAD83. A total of 21 links were used. Rocky points and capes

provided the most accurate features. Road network intersections proved to be the least accurate features but were used in areas where no other suitable points were found. A similar process was used for the image file.
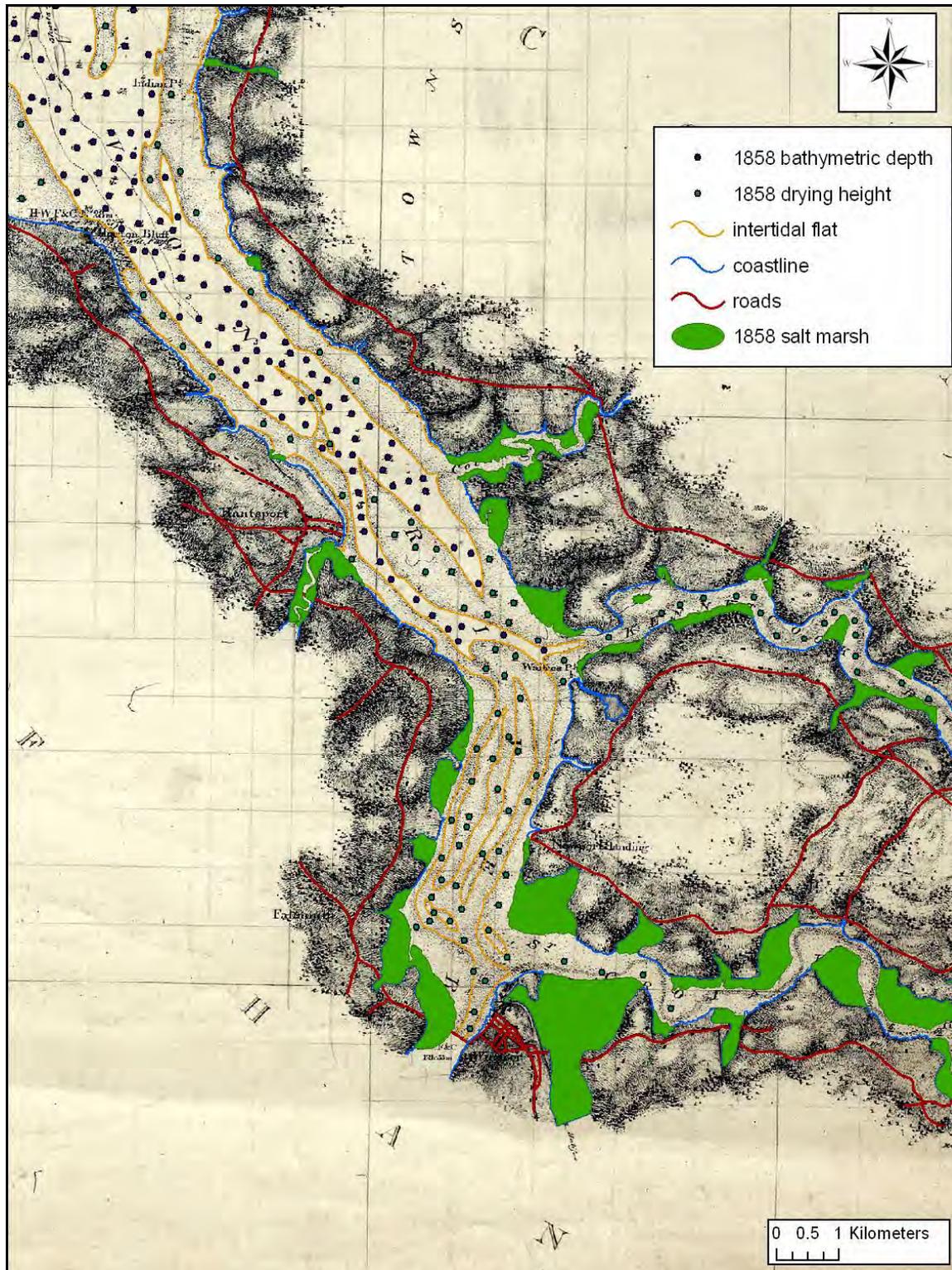
Figure 3.1: Digitzed features on 1858 British Admiralty Field Sheet D4801 from the United Kingdom Hydrographic Office.
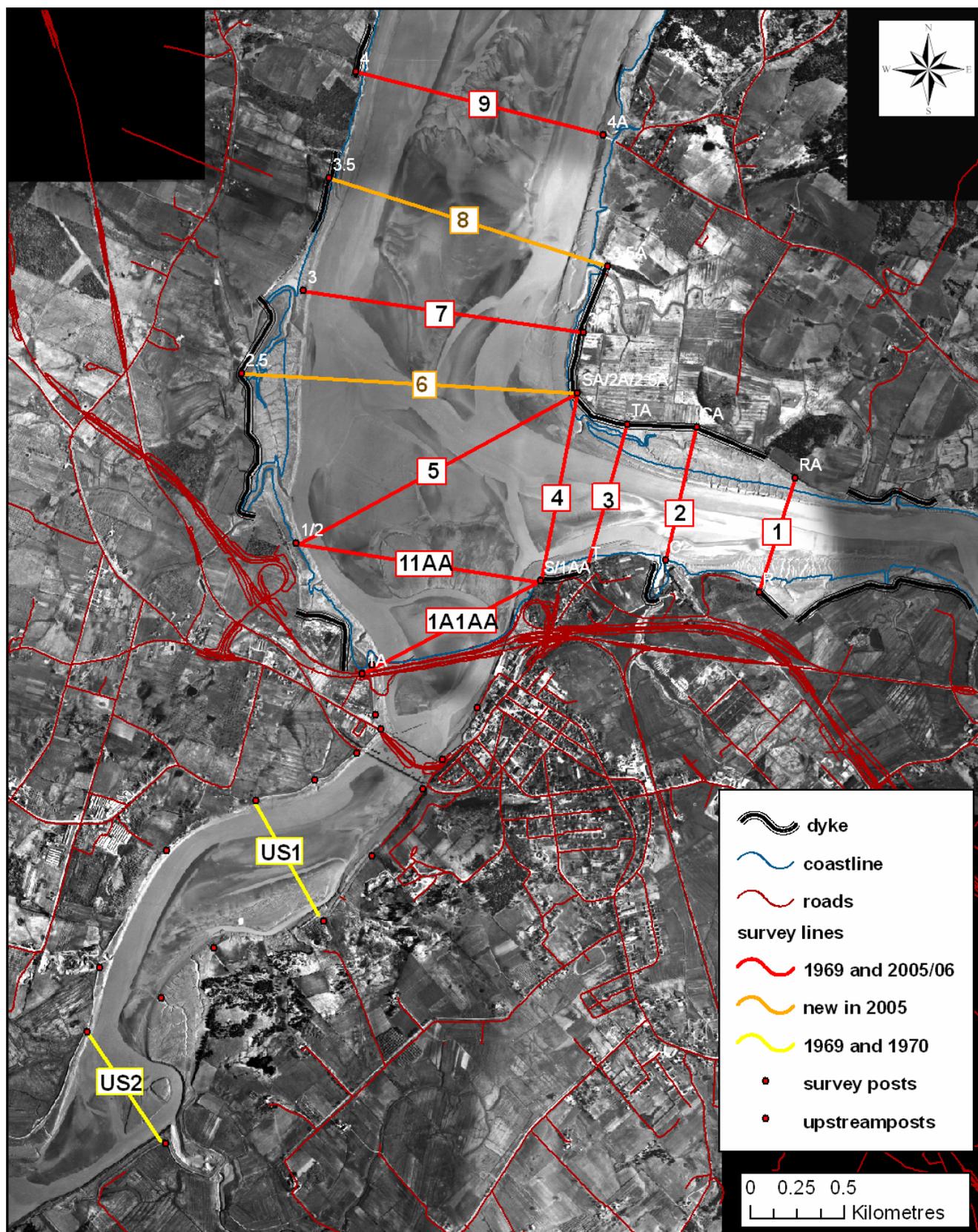
Figure 3.2 a)Location of historical and comtemporary survey lines closest to the Windsor causeway.   Although addional upstream surveys were conducted as indicated by the survey posts, those data were only collected in Nov 1970, after the causeway was completed and no comparable data are available.   Note the road and coast vector layers are based on data from 1986 to 1996 (Service NS Municipal Relations) overlain onto a 1964 digital photo mosaic.
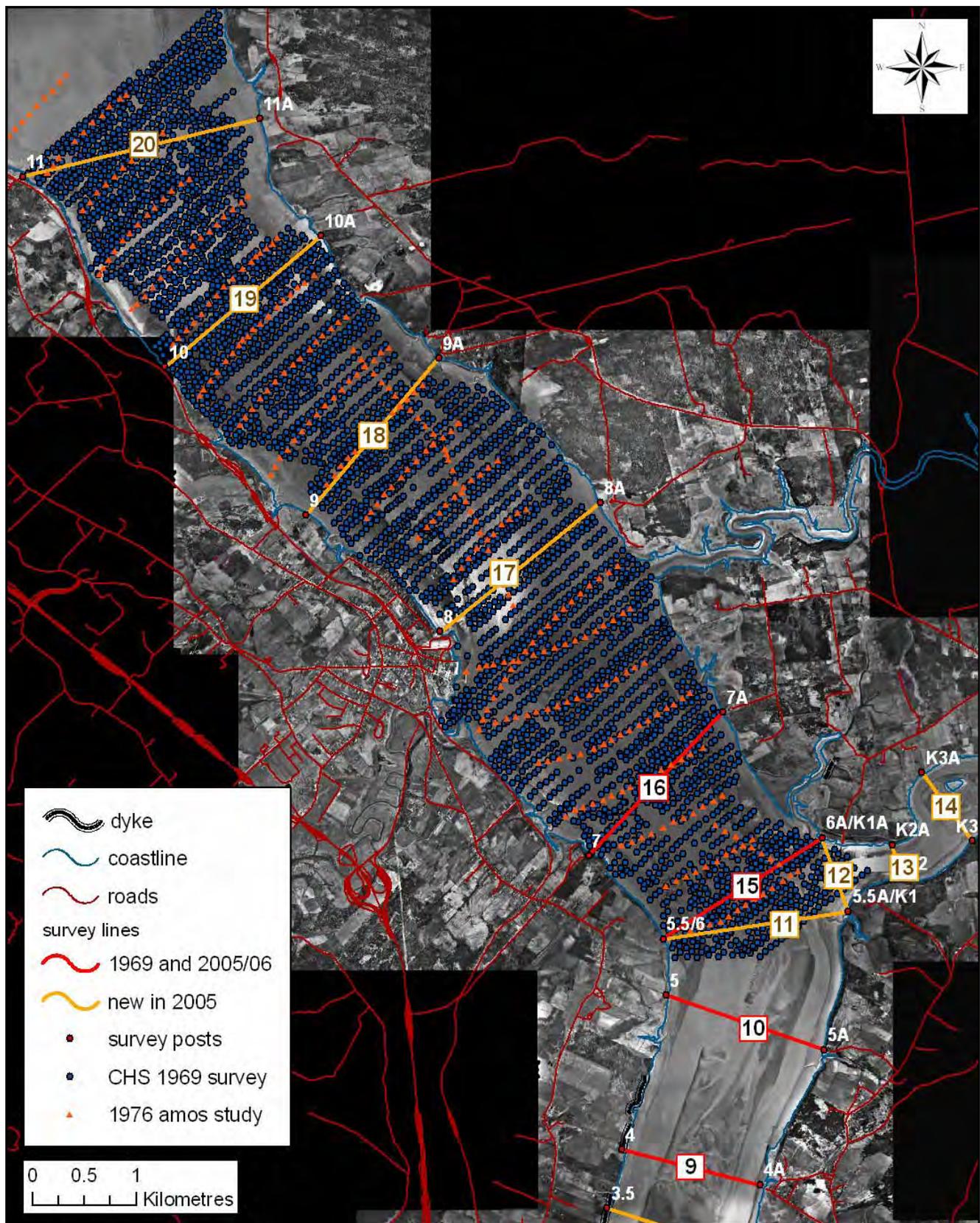
Figure 3.2 b)Location of historical and comtemporary survey lines near the mouth of the Avon River.   Note the road and coast vector layers are based on data from 1986 to 1996 (Service NS Municipal Relations) overlain onto a 1964 digital photo mosaic.

Since on-the-fly projection is not permitted in ArcMap for raster datasets, the image was first projected to UTM. The georeferencing toolbar was then used with the previous link table of 21 links. The image was rectified once again with an affine transformation to the NAD83 datum. A total of 673 soundings (converted to negative values) and drying heights in fathoms were converted to metres and modern chart datum using the adjustments presented in Table 3.1. These data were then converted to geodetic datum (CGVD28) by subtracting -7.23 m (CHS, 2007). Easting and northing coordinates for each point were computed from digitized feature geometry in ArcGIS. The 1858 shapefiles were added to a modern ArcMap document and were then checked against the position of resistant features such as rock outcrops visible on rectified air photo mosaics and satellite imagery. The position and values of a random sample of 50 points were vertified with the paper BA chart.

The CHS mylar field sheets were digitized at MP_SpARC at Saint Mary's University for comparison with the contempory surveys. Each sheet was registed using control points in UTM coordinates on a 44" x 60" Super L III GTCO Calcomp digitizing tablet. Shoreline, salt marsh, soundings, and drying heights were digitized and verified on-screen in ArcGIS against a 1:10,000 digital topographic map sheet. Appropriate attribute information (e.g. sounding values) was added systematically and conversions applied (Table 3.1) to convert to modern chart and geodetic datum. In total, 3842 points were digitized from the 1969 field sheets and 333 for the 1976 survey. Once completed, an attribute query was performed to identify points with incorrect elevational information (e.g. value of 0 or > 30) and a total of 25 points were corrected. Data were also plotted and patterns compared to the mylar copy. In addition, a random sample of 50 points was selected and verified against the original field sheet. No errors were discovered.

3.2.2   MMRA Cross Sectional Profiles

The MMRA undertook a field survey campaign during the construction of the Causeway to monitor changes in the cross sectional profiles in the Avon and St. Croix Rivers. Surveys were conducted by MMRA survey technicians along 12 transects downstream of the causeway and approximately 12 transects upstream of the future causeway (Figure 3.2). Posts were put in at either end of each line and a detailed sketch and description were recorded in field logs. Bathymetry was recorded using an echosounder on a small open boat guided between the two posts at high tide. A detailed record of the tide water levels during the survey was maintained to assist in interpretation of water levels. A marker was placed at either end of the line when an echosounding survey was no longer feasible due to water

level and standard rod and level surveying techniques were used to complete the profiles over the marsh itself. All of the downstream profiles were initiated in July 1969 and repeated in November 1969, however only those in the immediate vicinity of the causeway and along the St. Croix River were repeated in the Spring (May) and the Fall (November) until May 1971 (Table 3.2, Figure 3.2). These echo sounding profiles were then drafted to scale (point created for each topographic change in slope) on paper charts by the survey engineers and tied to geodetic datum (CGVD28). Profiles collected from both upstream and downstream sections of the existing causeway will be examined however, more emphasis will be placed on changes downstream due to a lack of contemporary information upstream.

Survey Lines	Map code	BA 1858	MMRA					CHS		Hughes Surveys & Saint Mary's Univ.		
			July 9-11 1969	Oct 28-30 & Nov 4-7 1969	May 26 1970	Nov.4 1970	May 1971	Oct. 1 1969	June 1 1976	Dec. 4-5 2005	June 23 2006	Aug. 6 2006
US1	US1		X	X		X						
US2	US2		X	X		X						
L1_SC_RRA	1		X	X	X	X	X			X	X	X
L2_SC_CCA	2		X	X	X	X	X			X	X	X
L3_SC_TTA	3		X	X	X	X	X			X	X	X
L4_SC_SSA	4	X	X	X	X	X	X			X	X	X
L1A_DS_1A1AA	1A1AA		X	X						X		X
L1_DS_11AA	11AA	X	X	X						X		X
L5_DS_22A	5	X	X	X	X	X				X	X	X
L6_DS_2.52.5A	6	X								X	X	X
L7_DS_33A	7	X	X	X	X	X				X	X	X
L8_DS_3.53.5A	8	X								X	X	X
L9_DS_44A	9	X	X	X	X	X				X	X	X
L10_DS_55A	10	X	X	X	X					X	X	X
L11_DS_5.55.5A	11	X						X		X		X
L12_DS_K1K1A	12	X						X		X		X
L13_DS_K2K2A	13	X								X		X
L14_DS_K3K3A	14	X								X		X
L15_DS_66A	15	X	X	X				X	X	X		X
L16_DS_77A	16	X	X	X				X	X	X		X
L17_DS_88A	17	X						X	X	X		X
L18_DS_99A	18	X						X	X	X		X
L19_DS_1010A	19	X						X	X	X		X
L20_DS_1111A	20	X						X	X	X		X

Table 3.2: Dates of bathymetric surveys used in the analysis and corresponding cross sectional lines. BA = British Admiralty, MMRA = Maritime Marshland Rehabilitation Administration; CHS = Canadian Hydrographic Service . Survey lines are presented in Figures 3.1 & 3.2.
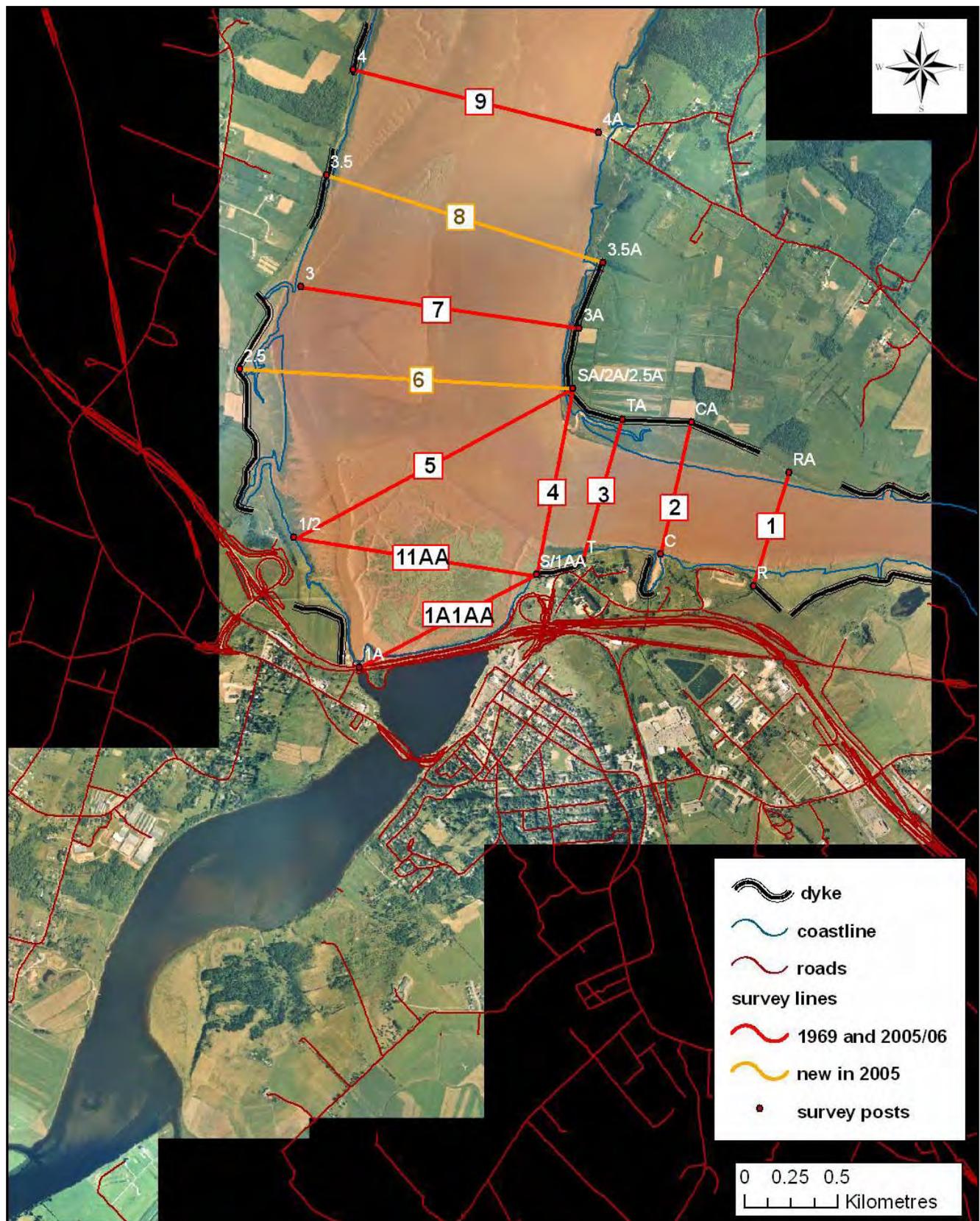
Figure 3.3 a) Location of historical MMRA and contemporary survey lines near the Windsor causeway overlain onto a 2003 digital air photo mosaic.
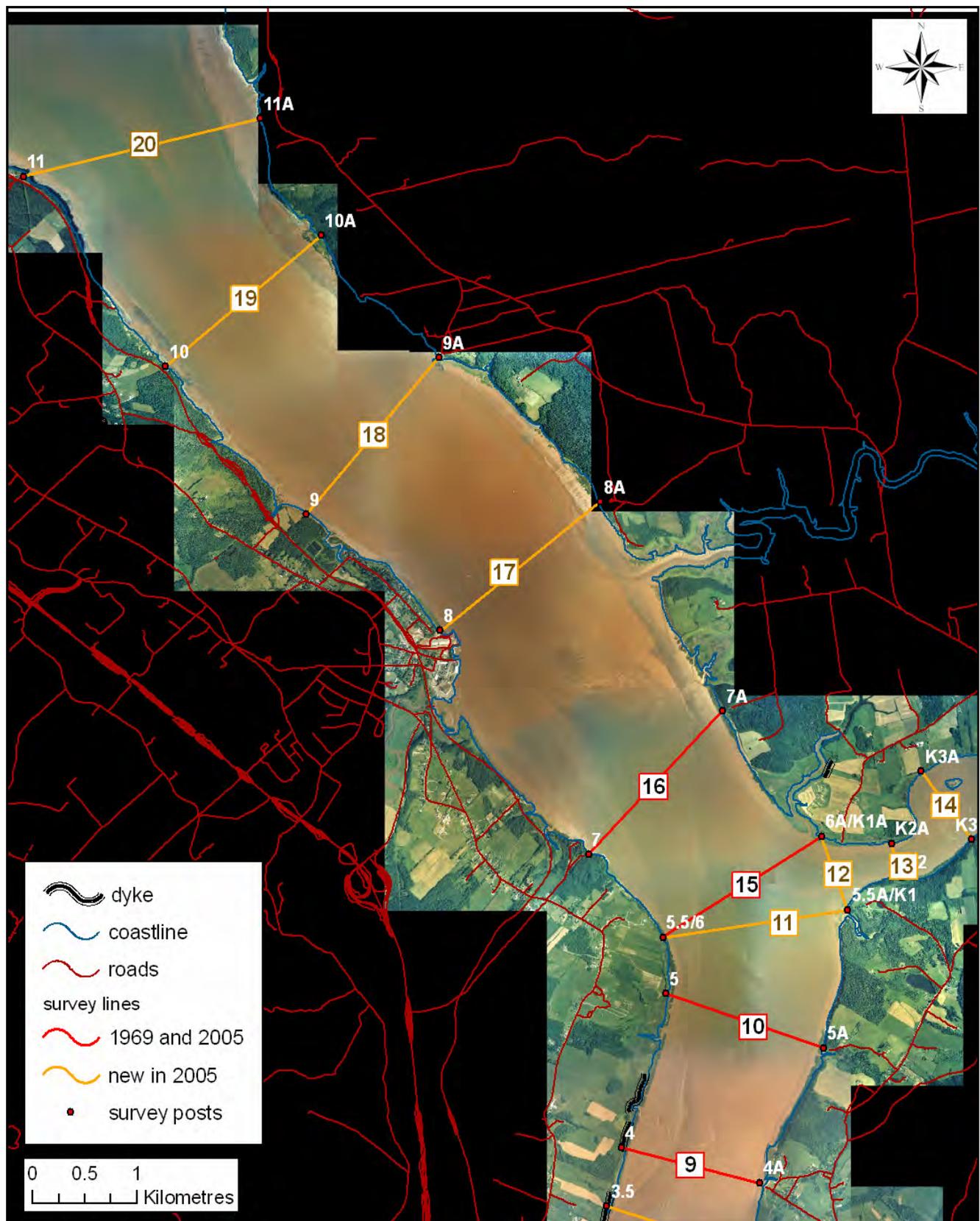
Figure 3.3 b)Location of historical and comtemporary survey lines closest to the mouth of the Avon River overlain onto a 2003 digital air photo mosaic. The June 2006 survey ended at line 16 whereas all of the lines were surveyed in August 2006.

The paper charts were digitized at MP_SpARC for comparison with the contemporary surveys. Each paper survey was registered using Cartesian coordinates on a 44" x 60" Super L III GTCO Calcomp digitizing tablet. Lines were digitized from post to post with the 'start post' indicated as zero on the paper chart in ArcMap[tm] 9.1 (ESRI[®], Redlands, CA).

Since the distance between survey points was greater than the distance between bathymetric points (2 m) on the contemporary surveys, the historical surveys needed to be densified. This step is critical for accurate comparison. In this procedure, vertices are added to an arc (line) at a specified interval (2 m). This was achieved using the ETGeoTools (ET Spatial Techniques, 2005) extension for ArcMap 9.1. The resultant densified lines were then converted to an ASCII text file using a 'Shape_To_Text' executable file (Taylor, 2003) and opened in Microsoft Excel. A custom template spreadsheet was created to convert the X and Y values from the digitized lines, representing orthometric distance in feet (X) from a certain starting post, and height above geodetic datum (Y), also in feet. The 2-D X,Y coordinates were converted to 3-D x,y,z values in metric units, representing Easting (x) and Northing (y) in the UTM map projection and the height above geodetic datum (z). The second step required the UTM Easting/Northing locations of the start and end posts of the cross-sectional line. These post coordinates were determined in consultation with Ken Carroll and Darrel Hingley of NS Dept of Agriculture, old field logs, and georeferenced air photo mosaics from the 1960s. Post coordinates were then extracted to create new point features. These coordinates were used in a range/bearing configuration to calculate the new x,y location for each distance value along the line. The z value was simply copied from the original metric 'Y' value.

In order to compare the exact position of the BA and CHS surveys to those collected in other years, points within 150 m either side of the established survey lines (Table 3.2 and Figure 3.2b) were selected in ArcMap and exported in csv format and inserted into another Excel spreadsheet template. The exported data were expressed as Easting (x), Northing (y) coordinates with elevation (z) values and were converted to a distance and elevation value suitable for comparison with the MMRA surveys. A custom spreadsheet was designed which effectively 'snapped' the data to a straight line using the post coordinates and trigonometry. A series of distance filters were applied to the data which excluded any point which was more than 50, 100 and 150m off line. A resultant straight line distance and associated elevation value was generated for each vertex. New x,y coordinates were generated relative to the survey posts using the above mentioned spreadsheet and ploted for each line.

Total monthly precipitation values are presented from 1969-1976 and 2005-2006 from the Kentville meteorological station (Figure 3.4) to identify any potential large run-off events that might influence the surveys. Details for tidal and meterological conditions for each survey are provided in Appendix A.
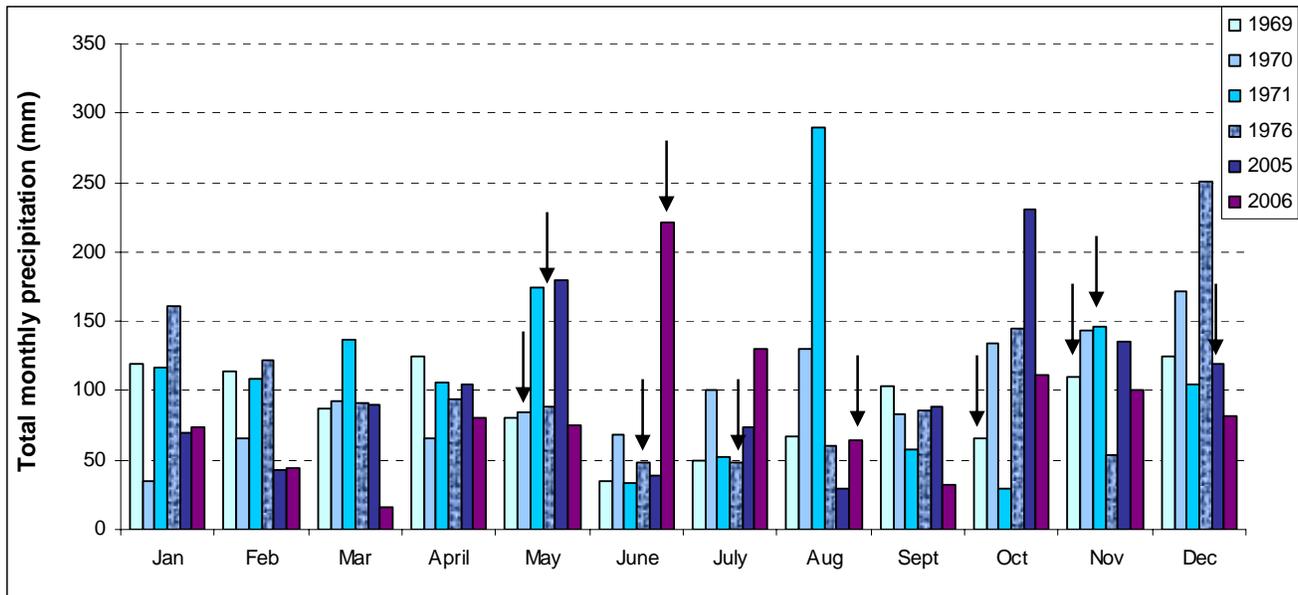
Figure 3.4: Total monthly precipitation at Kentville (45.07 N, -64.43 W). Months during which surveys were conducted indicated by an arrow.

3.2.3 Contemporary

Hughes Surveys and Consultants Inc, consulting engineers with experience in macrotidal surveys (e.g. Petitcodiac) were contracted to perform a contemporary survey of the Avon, St. Croix, and Kennetcook River estuaries. Originally scheduled for October 2005, surveys were postponed until December 4 & 5, 2005 due to a combination of weather restrictions and non-optimal tidal heights (e.g. not high spring tides). Heavy rainfall in October and November created freshet conditions so the resultant surveys likely represent lower bed elevations than are typically found in the Fall (Figure 3.4). Additional surveys were conducted on June 23 and Aug 6, 2006.

Surveys were conducted from a 20-foot welded aluminium Sounding Launch using a Knudsen 320 B/P Dual Frequency Digital Echo Sounder. Data were recorded at both 28 and 200 KHz in order to try and record the presence of fluid mud (US Army Corps of Engineers, 2002). Navigation and positioning as well as tide height monitoring were conducted using DGPS and Real Time Kinematic GPS techniques. Real time corrections for navigation to points (posts) supplied by MP_SpARC were performed using the Canadian Coast Guard Realtime Beacon (RTB). GPS data were post-processed for higher

precision against a Hughes operated base station set up over a geodetic benchmark at the Hantsport wharf. Data were also post processed against a survey monument installed at the Windsor Tide Gate (by Darrell Hingley, NSDA) and monument 69N142 at the Hantsport Wharf.   Three dimentional x,y,z coordinates of river bed elevation were computed using xyz post-processed DGPS values and subtracting the depth of echo sounding to produce a new z value. Appropriate offsets for the difference in location of the GPS antenna and the echo sounding equipment were applied.   All data were referenced to CGVD28 vertical datum.

Topographic surveys of the marsh surface were conducted using differential GPS survey techniques using a Leica GS50® single frequency GPS receiver in late November and early December, 2005 and late August 2006. Prior to the start of the survey on each line, the instrument was initialized at a known base point (e.g. post) and then the marsh and start of the adjacent mudflat zone were surveyed with data being collected as a kinematic phase chain. These data were then post processed using Leica® software against a base station collecting phase chain data at the Windsor tide gate. The surveys are accurate to within 0.10 m in the vertical plane.

Both bathymetric and marsh point survey data were displayed in ArcMap 9.1. Points were selected along the survey line of interest and the associated attribute table was exported and inserted into another Excel spreadsheet template. This permitted non relevant data to be excluded (e.g. boat turning). The exported data were expressed as Easting (x), Northing (y) coordinates with elevation (z) values, and were converted to a distance and elevation value suitable for comparison with the historical surveys. An additional distance filter was applied to the data which excluded any point which was more than 20 m off line. A resultant straight line distance and associated elevation value were generated for each vertex. These data were filtered using a 3 sample running mean to smooth the data.

Lines 1A_DS_1A1AA and 1_DS_11AA (Figure 3.3) were extrapolated from a digital elevation model (DEM) generated from a detailed survey of the Windsor marsh surface in July 2004 with the assistance of Darrel Hingley (NSDA). The DEM was created using the 'Topo to Raster' ArcInfo Toolbox function in ArcGIS 9.1 using digitized tidal creek thalwegs and elevation points. 'Topo to Raster' is an interpolation method specifically designed for the creation of hydrologically correct digital elevation models. It is based on the ANUDEM program developed by M. Hutchinson (1989) and uses an iterative finite difference interpolation technique. It is optimized to have the computational efficiency of local interpolation methods, such as Inverse Distance Weighted (IDW) interpolation,

without losing the surface continuity of global interpolation methods such as Kriging and Spline. TypeConvert v 2.3.5, ETgeoTools and ShapetoText were used to extract and convert the line data to point data suitable for inclusion in the analysis. These lines were re-surveyed in the field in August 2006 and plotted accordingly.

Profiles for each survey for each line were plotted in Excel and examined for consistency, accuracy, and depiction of realistic changes using the original paper charts, digital air photo mosaics, old marsh plans, and expert opinions of NSDA personnel familiar with the Avon system since the 1960s. A total of 4 lines needed to be corrected due to slight errors on the original field sheets, misinterpretation of data, or incorrect post locations. Much of this was due to the disappearance of a key feature (e.g. bank erosion or wharf decay) where an old post was situated. If it was determined that a post needed to be re-located, all of the data for that line were re-calculated using the new parameters. If the survey ended below either the HHWLT (Higher High Water Large Tides) or HHWMT (Higher High Water Mean Tides) level, it was extended up to either the 10 m contour from the NS 1;10,000 digital topographic series or nearest dyke to allow for proper cross section calculations. The coordinates of the intersection of the line and the 10 m contour were determined within ArcMap. These new coordinates were added to the lines (Figure 3.2) and calculations redone using the extended parameters.

3.2.4   Digital Elevation Model Generation

In order to address one of the primary questions associated with this project, namely what has been the impact of the construction of the Windsor causeway on the tidal prism, three digital elevation models were developed based on the availability of survey data for the entire length of the estuary. Digital Elevation Models (DEM) were generated for 1858, 1969 (using CHS Oct 1969 & MMRA Nov 69), and 2005. An additional 'short' DEM (downstream of the Kennetcook) was generated for the June 1976 survey as well. For each year, the thalwegs of the main tidal channels were digitized in a downstream direction as well as the outline of major emergent tidal bars. The latter polyline was assigned an elevation value based on the mean of the points that it crossed. Since formal ground surveys were not performed on all marshes, these were assigned a base value for all years of 6.5 m OD based on the results of the 2005 survey. The full potential tidal prism area was digitized as the shoreline and upland edge of marshes for each time period from the head of the Avon River to its mouth near Horton Bluff and upstream to the tidal limit on the St. Croix, Kennetcook, and Cogmagon rivers. Since the 1858 survey did not extend much upstream beyond the causeway, marsh areas were assumed to be between the HHWLT and HHWMT elevations. When compared with the boundaries of

the MMRA marsh bodies the estimated area appear relatively accurate. However, the position of the dykes in 1858 were not available for this project therefore the model generated will likely overestimate the prism area. The 1:10,000 digital spot elevations from the Nova Scotia Topographic Database (Service Nova Scotia and Municipal Relations) were used to represent areas outside of the surveyed areas. The average spacing of points is ~90 m cross track and ~ 40 m along track. The prism polygon was then used to erase 1:10,000 elevations beneath it in order to account for shoreline erosion and dyking. All of these data were then used to generate a DEM using the 'Topo to Raster' ArcInfo Toolbox function for each year. Resultant DEMs were compared to aerial photo mosaics, satellite images or original chart (e.g. 1858) representative of each time period to ensure that the location of the major bars and channels were accurately represented.   Since the initial 2005 DEM did not accurately reflect the complex marsh and mudflat growth adjacent to the causeway, a high resolution DEM from 2004 of the Windsor marsh/mudflat system was added to the larger model. This resulted in a larger and more accurate DEM.

In order to compare the modeled data with the field data, 3D Analyst was used to extract 3D topographic lines along each survey transect. TypeConvert v 2.3.5, ETgeoTools, and ShapetoText were then used to extract and convert the line data to point data suitable for inclusion in the analysis. Both the 1858 and 2005 models were within 1 m of the empirical data in the intertidal areas.   The 1969 model however significantly overestimated the tidal prism downstream of the Kennetcook River. It was hypothesized that the high density of points from the CHS Oct 1969 survey created a much larger weight in the model. Therefore, the model was re-generated using only points within 100 m either side of the profile lines. The resultant surface and curve was much more representative along the entire estuary.

3.2.5   *Hydraulic Geometry & Prism Calculations*

In order to examine the morphological changes in the Avon River channel over time, a series of hydraulic geometry parameters were calculated. Channel depth, width, and x-sectional area will control tidal discharge and current speed (Knigthon, 1984; Williams et al., 2002).   Since most of these parameters will vary depending on the tidal height used, all variables were calculated for both HHWLT and HHWMT at Hantsport. These values were obtained from the Canadian Hydrographic Service (CHS) Chart 4140, 1982 (Table 3.3). Values were then converted from chart to geodetic datum (pers comm. Charles O'Reiley, 2005) to be used with the survey data referenced to CGVD28 vertical datum. HHWLT refers to the 19 year average of the highest annual predicted high waters whereas HHWMT

represents the average of all of the higher high water from 19 years of prediction. Mean Water level (MWL) refers to the average of all hourly water levels over the available period of record (Forrester, 1983). These limits were applied to all survey dates and have not been adjusted for sea level rise.

Datum	Large tides		Average tides		Mean water level
	HHWLT	LLWLT	HHWMT	LLWMT	MWL
CGVD28 (m)	7.57	-7.33	5.77	-6.03	-0.03

Table 3.3: Geodetic elevations converted from chart datum values obtained from the CHS chart 4140 at Hantsport. Non-published conversion value obtained from Charles O'Reiley, CHS, 2005.

V	Tidal Prism (m^3)
A_i	Intertidal cross sectional area (m^2)
pw	Wetted perimeter (m)
w	Width (m)
H	Mean elevation (m CGVD28)
H_{min}	Minimum bed elevation (m CGVD28)
D	Maximum water depth (m)
d	Mean water depth (m)

Table 3.4: Definitions and abbreviations used for analysis of hydraulic geometry

All of the data were analyzed in Microsoft Excel and calculations were performed relative to the intersection of the segment cross sectional line with the tidal limit horizontal plane. Parameters calculated and abbreviations used are summarized in Table 3.5. Cross sectional areas (A) were calculated as the area of water contained in the channel below either the HHWLT and HHWMT tidal limits. These values were obtained using a modified Trapezoid rule (A = sum of trapezoid areas between water level and bed elevation calculated from $(b_1+b_2) \cdot h/2$ between each sample point). In the majority of cases, the distance between sample points was 2 m. Intertidal
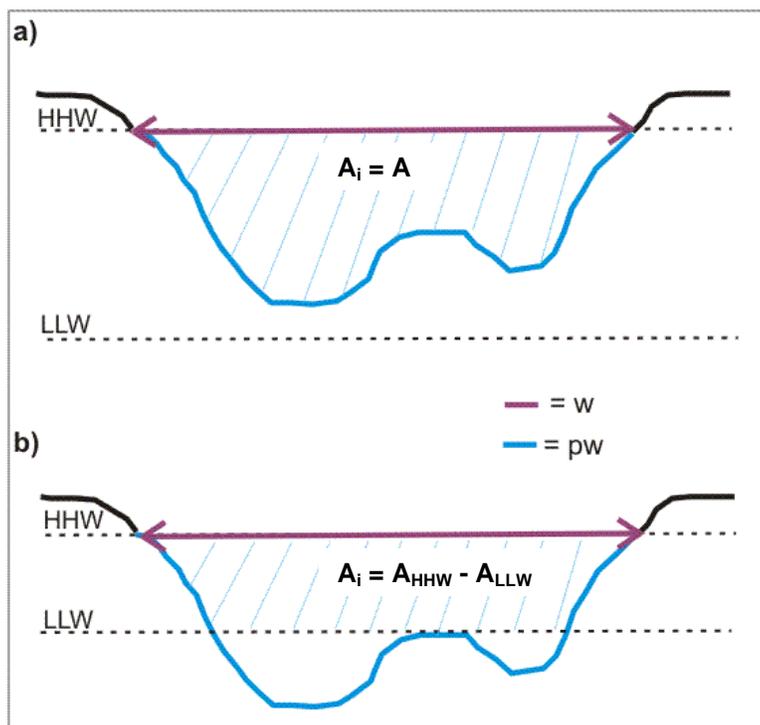
Figure 3.5 : a) Intertidal cross sectional area (A_i) when LLW level falls below the lowest surveyed bed elevation; b) Intertidal cross sectional area measured as the difference between cross sectional areas calculated for HHW and LLW. The geodetic elevation of these tidal limits will vary depending on whether the calculations are being performed for large tides or average tides. Channel width (w) and wetted perimeter (pw) are also indicated.

cross sectional area (A_i) is defined as the amount of water moving within the channel. It is calculated as the difference between the HHW and LLW cross sectional area values (Figure 3.5). In most cases, the LLW values were below the measured bed elevations. In those cases, the lower limit for the A_i calculations was taken as the bed elevation and is equal to the cross sectional area (Figure 3.5).

The tidal prism (V) is defined as the volume of water that moves through the estuary over one tidal cycle. In order to examine how the tidal prism changes with distance from the head of the estuary, the prism was calculated as the upstream volume of water that must pass through each cross section. This was either calculated mathematically or by using DEMs for each cross section. The digitized prism polygon shapefile was segmented using Arctoolbox into segments representing the planimetric area between pairs of survey lines. An additional field was added to the attribute table and assigned a value of 1. The polygons were converted to raster and multiplied using a raster calculator with the appropriate DEM (1858, 1969, or 2005). Areas that were outside of the prism were then effectively erased. The volume was calculated for each section using the Functional Surface function in 3D Analyst ArcToolbox. The surface volume was calculated below either the 5.77 (HHWMT) or 7.57 (HHWLT) reference planes as well as the -6.03 (LLWMT) and -7.33 (LLWLT) lower tidal limits. Similar to the A_i calculation, the resultant prism is the difference between HHW and LLW at each section. The total prism for each time period was then calculated as the sum of all segments.

In addition, a crude estimate of the prism was determined for each survey date by determining the mean of calculated cross sectional area between each line multiplied by the distance between them. This does result in a slight overestimation of the prism as it does not account for bathymetric variations between each line. However, it is useful to compare the patterns of change within the estuary, and since the width of the river remains relatively constant, it is a more effective approach than using the standard trapezoid model. The June 1976 survey was excluded since no data were available upstream of the Kennetcook River.

Wetted perimeter (pw) is the distance along a cross sectional profile that is below the water level. Channel width was calculated as the horizontal distance between the channel banks where the tide intersects the cross sectional profile. Both mean and minimum elevations were derived directly from the survey data and are presented relative to the CGVD28 datum. These values will not vary between tide levels. Maximum water depth (D) was calculated as the tide level minus the minimum surveyed elevation. Mean depth was calculated as the tide level minus the mean elevation.

3.2.6   Assumptions and Limitations of the Analysis

The accuracy of any analysis is inherently dependent on the quality of the input data being used in the analysis. Although there are likely some differences in the quality of the historical data, for this study the level of accuracy will be assumed to be equal, and the precision of the resultant findings is limited more by the sampling frequency and spatial distribution of the points. The results, particularly the prism calculations, should be interpreted as relative findings rather than absolute values. The prism calculations will be dependent on the tide level used, and therefore may vary between different studies. In additon, we assume a horizontal water surface and minimal freshwater input during the tidal cycle. The largest uncertainly in the study results from having to assume the amount of marsh area above the causeway in 1858 and not having accurate elevation values for the marsh surfaces prior to 2005. In addition, the tide limits (e.g.HHWLT) in 1858 were not adjusted to account for sea level rise.

3.3   Analysis of Intertidal Ecosystems

3.3.1   Aerial photo mosaics & Satellite Imagery

Digital aerial photo mosaics were created in a previous study (van Proosdij and Horne, 2006) at MP_SpARC at Saint Mary's University. Relevant flight lines were identified and individual aerial photographs were examined and assessed for suitability for intertidal analysis (i.e. salt marsh and marsh / mudflat boundary were visible). Air photos were scanned to provide a 1-m ground resolution. The images were then georeferenced and rectified in ArcMap 9.1 using 1:10,000 digital topographic map sheets and referenced to UTM Zone 20N NAD 83 CSRS 98. Mosaics were generated using a custom Arc Macro Language tool. The macrotidal conditions of the upper Bay of Fundy combined with timing of the flights present considerable challenges to the seamless creation of images. Flight lines are generally flown along a west-east transect within each county, essentially bisecting the Southern Bight. As a result, tidal conditions were not comparable over the entire mosaic. Furthermore, since flights are flown on a county basis, this can result in the western shore of the Avon River being flown as much as 4 years before or after the eastern shore. For example, Hants County was flown in 1973, 1981, 1992, and 2003/2004 while the adjacent Kings County was flown in 1977, 1987, 1992, and 2002 (van Proosdij and Horne, 2006). At times, a county may also be divided even further (e.g. Hants 2003/2004). Additional details of the mosaic process are presented in van Proosdij and Horne, 2006. Since the interpretation of intertidal features will be influenced by the level of the

tide, Appendix A contains a chart in which the geodetic tide elevation was determined using the flight time and CHS tidal predictions for that date using *Tides and Currents* software.

Available satellite archive images were procured by MP_SpARC and used to help suplement the interpretation of changes in the system over the last ten years.   Table 3.5 summarizes the images and scale used for the analysis.   The IKONOS imagery (both panchromatic and multispectral) was orthorectified using a 1:10,000 NS digitial topographic data and DEM for the area using Ortho Engine in PCI Geomatica. ASTER imagery was not orthorectified at this time however comparison with the 1:10,000 planimetric layer illustrates that the processed image does line up (e.g. roads and dykes) quite well with the polyline data. These images were used primarily to examine the changes in the position of the main tidal thalweg and change in intertidal bar features, not for quantification purposes at this time.

Satellite	Date	Resolution	Type	Time (ADT)	Tide (m CGVD28)
Landsat 7	Sept 13, 1999	28.5 m	multispectral		
ASTER	Sept 22, 2000	15 m	multispectral	12:39	-2.29
IKONOS	March 20, 2002	4 m	Multispectral	13:34	-2.11
IKONOS	March 20, 2002	0.82 m	Panchromatic	13:34	-2.11
ASTER	Sept 30, 2002	15 m	multispectral	12:13	-1.80
ASTER	May 19, 2003	15 m	multispectral	12:19	-2.51
ASTER	July 12, 2005	15 m	multispectral	12:18	-4.76
IKONOS	Sept 19,2007	4 m	multispectral	12:20	-3.73
IKONOS	Sept 19,2007	0.82 m	panchromatic	12:20	-3.73

Table 3.5 : Details of satellite images used within this project.

3.3.2   Salt Marsh Habitat Quantification

The amount of salt marsh habitat was determined for each air photo mosaic based on the area of digitized polygons within ArcGIS 9.1. Since the boundaries between high and low marsh vegetation types were very difficult to determine from the aerial photographs without any field ground truthing, salt marsh habitat polygons incorporated both high and low marsh zones as defined by the mudflat or upland boundary.   For some areas, particularly in the early mosaics, marsh area was very difficult to distinguish from adjacent mudflat.   Surveyed dyke lines were used to help define the upland boundaries, as were GIS polygons of 'incorporated' marshes supplied by the NSDA. Old marsh surveys from the MMRA and NSDA were used in other areas as well as consultation with Ken Carroll (NSDA).   This study incorporates salt marsh areas both upstream and downstream of the Windsor

causeway. The extent of the 1858 salt marsh upstream was estimated based on the elevational contours and it is likely an overestimation since it does not account for any dykes that may have been present in 1858. Since the spatial area covered by each air photo mosaic is different due to limitations with flight lines and low tide conditions, normalization procedures were required to facilitate comparison between years (refer to van Proosdij and Horne, 2006 for detailed extents of air photographs). Marsh area was normalized by the area of the mosaic occupying the zone below the 10 m topographic land contour. Upland boundaries were not as critical for this study. The main objective of incorporating marsh areas in the analysis of changes in intertidal geomorphology was to identify zones of accretion and erosion. Salt marsh habitats common to all of the mosaics were also extracted for direct comparison. Additionally, in order to assess the effects of dyking, changes in marsh habitat were categorized into those resulting directly from the construction of a dyke, and those attributed to 'natural' or potential human impacts seaward of the new dyke. The position of the modern dykes were taken from the NSDA GIS database, and location of the older dykes determined from the aerial photographs.

3.3.3 Intertidal Features

Changes in the position of the main tidal channel thalweg and intertidal bars were examined by digitizing their boundaries from the aerial photo mosaics and satellite imagery. Bar features were classed as either primary or secondary based on degree of emergence relative to the tide. For example, a feature that would be exposed at low neap tides would be classified as primary (e.g. Windsor mudflat) and those exposed only on low spring tides are classified as secondary. Channel thalwegs were also interpreted as either being a dominant channel or only operational during higher tides. This was determined by the presence or absence of water in the channel at low tide. Intertidal bedforms were interpreted primarily from the high resolution IKONOS panchromatic images and field observations.

3.3.4 Assumptions and Limitations

There are a number of assumptions and limitations in the spatial and temporal analysis of salt marsh and intertidal features using either aerial photography or satellite imagery. The results are limited to the dates during which appropriate imagery can be located and to the level of the tide. For example, little is known regarding the amount of salt marsh in the 1980s in this region since any aerial photography flown was at high tide and satellite images are not available. Therefore, only images where the entire marsh surface and initial mudflat are visible were used during this analysis and tide

levels were calculated for each image. Intertidal features such as sand and mudflats were only interpreted if the images were at low tide and the majority of the channels were clearly defined. In addition, one must assume that the change in marsh habitat is linear between years. For example, if the sequence is determined to be progradational then we assume that there is not an intermediate period of erosion in the intervening years. Some error will be introduced during the rectification and digitizing process and other studies have shown that the level of accuracy of interpreting historical images is around ±10 m.

4.0   RESULTS

4.1   Cross Sectional Profiles

Figures 4.1, 4.3 and 4.4 present the cross sectional profiles and associated hydraulic geometry graphs for lines on the St. Croix, Avon, and Kennetcook Rivers respectively. Due to the wide range of channel widths and depths from the causeway to the mouth of the Avon River, vertical and horizontal scales on the graphs vary. Data are presented for both large and mean tides in order to compare changes which occur primarily within the tidal river channel (e.g. below HHWMT) with changes of the whole intertidal profile including the marsh surface (e.g. between HHWMT and HHWLT). Data for the 1858 and 1976 Amos surveys are presented as the original point values, not the interpolated curve to demonstrate fit with modern data. Refer to Figures 3.2 and 3.3 for location of the survey lines. Three standard measures of channel form are also presented: the width to mean depth ratio (w/d), the width to max depth ration (w/D), and max to mean depth ratio (D/d) (Myrick and Leopold, 1963) (Table 4.1). In general, as the w/d ratio increases, the form of the river is becoming wider and shallower. If the opposite occurs, it is generally becoming deeper and narrower. A large D/d ratio generally indicates the presence of a deep channel relative to the surrounding bathymetry. As the D/d ratio becomes closer to 1, the channel exhibits a relatively flat form as seen in the mud and sand flat areas.

4.1.1. Description of Changes in the St. Croix River

The most noticeable changes in the cross sectional profiles within the St. Croix river occur on Lines 1 (Fig 4.2a) and 2 (Fig 4.2b) as erosion of the north river bank and associated salt marsh habitat by as much as 62 m occurred between May 1971 and December 2005.   This represents approximately 411 m^2 in marsh loss (vertical plane). In Line 1, there is evidence of extensive growth of a mudflat deposit along the southern shore (Fig 4.2a) which becomes vegetated most likely by *Spartina alterniflora* between 1973 and 1992 (Fig 4.2e). This extends the southern shore by approximately 20 m since 1971 and represents an accumulation of sediment 8.7 m deep since November 1969. However, in 1858 there was no salt marsh evident along the north shore on Line 1 and the position of the shoreline was close to the modern dykeline. The cross sectional remained relatively constant over the study period. The width of the river appears to have been approximately 50 m wider and about 2 m shallower in 1858 than in 2005 and 2006 (Fig 4.2a to 4.2c). Although there has been approximately 50 m of marsh erosion along Line 2 on the North shore between the 1970s and 2005/2006, the 2005/2006 marsh extent is 175 m wider than in 1858 (Fig 4.2). There is a statistically significant increase in cross

sectional area since July 1969 (R^2 = 0.816, F=11.998, p=0.013). On Line 3, salt marsh has expanded approximately 175 m into the St. Croix since 1858 and subsequently reduced the width by 24%. However, the minimum bed elevation has increased as the channel has deepened (Fig 4.2c) allowing the cross sectional area to remain relatively constant.

Figure 4.1: New growth of Spartina alterniflora along north shore of St. Croix along lines 2 and 3 on new mudflat developing. Photo by D. van Proosdij in August 2006.

Closer to the Avon River, there is a general narrowing of the St. Croix River channel by approximately 75 m from 1858 to 1969 and an additional 108 m from the 1970s to 2005/2006 (Table 4.1b) as mud and marsh accumulates at either end of the Line 4.   Interestingly, the 1858 bed elevation data point falls almost exactly at the level of the 1970 cross section suggesting that there may have been little variation in depth. However, given the limited amount of data this cannot be stated with certainty. There has however, been a statistically significant decrease in cross sectional area over time (R^2=0.762, F=8.303, p=0.028).
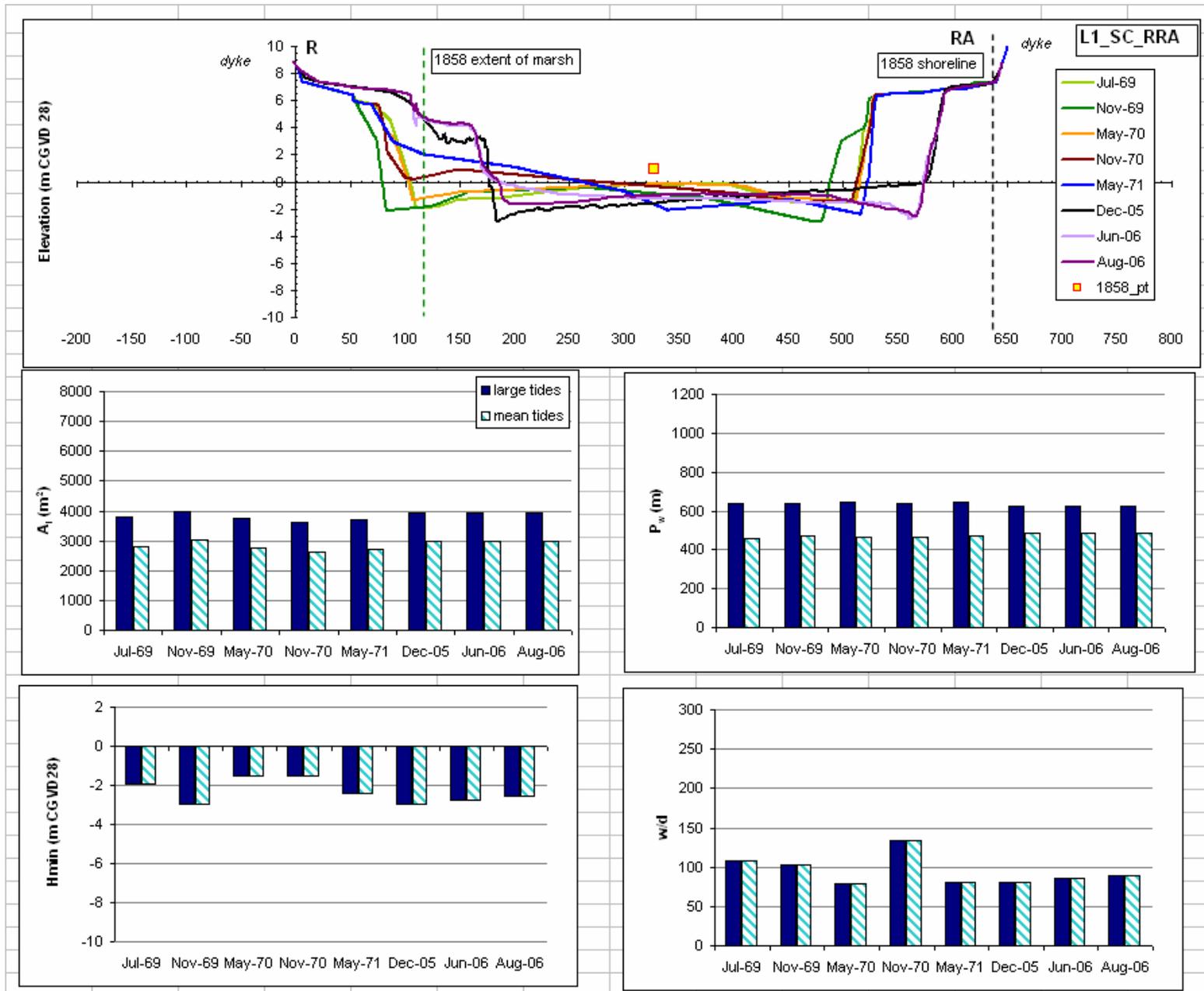
Figure 4.2a: Cross sectional profile for Line1_SC_RRA and associated hydraulic geometry parameters on the St. Croix River. Vertical exaggeration on cross sectional profiles = 50 X. Distance on cross sectional profile in metres. Refer to figure 4.1e for position of line.
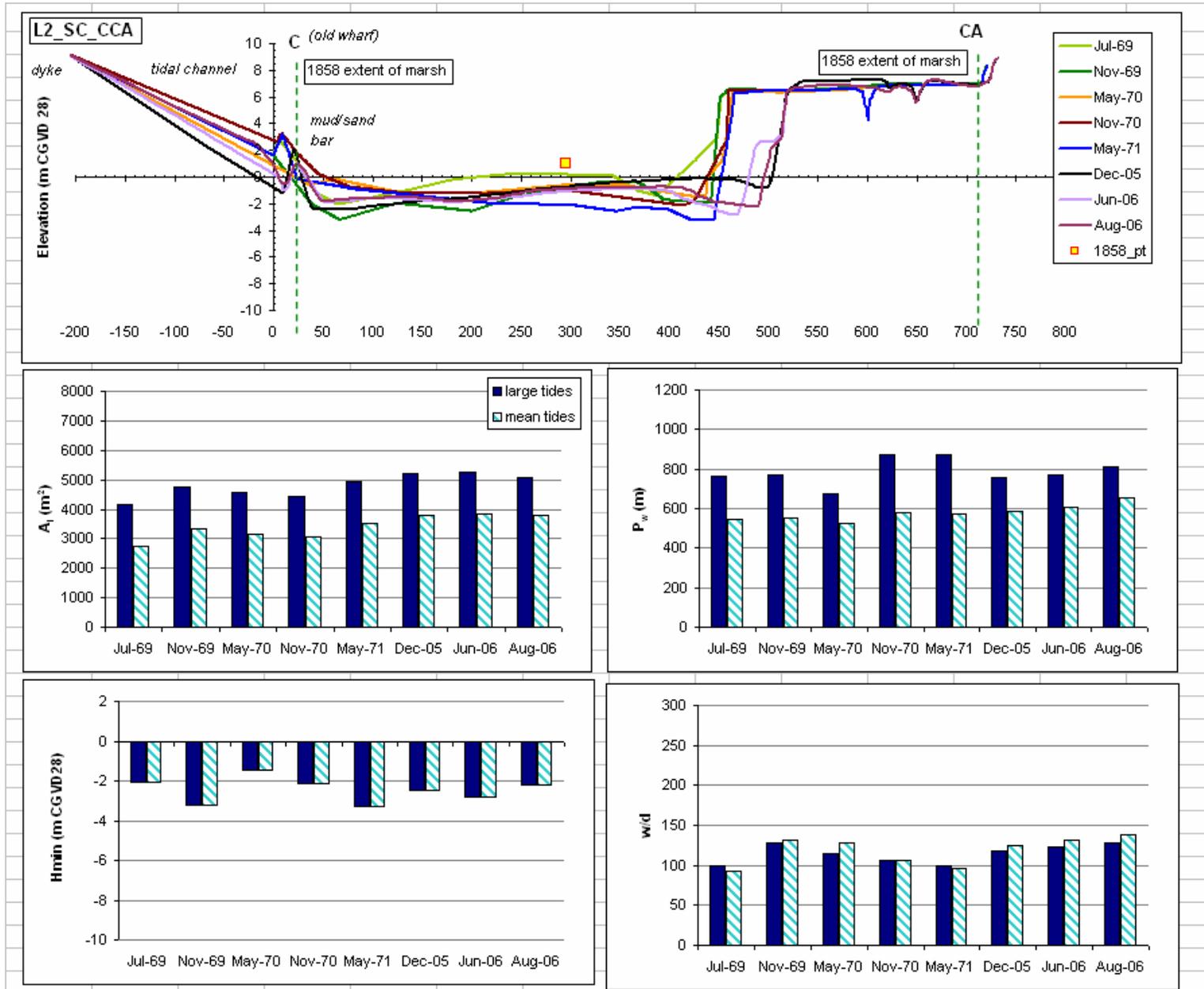
Figure 4.2b: Cross sectional profile for Line2_SC_C and associated hydraulic geometry parameters on the St. Croix River. Vertical exaggeration on cross sectional profiles = 50 X. Distance on cross sectional profile in metres. Prism and cross sectional area calculations are to be interpreted with some caution due to significant extrapolation on southern bank due to low elevation at the start of the survey and position of line within a tidal creek. Refer to Figure 4.1e for position of line.
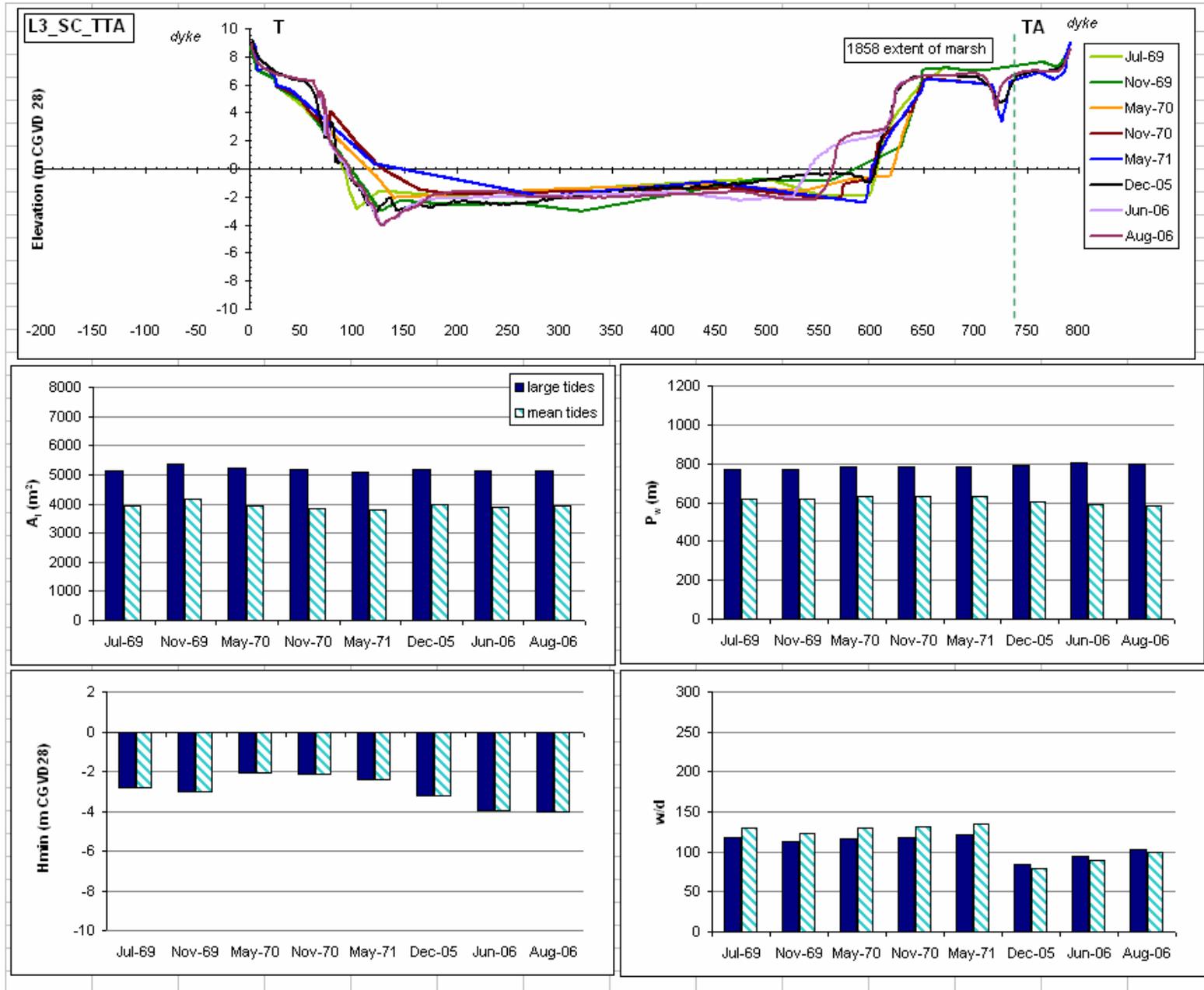
Figure 4.2c: Cross sectional profile for Line3_SC_TTA and associated hydraulic geometry parameters on the St. Croix River. Vertical exaggeration on cross sectional profiles = 50 X. Distance on cross sectional profile in metres. Refer to figure 4.1e for position of line.
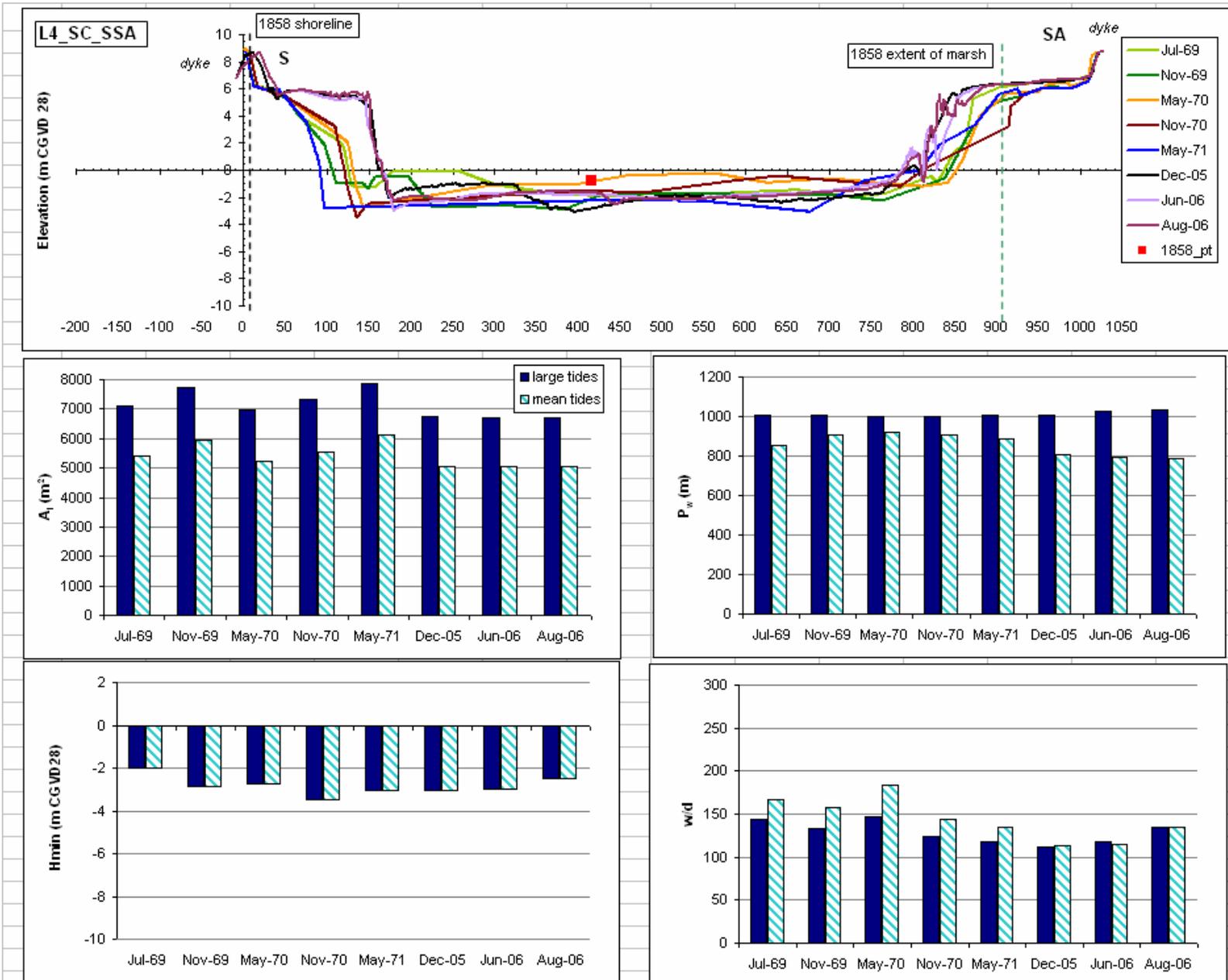
Figure 4.2d: Cross sectional profile for Line4_SC_SSA and associated hydraulic geometry parameters on the St. Croix River. Vertical exaggeration on cross sectional profiles = 50 X. Distance on cross sectional profile in metres. Refer to figure 4.1e for position of line.
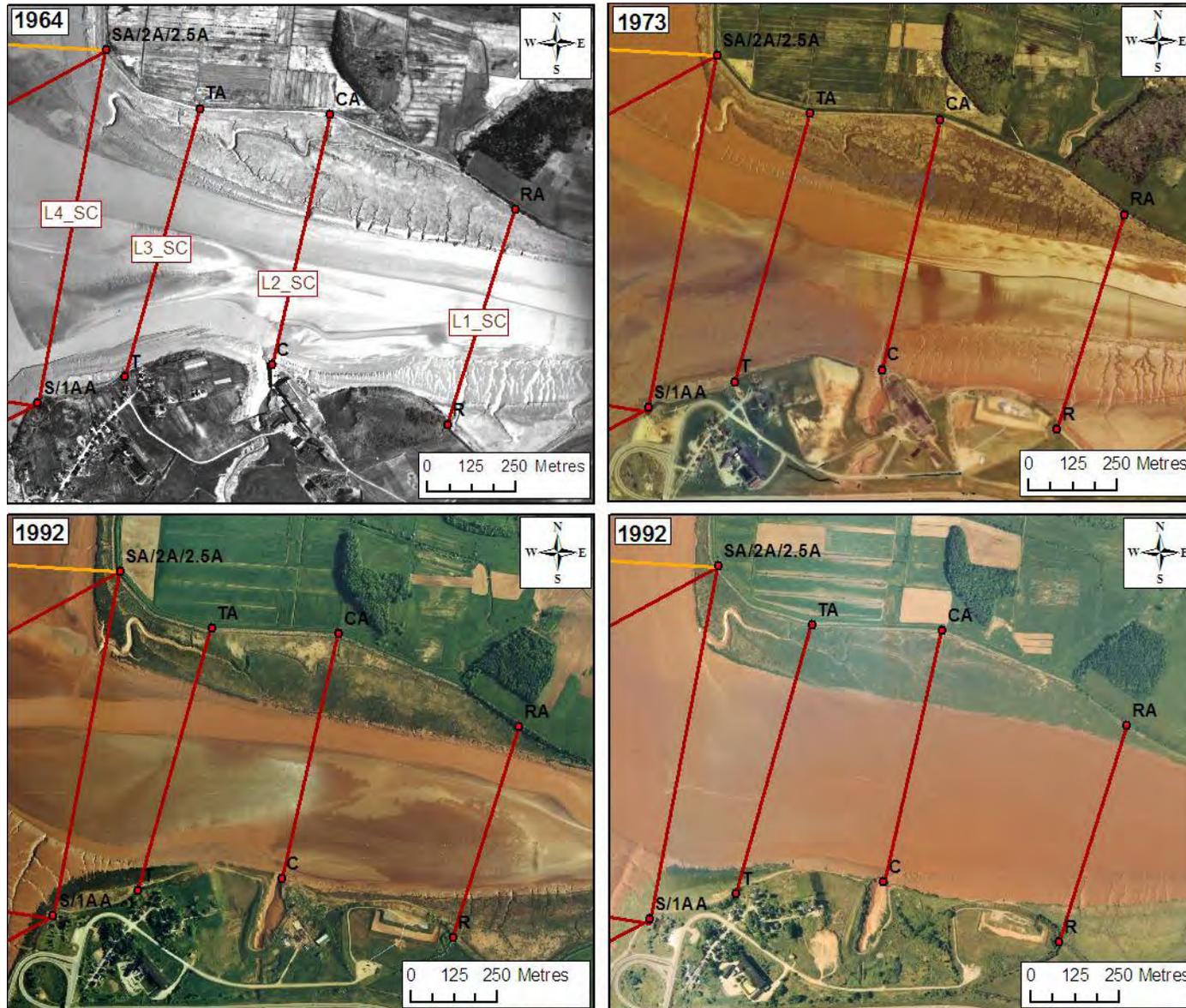
Figure 4.2e: Location of St. Croix cross sections lines 1-4. Note shift of main channel thalweg from south to north shore and associated marsh erosion from 1964 to 2003.

a) LARGE TIDES

Date	Line	Distance between	total dist	A_i	pw	H	Hmin	d	D	w	w/d	w/D	D/d
Jul-69	L1_SC_R	0	1190	3781	639	1.5	-2.0	6.0	9.5	635	105	67	1.6
	L2_SC_C	548	642	4178	767	1.9	-2.1	5.6	9.6	765	136	79	1.7
	L3_SC_T	386	256	5138	771	1.0	-2.8	6.6	10.4	769	117	74	1.6
	L4_SC_S	256	0	7110	1005	0.6	-2.0	6.9	9.6	1003	145	105	1.4
Nov-69	L1_SC_R	0	1190	4000	639	1.2	-3.0	6.4	10.6	635	100	60	1.7
	L2_SC_C	548	642	4772	768	0.3	-3.2	7.2	10.8	765	106	71	1.5
	L3_SC_T	386	256	5349	773	0.8	-3.0	6.8	10.6	771	113	73	1.6
	L4_SC_S	256	0	7719	1007	0.0	-2.9	7.5	10.5	1006	134	96	1.4
May-70	L1_SC_R	0	1190	3734	642	-0.1	-1.5	7.7	9.1	639	83	70	1.2
	L2_SC_C	548	642	4560	673	-0.2	-1.2	7.7	8.8	670	87	76	1.1
	L3_SC_T	386	256	5239	783	0.9	-2.1	6.7	9.6	780	117	81	1.4
	L4_SC_S	256	0	6977	1000	0.8	-2.7	6.8	10.3	999	147	97	1.5
Nov-70	L1_SC_R	0	1190	3606	641	2.3	-1.5	5.3	9.1	639	121	70	1.7
	L2_SC_C	548	642	4428	876	2.3	-1.3	5.3	8.8	768	145	87	1.7
	L3_SC_T	386	256	5163	784	1.0	-2.1	6.6	9.7	780	118	80	1.5
	L4_SC_S	256	0	7317	1003	-0.5	-3.5	8.1	11.0	1001	124	91	1.4
May-71	L1_SC_R	0	1190	3691	642	0.0	-2.4	7.5	10.0	639	85	64	1.3
	L2_SC_C	548	642	4938	873	1.5	-3.3	6.1	10.8	768	127	71	1.8
	L3_SC_T	386	256	5084	783	1.1	-2.4	6.5	10.0	780	121	78	1.5
	L4_SC_S	256	0	7887	1008	-1.0	-3.1	8.5	10.6	1001	117	94	1.2
Dec-05	L1_SC_R	0	1190	3955	627	-0.2	-3.0	7.7	10.5	620	80	59	1.4
	L2_SC_C	548	642	5216	759	0.7	-2.5	6.9	10.0	814	118	81	1.5
	L3_SC_T	386	256	5183	787	-1.5	-3.2	9.1	10.8	762	84	71	1.2
	L4_SC_S	256	0	6737	1005	-1.3	-3.1	8.9	10.6	995	112	94	1.2
Jun-06	L1_SC_R	0	1190	3918	624	0.1	-2.8	7.5	10.3	618	83	60	1.4
	L2_SC_C	548	642	5239	772	0.8	-2.8	6.7	10.4	822	122	79	1.5
	L3_SC_T	386	256	5115	807	-0.6	-4.0	8.2	11.6	778	95	67	1.4
	L4_SC_S	256	0	6715	1030	-0.9	-3.0	8.4	10.6	996	118	94	1.3
Aug-06	L1_SC_R	0	1190	3913	623	0.3	-2.5	7.2	10.1	618	86	61	1.4
	L2_SC_C	548	642	5079	813	0.9	-2.2	6.7	9.8	850	127	87	1.5
	L3_SC_T	386	256	5139	797	0.0	-4.0	7.5	11.6	778	103	67	1.5
	L4_SC_S	256	0	6691	1033	0.1	-2.5	7.4	10.0	996	134	99	1.4

b) MEAN TIDES

Date	Line	Distance between	total dist	A_i	pw	H	Hmin	d	D	w	w/d	w/D	D/d
Jul-69	L1_SC_R	0	1190	2811	459	1.5	-2.0	4.2	7.7	456	108	59	1.8
	L2_SC_C	548	642	2760	549	1.9	-2.1	3.8	7.8	547	142	70	2.0
	L3_SC_T	386	256	3953	617	1.0	-2.8	4.8	8.6	615	129	71	1.8
	L4_SC_S	256	0	5394	856	0.6	-2.0	5.1	7.8	854	166	110	1.5
Nov-69	L1_SC_R	0	1190	3029	471	1.2	-3.0	4.6	8.8	468	102	53	1.9
	L2_SC_C	548	642	3354	551	0.3	-3.2	5.4	9.0	548	101	61	1.7
	L3_SC_T	386	256	4166	619	0.8	-3.0	5.0	8.8	618	123	70	1.8
	L4_SC_S	256	0	5950	906	0.0	-2.9	5.7	8.7	906	158	105	1.5
May-70	L1_SC_R	0	1190	2759	464	-0.1	-1.5	5.9	7.3	461	79	63	1.2
	L2_SC_C	548	642	3134	522	-0.2	-1.2	5.9	7.0	519	87	74	1.2
	L3_SC_T	386	256	3932	633	0.9	-2.1	4.9	7.8	631	129	81	1.6
	L4_SC_S	256	0	5225	918	0.8	-2.7	5.0	8.5	916	183	108	1.7
Nov-70	L1_SC_R	0	1190	2631	464	2.3	-1.5	3.5	7.3	461	133	63	2.1
	L2_SC_C	548	642	3057	577	2.3	-1.3	3.5	7.0	574	163	82	2.0
	L3_SC_T	386	256	3856	634	1.0	-2.1	4.8	7.9	631	132	80	1.7
	L4_SC_S	256	0	5558	908	-0.5	-3.5	6.3	9.2	906	144	98	1.5
May-71	L1_SC_R	0	1190	2714	469	0.0	-2.4	5.7	8.2	461	81	56	1.4
	L2_SC_C	548	642	3519	571	1.5	-3.3	4.3	9.0	574	134	64	2.1
	L3_SC_T	386	256	3782	633	1.1	-2.4	4.7	8.2	631	135	77	1.8
	L4_SC_S	256	0	6125	885	-1.0	-3.1	6.7	8.8	906	134	103	1.3
Dec-05	L1_SC_R	0	1190	2995	486	-0.2	-3.0	5.9	8.7	479	80	55	1.5
	L2_SC_C	548	642	3799	589	0.7	-2.5	5.1	8.2	633	124	77	1.6
	L3_SC_T	386	256	3956	602	-1.5	-3.2	7.3	9.0	580	80	65	1.2
	L4_SC_S	256	0	5068	810	-1.3	-3.1	7.1	8.8	798	113	90	1.2
Jun-06	L1_SC_R	0	1190	2965	489	0.1	-2.8	5.7	8.5	485	85	57	1.5
	L2_SC_C	548	642	3844	607	0.8	-2.8	4.9	8.6	644	131	75	1.7
	L3_SC_T	386	256	3899	593	-0.6	-4.0	6.4	9.8	568	89	58	1.5
	L4_SC_S	256	0	5057	792	-0.9	-3.0	6.6	8.8	762	115	87	1.3
Aug-06	L1_SC_R	0	1190	2961	487	0.3	-2.5	5.4	8.3	484	89	58	1.5
	L2_SC_C	548	642	3772	654	0.9	-2.2	4.9	8.0	676	139	84	1.6
	L3_SC_T	386	256	3923	580	0.0	-4.0	5.7	9.8	568	99	58	1.7
	L4_SC_S	256	0	5029	786	0	-2	6	10	760	135	76	1.8

Table 4.1: Summary of hydraulic geometry parameters and measures of channel form for lines on the St. Croix River from July 1969 to August 2006 where available for a) large tides and b) mean tides. Total distance = distance from confluence of Avon and St. Croix Rivers. Refer to Table 3.4 for additional abbreviations.

Seasonal cyclicity is evident within most lines on the St. Croix River. On Line 1, the southern bank had retreated approximately 20 m between July and November 1969 but in May 1970 had expanded back to the July 1969 level (Fig 4.2a). This phenomenon is also observed along the south shore on Line 4: bank erosion of 14 m from July 1969 to November 1969, expansion by 24.2 m and by May 1971 the extent of the bank was at the same distance from the post as it was in July 1969. A marked period of erosion (29 m) was recorded between November 1970 and May 1971 (Fig.4.2d), yet by 1992 mudflat and marsh deposits are visible on the aerial photographs (Fig 4.2e) and by 2005 the south bank along Line 4 had extended by 74 m (Fig 4.2d), back to the edge of the 1858 salt marsh. On Line 2 the same phenomena was observed in the bed elevation, with a decrease in elevation (at point 200 m Fig 4.2b) of 2.45 m July 1969 to November 1969 followed by an increase of 1.02 m by May 1970. The sequence of changes in bed elevations along Line 4 in the central portion of the channel (point 500 m Fig 4.2d) show the disappearance and potential shift of an intertidal bar present in May 1970 and a return to 1969 bed elevation levels in December 2005. Triggers between an erosion or accretion phase on either channel bank appears to coincide with a shift in the thalweg of the main channel. This shift has now facilitated the deposition and creation of a new mudflat in 2006 along the north shore near lines 2 and 3 which in August 2006 had colonies of Spartina *alterniflora* becoming established (Figure 4.1). However, despite erosion of marsh along the shoreline at a number of locations, overall there is generally more salt marsh seaward of the dykes than in 1858. This has resulted in an overall narrowing of the main river channel.

a) Large Tides	**% Change in Cross Sectional Area between Surveys**						
	1969 to 1970	**1970 to 1971**	**1971 to 2005**	**2005 to 2006**	**1969 to 2005**	**1969 to 2006**	**1971 to 2006**
L1_SC_RRA	-5.7	0.6	7.1	-1.0	0.6 (±4.0)	0.6 (±4.0)	6.1
L2_SC_CCA	0.4	9.9	5.6	-1.1	15.3 (±11.0)	15.3 (±10.7)	4.5
L3_SC_TTA	-0.8	-2.2	1.9	-1.1	-2.2 (±2.8)	-2.2 (±2.8)	0.8
L4_SC_SSA	-3.6	10.4	-14.6	-0.5	-9.6 (±5.3)	-9.6 (±5.2)	-15.0
b) Mean Tides	**% Change in Cross Sectional Area between Surveys**						
	1969 to 1970	**1969 to 1976**	**1976 to 2005**	**2005 to 2006**	**1969 to 2005**	**1969 to 2006**	**1971 to 2006**
L1_SC_RRA	-7.7	0.7	10.4	-1.1	2.6 (±5.4)	1.5 (±5.4)	9.2
L2_SC_CCA	1.2	13.7	8.0	0.2	24.3 (±17.2)	24.6 (±17.1)	8.2
L3_SC_TTA	-4.1	-2.9	4.6	-1.1	-2.6 (±3.6)	-3.6 (±3.6)	3.4
L4_SC_SSA	-5.0	13.6	-17.3	-0.5	-10.6 (±6.2)	-11.1 (±6.2)	-17.7

Table 4.2: Percent change in cross sectional area between years along the St. Croix River. Negative values indicate a decrease in area whereas positive values indicate an increase in cross sectional area. Values in brackets represents the seasonal variability in the data where applicable. Data are presented for a) Large Tides and b) Mean Tides.

Despite the relatively large shifts in channel bank position, the cross sectional area and wetted perimeter, Lines 1 & 3 remain quite constant between the time periods (Figs 4.2a & d; Table 4.1). This indicates that although the form of the river channel is changing, primarily due to a shift in the main channel thalweg from the south to the north shore of the river (Fig 4.2e), the hydraulic capacity of the system has not changed. Seasonal fluctuations in cross sectional area by as much as 600 m^2 are clearly evident on Line 4, the closest line to the confluence of the Avon and St. Croix rivers (Fig 4.2d; Table 2).   It should be noted that the changes recorded for Line 2 should be interpreted with caution due to the position of the line (Fig 4.2e) and extrapolation for the area calculations on the south shore. In addition, this is also the outlet for a large aboiteaux which could temporarily but significantly deepen the channel after a heavy rainfall due to subsequent freshwater discharge. In general, the data suggest that there is considerable seasonal and inter annual variability, however, when one examines the net changes in cross sectional area from July 1969 to 2006, Lines 1 and 3 show between 6.1 and 0.8% increase in cross sectional area and Line 4 exhibits a 15 % decrease in area for large tides (Table 4.2).

4.1.2. Description of Changes in the Avon River

Although minimal data are available for upstream of the Windsor causeway, between July 1969 and October 1970 after the causeway had been completed, there was minimal decrease in cross sectional area and the width remained relatively constant despite a shift in the position of the channel at US2. The w/d ratio (Table 4.3; Fig 4.3a,b) however decreases, suggesting a general flattening of the channel.

Overall, the most notable changes in cross sectional form since 1969 have occurred in lines closest to the causeway (Fig. 4.3g; Table 4.3 to 4.5).   Both lines 1A (Fig 4.3d) and 1 (Fig4.3e) saw a general decrease in mean bed elevation of around 1 m between July 1969 and November 1969, particularly in the western channel in Line 1 (Table 4.3). An intertidal bar is also evident near the center of the river channel. It is unknown if the 1858 data points represent that feature in 1858 or if they represent the bed elevation. The chart does indicate that the marsh along the western shore was about 150 m from the 1969 shoreline on Line 1 and 200 m on Line 1A, sloping towards the other shore (Figs 4.3d,e). In addition, the elevation of the bottom of the channel in 1969 appears to be very close to the 1858 level. However, between 1969 and December 2005, a sediment layer approximately 6.5 m (Fig 4.3e) deep has accumulated in the central section (point 600 m on profile) in the vicinity of an intertidal bar that was present in 1963 (Fig 4.3g). Additionally, the thalweg of the tidal creek which runs parallel to the causeway (Fig 4.3f) has filled in with approximately 3.8 m of sediment. This surface is now at the

limit of the HHWMT level. These changes resulted in a 75% and 92% decrease in cross sectional area for large and mean tides respectively (Table 4.5) along Line 1A by August 2006. Line 1 has also decreased in cross sectional area by at least half to three quarters (Table 4.5). A 24 % decrease in area from 2005 to 2006 alone was recorded at Line 1A. These decreases are statistically significant (Table 4.6). The wetted perimeter for large tides remained fairly constant along that line, however, its value decreased by half when calculated for mean tides due to the limited amount of channel area below the HHWMT line. This also resulted in a marked difference between w/d and also D/d ratios between the 1960s and the present day.

The intertidal cross sectional area at Line 5 (Fig 4.3f,g) decreased significantly by 22.5% since closure of the causeway with an additional 1.8% from December 2005 to the Summer of 2006 (Table 4.5, 4.6) for large tides. It picks up the major shift (219 m) in the location of the tide gate channel and the infilling of the new channel by around 2 m of sediment (Fig 4.3f). However, a total of 10 m of sediment has accumulated in the location of the old tide gate channel. Much of the decrease in area was due to the expansion and elongation of the Windsor mudflat/salt marsh system (Figure 4.3g). The present day bed elevation of the main Avon River channel along the eastern portion of the line (Fig 4.3f,g) has decreased down to the 1969 base level. As in the previous line, the wetted perimeter remains relatively constant between the study periods. The w/d and D/d ratios in the present day are quite similar to those recorded for May 1970 and July 1969.

Further downstream Lines 6 and 7 cross an intertidal bar feature which is now being referred to as the Newport Bar (Daborn and Brylinsky, 2004). Almost 6 m of sediment has accumulated at that location since 1858 (Figure 4.3h) along line 6. It has accumulated between 7.1 (in old channel) and 2.9 m of sediment since July 1969 (Fig 4.3i). However the western bank of the river saw approximately 150 m of erosion resulting in approximately 1500 m^3 loss of sediment. The position of the modern shoreline is in almost the same position as the shoreline in 1858. While the eastern shore exhibits minimal change in position there is a deepending of the tidal channel thalweg against that bank by 2006 (Fig 4.3i). Inter annual fluctuations in cross sectional area are observed (Table 4.3-4.5), yet there has been only a small change in cross sectional area from November 1970 to December 2005 despite large apparent changes in the profiles and air photographs (Fig 4.3k). There was a 10-14% decrease in cross sectional area between 1969 and December 2005 (Table 4.5), and there was a further 4 to 3% decrease from 2005 to 2006.
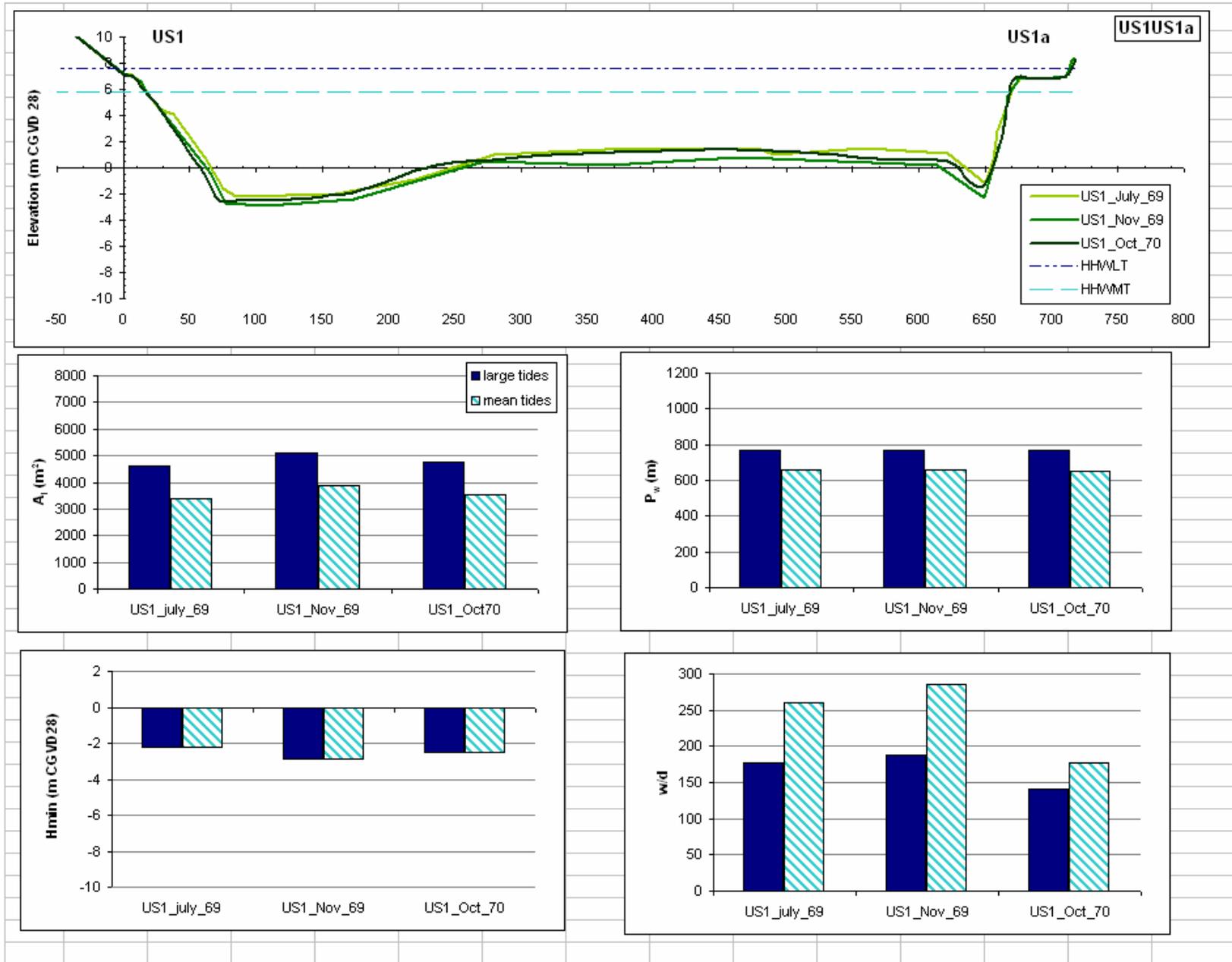
Figure 4.3a: Cross sectional profile for Line US1US1a and associated hydraulic geometry parameters upstream of the Windsor Causeway on the Avon River. Vertical exaggeration on cross sectional profiles = 42.5 X. Distance on cross sectional profile in metres.
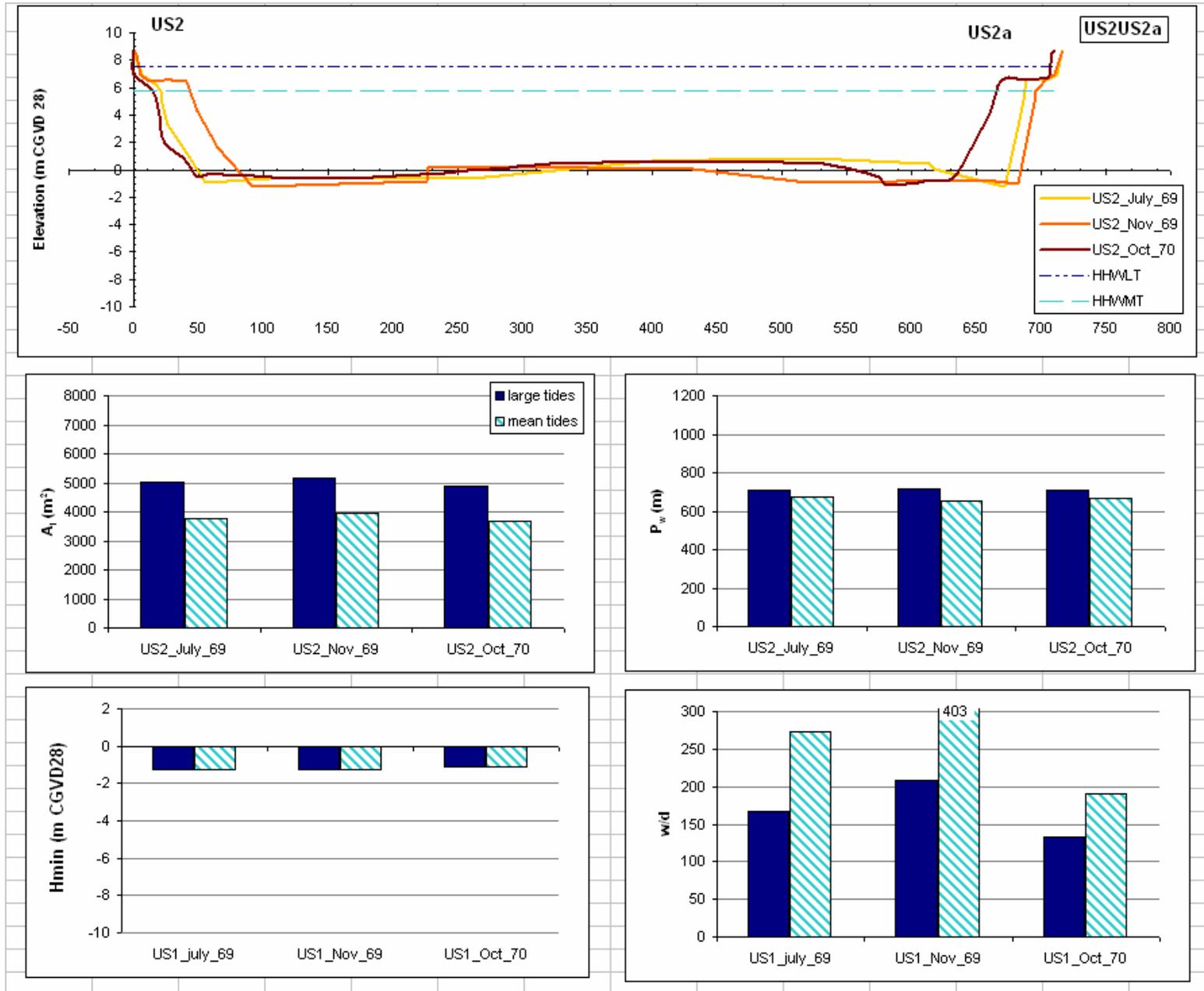
Figure 4.3b: Cross sectional profile for Line US2US2a and associated hydraulic geometry parameters upstream of the Windsor Causeway on the Avon River. Vertical exaggeration on cross sectional profiles = 42.5 X. Distance on cross sectional profile in metres.
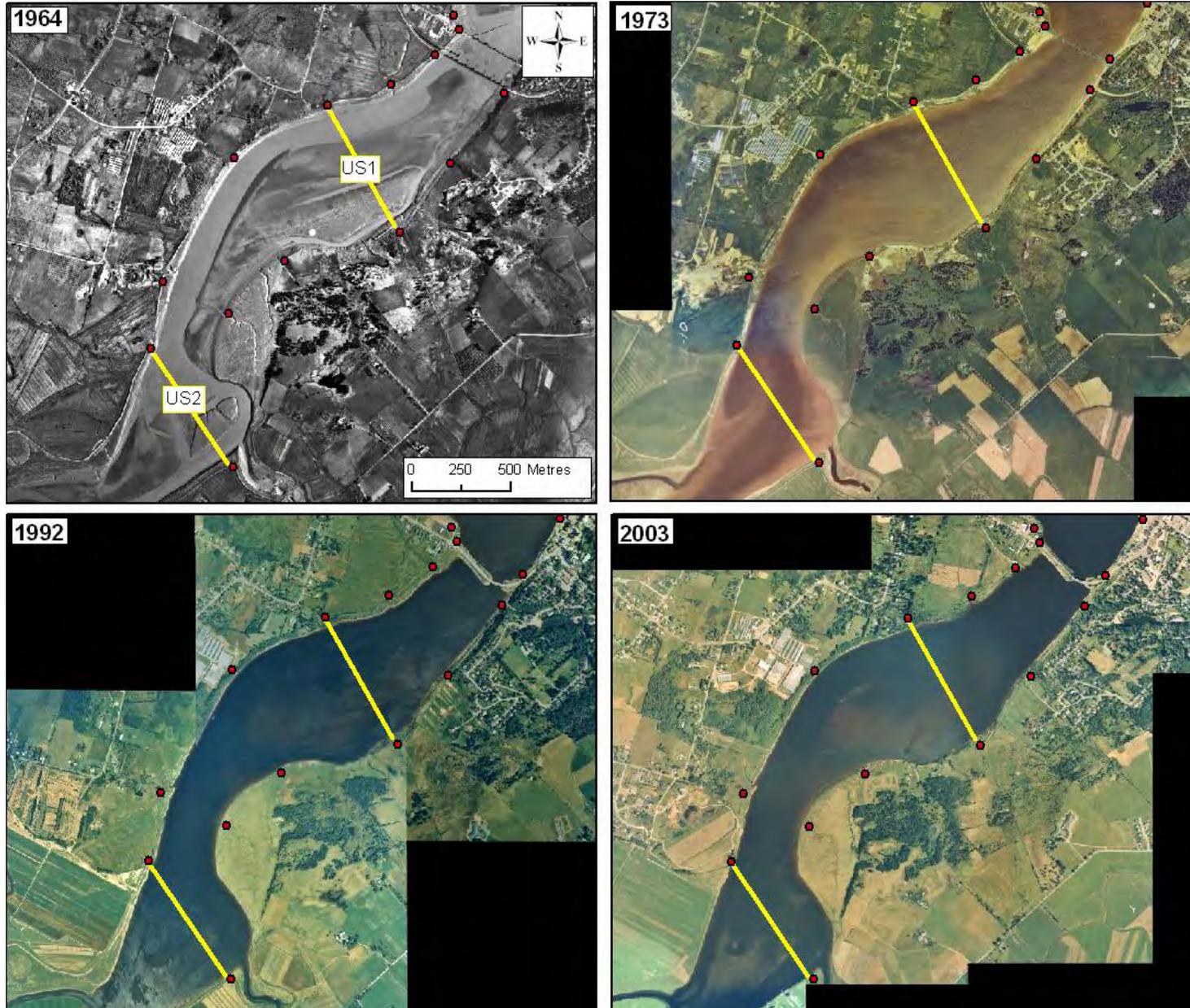
Figure 4.3c: Location of upstream cross section lines US1 and US2. Full tidal flow blocked in July 1970. Note growth of vegetation on original mudflat/low marsh.
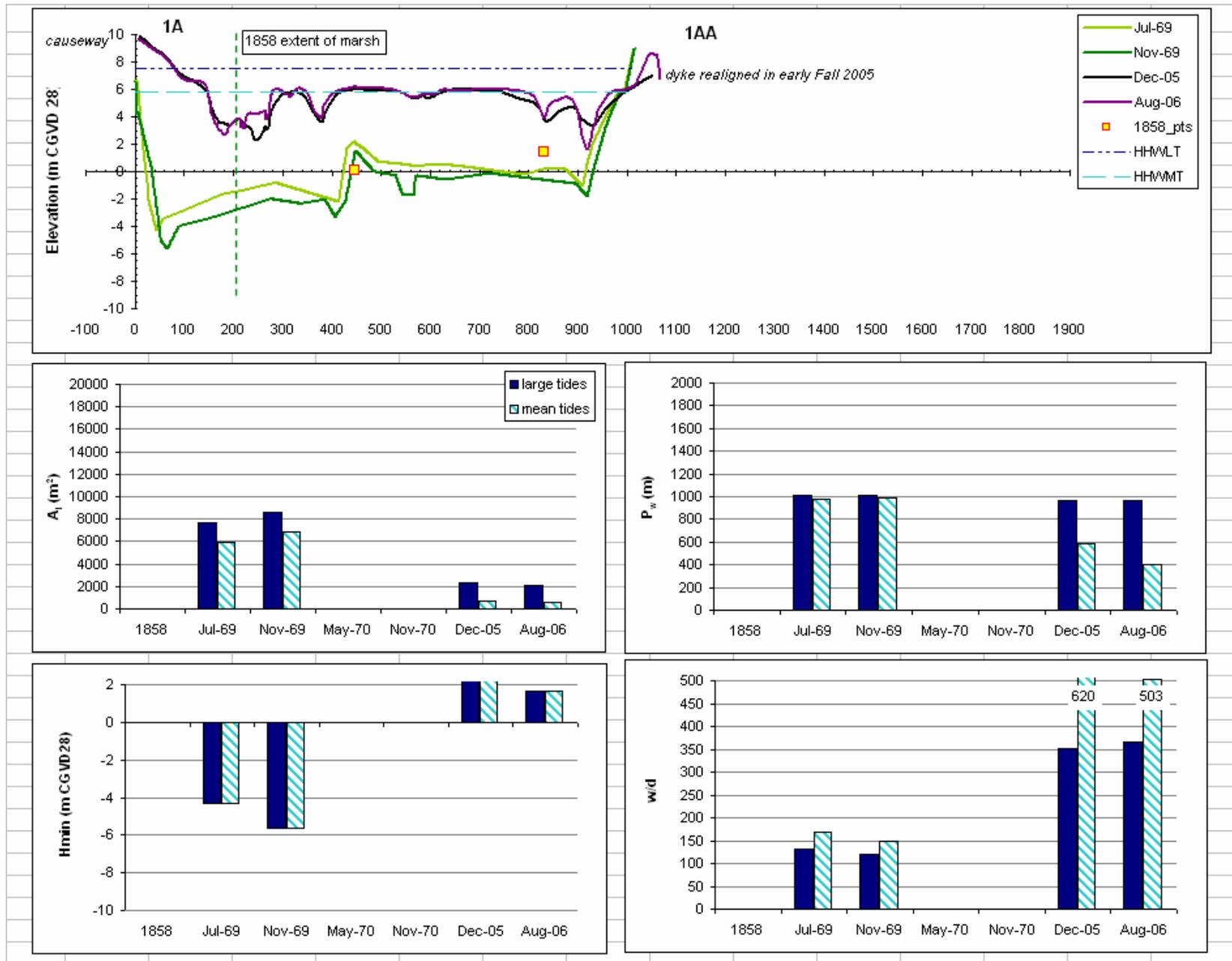
Figure 4.3d: Cross sectional profile for Line 1_DS_1A1AA and associated hydraulic geometry parameters on the Avon River. Note change in vertical exaggeration on cross sectional profiles to 100 X. Distance on cross sectional profile in metres.
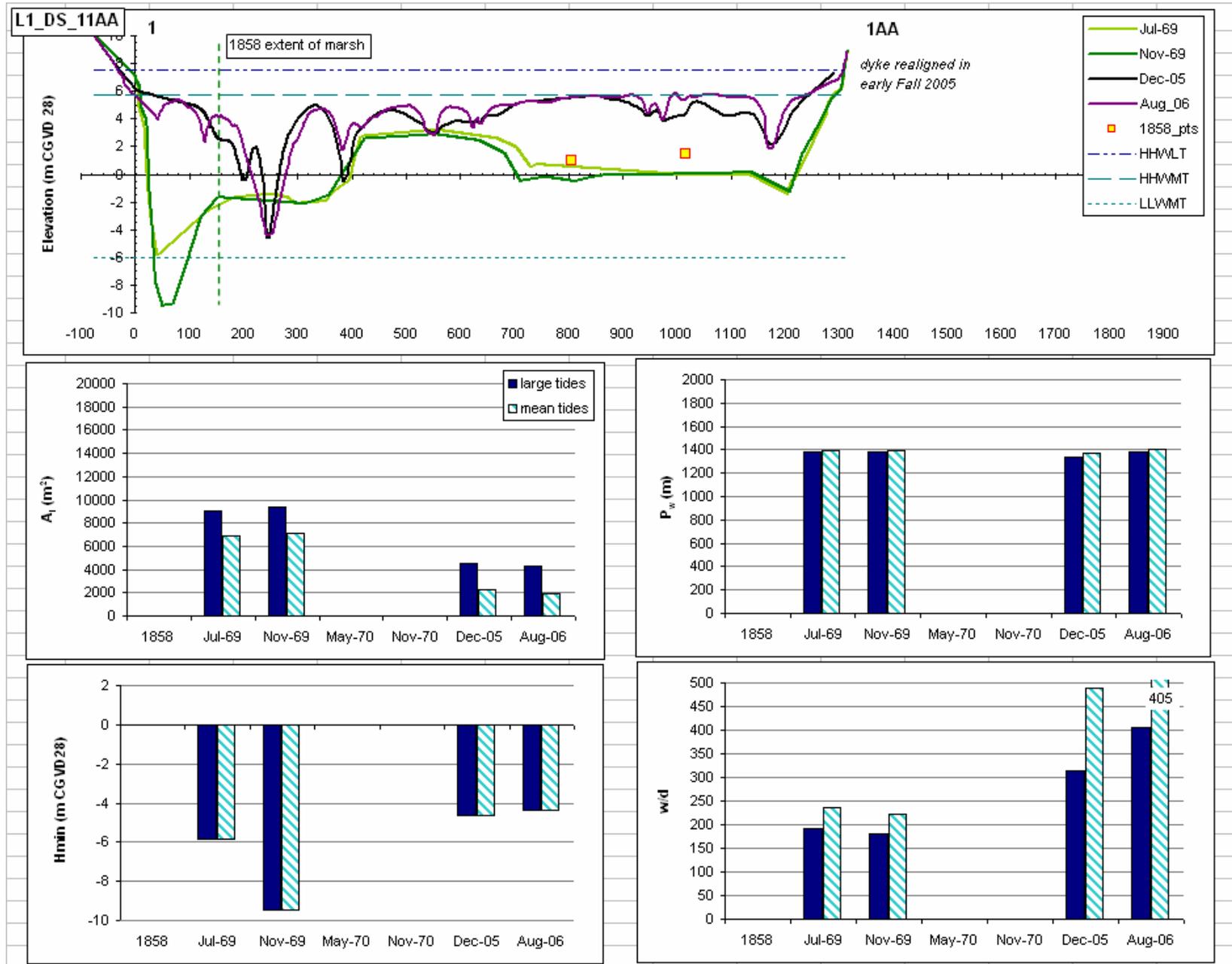
Figure 4.3e: Cross sectional profile for Line1_DS_11AA and associated hydraulic geometry parameters on the Avon River. Vertical exaggeration on cross sectional profiles = 100 X. Distance on cross sectional profile in metres.
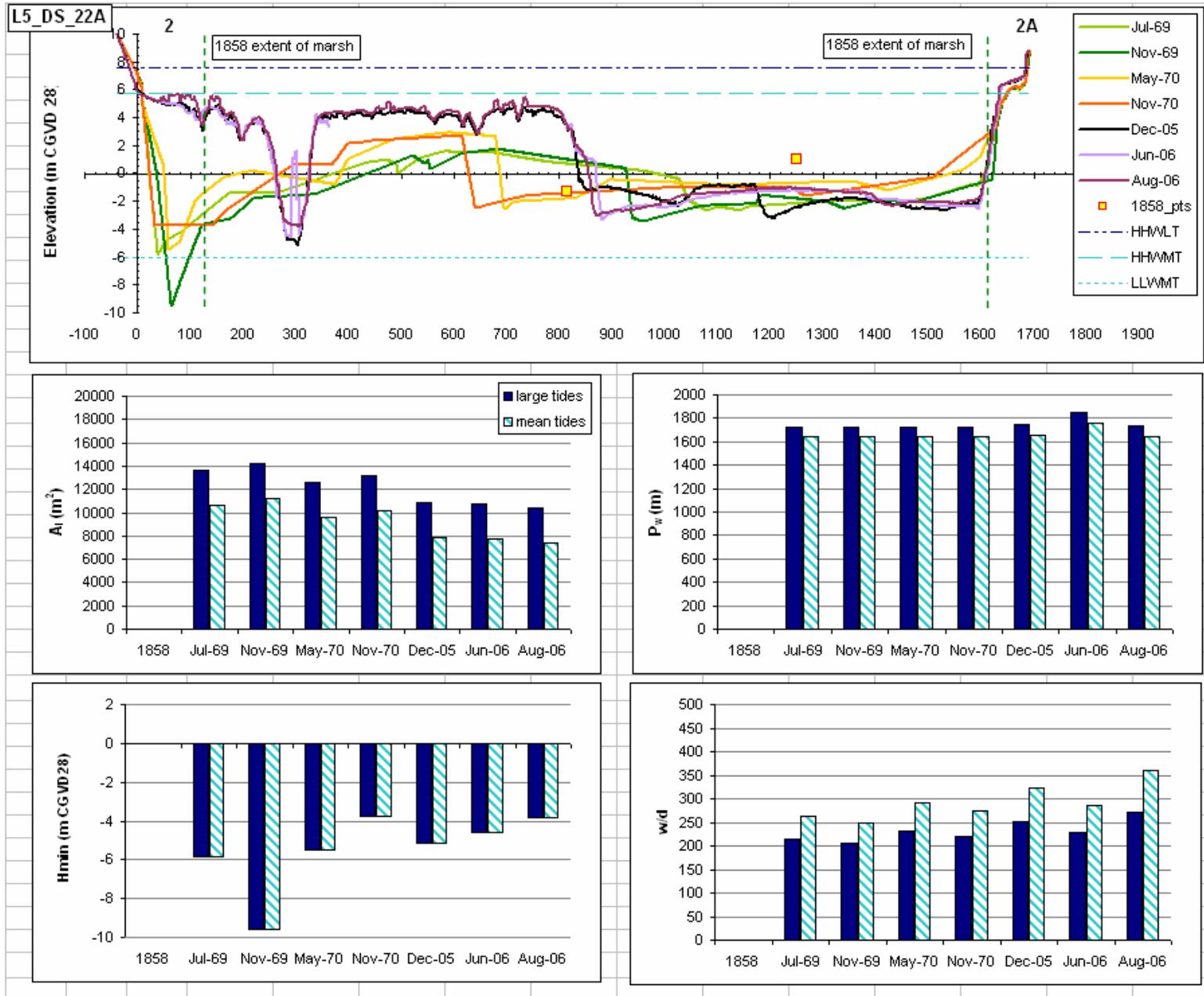
Figure 4.3f: Cross sectional profile for Line5_DS_22A and associated hydraulic geometry parameters on the Avon River. Vertical exaggeration on cross sectional profiles = 100 X. Distance on cross sectional profile in metres.
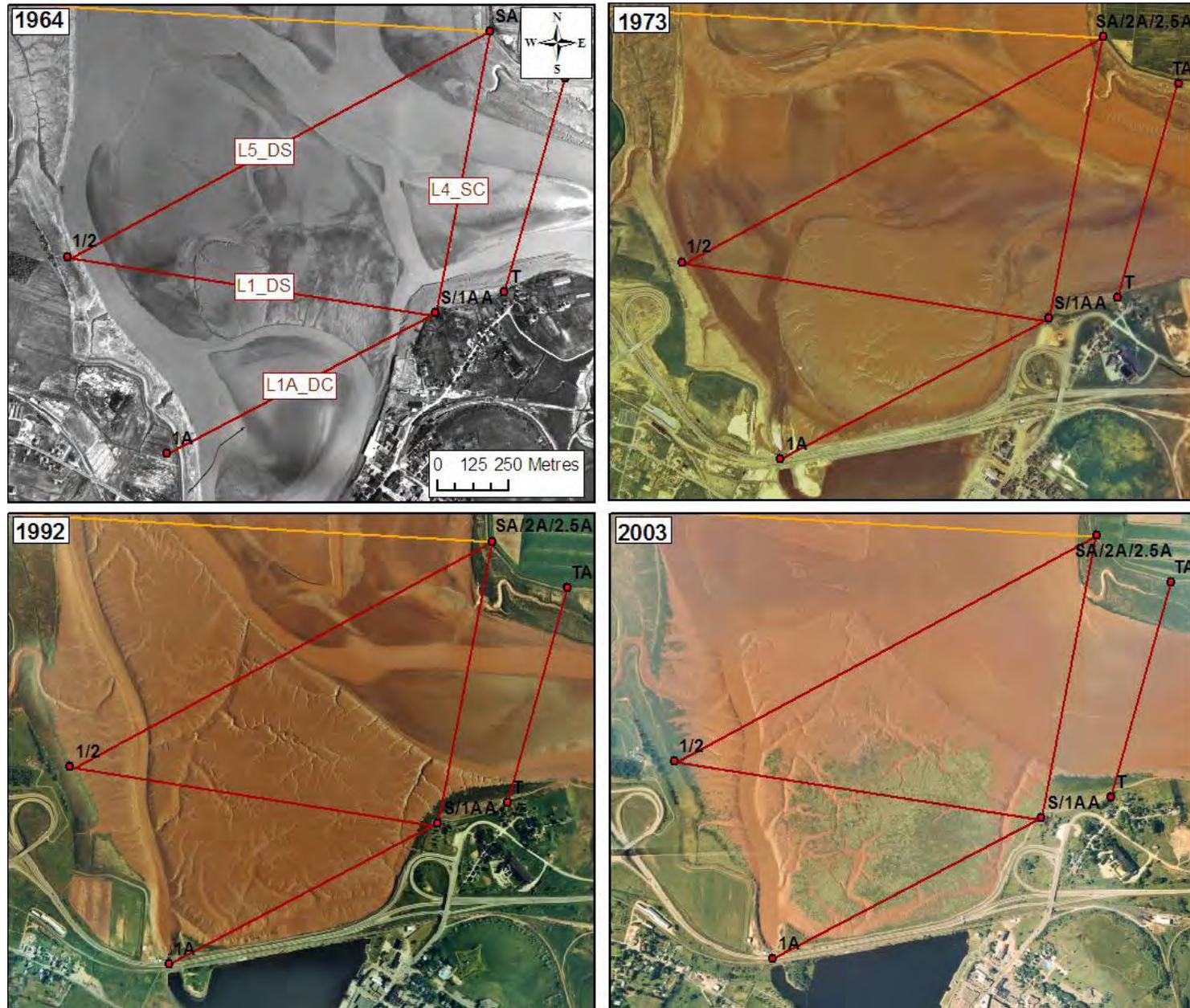
Figure 4.3g: Location of downstream survey lines 1A, 1 and 5. Note changes in channel thalwegs, bar location and marsh growth from 1964 to 2003.
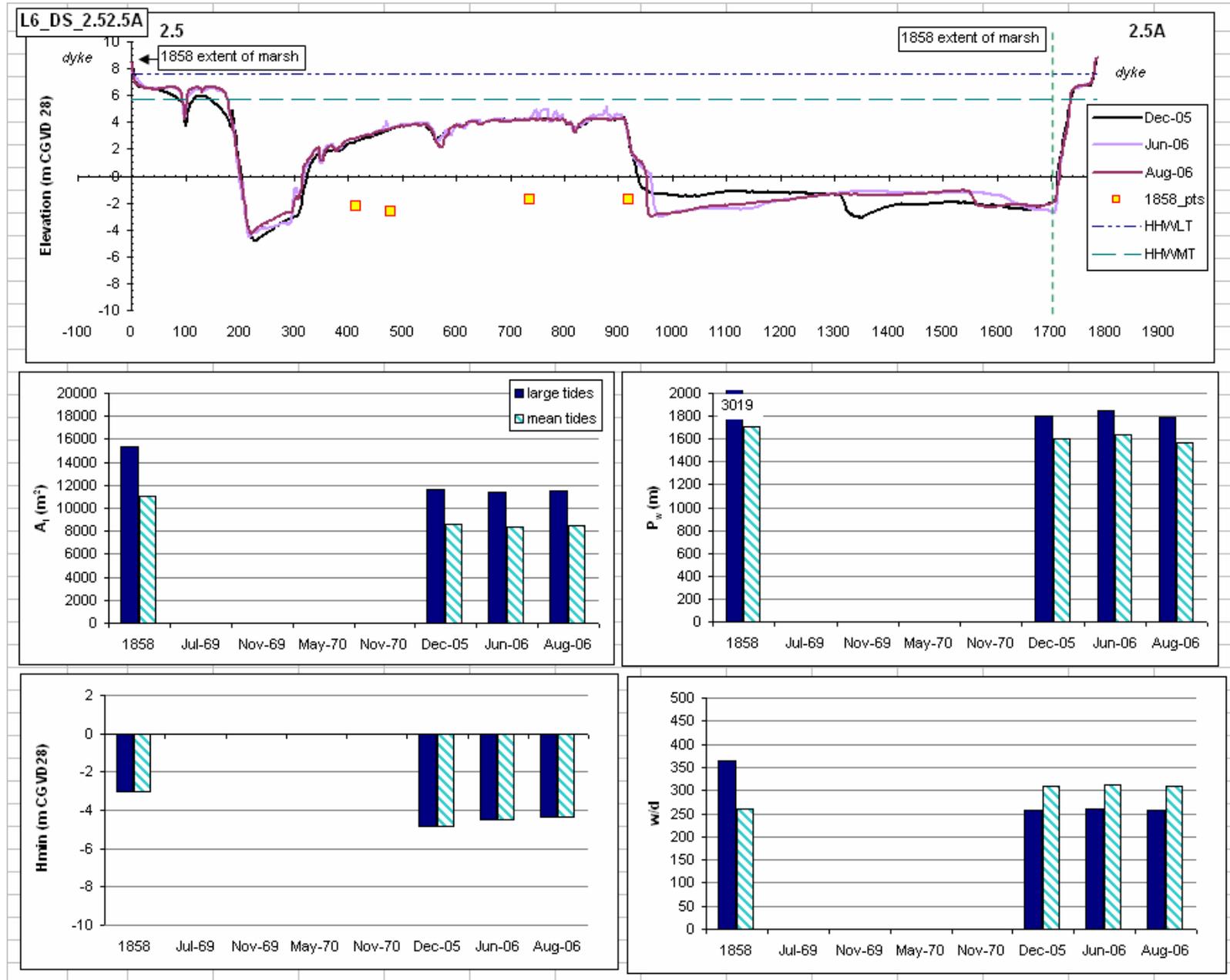
Figure 4.3h: Cross sectional profile for Line6_DS_2.52.5A and associated hydraulic geometry parameters on the Avon River. Vertical exaggeration on cross sectional profiles = 100 X. Distance on cross sectional profile in metres.
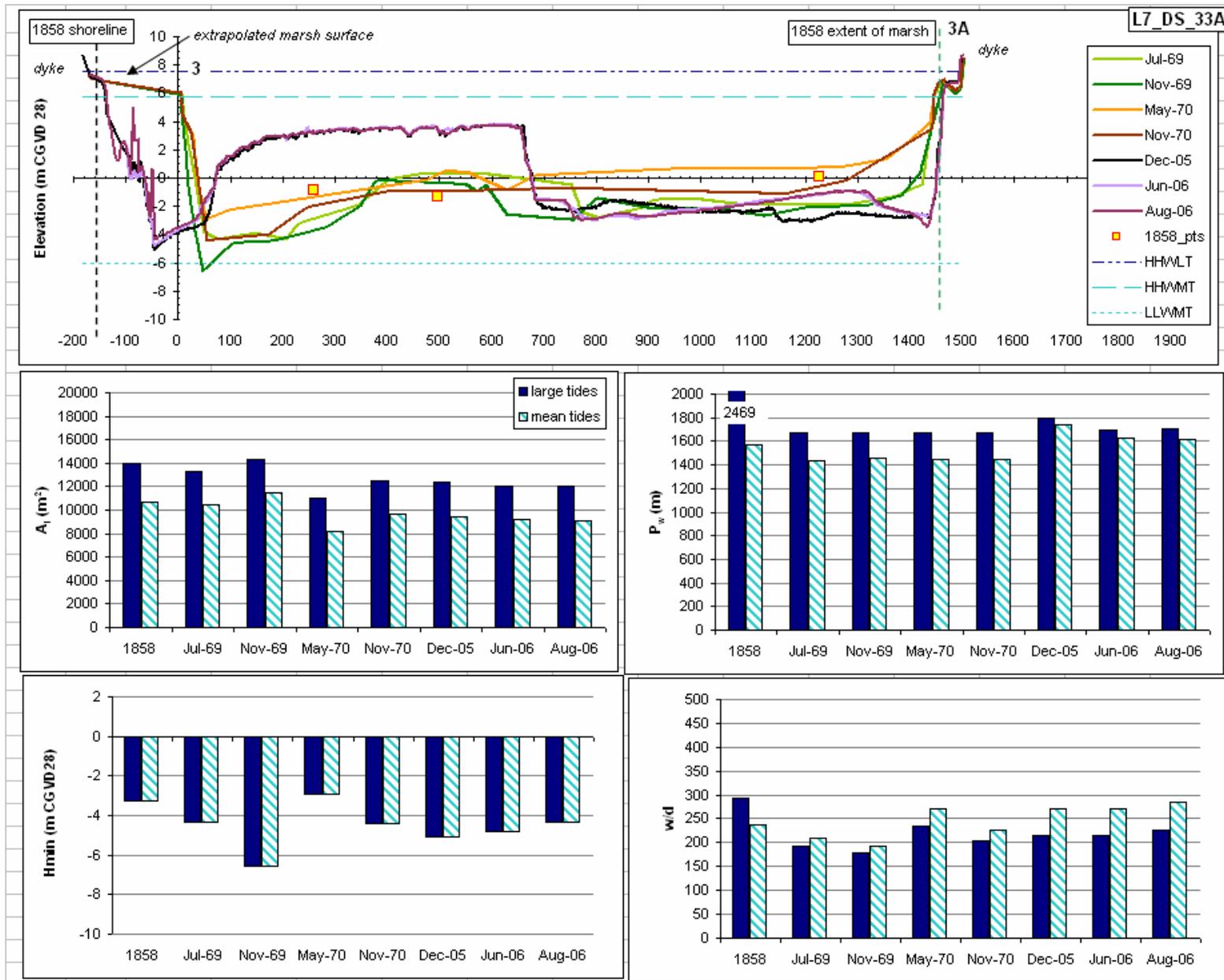
Figure 4.3i: Cross sectional profile for Line7_DS_33A and associated hydraulic geometry parameters on the Avon River. Vertical exaggeration on cross sectional profiles = 100 X. Distance on cross sectional profile in metres.
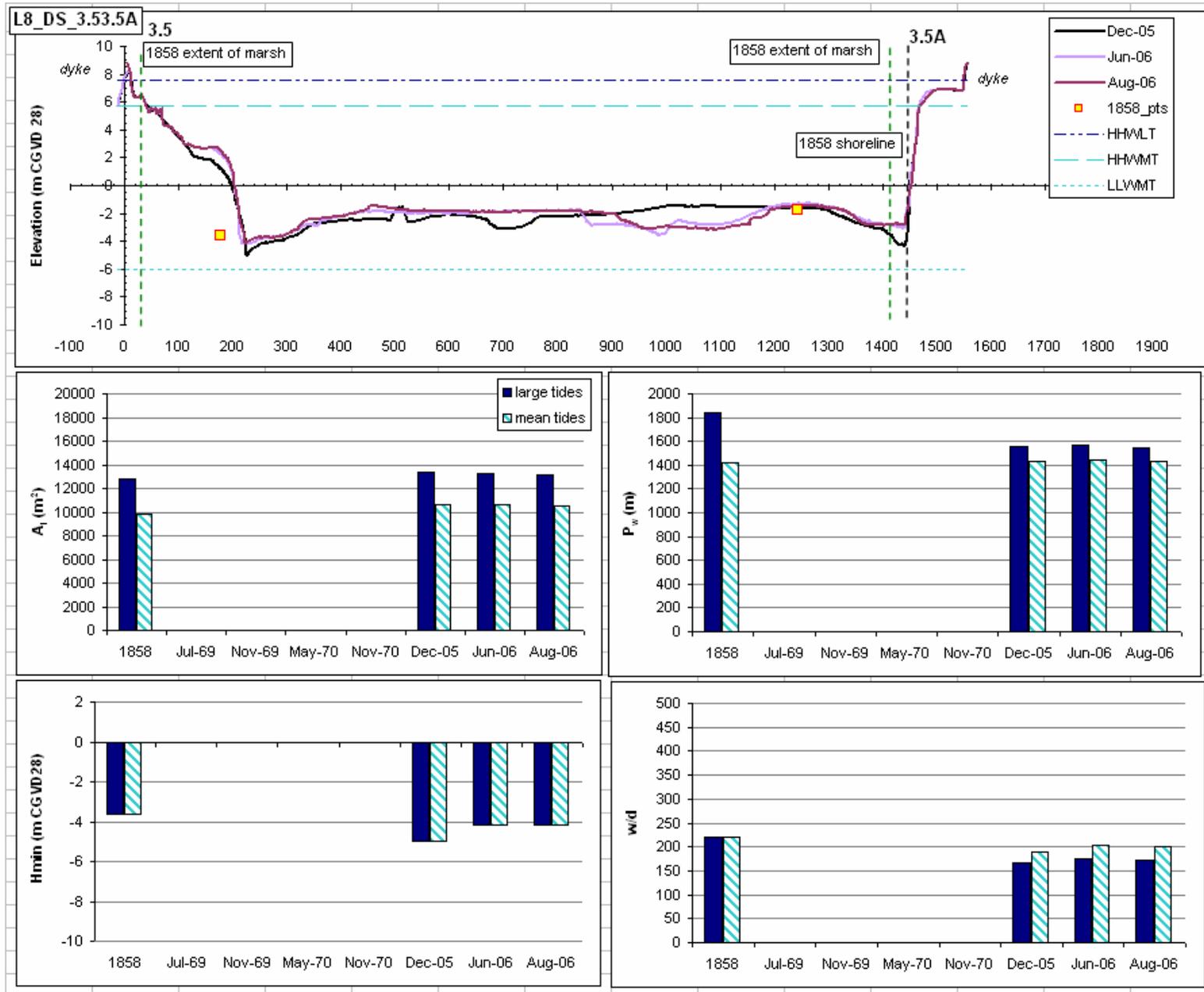
Figure 4.3j: Cross sectional profile for Line8_DS_3.53.5A and associated hydraulic geometry parameters on the Avon River. Vertical exaggeration on cross sectional profiles = 100 X. Distance on cross sectional profile in metres.
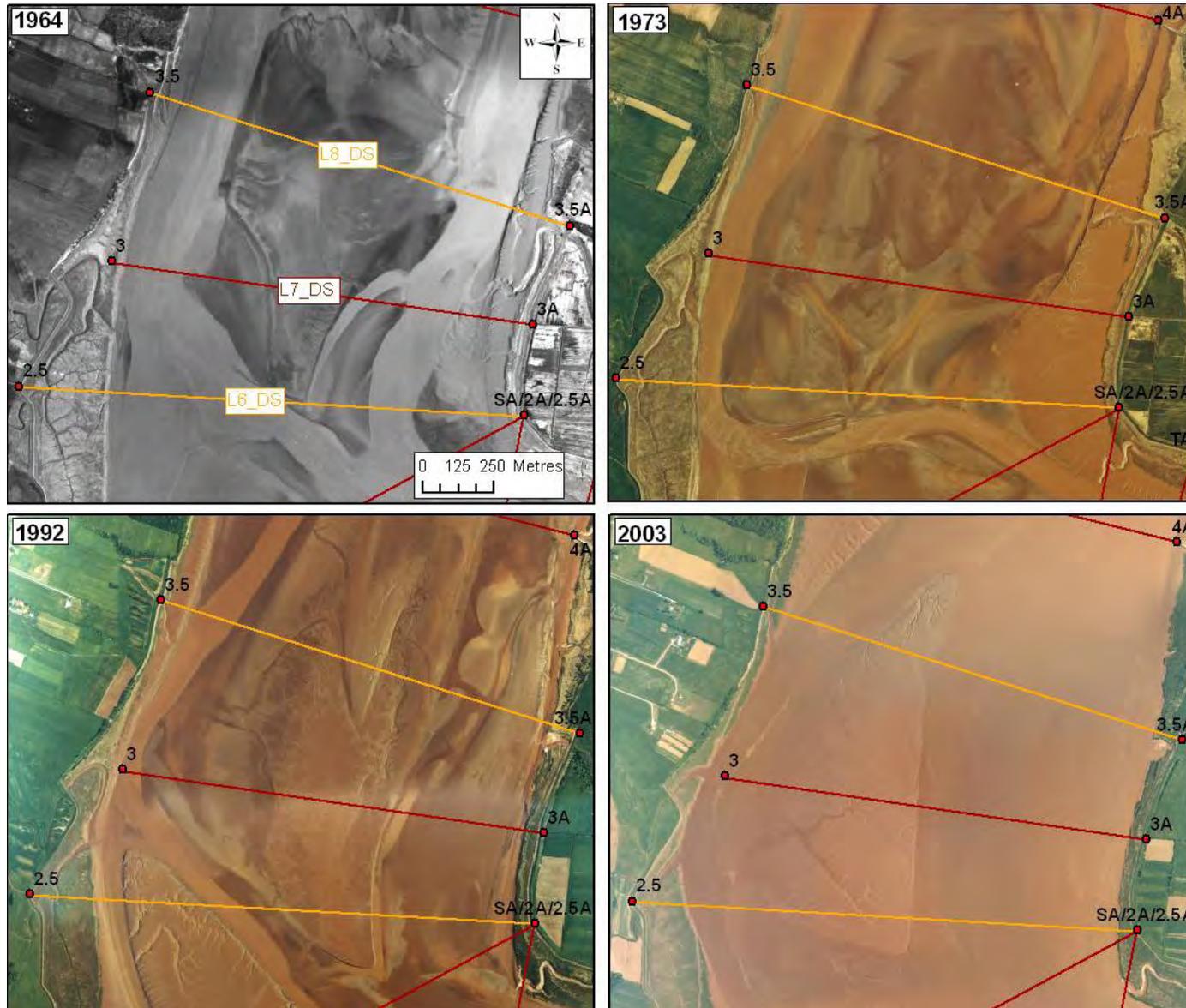
Figure 4.3k: Location of downstream survey lines 6,7 and 8. Note changes in channel thalwegs, bar location and marsh loss on west bank from 1964 to 2003. A new marsh post '3' was added in 2005 for navigational purposes due to erosion of the west bank however all calculations were performed relative to the original stake 3.
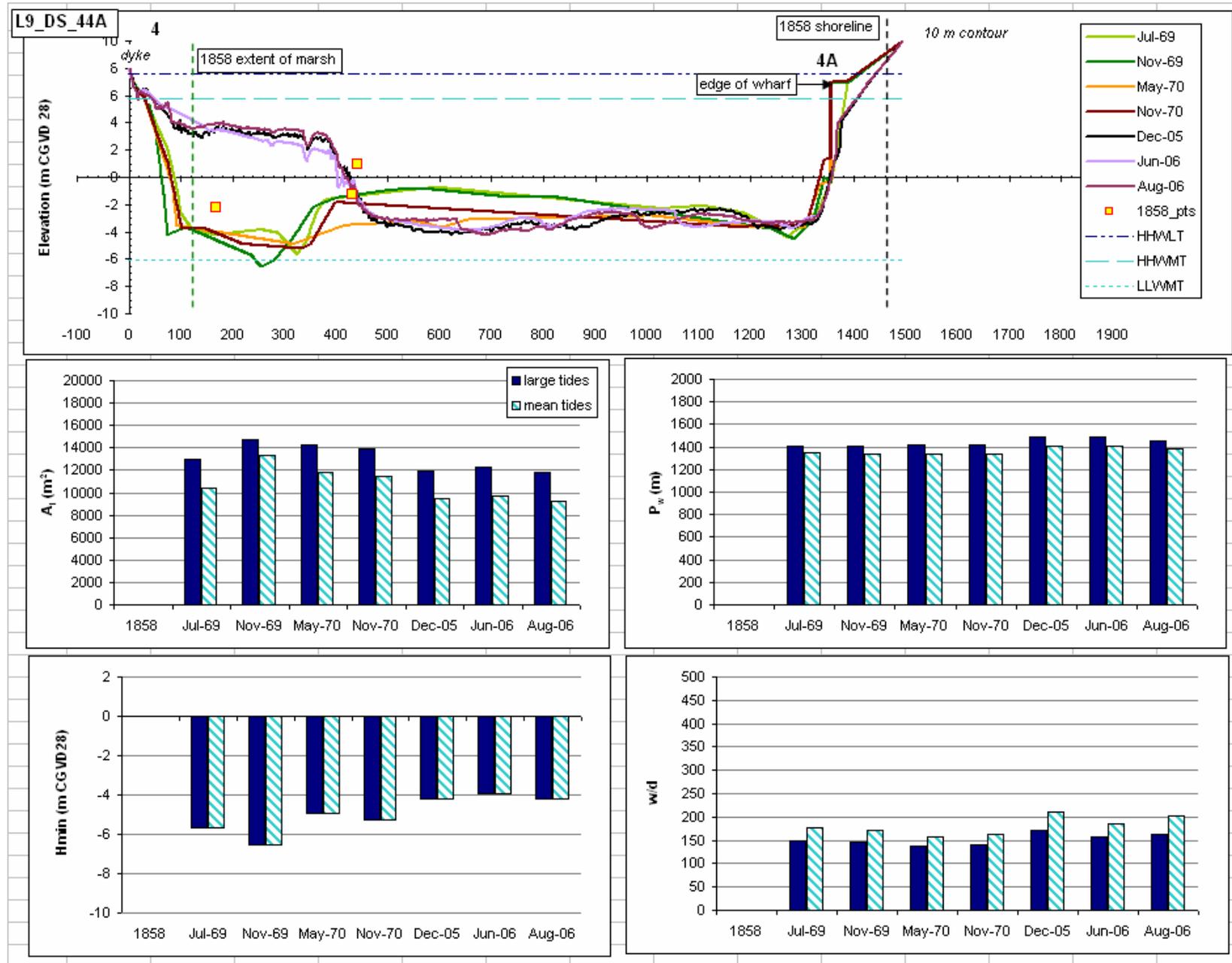
Figure 4.3l: Cross sectional profile for Line9_DS_44A and associated hydraulic geometry parameters on the Avon River. Vertical exaggeration on cross sectional profiles = 100 X. Distance on cross sectional profile in metres.
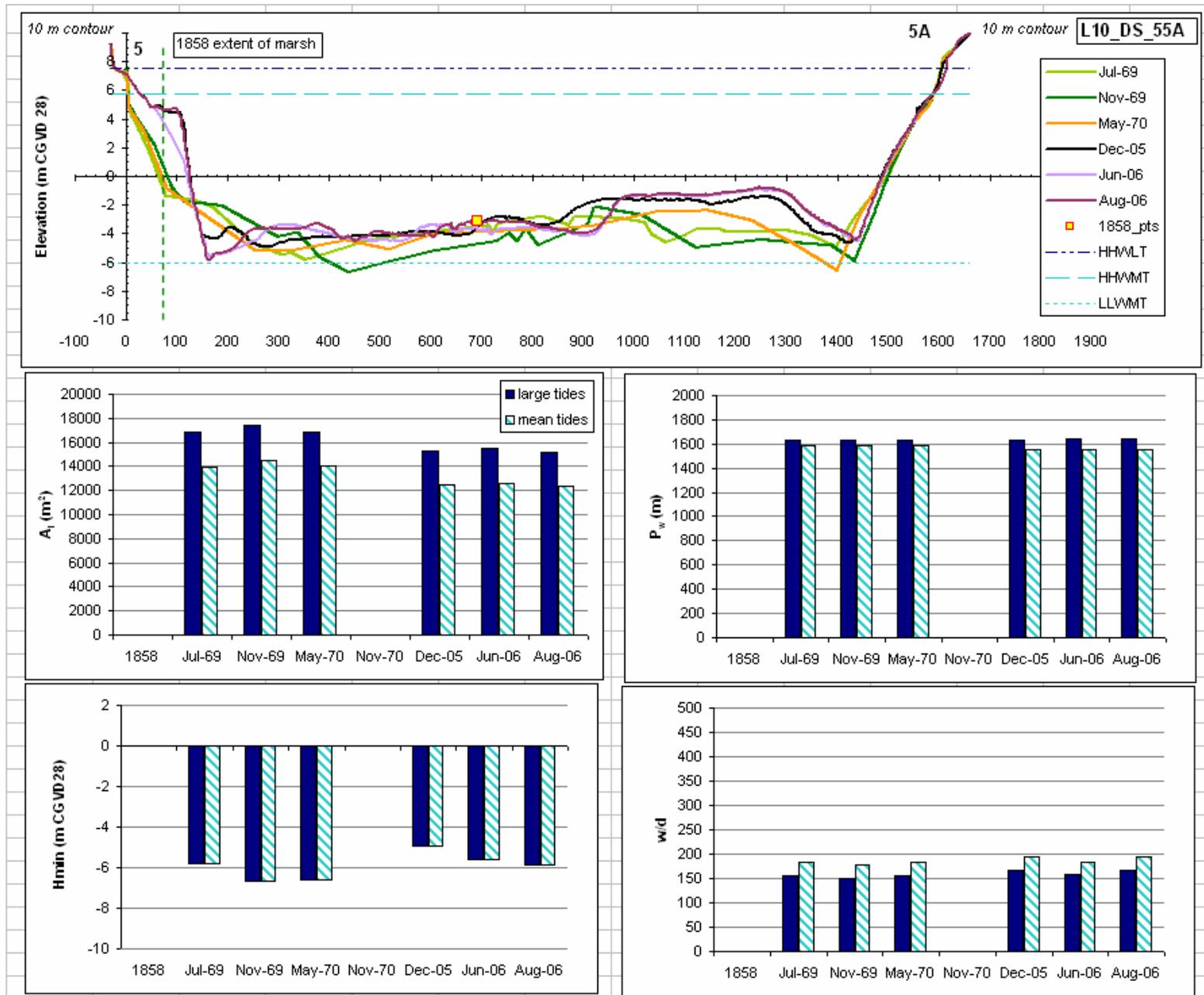
Figure 4.3m: Cross sectional profile for Line10_DS_55A and associated hydraulic geometry parameters on the Avon River. Vertical exaggeration on cross sectional profiles = 100 X. Distance on cross sectional profile in metres.
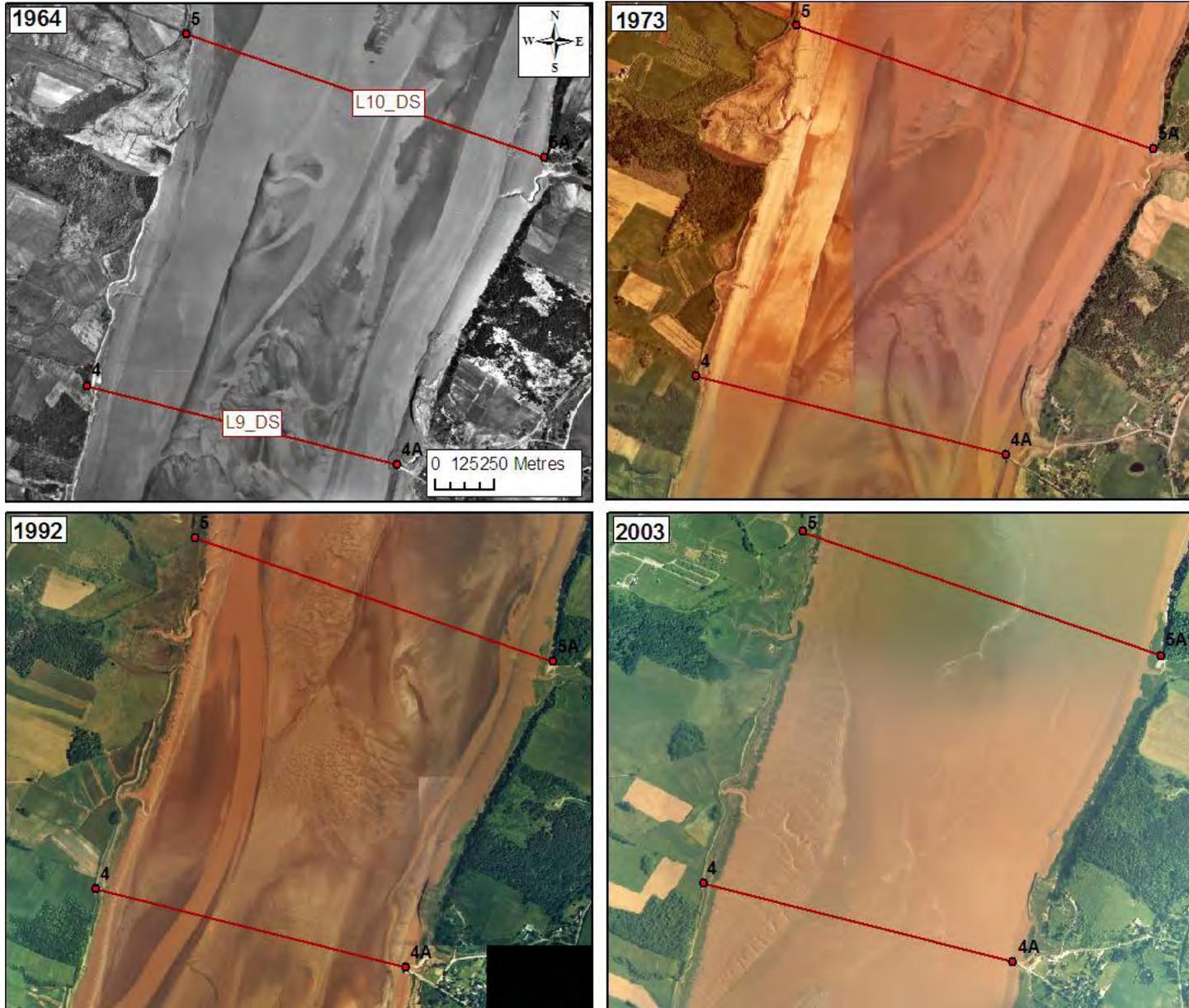
Figure 4.3n: Location of downstream survey lines 9 and 10. Note changes in channel thalwegs, bar location and marsh and mudflat expansion on west bank from 1964 to 2003.
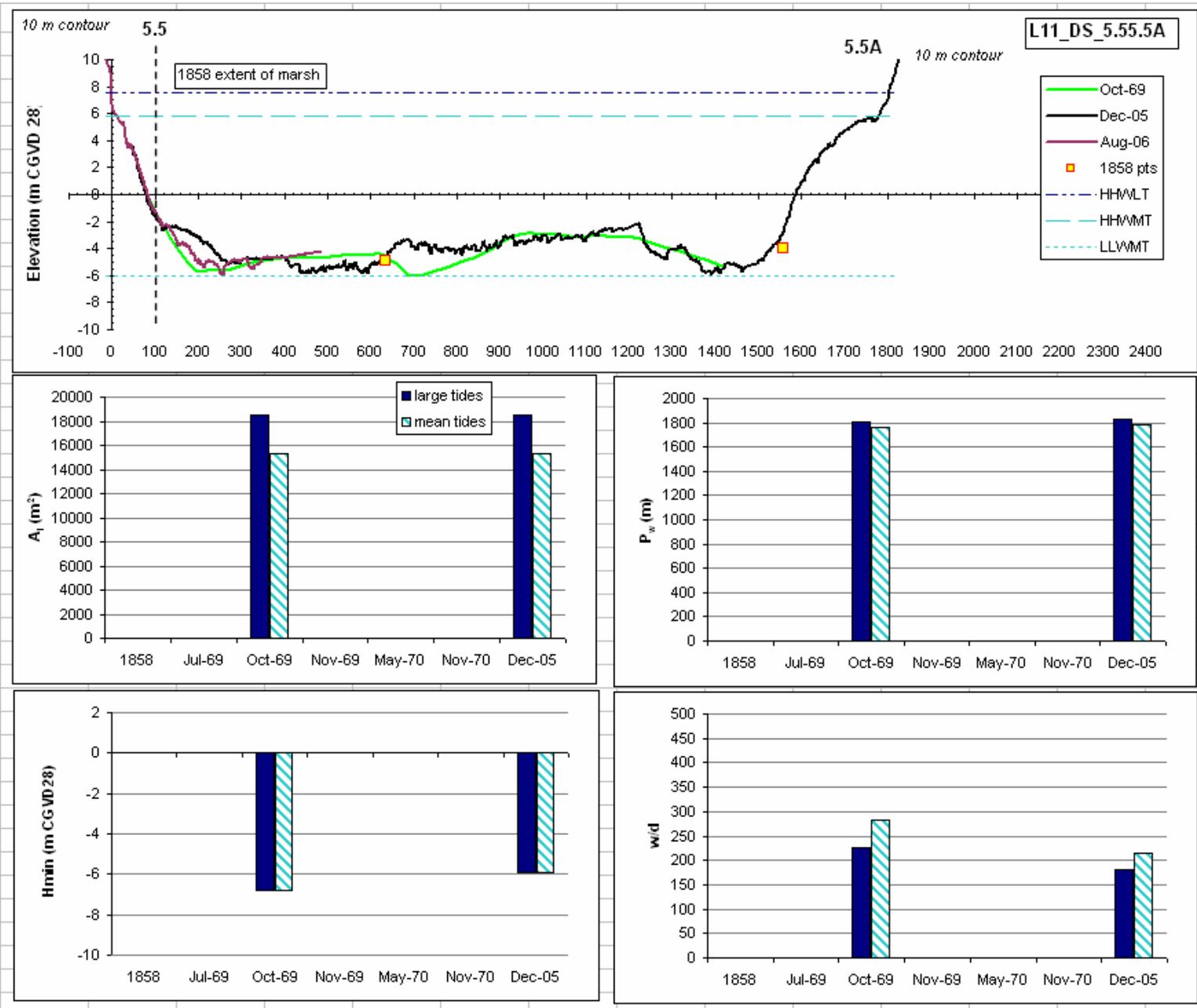
Figure 4.3o: Cross sectional profile for Line11_DS_5.55.5A and associated hydraulic geometry parameters on the Avon River. Note change in vertical exaggeration on cross sectional profiles to 125 X. Distance on cross sectional profile in metres.
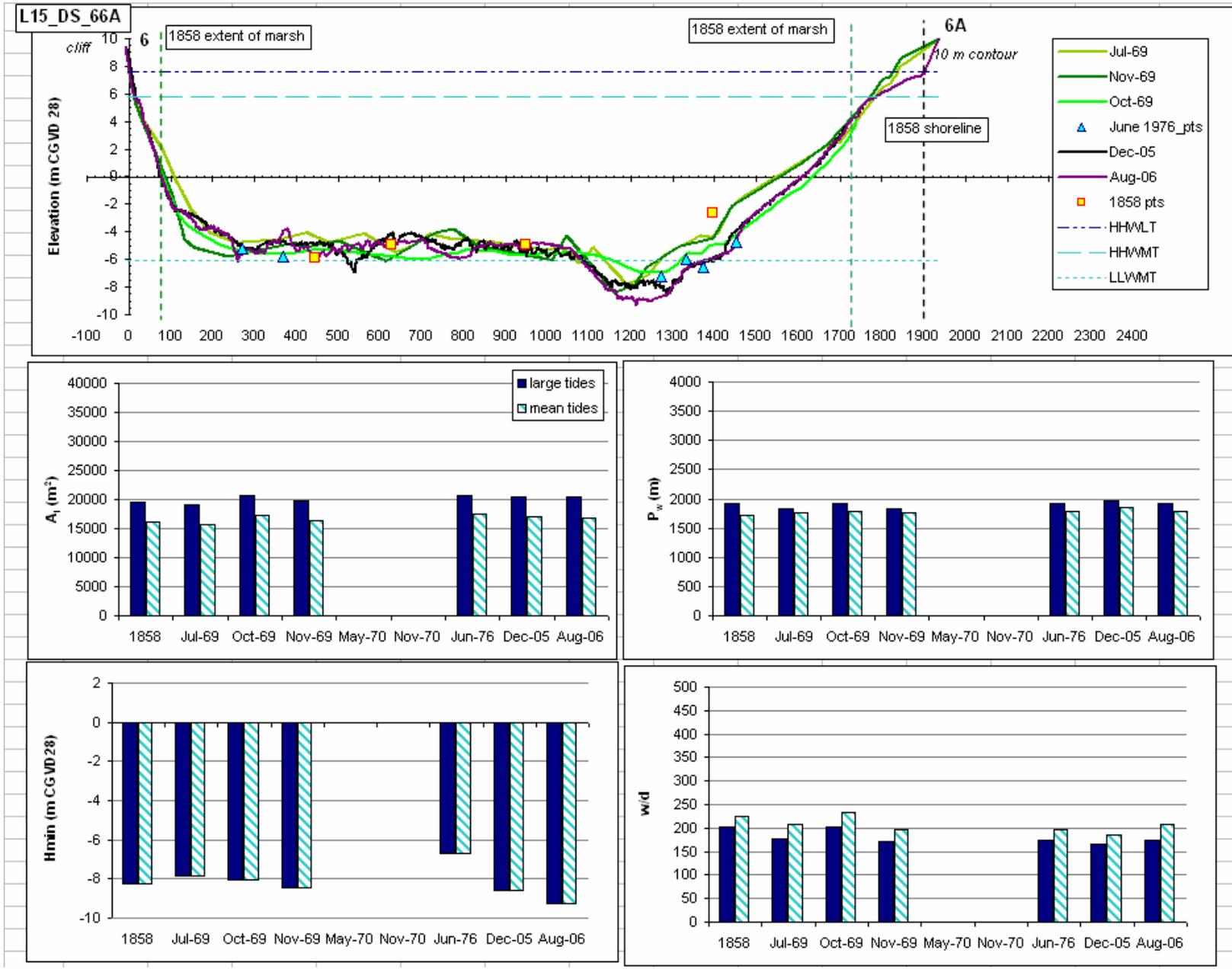
Figure 4.3p: Cross sectional profile for Line15_DS_66A and associated hydraulic geometry parameters on the Avon River. Vertical exaggeration on cross sectional profiles = 125 X. Note change in scale on y axis for cross sectional area and wetted perimeter. Distance on cross sectional profile in metres.
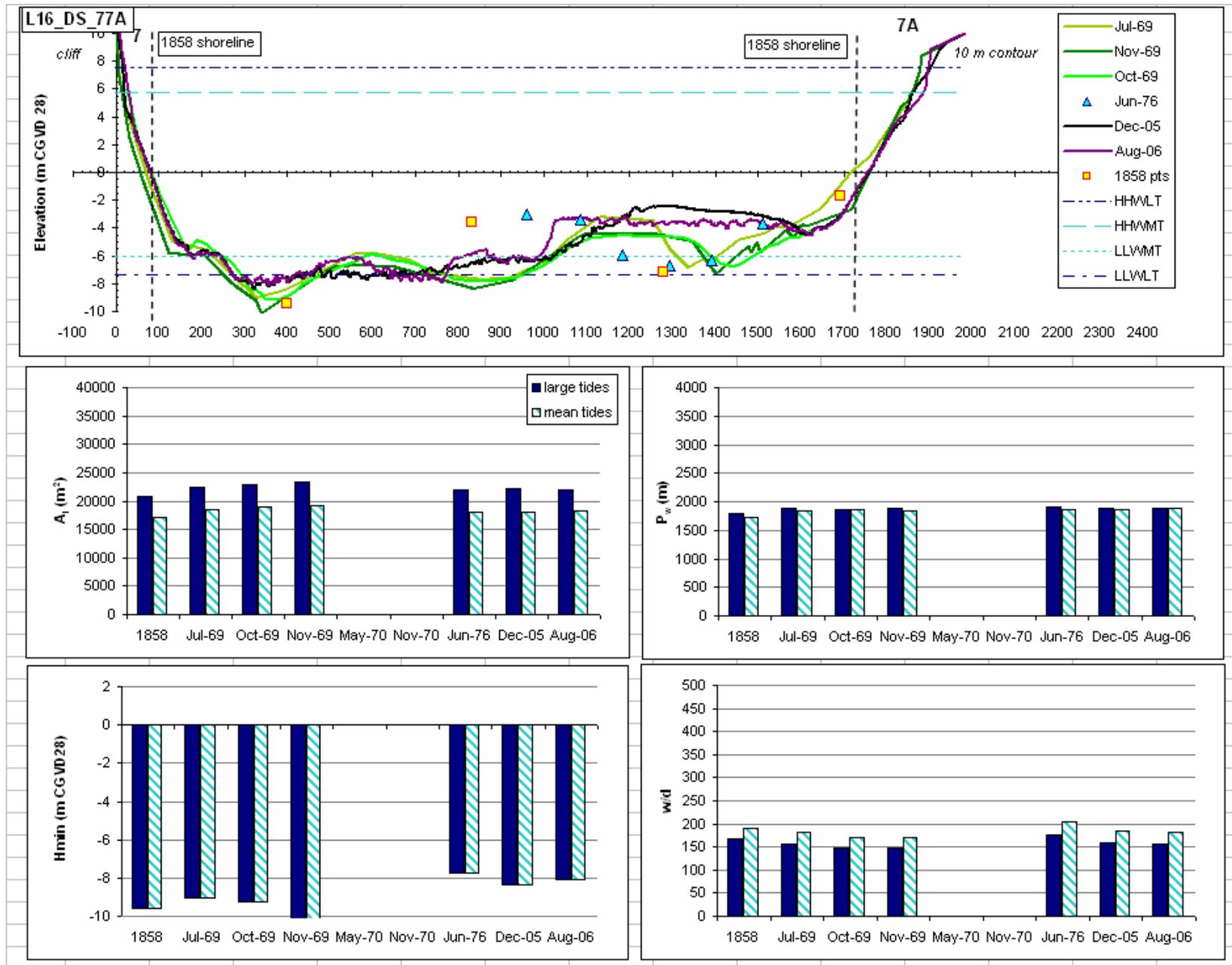
Figure 4.3q: Cross sectional profile for Line16_DS_77A and associated hydraulic geometry parameters on the Avon River. Vertical exaggeration on cross sectional profiles =125 X. Distance on cross sectional profile in metres.
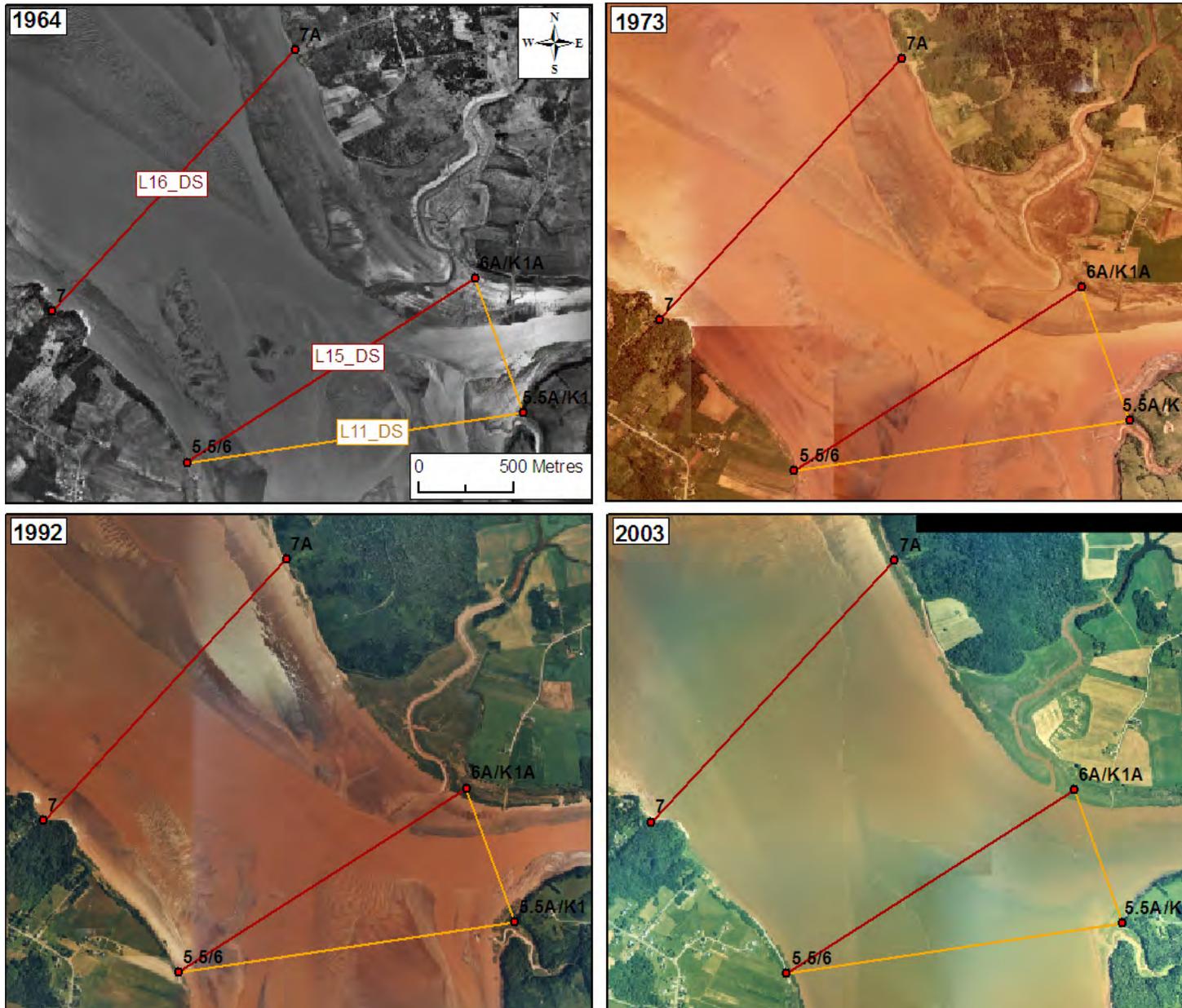
Figure 4.3r: Location of downstream survey lines 11,15 and 16. Minor changes in channel thalweb and bar location from 1964 to 2003.
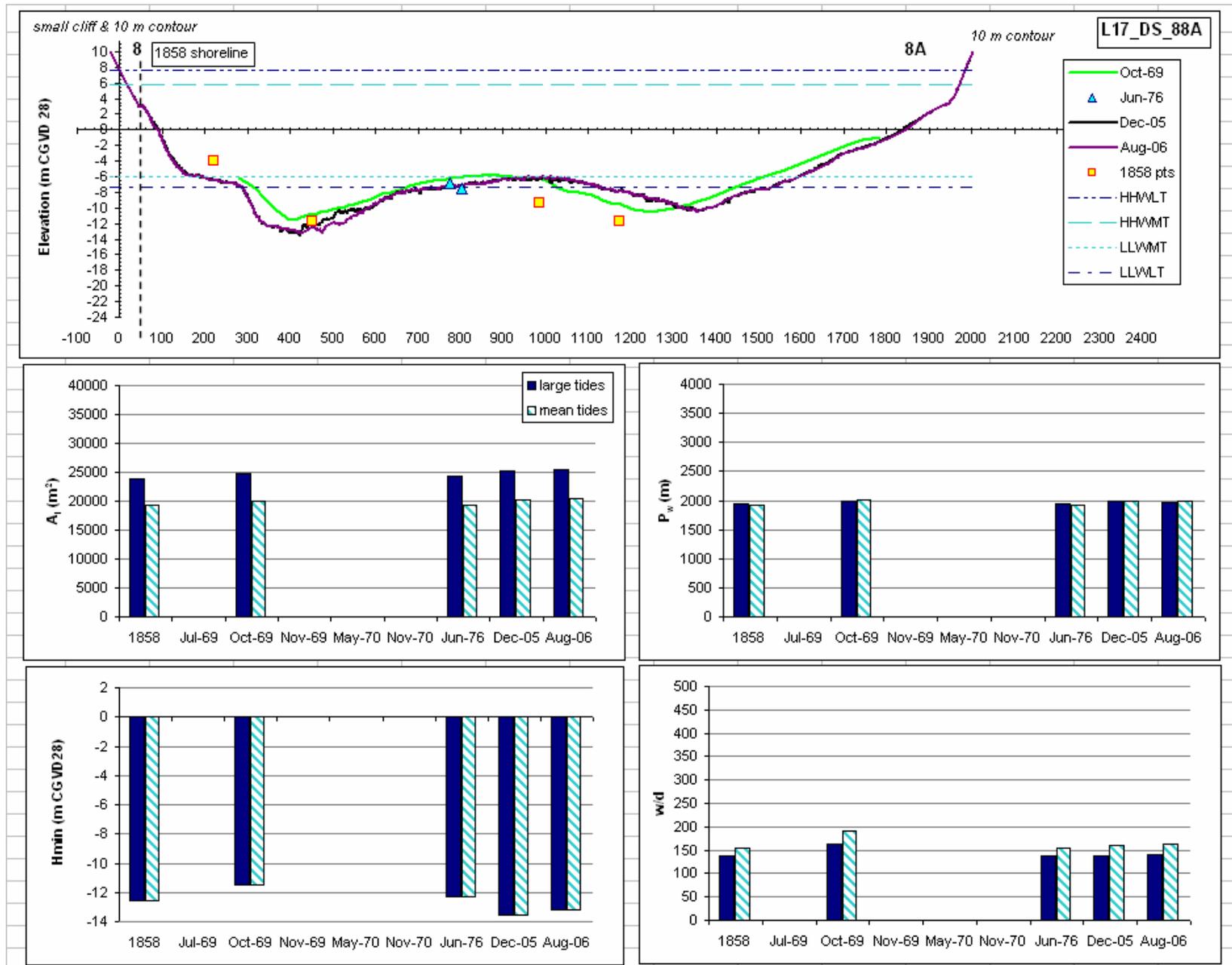
Figure 4.3s: Cross sectional profile for Line17_DS_88A and associated hydraulic geometry parameters on the Avon River. Note change in vertical exaggeration on cross sectional profiles to 73 X. Distance on cross sectional profile in metres.
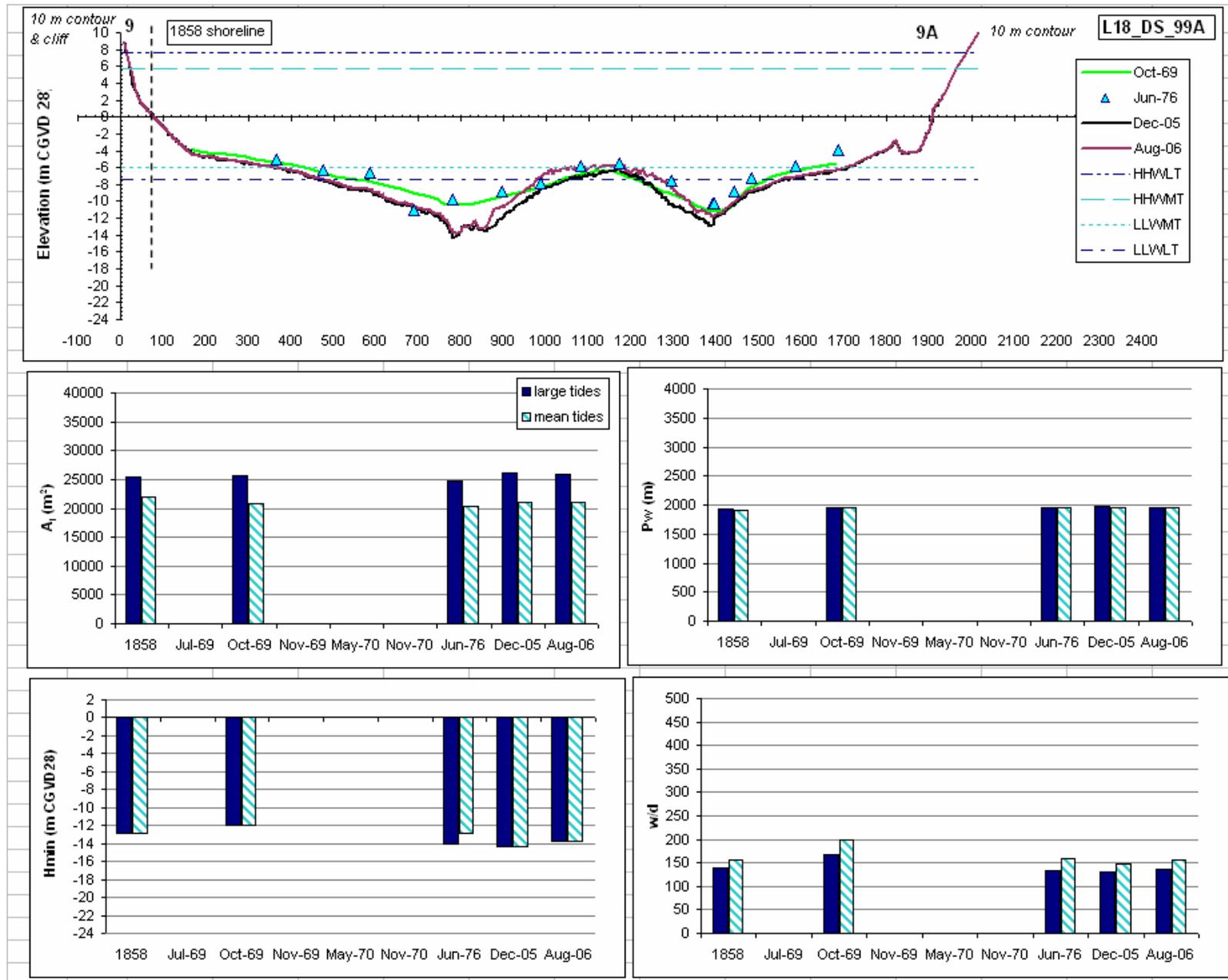
Figure 4.3t: Cross sectional profile for Line18_DS_99A and associated hydraulic geometry parameters on the Avon River. Vertical exaggeration on cross sectional profiles = 73 X. Note change in scale for minimum bed elevation. Distance on cross sectional profile in metres.
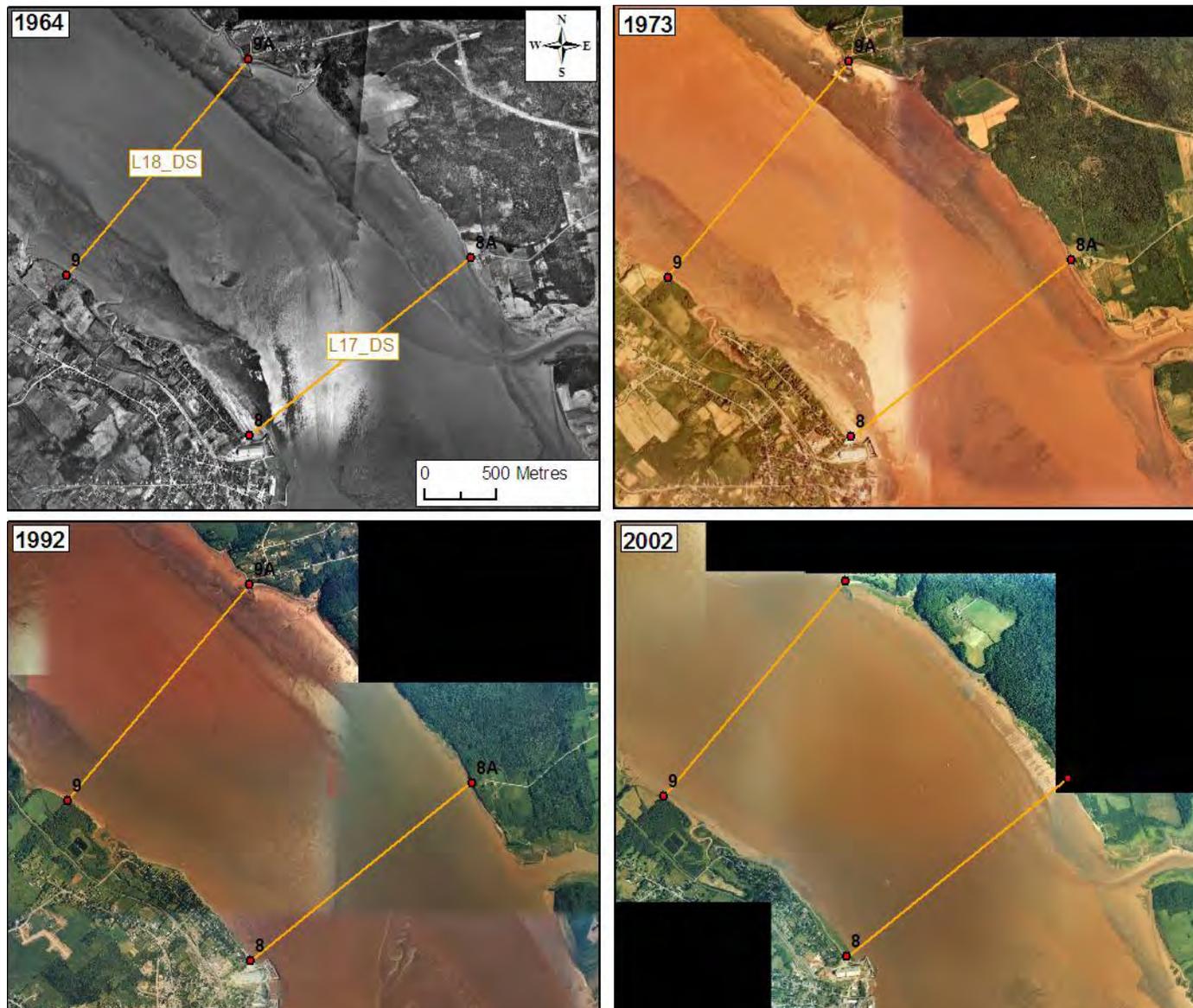
Figure 4.3u: Location of downstream survey lines 17 and 18. Note relative stability of position of the main channel thalwegs and bar locations from 1964 to 2003.
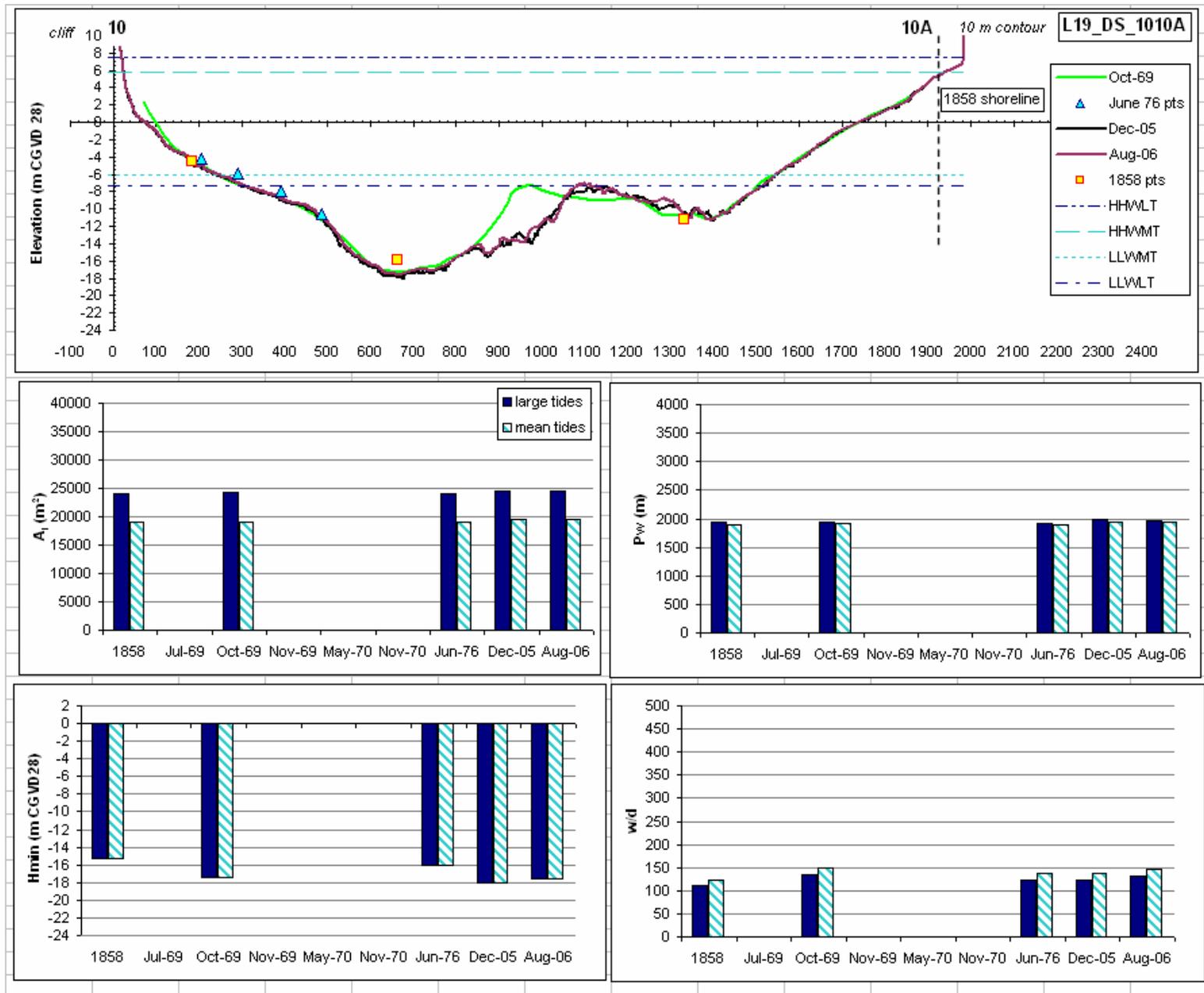
Figure 4.3v: Cross sectional profile for Line19_DS_1010A and associated hydraulic geometry parameters on the Avon River. Vertical exaggeration on cross sectional profiles = 73 X. Note change in scale for minimum bed elevation. Distance on cross sectional profile in metres.
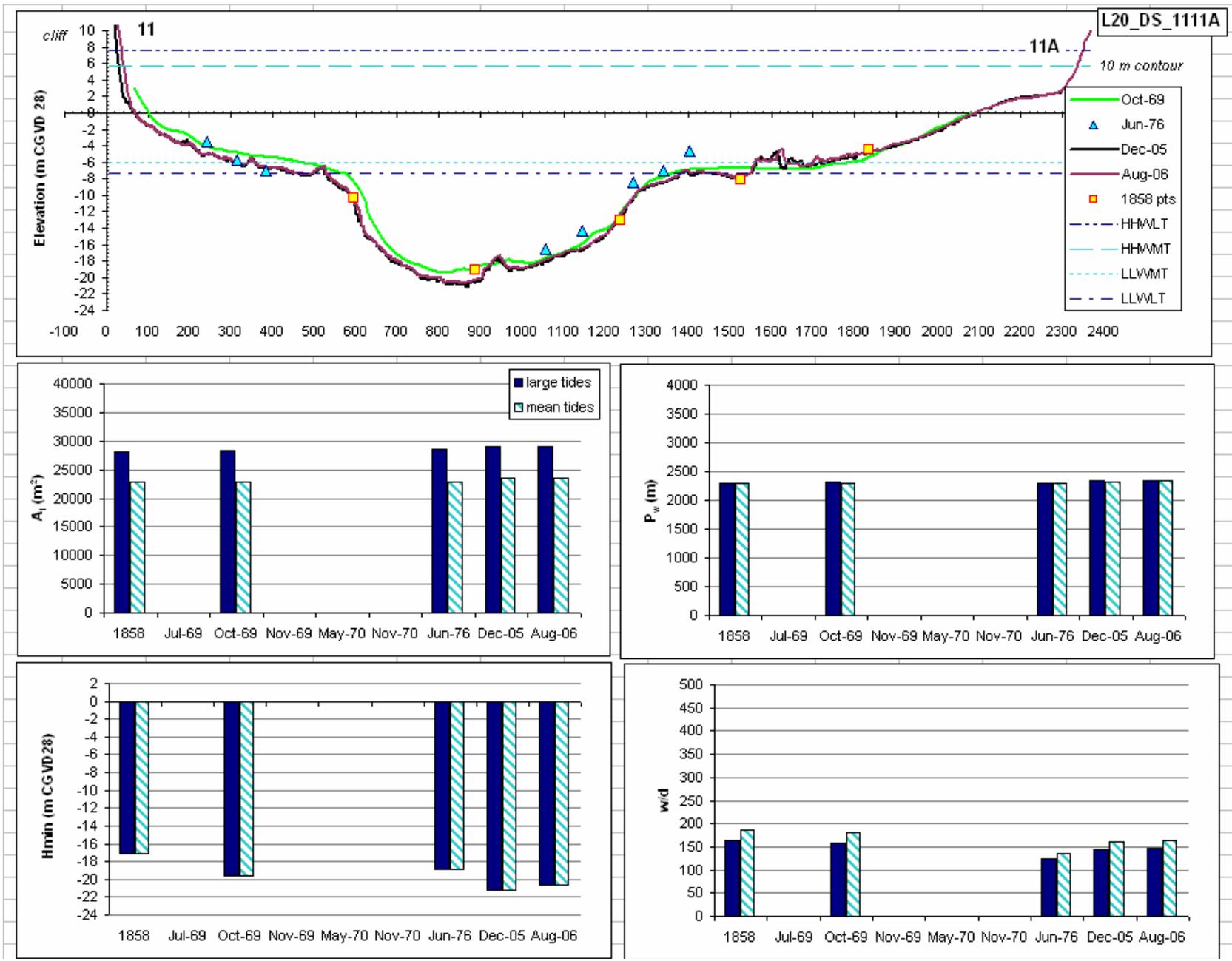
Figure 4.3w: Cross sectional profile for Line20_DS_1111A and associated hydraulic geometry parameters on the Avon River. Vertical exaggeration on cross sectional profiles = 73 X. Distance on cross sectional profile in metres.
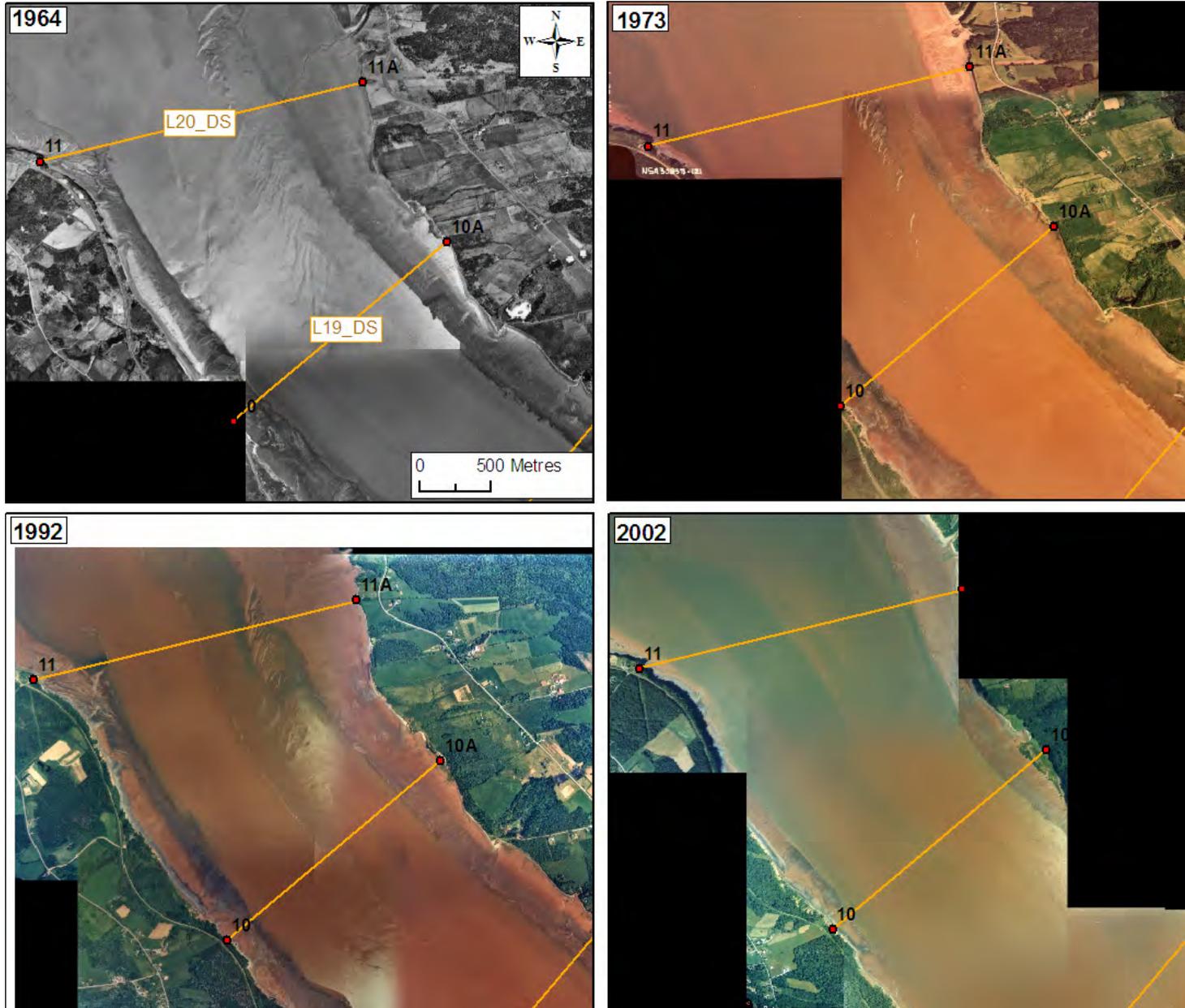
Figure 4.3x: Location of downstream survey lines 19 and 20. Note relative stability of position of the main channel thalwegs and bar locations from 1964 to 2003.

Avon River - Large Tides

Date	Line	Distance between	total dist	A_i	pw	H	Hmin	d	D	w	w/d	w/D	D/d
1858	L6_DS_5.55.5A	469	9947	15365	3019	-0.7	-3.0	8.3	10.6	3008	363	283	1.3
	L7_DS_33A	385	10332	14027	2469	-0.8	-3.3	8.4	10.8	2468	294	228	1.3
	L8_DS_3.53.5A	511	10843	12822	1835	-0.7	-3.6	8.3	11.2	1835	221	164	1.3
	L15_DS_66A	428	14321	19562	1911	-1.8	-8.2	9.4	15.8	1910	203	121	1.7
	L16_DS_77A	1333	15654	20747	1803	-3.3	-9.6	10.8	17.1	1801	166	105	1.6
	L17_DS_88A	2453	18107	23960	1950	-6.7	-12.5	14.3	20.1	1948	137	97	1.4
	L18_DS_99A	1892	19999	25514	1935	-6.4	-12.8	14.0	20.4	1933	138	95	1.5
	L19_DS_1010A	1802	21801	23998	1936	-9.7	-15.3	17.3	22.9	1927	111	84	1.3
	L20_DS_1111A	1791	23592	28174	2305	-6.4	-17.1	14.0	24.7	2294	164	93	1.8
Jul-69	US1	5435	5435	4606	771	3.2	-2.2	4.3	9.8	769	178	79	2.3
	US2	1451	6886	5019	712	3.3	-1.2	4.3	8.8	709	167	81	2.1
	L1A_DS_1A1AA	1558	8444	7732	1010	0.0	-4.3	7.6	11.9	1005	132	85	1.6
	L1_DS_11AA	486	8930	9002	1378	0.4	-5.9	7.2	13.4	1374	190	102	1.9
	L5_DS_22A	548	9478	13641	1726	-0.5	-5.8	8.0	13.4	1722	214	129	1.7
	L7_DS_33A	385	10332	13345	1674	-1.1	-4.3	8.7	11.9	1672	193	140	1.4
	L9_DS_44A	624	11467	12930	1405	-1.8	-5.7	9.4	13.2	1403	149	106	1.4
	L10_DS_55A	1483	12950	16807	1629	-2.8	-5.8	10.4	13.4	1627	157	121	1.3
	L15_DS_66A	428	14321	19161	1837	-2.8	-7.8	10.3	15.4	1836	178	119	1.5
	L16_DS_77A	1333	15654	22517	1875	-4.5	-9.0	12.0	16.6	1873	156	113	1.4
Oct-69	L11_DS_5.55.5A	943	13893	18564	1811	-0.4	-6.8	8.0	14.4	1801	225	125	1.8
	L15_DS_66A	428	14321	20654	1910	-1.9	-8.0	9.4	15.6	1905	202	122	1.7
	L16_DS_77A	1333	15654	23001	1866	-5.1	-9.2	12.7	16.8	1868	147	111	1.3
	L17_DS_88A	2453	18107	24844	1989	-4.5	-11.5	12.0	19.0	1957	163	103	1.6
	L18_DS_99A	1892	19999	25652	1959	-4.0	-12.0	11.6	19.6	1946	168	100	1.7
	L19_DS_1010A	1802	21801	24247	1939	-6.9	-17.4	14.5	24.9	1927	133	77	1.7
	L20_DS_1111A	1791	23592	28422	2308	-6.9	-19.6	14.5	27.2	2294	158	84	1.9
Nov-69	US1	5435	5435	5081	771	3.5	-2.9	4.1	10.5	768	188	73	2.6
	US2	1451	6886	5176	714	4.2	-1.2	3.4	8.8	710	208	81	2.6
	L1A_DS_1A1AA	1558	8444	8609	1012	-0.9	-5.7	8.5	13.2	1007	119	76	1.6
	L1_DS_11AA	486	8930	9352	1378	0.0	-9.5	7.6	17.1	1372	181	80	2.3
	L5_DS_22A	548	9478	14275	1726	-0.9	-9.6	8.4	17.1	1721	204	100	2.0
	L7_DS_33A	385	10332	14299	1677	-1.8	-6.6	9.3	14.1	1671	179	118	1.5
	L9_DS_44A	624	11467	14778	1412	-2.0	-6.6	9.6	14.1	1403	146	99	1.5
	L10_DS_55A	1483	12950	17451	1632	-3.2	-6.7	10.8	14.3	1629	151	114	1.3
	L15_DS_66A	428	14321	19831	1826	-3.1	-8.4	10.7	16.0	1825	170	114	1.5
	L16_DS_77A	1333	15654	23440	1876	-5.0	-10.1	12.6	17.7	1874	149	106	1.4
May-70	L5_DS_22A	548	9478	12614	1726	0.1	-5.5	7.4	13.1	1721	232	132	1.8
	L7_DS_33A	385	10332	11001	1672	0.4	-2.9	7.1	10.5	1669	234	159	1.5
	L9_DS_44A	624	11467	14246	1424	-2.7	-4.9	10.2	12.5	1402	137	112	1.2
	L10_DS_55A	1483	12950	16871	1634	-2.9	-6.6	10.4	14.1	1630	156	115	1.4
Nov-70	US1	5435	5435	4772	771	2.1	-2.5	5.5	10.1	768	141	76	1.8
	US2	1451	6886	4888	710	2.3	-1.1	5.3	8.7	707	133	81	1.6
	L5_DS_22A	1558	9478	13219	1725	-0.2	-3.7	7.8	11.3	1721	221	152	1.5
	L7_DS_33A	385	10332	12520	1673	-0.6	-4.4	8.1	12.0	1670	205	139	1.5
	L9_DS_44A	624	11467	13883	1419	-2.4	-5.2	10.0	12.8	1402	141	109	1.3
Jun-76	L15_DS_66A	428	14321	20765	1910	-3.3	-6.7	10.9	14.3	1905	175	134	1.3
	L16_DS_77A	1333	15654	21945	1900	-2.9	-7.7	10.4	15.3	1837	176	120	1.5
	L17_DS_88A	2453	18107	24390	1950	-6.6	-12.2	14.2	19.8	1948	137	98	1.4
	L18_DS_99A	1892	19999	24855	1959	-7.0	-14.1	14.5	21.7	1948	134	90	1.5
	L19_DS_1010A	1802	21801	24123	1922	-7.9	-16.0	15.5	23.6	1914	123	81	1.5
	L20_DS_1111A	1791	23592	28684	2304	-11.0	-18.9	18.6	26.5	2294	123	87	1.4

Table 4.3: Summary of hydraulic geometry parameters and measures of channel form for lines on the Avon River from 1858 to August 2006 where available for large tides. Distance = distance between lines, Total Distance = distance from head of tide on the Avon River. Refer to Table 3.4 for additional abbreviations.

Date	Line	Distance between	total dist	A_i	pw	H	Hmin	d	D	w	w/d	w/D	D/d
Dec-05	L1A_DS_1A1AA	143	8444	2303	967	4.8	2.3	2.8	5.3	963	350	183	1.9
	L1_DS_11AA	486	8930	4513	1342	3.3	-4.6	4.3	12.2	1342	313	110	2.8
	L5_DS_22A	548	9478	10811	1743	0.7	-5.2	6.8	12.7	1719	252	135	1.9
	L6_DS_5.55.5A	469	9947	11679	1801	0.6	-4.8	6.9	12.4	1777	257	143	1.8
	L7_DS_33A	385	10332	12400	1798	-0.2	-5.1	7.7	12.7	1666	216	131	1.6
	L8_DS_3.53.5A	511	10843	13347	1559	-1.8	-5.0	9.3	12.6	1550	166	123	1.3
	L9_DS_44A	624	11467	11953	1483	-0.8	-4.2	8.4	11.8	1427	171	121	1.4
	L10_DS_55A	1483	12950	15331	1634	-2.2	-4.9	9.8	12.5	1625	166	130	1.3
	L11_DS_5.55.5A	943	13893	18512	1825	-2.4	-5.9	10.0	13.5	1804	180	134	1.3
	L15_DS_66A	428	14321	20395	1976	-3.8	-8.6	11.4	16.1	1898	166	118	1.4
	L16_DS_77A	1333	15654	22132	1876	-4.4	-8.4	12.0	15.9	1891	158	119	1.3
	L17_DS_88A	2453	18107	25332	1994	-6.7	-13.6	14.2	21.2	1973	139	93	1.5
	L18_DS_99A	1892	19999	26102	1978	-7.3	-14.3	14.9	21.9	1953	131	89	1.5
	L19_DS_1010A	1802	21801	24583	1981	-8.3	-18.1	15.8	25.7	1964	124	76	1.6
	L20_DS_1111A	1791	23592	29128	2331	-8.5	-21.2	16.1	28.7	2324	145	81	1.8
Jun-06	L5_DS_22A	548	9478	10792	1849	0.1	-4.6	7.5	12.1	1720	230	142	1.6
	L6_DS_5.55.5A	469	9947	11422	1847	0.7	-4.5	6.8	12.1	1774	260	147	1.8
	L7_DS_33A	385	10332	12077	1690	-0.1	-4.8	7.7	12.4	1664	216	135	1.6
	L8_DS_3.53.5A	511	10843	13264	1564	-1.3	-4.2	8.9	11.8	1550	175	132	1.3
	L9_DS_44A	624	11467	12255	1484	-1.5	-3.9	9.1	11.5	1427	157	124	1.3
	L10_DS_55A	1483	12950	15499	1644	-2.7	-5.6	10.3	13.2	1635	159	124	1.3
Aug-06	L1A_DS_1A1AA	143	8444	2070	965	5.0	1.6	2.6	5.9	956	366	161	2.3
	L1_DS_11AA	486	8930	4238	1382	4.2	-4.4	3.4	11.9	1376	405	115	3.5
	L5_DS_22A	548	9478	10436	1730	1.3	-3.8	6.3	11.4	1718	272	151	1.8
	L6_DS_5.55.5A	469	9947	11489	1787	0.7	-4.4	6.9	11.9	1777	258	149	1.7
	L7_DS_33A	385	10332	12038	1712	0.2	-4.3	7.4	11.9	1664	225	140	1.6
	L8_DS_3.53.5A	511	10843	13187	1546	-1.3	-4.2	8.9	11.8	1541	173	131	1.3
	L9_DS_44A	624	11467	11779	1448	-1.1	-4.2	8.7	11.8	1423	164	121	1.4
	L10_DS_55A	1483	12950	15204	1642	-2.2	-5.9	9.8	13.4	1635	167	122	1.4
	L15_DS_66A	428	14321	20427	1913	-3.4	-9.3	11.0	16.9	1905	173	113	1.5
	L16_DS_77A	1333	15654	22078	1890	-4.5	-8.1	12.1	15.7	1884	156	120	1.3
	L17_DS_88A	2453	18107	25405	1972	-6.4	-13.2	13.9	20.8	1973	141	95	1.5
	L18_DS_99A	1892	19999	25835	1963	-6.6	-13.8	14.2	21.4	1948	137	91	1.5
	L19_DS_1010A	1802	21801	24542	1965	-7.5	-17.6	15.0	25.1	1963	131	78	1.7
	L20_DS_1111A	1791	23592	28980	2337	-8.2	-20.7	15.8	28.3	2310	147	82	1.8

Header for table: **Hydraulic geometry Large Tides**

Table 4.3: Summary of hydraulic geometry parameters and measures of channel form for lines on the Avon River from 1858 to August 2006 where available for large tides. Distance = distance between lines, Total Distance = distance from head of tide on the Avon River. Refer to Table 3.4 for additional abbreviations.

Avon River - Mean Tides

Date	Line	Distance between	total dist	A_i	pw	H	Hmin	d	D	w	w/d	w/D	D/d
1858	L6_DS_5.55.5A	469	9947	11270	1703	-0.7	-3.0	6.5	8.8	1702	262	193	1.4
	L7_DS_33A	385	10332	10715	1573	-0.8	-3.3	6.6	9.0	1573	239	174	1.4
	L8_DS_3.53.5A	511	10843	9777	1424	-0.7	-3.6	6.5	9.4	1424	220	152	1.4
	L15_DS_66A	428	14321	16211	1713	-1.8	-8.2	7.6	14.0	1712	226	122	1.8
	L16_DS_77A	1333	15654	17161	1728	-3.3	-9.6	9.0	15.3	1727	191	113	1.7
	L17_DS_88A	2453	18107	19358	1914	-6.7	-12.5	12.5	18.3	1912	154	104	1.5
	L18_DS_99A	1892	19999	22052	1908	-6.4	-12.8	12.2	18.6	1907	157	103	1.5
	L19_DS_1010A	1802	21801	19070	1903	-9.7	-15.3	15.5	21.1	1892	122	90	1.4
	L20_DS_1111A	1791	23592	22755	2301	-6.4	-17.1	12.2	22.9	2285	188	100	1.9
Jul-69	US1	5435	5435	3383	659	3.2	-2.2	2.5	8.0	657	260	82	3.2
	US2	1451	6886	3777	673	3.3	-1.2	2.5	7.0	670	273	96	2.9
	L1A_DS_1A1AA	1558	8444	5939	981	0.0	-4.3	5.8	10.1	978	168	97	1.7
	L1_DS_11AA	486	8930	6840	1288	0.4	-5.9	5.4	11.6	1285	237	110	2.1
	L5_DS_22A	548	9478	10627	1643	-0.5	-5.8	6.2	11.6	1639	263	142	1.9
	L7_DS_33A	385	10332	10488	1440	-1.1	-4.3	6.9	10.1	1438	209	142	1.5
	L9_DS_44A	624	11467	10465	1351	-1.8	-5.7	7.6	11.4	1350	177	118	1.5
	L10_DS_55A	1483	12950	13929	1583	-2.8	-5.8	8.6	11.6	1582	184	136	1.4
	L15_DS_66A	428	14321	15785	1770	-2.8	-7.8	8.5	13.6	1769	207	130	1.6
	L16_DS_77A	1333	15654	18435	1846	-4.5	-9.0	10.2	14.8	1845	180	125	1.4
Oct-69	L11_DS_5.55.5A	943	13893	15352	1762	-0.4	-6.8	6.2	12.6	1758	284	140	2.0
	L15_DS_66A	428	14321	17265	1782	-1.9	-8.0	7.6	13.8	1778	233	129	1.8
	L16_DS_77A	1333	15654	18912	1853	-5.1	-9.2	10.9	15.0	1851	170	123	1.4
	L17_DS_88A	2453	18107	20089	2010	-4.5	-11.5	10.2	17.2	1960	192	114	1.7
	L18_DS_99A	1892	19999	20847	1946	-4.0	-12.0	9.8	17.8	1949	199	110	1.8
	L19_DS_1010A	1802	21801	19138	1906	-6.9	-17.4	12.7	23.1	1892	150	82	1.8
	L20_DS_1111A	1791	23592	22890	2303	-6.9	-19.6	12.7	25.4	2285	180	90	2.0
Nov-69	US1	5435	5435	3861	658	3.5	-2.9	2.3	8.7	656	286	76	3.8
	US2	1451	6886	3943	653	4.2	-1.2	1.6	7.0	649	403	93	4.3
	L1A_DS_1A1AA	1558	8444	6808	989	-0.9	-5.7	6.7	11.4	986	148	86	1.7
	L1_DS_11AA	486	8930	7130	1288	0.0	-9.5	5.8	15.3	1283	222	84	2.6
	L5_DS_22A	548	9478	11215	1646	-0.9	-9.6	6.6	15.3	1642	248	107	2.3
	L7_DS_33A	385	10332	11439	1456	-1.8	-6.6	7.5	12.3	1451	193	118	1.6
	L9_DS_44A	624	11467	13345	1332	-2.0	-6.6	7.8	12.3	1325	170	108	1.6
	L10_DS_55A	1483	12950	14541	1587	-3.2	-6.7	9.0	12.5	1586	176	127	1.4
	L15_DS_66A	428	14321	16445	1759	-3.1	-8.4	8.9	14.2	1758	197	124	1.6
	L16_DS_77A	1333	15654	19168	1847	-5.0	-10.1	10.8	15.9	1845	171	116	1.5
May-70	L5_DS_22A	548	9478	9602	1644	0.1	-5.5	5.6	11.3	1640	291	146	2.0
	L7_DS_33A	385	10332	8163	1442	0.4	-2.9	5.3	8.7	1440	270	166	1.6
	L9_DS_44A	624	11467	11815	1342	-2.7	-4.9	8.4	10.7	1324	157	124	1.3
	L10_DS_55A	1483	12950	13995	1588	-2.9	-6.6	8.6	12.3	1586	184	128	1.4
Nov-70	US1	5435	5435	3552	649	2.1	-2.5	3.7	8.3	647	176	78	2.3
	US2	1451	6886	3656	668	2.3	-1.1	3.5	6.9	666	190	97	2.0
	L5_DS_22A	1558	9478	10206	1644	-0.2	-3.7	6.0	9.5	1641	275	173	1.6
	L7_DS_33A	385	10332	9684	1442	-0.6	-4.4	6.3	10.2	1440	227	141	1.6
	L9_DS_44A	624	11467	11451	1338	-2.4	-5.2	8.2	11.0	1324	162	120	1.3
Jun-76	L15_DS_66A	428	14321	17466	1781	-3.3	-6.7	9.1	12.5	1778	196	143	1.4
	L16_DS_77A	1333	15654	17979	1861	-2.9	-7.7	8.6	13.5	1767	205	131	1.6
	L17_DS_88A	2453	18107	19431	1913	-6.6	-12.2	12.4	18.0	1912	154	106	1.5
	L18_DS_99A	1892	19999	20316	1946	-6.4	-12.8	12.2	18.6	1950	160	105	1.5
	L19_DS_1010A	1802	21801	19052	1898	-7.9	-16.0	13.7	21.8	1887	138	87	1.6
	L20_DS_1111A	1791	23592	22954	2300	-11.0	-18.9	16.8	24.7	2285	136	93	1.5

Table 4.4: Summary of hydraulic geometry parameters and measures of channel form for lines on the Avon River from 1858 to August 2006 where available for mean tides. Distance = distance between lines, Total Distance = distance from head of tide on the Avon River. Refer to Table 3.4 for additional abbreviations.

Date	Line	Distance between	total dist	A_i	pw	H	Hmin	d	D	w	w/d	w/D	D/d
Dec-05	L1A_DS_1A1AA	143	8444	694	585	4.8	2.3	1.0	3.5	590	620	171	3.6
	L1_DS_11AA	486	8930	2208	1224	3.3	-4.6	2.5	10.4	1219	489	117	4.2
	L5_DS_22A	548	9478	7810	1650	0.7	-5.2	5.0	10.9	1619	322	148	2.2
	L6_DS_5.55.5A	469	9947	8581	1607	0.6	-4.8	5.1	10.6	1591	310	150	2.1
	L7_DS_33A	385	10332	9466	1737	-0.2	-5.1	5.9	10.9	1604	271	147	1.8
	L8_DS_3.53.5A	511	10843	10667	1436	-1.8	-5.0	7.5	10.8	1430	190	133	1.4
	L9_DS_44A	624	11467	9422	1406	-0.8	-4.2	6.6	10.0	1379	211	139	1.5
	L10_DS_55A	1483	12950	12471	1556	-2.2	-4.9	8.0	10.7	1547	194	145	1.3
	L11_DS_5.55.5A	943	13893	15292	1783	-2.4	-5.9	8.2	11.7	1765	215	151	1.4
	L15_DS_66A	428	14321	17073	1863	-3.8	-8.6	9.6	14.3	1780	185	124	1.5
	L16_DS_77A	1333	15654	18044	1867	-4.4	-8.4	10.2	14.1	1872	184	132	1.4
	L17_DS_88A	2453	18107	20341	2000	-6.7	-13.6	12.4	19.4	1983	159	102	1.6
	L18_DS_99A	1892	19999	21077	1964	-7.3	-14.3	13.1	20.1	1954	149	97	1.5
	L19_DS_1010A	1802	21801	19446	1946	-8.3	-18.1	14.0	23.9	1923	137	81	1.7
	L20_DS_1111A	1791	23592	23440	2326	-8.5	-21.2	14.3	26.9	2312	162	86	1.9
Jun-06	L5_DS_22A	548	9478	7788	1756	0.1	-4.6	5.7	10.3	1625	286	157	1.8
	L6_DS_5.55.5A	469	9947	8385	1633	0.7	-4.5	5.0	10.3	1567	312	153	2.0
	L7_DS_33A	385	10332	9149	1628	-0.1	-4.8	5.9	10.6	1602	271	152	1.8
	L8_DS_3.53.5A	511	10843	10584	1442	-1.3	-4.2	7.1	10.0	1431	203	144	1.4
	L9_DS_44A	624	11467	9675	1405	-1.5	-3.9	7.3	9.7	1361	187	141	1.3
	L10_DS_55A	1483	12950	12627	1558	-2.7	-5.6	8.5	11.4	1553	183	137	1.3
Aug-06	L1A_DS_1A1AA	143	8444	525	398	5.0	1.6	0.8	4.1	407	503	99	5.1
	L1_DS_11AA	486	8930	1898	1214	4.2	-4.4	1.6	10.1	1205	755	119	6.4
	L5_DS_22A	548	9478	7436	1641	1.3	-3.8	4.5	9.6	1623	360	169	2.1
	L6_DS_5.55.5A	469	9947	8460	1571	0.7	-4.4	5.1	10.1	1564	308	155	2.0
	L7_DS_33A	385	10332	9108	1621	0.2	-4.3	5.6	10.1	1594	285	158	1.8
	L8_DS_3.53.5A	511	10843	10513	1436	-1.3	-4.2	7.1	10.0	1434	202	144	1.4
	L9_DS_44A	624	11467	9247	1382	-1.1	-4.2	6.9	10.0	1386	201	139	1.4
	L10_DS_55A	1483	12950	12332	1556	-2.2	-5.9	8.0	11.6	1553	194	134	1.5
	L15_DS_66A	428	14321	16818	1784	-3.4	-9.3	9.2	15.1	1905	207	127	1.6
	L16_DS_77A	1333	15654	18163	1883	-4.5	-8.1	10.3	13.9	1879	183	135	1.4
	L17_DS_88A	2453	18107	20419	1978	-6.4	-13.2	12.1	19.0	1983	163	104	1.6
	L18_DS_99A	1892	19999	21083	1950	-6.6	-13.8	12.4	19.6	1950	157	100	1.6
	L19_DS_1010A	1802	21801	19421	1930	-7.5	-17.6	13.2	23.3	1922	145	82	1.8
	L20_DS_1111A	1791	23592	23448	2336	-8.2	-20.7	14.0	26.5	2299	165	87	1.9

Table 4.4: Summary of hydraulic geometry parameters and measures of channel form for lines on the Avon River from 1858 to August 2006 where available for mean tides. Distance = distance between lines, Total Distance = distance from head of tide on the Avon River. Refer to Table 3.4 for additional abbreviations.

a) Large Tides	**% Change in Cross Sectional Area Between Years**							
	1858 to 1969	**1969 to 1970**	**1969 to 1976**	**1976 to 2005**	**2005 to 2006**	**1858 to 2005**	**1969 to 2005**	**1969 to 2006**
L1A_DS_1A1AA					-10.1		-71.8 (±2.1)	-74.7(±1.9)
L1_DS_DS_11AA					-6.1		-50.8 (±1.3)	-53.8 (±1.2)
L5_DS_22A		-7.5			-1.8		-22.5 (±2.5)	-24.0 (±2.4)
L6_DS_2.52.5A					-1.9	-23.7		
L7_DS_33A	-1.5	-14.9			-2.8	-11.6	-10.3 (±4.4)	-12.8 (±4.3)
L8_DS_3.53.5A					-0.9	4.1		
L9_DS_44A		1.5			0.5		-13.7 (±8.2)	-13.3 (±8.1)
L10_DS_55A		-1.5			0.1		-10.5 (±2.4)	-10.4 (±2.4)
L11_DS_5.55.5A					0.0		-0.3 (±0.0)	
L15_DS_66A	1.6		4.4	-1.8	0.2	4.3	2.6 (±3.9)	2.7 (±3.9)
L16_DS_77A	10.8		-4.5	0.9	-0.2	6.7	-3.7(±1.9)	-4.0 (±1.9)
L17_DS_88A	3.7		-1.8	3.9	0.3	5.7	2.0	2.3
L18_DS_99A	0.5		-3.1	5.0	-1.0	2.3	1.8	0.7
L19_DS_1010A	1.0		-0.5	1.9	-0.2	2.4	1.4	1.2
L20_DS_11A	0.9		0.9	1.6	-0.5	3.4	2.5	2.0
b) Mean Tides	**% Change in Cross Sectional Area Between Years**							
	1858 to 1969	**1969 to 1970**	**1969 to 1976**	**1976 to 2005**	**2005 to 2006**	**1858 to 2005**	**1969 to 2005**	**1969 to 2006**
L1A_DS_1A1AA					-24.2		-89.1 (±1.1)	-91.8 (±0.8)
L1_DS_DS_11AA					-14.1		-68.4 (±0.9)	-72.8 (±0.8)
L5_DS_22A		-9.3			-2.5		-28.5 (±2.7)	-30.3 (±2.6)
L6_DS_2.52.5A					-1.8	-23.9		
L7_DS_33A	2.3	-18.6			-3.6	-11.7	-13.7 (±5.3)	-16.7 (±5.1)
L8_DS_3.53.5A					-1.1	9.1		
L9_DS_44A		-2.3			0.4		-20.9 (±13.7)	-20.5 (±13.5)
L10_DS_55A		-1.7			0.1		-12.4 (±2.7)	-12.3 (±2.6)
L11_DS_5.55.5A					0.0		-0.4 (±0.0)	
L15_DS_66A	1.8		5.9	-2.3	-1.5	5.3	3.5 (±4.6)	1.9 (±4.6)
L16_DS_77A	9.8		-4.6	0.4	0.7	5.1	-4.2(±1.9)	-3.6 (±1.9)
L17_DS_88A	3.8		-3.3	4.7	0.4	5.1	1.3	1.6
L18_DS_99A	-5.5		-2.5	3.7	0.0	-4.4	1.1	1.1
L19_DS_1010A	0.4		-0.5	2.1	-0.1	2.0	1.6	1.5
L20_DS_11A	0.6		0.3	2.1	0.0	3.0	2.4	2.4

Table 4.5: Percent change in cross sectional area between years along the Avon River. Negative values indicate a decrease in area (e.g. siltation or marsh growth) whereas positive values indicate an increase in cross sectional area. Values in brackets represents the seasonal variability in the data where applicable. Data are presented for a) Large Tides and b) Mean Tides.

Line	Distance from head of tide (m)	Distance from causeway (m)	R^2	F ratio	P value
L1A_DS_1A1AA	8444	143	0.983	176.029	**0.006**
L1_DS_DS_11AA	8930	471	0.996	849.649	**0.001**
L5_DS_22A	9478	1019	0.890	49.442	**0.001**
L6_DS_2.52.5A	9947	1488	0.996	741.979	**0.010**
L7_DS_33A	10332	1873	0.086	1.655	0.246
L8_DS_3.53.5A	10843	2384	0.958	22.161	***0.042**
L9_DS_44A	11467	3008	0.616	10.630	**0.022**
L10_DS_55A	12050	4491	0.928	65.731	**0.001**
L11_DS_5.55.5A	13893	5434	NA	NA	NA
L15_DS_66A	14321	5862	0.024	1.148	0.333
L16_DS_77A	15654	7195	0.164	2.176	0.200
L17_DS_88A	18107	9638	0.433	4.058	0.137
L18_DS_99A	19999	11540	0.396	3.628	0.153
L19_DS_1010A	21801	13342	0.255	2.369	0.221
L20_DS_11A	23592	15133	0.495	4.918	0.113

*Table 4.6: Results of ordinary least squared linear regression of changes in cross sectional area over time for large tides using Systat ^{tm}. Bold indicates statistical significance at the 95% confidence interval. * indicates significant increase in cross sectional area. All other significant values indicate decrease in area.*

The formation of the large intertidal bar did have an affect on increasing the wetted perimeter. By Line 8, the present day bed elevation is very similar to that in 1858 (Figure 4.2j). The eastern shore has retreated by approximately 100 m since 1858 and a new mudflat is developping along the western shore. This has resulted in a small, but statistically significant increase in the cross sectional area (9%) by deepening the main channel (Tables 4.5, 4.6).

Line 9 (Fig 4.3l) clearly depicts the extensive mudflat and expanding salt marsh which has developed on the western shore after the channel thalweg shifted in 1973 (Fig 4.3n). Once again there is an example of cyclicity in the location of the marsh edge along the western shore, with recession of around 85 m from 1858 to 1969/1970 followed by 335 m of progradation. The new mudflat is approximately 6.1 m deep (Fig 4.3l). Conversely, the bed of the new channel has lowered by 3.5 m (measured at 600 m from post 4). The thalweg closest to the old wharf at 4A has maintained a relatively constant bed elevation (Fig4.3l) and position (Fig4.3n), most likely since 1858 judging by the chart. Changes in cross sectional area are statistically significant (14 to 21%) from 1969 to 2006 (Tables 4.5, 4.6), however, seasonal variability alone in the intertidal cross sectional surveys ranges from 8 to 14%.

Line 10 (Fig 4.2m) shows very little change in the overall form of the cross sectional profile, with new marsh developing along the western shore and gradual accumulation of an intertidal bar along the eastern edge. This bar however remains quite low and represents about 2.3 m of accumulation. The bed elevation in the centre of the channel in 2005/2006 is the same as it was in 1858. There has been about a 10-12% (±2.5%) decrease in intertidal cross sectional channel area (Table 4.5) since 1969 which is statistically significant at the 95% confidence level (Table 4.6).   However the wetted perimeter, w/d, and D/d ratio show very little change.

Line 11 is quite stable, with negligiable change in cross sectional area since 1969. The salt marsh near Mitchener Point (Fig 1.2) has receeded by about 75 m back to the cliff line (Fig 4.3r) since 1858. Line 15 (Fig 4.3p), located downstream of the confluence of Avon and Kennetcook Rivers, depicts very little change in cross sectional area or form. The 1858 and 1976 data points lie almost perfectly along the existing bed level. The salt marsh depicted in the 1858 chart appears to have been eroded on the western shore while pockets remain on the eastern shore. Aerial photographs (Fig 4.3r) illustrate the relative stability of the location of the main channel thalwegs and which is reflected in the intertidal cross sectional area comparisons. A 4 to 6% increase in area was measured between 1969 and 1976, and then a decrease was measured to 2006. The result from 1969 to 2005 is a general increase (3 to 3.5%)(±4%) in cross sectional area and intertidal cross sectional area (Tables 4.5, 4.6), and is essentially deepening as the thalweg on the eastern edge continues to incise. Line 16 (Fig 4.2q) depicts a very similar trend and only 4%(±2%) decrease in cross sectional area and associated intertidal cross sectional area (Table 4.5).   The decrease is associated with an intertidal bar starting to develop along the eastern section of the profile (Fig 4.3r). This bar is not a new feature, rather it is the tail end of the Shad Bar (Figure 1.1) which periodically welds to the shoreline and is visible on aerial photographs since the 1960s and in the bathymetric data from both 1858 and 1976 (Fig 4.3q).

After line 17, there is a small increase in intertidal cross sectional area of around 2% since 1969 and 6% from 1858 (Table 4.5). The 1976 survey points fall right on the 2005/2006 survey profiles. Past this point, the minimum elevation of the two main channels is below the LLWLT and has been decreasing since 1969 (Fig 4.2a).   The changes in bed elevation (e.g. ~ 4 m increase 1200 m from post 8 since 1858) occur below that level. This deepening is observed on lines 18-20 with 100 m of cliff recession estimated on the western shore of Line 19. The intertidal cross sectional area increases from between 2 to 3.5 % (Table 4.5).   Line 19 shows evidence of the migration of the crest of an intertidal

bar (Fig 4.2v) yet minimal nearshore lowering. Line 20 has deepened (2.5%) since 1969 although is now at the same level as it was in 1858 and 1976 (Fig 4.2w).

4.1.3 Description of Changes in the Kennetcook River

Along the Kennetcook river there appears to have been a general increase in cross sectional area and deepening of the channel (Fig 4.4a-c; Table 4.7). The width of the river has decreased by about 150 m, most notably on Line 13 through marsh erosion (Fig 4.4b). The 1858 chart depicts what appears to be either a causeway or a dyke which passes through a small bedrock core island (Fig 4.4d). As this position cannot be verified, and as other evidence was not found for its existence during this research, it was excluded in the prism analysis. The main thalweg of the channel in 1858 does however appear to be located along the opposite shore from the present day.

a) Kennetcook River - Large Tides

Date	Line	Distance between	total dist	A_i	pw	H	Hmin	d	D	w	w/d	w/D	D/d
Oct-69	L12_K1K1a			6408	744	-1.5	-6.8	7.3	12.6	739	101	59	1.7
Dec-05	L12_K1K1a			6723	753	-1.3	-7.9	8.9	15.4	744	84	48	1.7
	L13_K2K2a			3916	480	-3.5	-8.2	11.0	15.8	362	33	23	1.4
	K14_K3K3a			8754	837	-3.5	-8.4	11.0	15.9	831	75	52	1.4
Aug-06	L12_K1K1a			6748	745	-2.2	-7.9	9.7	15.5	739	76	48	1.6
	L13_K2K2a			3924	349	-3.6	-8.1	11.2	15.7	355	32	23	1.4
	K14_K3K3a			8767	833	-3.5	-5.5	11.1	13.1	833	75	64	1.2

b) Kennetcook River - Mean Tides

Date	Line	Distance between	total dist	A_i	pw	H	Hmin	d	D	w	w/d	w/D	D/d
Oct-69	L12_K1K1a			5066.3	676	-1.5	-6.8	7.3	12.6	676	93	54	1.7
Dec-05	L12_K1K1a			5210.3	699	-1.3	-7.9	7.1	13.6	695	98	51	1.9
	L13_K2K2a			3101.2	370	-3.5	-8.2	9.2	14.0	339	37	24	1.5
	K14_K3K3a			7070.1	814	-3.5	-8.4	9.2	14.1	829	90	59	1.5
Aug-06	L12_K1K1a			5230.1	677	-2.2	-7.9	7.9	13.7	676	85	49	1.7
	L13_K2K2a			3113	344	-3.6	-8.1	9.4	13.9	339	36	24	1.5
	K14_K3K3a			7309.5	819	-3.5	-5.5	9.3	11.3	805	87	72	1.2

Table 4.7: Summary of hydraulic geometry parameters and measures of channel form for lines on the Kennetcook River from 1858 to August 2006 where available for a)large and b) mean tides. Distance = distance between lines, Total Distance = distance from head of tide on the Avon River. Refer to Table 3.4 for additional abbreviations.
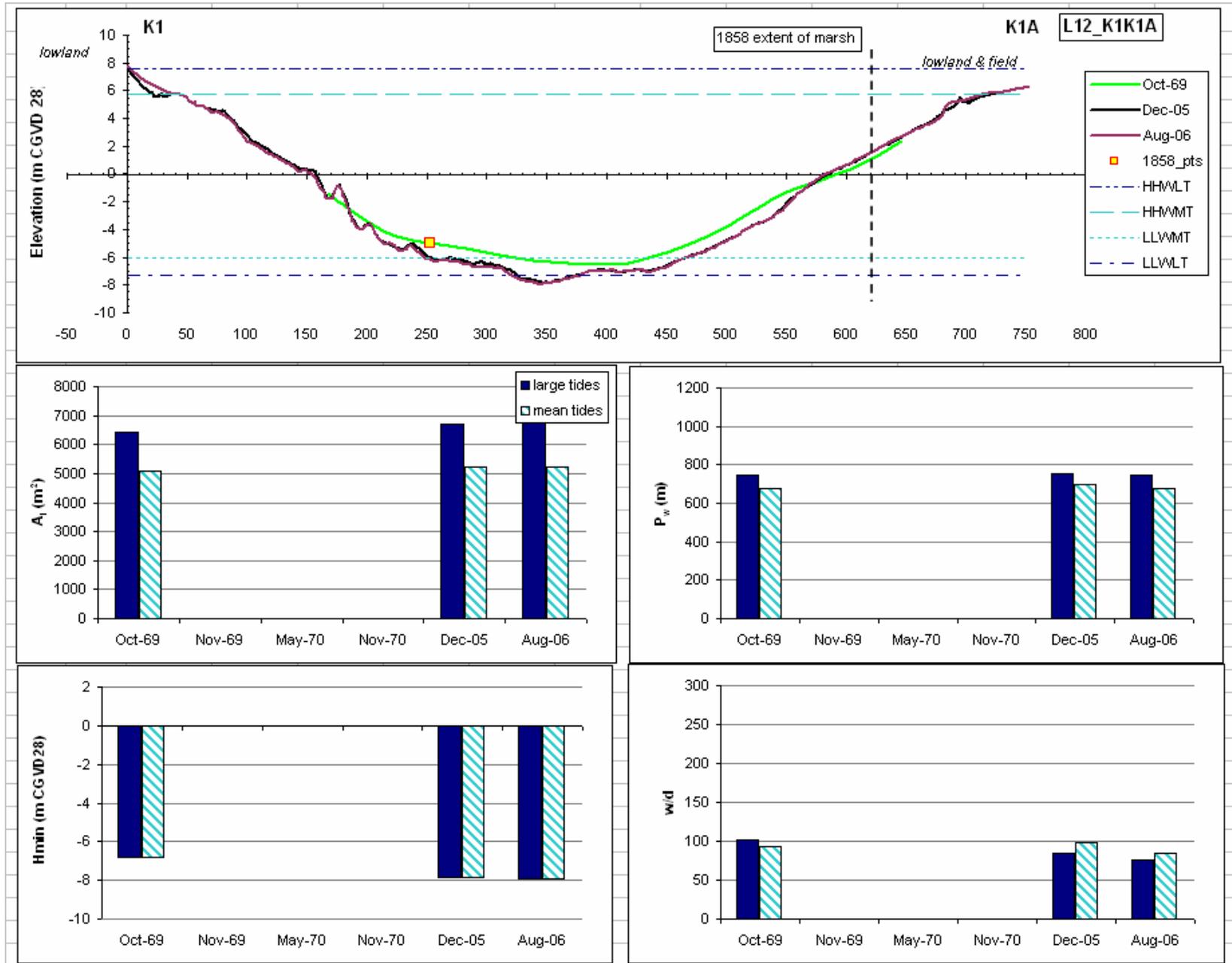
Figure 4.4a: Cross sectional profile for Line12_DS_K1K1A and associated hydraulic geometry parameters along the Kennetcook River. Vertical exaggeration on cross sectional profile = 42.5. Distance on cross sectional profile in metres. The section of the profile near K1A could not be extended further due to the extensive lowland area adjacent to it.
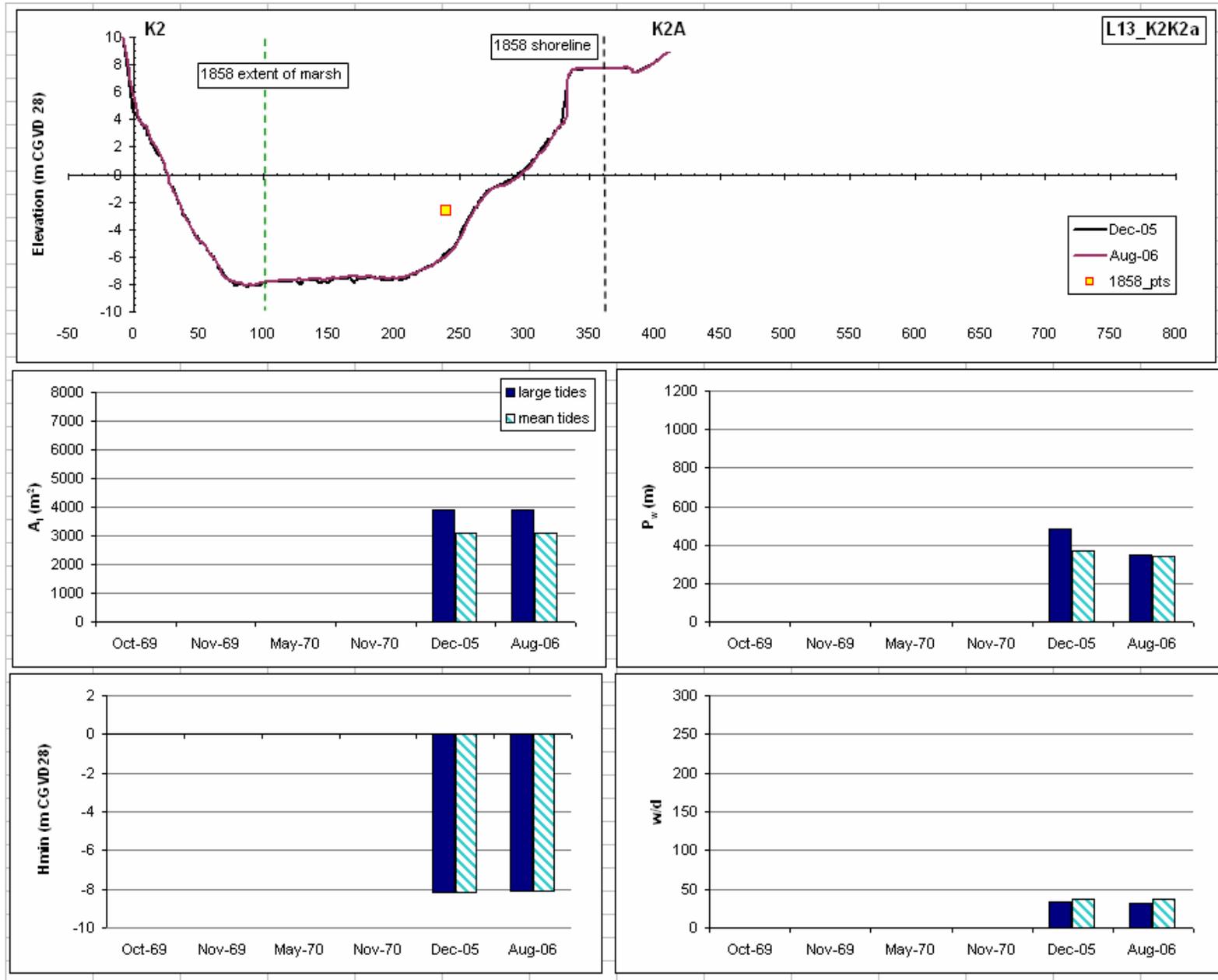
Figure 4.4b: Cross sectional profile for Line13_DS_K2K2A and associated hydraulic geometry parameters along the Kennetcook River. Vertical exaggeration on cross sectional profile = 42.5. Distance on cross sectional profile in metres.
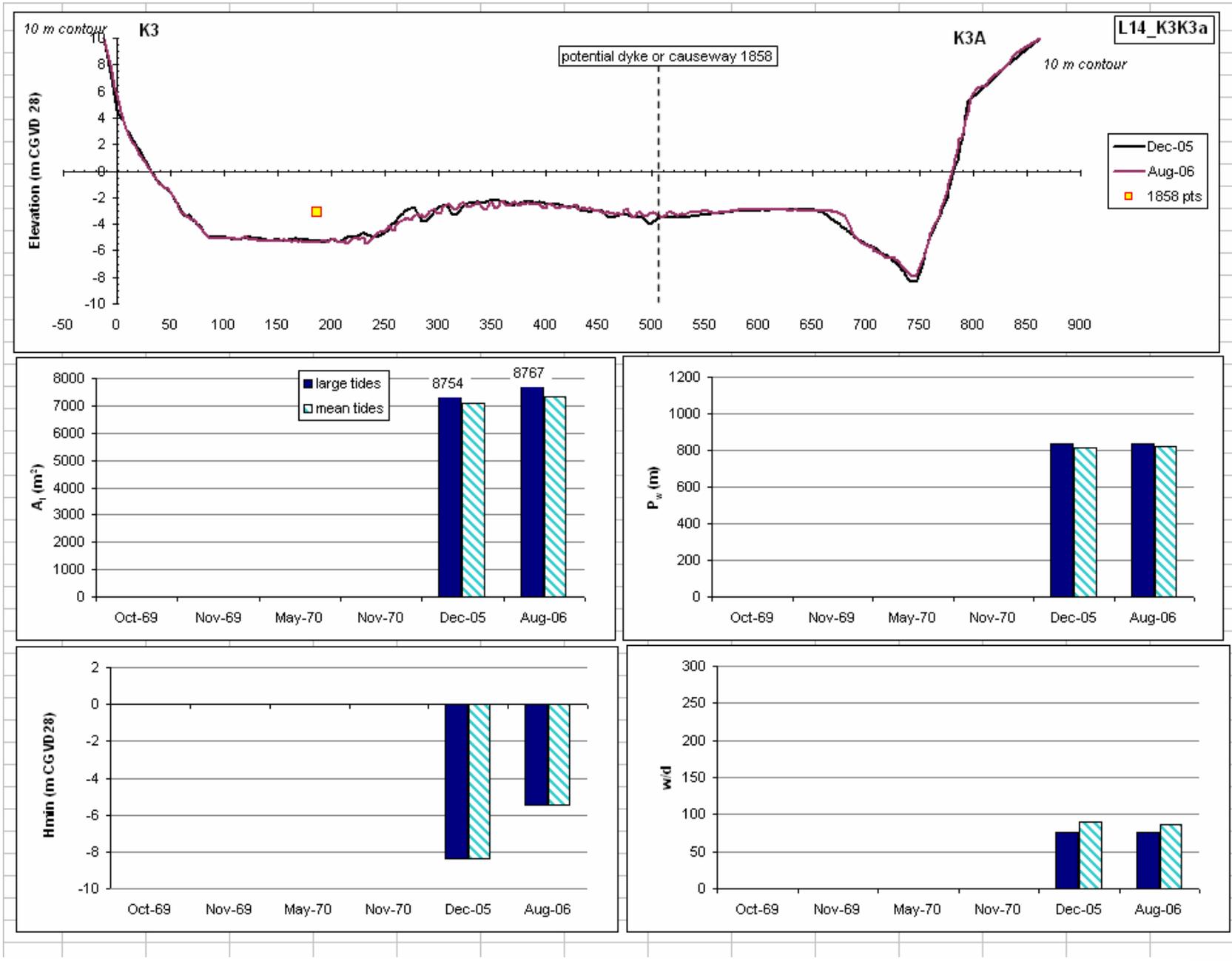
Figure 4.4c: Cross sectional profile for Line14_DS_K3K3A and associated hydraulic geometry parameters along the Kennetcook River. Vertical exaggeration on cross sectional profile = 42.5. Distance on cross sectional profile in metres. Note potential dyke or causeway that was visible on 1858 map. The position or existence of this dyke could not be verified and however since the thalweg was indicated as being along the opposite shore, it is possible.
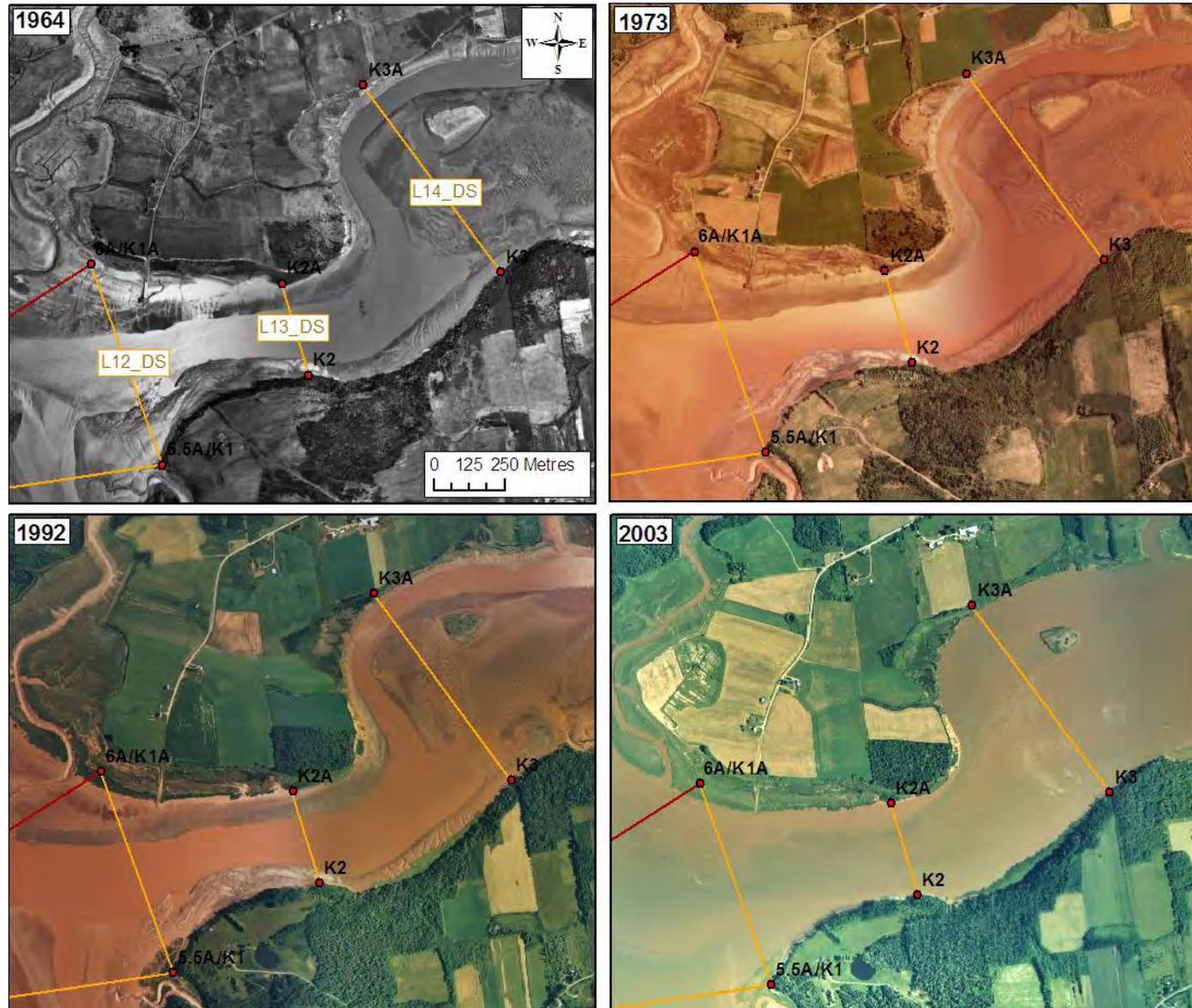
Figure 4.4d: Location of downstream survey lines 12, 13 and 14 on the Kennetcook River.

4.1.4   *Downstream Changes in Cross Section Form along the Avon River*

All of the hydraulic geometry parameters for each line were plotted against distance from the former tidal head of the Avon River (Fig. 1.2) near Windsor Forks and are presented in Figures 4.5 to 4.7.   In general, there is an increase in the intertidal channel cross sectional area with increasing distance from the head of the estuary for both large (Fig 4.5a), and mean tides (Fig 4.6a). The shape of the curve is quite similar for all lines and years including 1858 with the exception of lines within the first 1500 m downstream of the causeway after its construction.   In that region the difference is quite marked. Surveys conducted after the causeway was completed in July 1970 tend to have lower cross sectional areas until the Kennetcook river. After this point, the rate of change decreases but there is a general increase in intertidal cross sectional area per year.

The width of the Avon River increases very rapidly in the first 1500 m until just downstream of where it is joined by flows from the St. Croix River (Fig 4.5d and 4.6d) after which time there is a sharp decrease in width until Line 9, 3000 m downstream (Table 7; Fig 18c). This corresponds to the area in which numerous intertidal bars (e.g. Newport Bar) split the flow into two smaller channels and new marsh growth has been recorded along the western bank (Fig 11a, 16e-h). This splitting also causes an increase in the wetted perimeter (Fig 19a).   A more gradual increase in channel width continues beyond the Kennetcook and remains relatively constant until line 10 at the mouth of the Avon River. There are no significant differences in the shape of the curves from 1969 to 2005. There is however a marked variation in both wetted perimeter and width in 1858 for large tides (Fig 4.5c,d), likely associated with removing marsh area due to dyking.

Both minimum bed elevation relative to CGVD28 datum and mean bed elevation exhibit a general decreasing trend with increasing distance from the causeway (Fig 4.5e,f). Most of the variability in bed elevation levels out after the first 2000 m from the causeway. Lowest elevations were recorded in November 1969 (up until Line 16) and those recorded in June and August 2006 were similar to or lower than those recorded in the 1970s (Fig 4.5e) with the exception of the first 500 or so metres downstream of the causeway. Beyond Line 16, minimum bed elevations in 2006 are lower than those in 1969 or 1858.   Directly adjacent to the causeway, there is more than a 5 m difference in the minimum bed elevation. However, after this point the minimum bed elevation has remained at almost the same level since 1969 (with the exception of the decrease in November 1969) (Fig 4.5e).
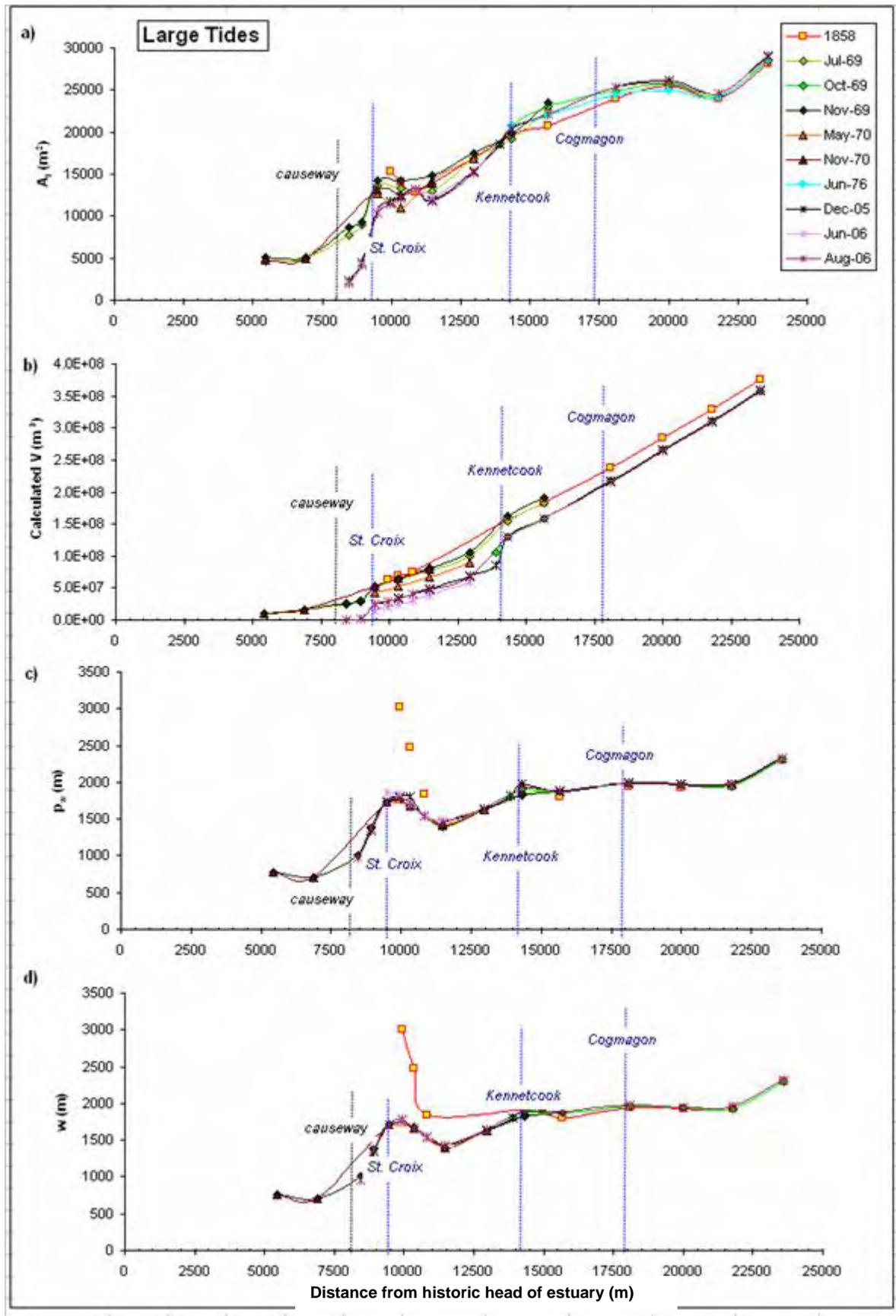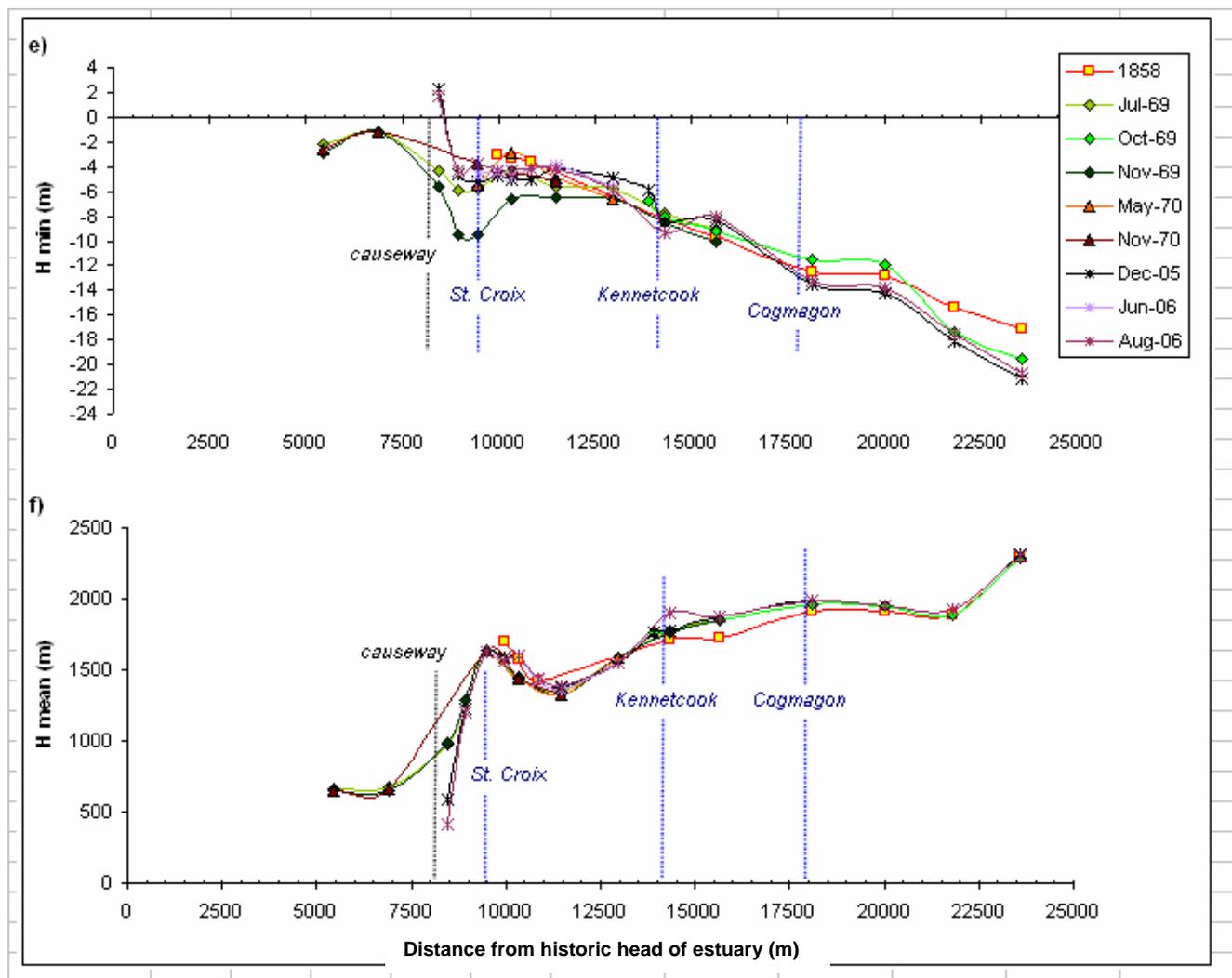
Figure 4.5: Downstream changes in channel form parameters for large tides for a) intertidal cross sectional area; b) tidal prism; c) wetted perimeter; d) width; e) minimum bed elevation (m CGVD28) and f) mean elevation (m CGVD28). Historic head of the Avon River estuary is located approximately 8 km upstream of the Windsor causeway.
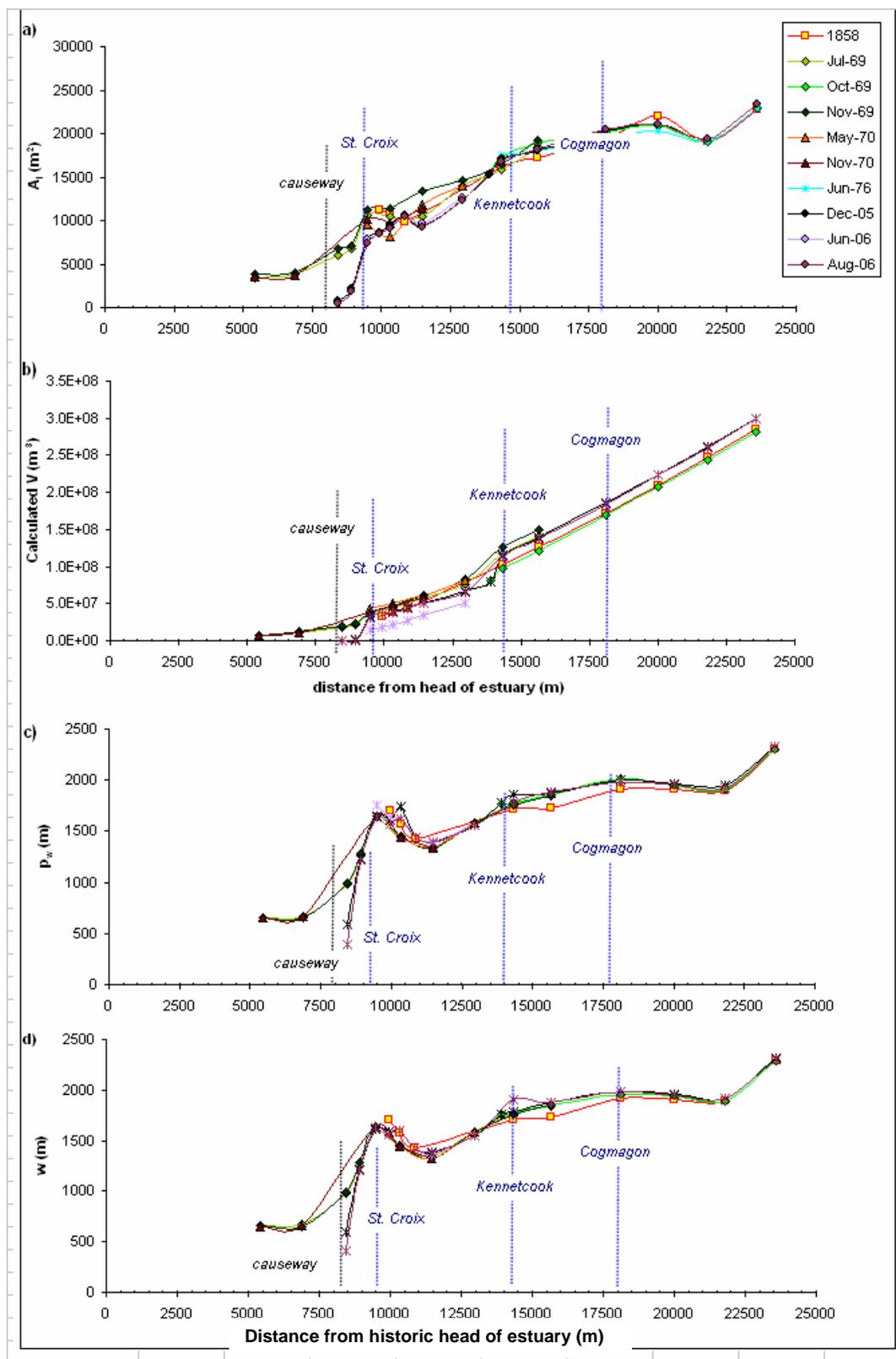
Figure 4.6: Downstream changes in channel form parameters for mean tides for a) intertidal cross sectional area; b) tidal prism ; c) wetted perimeter and d) width
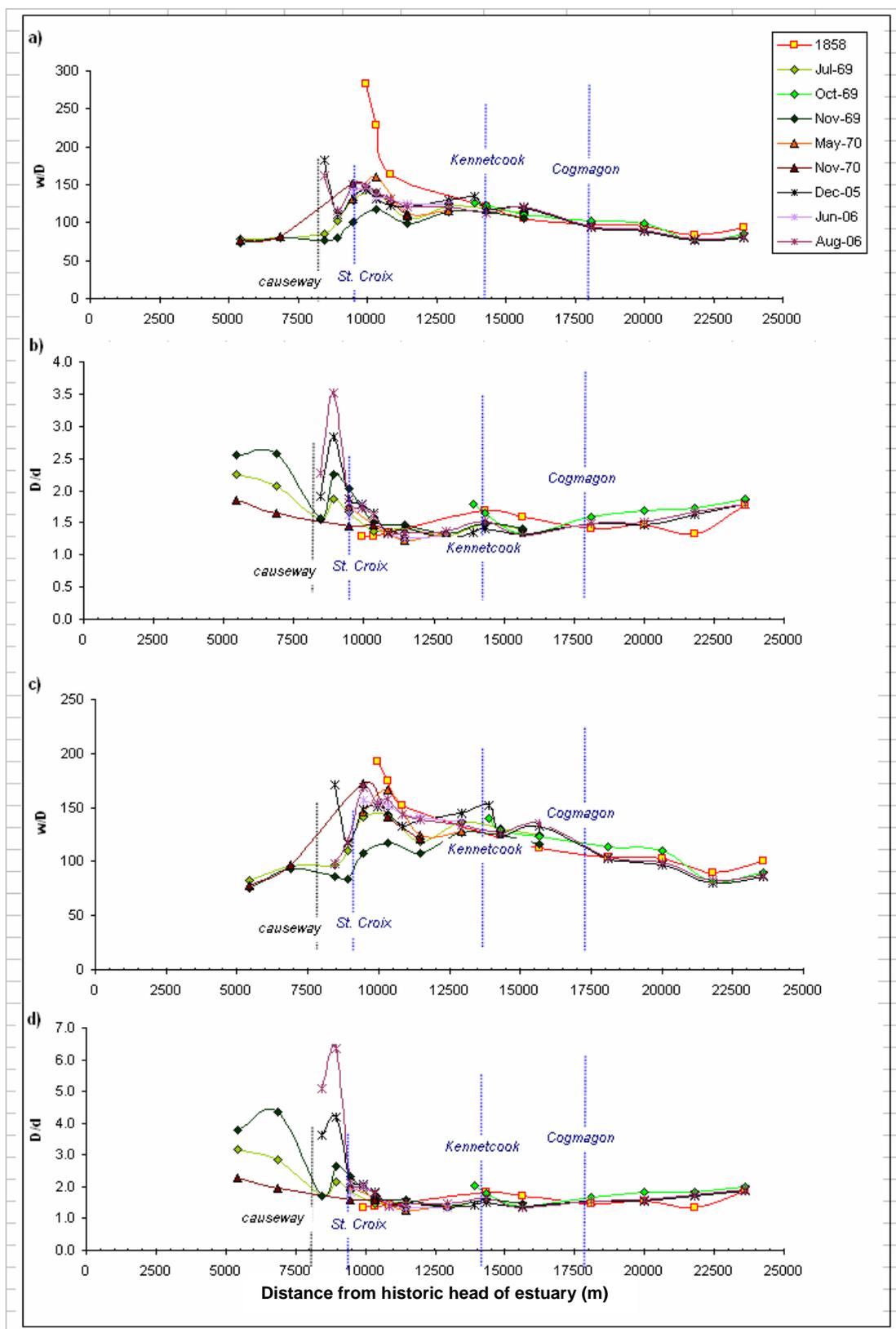
Figure 4.7: Downstream changes in channel form ratios for large tides a) width/min depth; b) min depth / mean depth and mean tides; c) width/min depth; d) mind depth/mean depth.

The mean bed elevation however has increased noticeably within the first 1000 m of the causeway which is seen as the large mudflat and marsh system which has developed (Fig 4.3g) downstream of the structure. An additional area of accumulation occurs around 3000 m downstream reflecting the growth of an extensive mudflat and new marsh along the western shore (Fig 4.3k,m). Figure 4.7 effectively illustrates two pivot points around which there are marked changes in channel cross sectional form. Based on the w/d and D/d ratios, this pivot point occurs around the 1000 m downstream of the causeway (or ~9500 m from head of estuary) mark at Line 5 where the St. Croix River joins the Avon (Fig 4.3f, 4.7). The second point occurs close to Line 7, 10.5 km downstream from the head of the estuary and primarily affects the 1858 curve for large tides. Upstream of that point there has been extensive dyking. The mean tide curve is not affected since it is below the level of most marshes that would have been dyked. Beyond this point, all of the survey dates display a very similar, gradually decreasing trend with increasing distance. This maintenance of channel form is particularly evident in examining the D/d ratios (Fig 4.7b,d).

4.1.4. Downstream Changes in Tidal Prism

Using the tidal prism results generated from the GIS, one can examine the influence of removing a portion of the tidal prism on the overall curve. In general, the tidal prism increases as one moves further down the estuary. After the construction of the causeway, the prism was reduced by about 7 % (Table 4.8), and this effect was then carried down the estuary (Fig 4.8a). If this amount was subtracted from the total prism for 1969 and 1858, then the resultant curve would represent changes in the tidal prism due to factors downstream of the causeway. Figure 4.8b shows that there is very little variation in the slope or position of the line once the upstream value has been removed.

a) HHWLT (7.57 m CGVD28)

Year	Full Tidal Prism (m^3 x 10^{-6})	upstream causeway (m^3 x 10^{-6})	St. Croix (m^3 x 10^{-6})	Kennetcook (m^3 x 10^{-6})
1858	376.8	21.2	19.6	24.5
1969	349.5	19.3	15.3	31.3
2005	324.5		17.8	37.2
% change				
1858 to 1969	-7.3	-9.0	-22.0	27.8
1969 to 2005	-7.2	-100.0	16.1	18.9

b) HHWMT (5.77 m CGVD28)

Year	Full Tidal Prism (m^3 x 10^{-6})	upstream causeway (m^3 x 10^{-6})	St. Croix (m^3 x 10^{-6})	Kennetcook (m^3 x 10^{-6})
1858	282.0	10.5	8.3	15.8
1969	269.1	13.3	9.9	22.3
2005	248.3	0.0	12.0	28.1
% change				
1858 to 1969	-4.6	27.2	19.5	41.8
1969 to 2005	-7.7	-100.0	21.3	26.0

Table 4.8: Change in tidal prism and contribution from upstream Avon, St. Croix and Kennetcook Rivers for a) large tides (7.57. m geodetic) and b) mean tides (5.77 m geodetic)
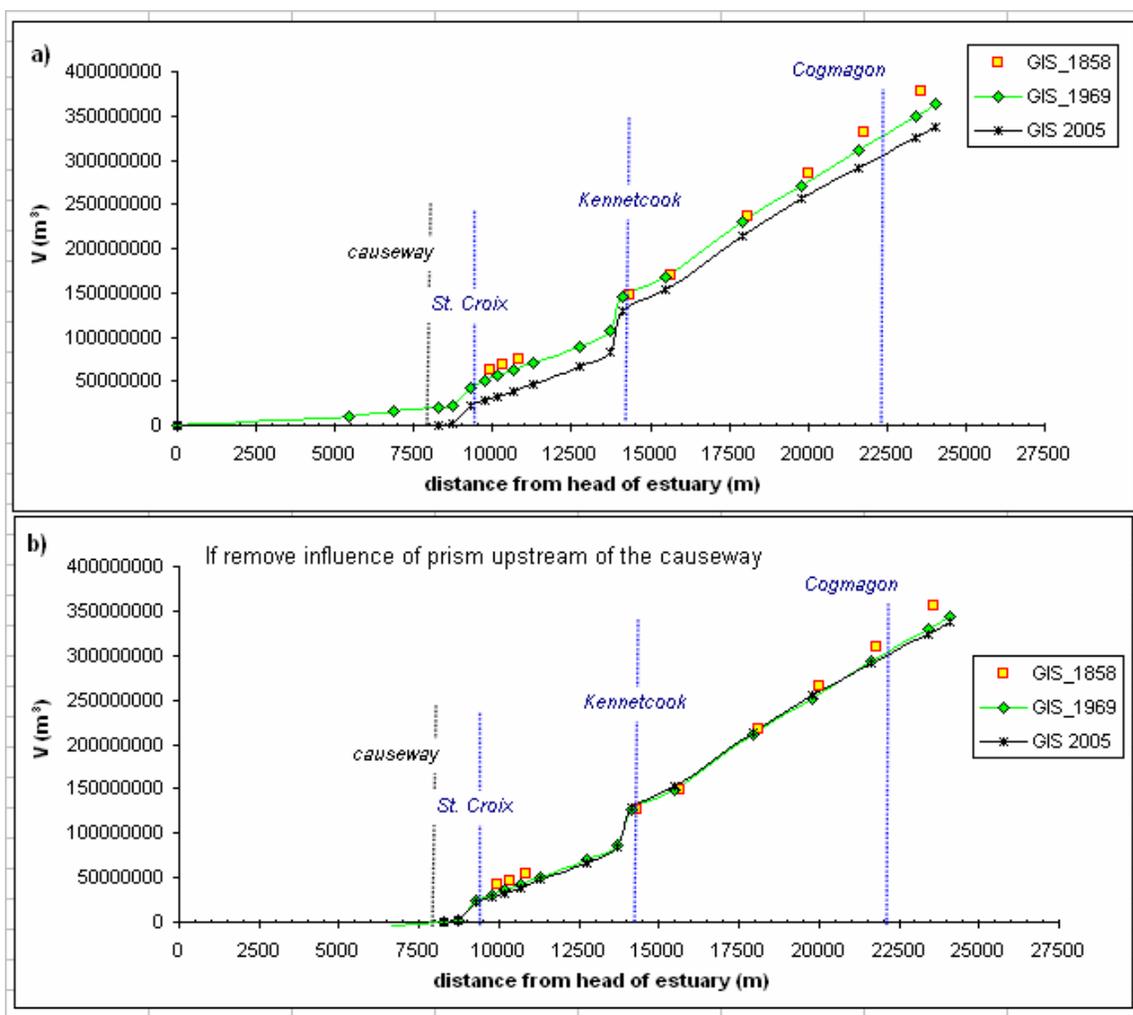
Figure 4.8: change in tidal prism calculated from GIS analysis with increasing distance from head of the Avon River for a) full tidal prism and b) volume of prism 'lost' upstream of the causeway removed.
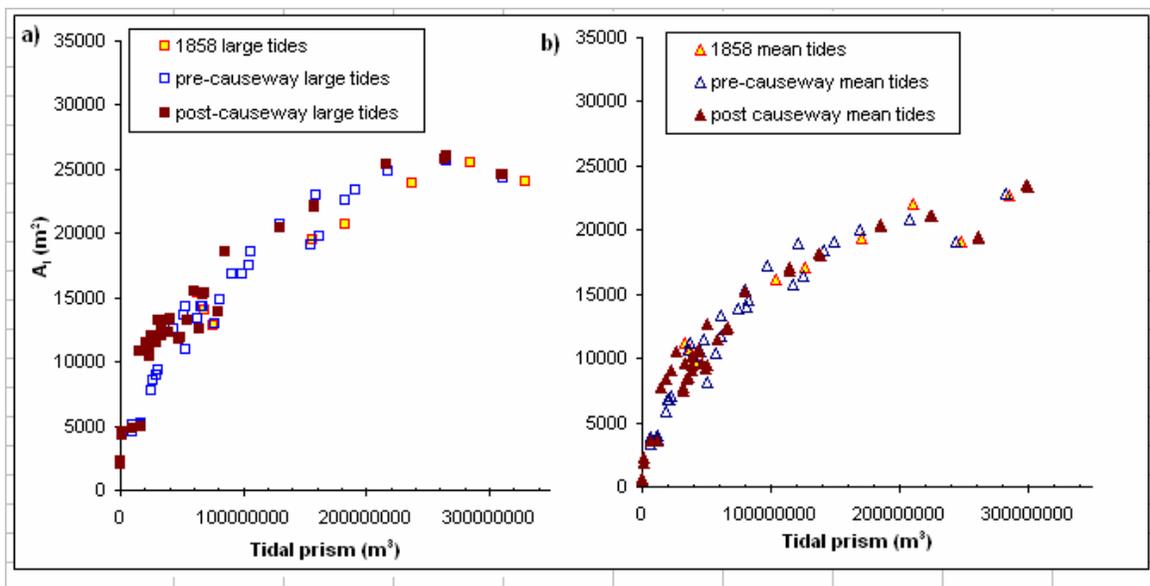
Figure 4.9: Change in intertidal cross sectional area as a function of the tidal prism for a) large (7.57 m) and b) mean (5.77m) tides.

Plotting cross sectional area versus tidal prism pre and post causeway also does not show a large difference in the position of the curve (Figure 4.9).

One of the main issues to be examined within this report is how the estuary has responded to a change in the volume of the tidal prism associated primarily with construction of the Windsor causeway. The basic assumption is that a homogeneous estuary will be in an equilibrium state when no long-term changes in cross sectional area take place (Bray et al., 1982). This indicates that the bed shear stress is approximately uniform over the estuary, and for this situation one assumes that the tidal velocity is essentially uniform at all cross sections. This can be expressed by calculating and examining a characteristic constrant for the estuary (parameter '*a*') and was used by Bray et al. to assess the effects of the construction of the Peticodiac causeway.

[1] $$a = \frac{AT}{\tilde{V}}$$

Where A = cross sectional area below the reference tide elevation (e.g. HHWLT)
V = corresponding volume passing the section
T = time during which the tide is flowing through the channel (or total innundation time)
a = characteristic constant for the estuary.

The variable 'T' was calculated using *FloodMetric 0.5* and the appropriate digital elevation model and CHS tide data exported from *Tides and Currents* software for Hantsport at 1 min intervals for the 2:01 am AT tide on March 21, 2007. These data are then plotted with distance from the head of the tide (Figure 4.10) for both pre and post causeway construction. *"Values from 'a' that deviate from average values for an estuary in equilibrium suggest the presence of some constraint due to a geological control or the works of man" (Bray et al., 1982 p. 299).* Values of 'a' deviate significantly at lines 1 and 1A (*a* = 244 and 606 respectively), and to a lesser extent after the St. Croix joins the Avon River until around 11000 m from the head of the estuary (~ 7.2 km downstream of the causeway), after which there is no difference. This parameter can also be used to estimate the point at which the estuary is dominated by fluvial or estuarine processes. In the Avon system, this occurs approximately 11 km from the head of the estuary, about mid way between the St. Croix and the Kennetcook Rivers (Fig 4.10b).

Digital elevation models were created for 1858, 1969, and 2005 (Fig 4.11). Most of the change between 1858 and 1969 occurred mostly in the central portion of the estuary and deepening of the channels on either side (Fig 4.11c). These channels continued to incise between 1969 and 2005 despite

considerable accretion and bar development .   The St. Croix and the Kennetcook are both lowering in bed elevation.
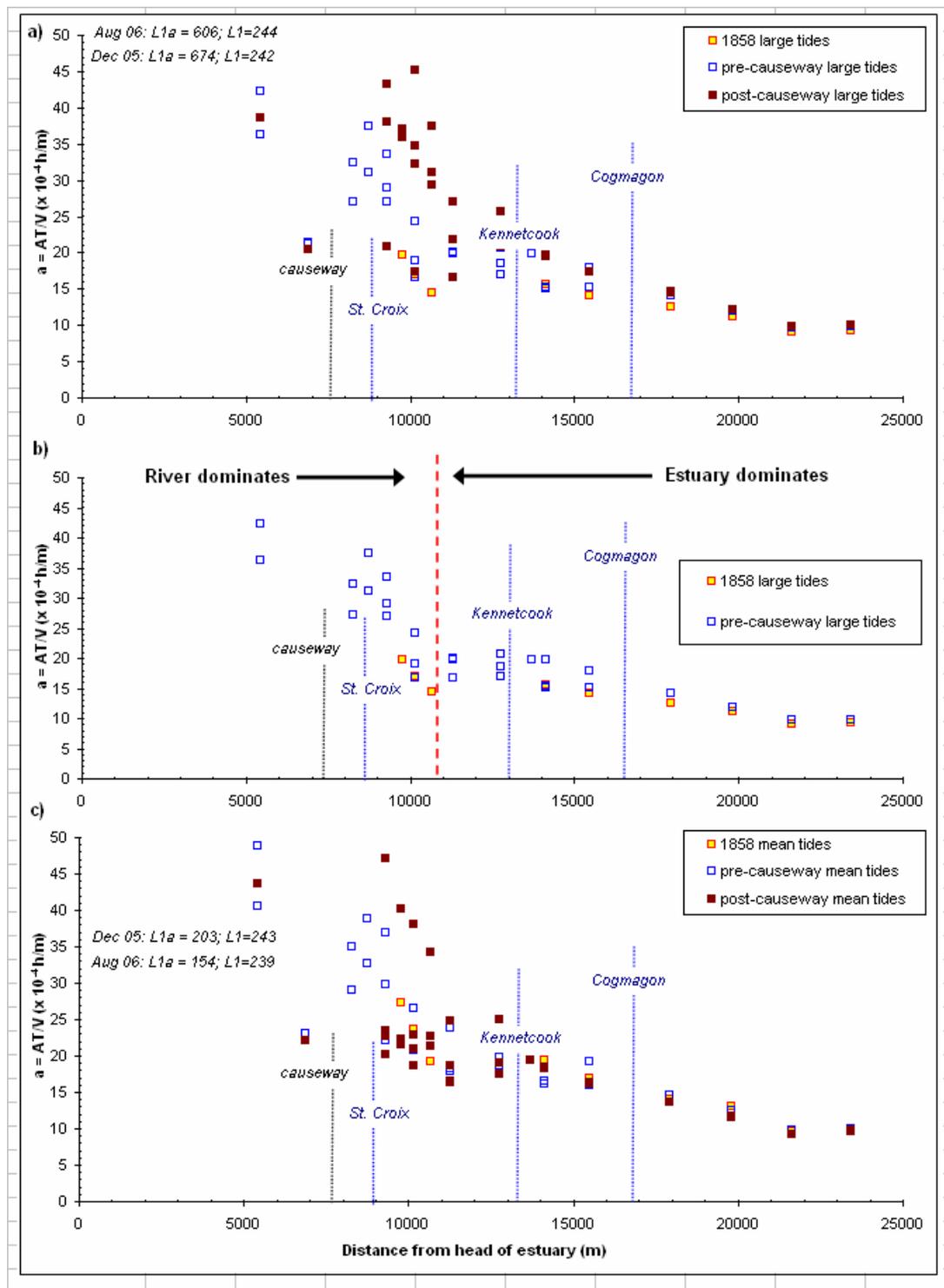
Figure 4.10: Variation in parameter 'a' (=AT/V) (Bray et al., 1982) with distance from head of tide for a) large tides pre and post causeway; b) pre-causeway large and mean tides and c) mean tides pre and post causeway. A = intertidal cross sectional area, V = tidal prism above cross section and T = length of time during which there is tidal water in the channel
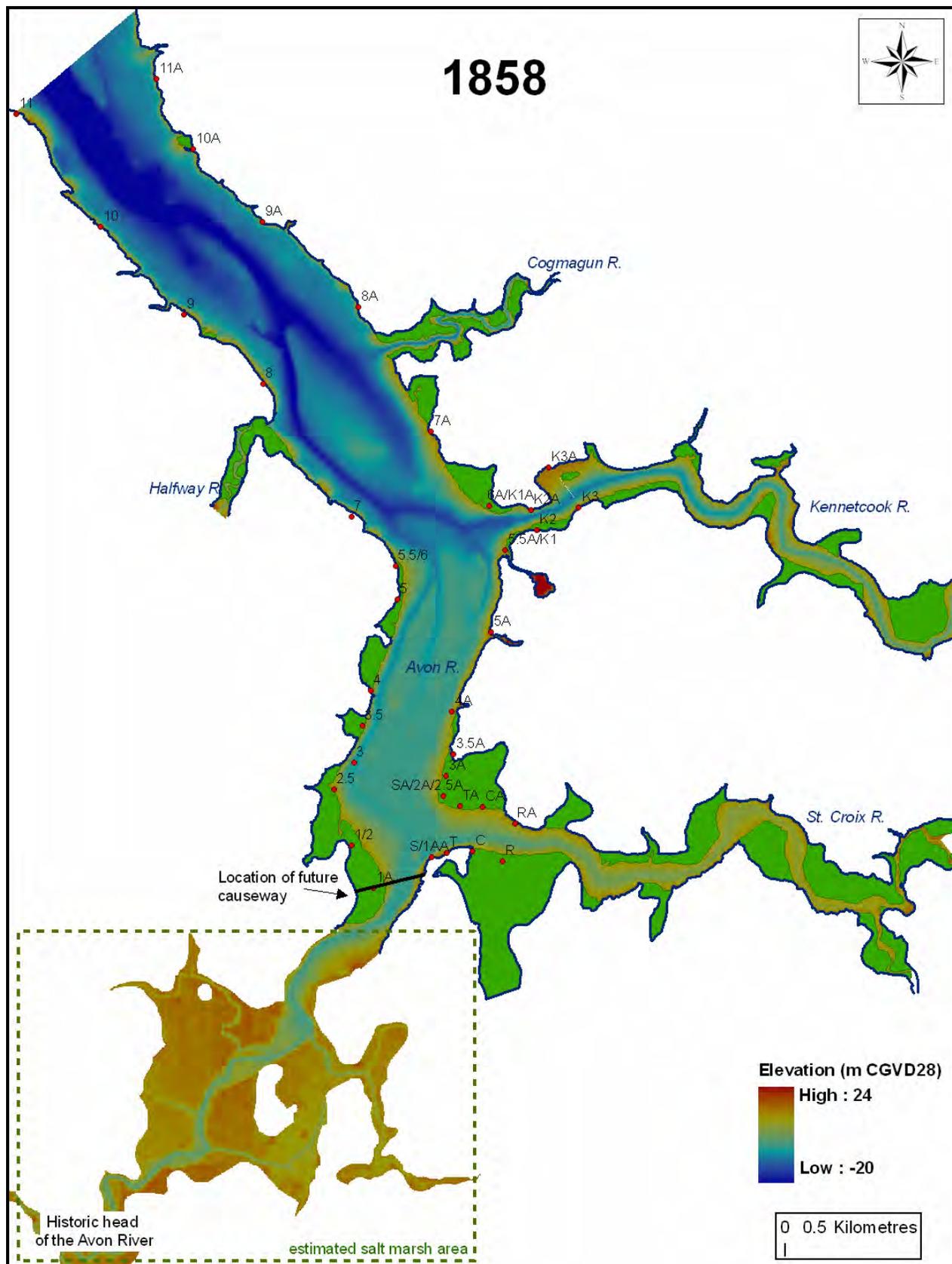
Figure 4.11a): Digital elevation model generated for 1858 for full tidal prism. Note that the areas upstream of the causeway are estimate values since no data were available. Marsh areas are in green and survey posts are provided for reference. Dyked marshes are not shown.
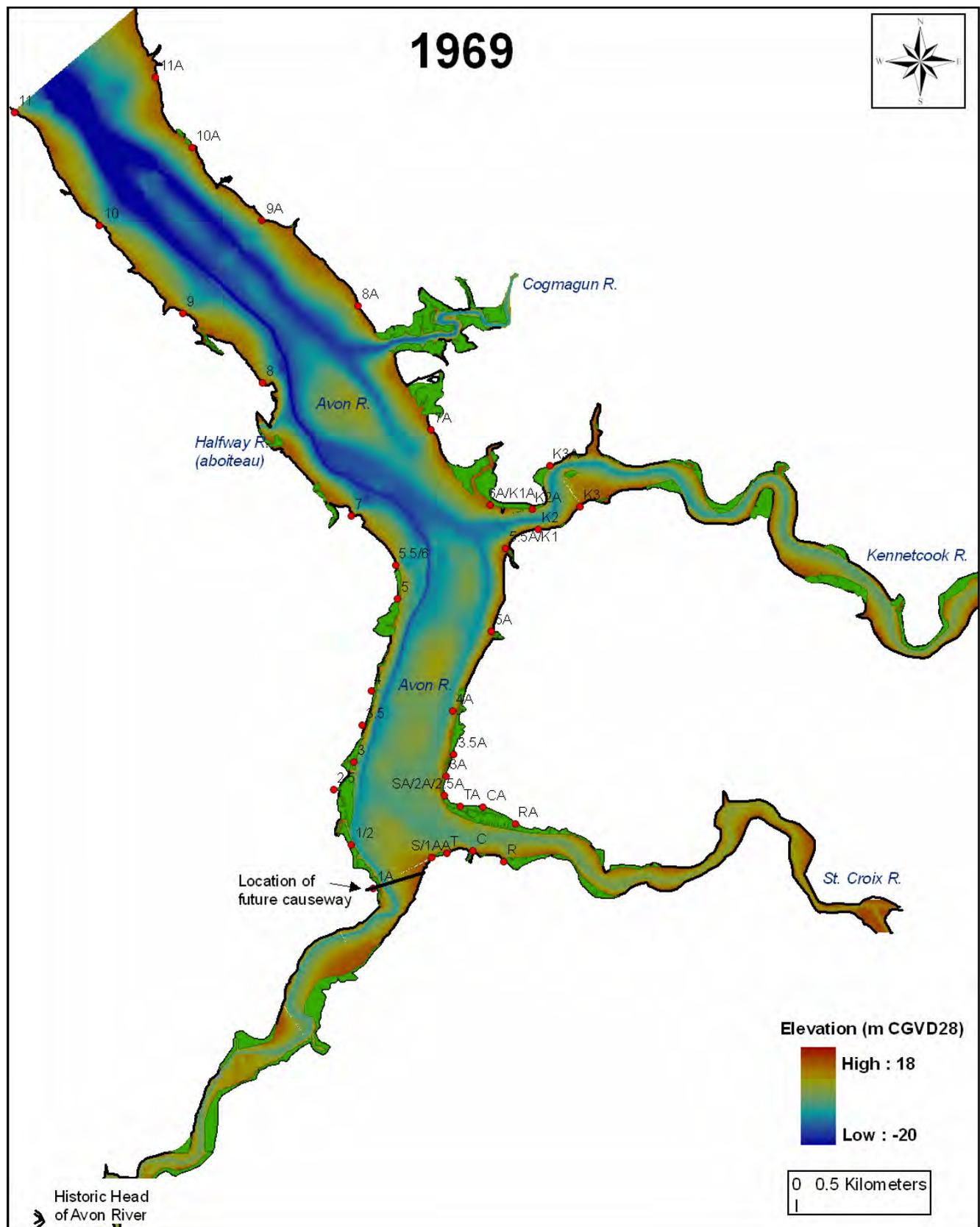
Figure 4.11b): Digital elevation model generated for 1969 for full tidal prism. Marsh areas for 1964 are in green and survey posts are provided for reference. Salt marsh in green. Dyked marshes excluded.
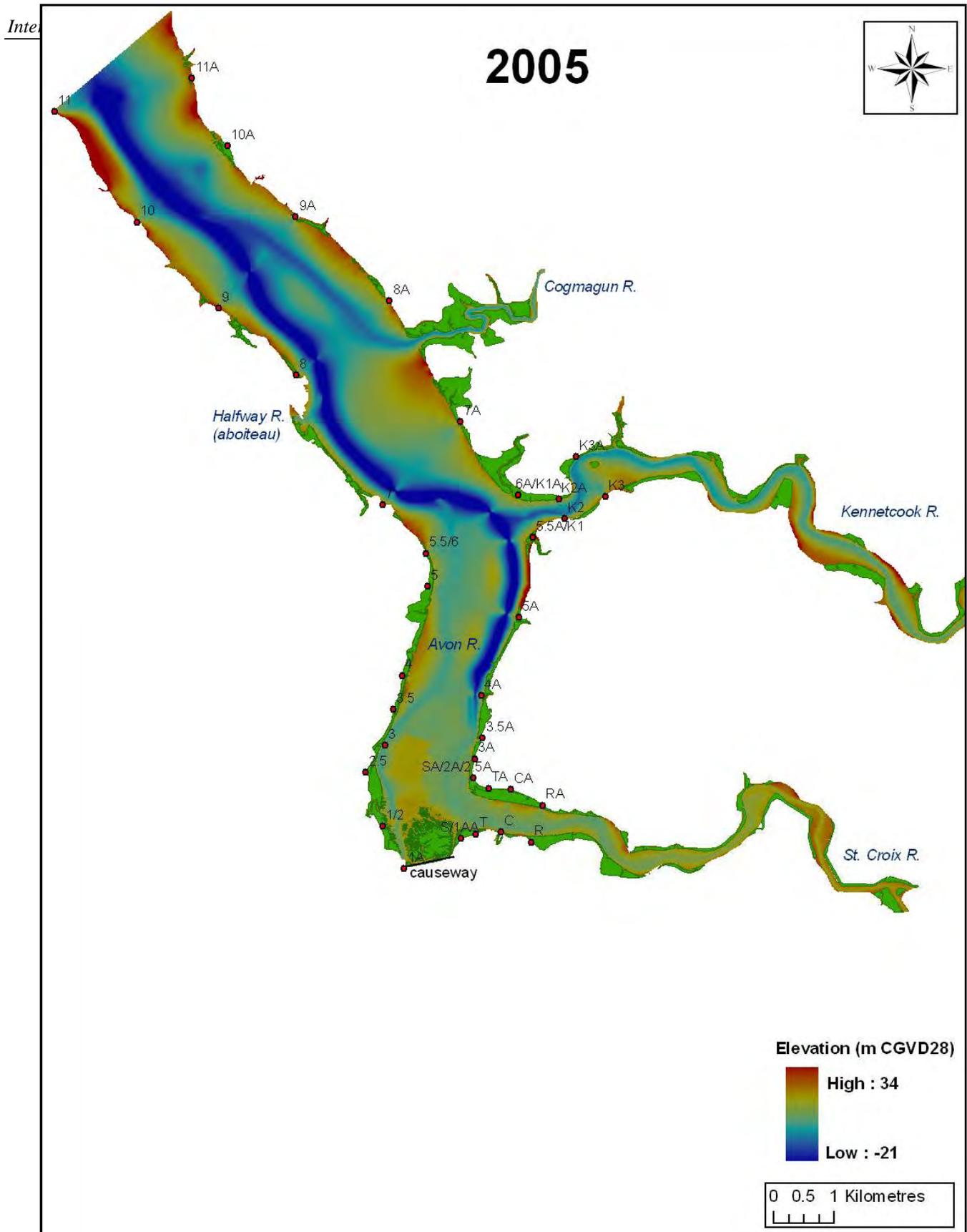
2005

Figure 4.11c): Digital elevation model generated for 2005 for full tidal prism. Marsh areas for 2003 are in green and survey posts are provided for reference.

4.2 Salt Marsh Habitat

The air photo mosaics and digitized salt marsh polygons were examined within the ArcGIS environment. Marsh area is expressed as a percentage of the total prism area or common prism area (Table 4.9a,b). Two scenarios are provided for 1858, with or without estimated salt marsh upstream of the causeway. This is due to the lack of reliable data in the area and position of dykes in 1858 (Table 4.9c). In general, there is an overall decrease in marsh area from 1858 to 1964 with the exception of 1955 (Table 4.9). Over the following decade however the percentage of marsh area remains constant at around 11 % and begins to increase slightly in 1992. By 2003, the proportion of the Avon River study area covered by salt marsh vegetation had increased and exceeded 1955 levels, however, it did not exceed the 1858 levels (Table 4.9b). If the upstream section for 1858 is included, there is a consistant decrease in the percentage of marsh area from 1858 to 1992, increasing to 16% in 2003 and 18% in 2007 with new marsh growth at the causeway. In order to distinguish between marsh 'lost' due to natural processes such as channel migration and dyking, the marsh area was divided into two sections, in front and behind the dyke. Overall there was an 87% loss of salt marsh from 1858 to 1955 (including upstream of the causeway) and an additional 13% loss from 1955 to 1964. It is estimated that 11% of the proportion of marsh loss was due to 'natural causes' and 89% due to dyking. This value however should be interpreted with caution due to the poor reliability of the 1858 data upstream.

a) Full tidal prism at HHWLT	1858	1944	1955	1964	1973	1992	2003	2007
Planimetric area of full tidal prism (km^2)	62.17	446.45	44.30	43.99	39.95	39.95	39.95	39.95
Prism clipped to mosaic area if needed	49.60	18.59	14.53	43.96	39.95	34.99	39.95	35.03
Marsh area within clipped prism (km^2)	12.02	1.90	1.96	4.02	3.66	2.78	4.59	3.78
Marsh area (% of prism)	24	10	13	9	9	8	11	11

b) Common prism at HHWLT (excludes upstream 1858)	1858	1944	1955	1964	1973	1992	2003	2007
Common prism area (km^2)	13.93	9.71	9.53	9.25	8.69	8.75	8.75	8.75
Marsh area (km^2)	5.19	1.04	1.53	0.94	1.05	1.13	1.57	1.80
Marsh area (% of common prism)	37	11	14	10	12	13	18	21

c) common prism at HHWLT (includes upstream 1858)	1858	1944	1955	1964	1973	1992	2003	2007
Common prism area (km^2)	27.98	NA	14.68	14.37	10.44	10.48	10.48	10.48
Marsh area (km^2)	14.93		1.96	1.68	1.11	1.20	1.66	1.89
Marsh area (% of common prism)	53		13	12	11	11	16	18

*Table 4.9: Marsh area calculated for each aerial photo mosaic. **A)** marsh areas are presented as a % of the marsh area contained within the area that is flooded at HHWLT clipped to the area covered by the air photo mosaic. It does NOT include estimate salt marsh upstream of the causeway; **b)** same as in 'a' however restricted to only the 'common' spatial area for all years (Figs 4.13 – 4.16) and **c)** including the estimated 9.8 km^2 of marsh upstream of the causeway assuming no dykes are present.*

In order to examine the influence of dyking, hypsometric curves were calculated using *FloodMetrics 0.5*. The hypsometric curve illustrates the planimetric area flooded, and volume of water above a raster Digital Elevation Model (DEM) for a given elevation value (Figure 4.12). The planimetric area is calculated by determining whether the height value of each pixel is equal to or less than the given elevation interval. If the pixel is lower than the given interval (water level), the area of that pixel is calculated by squaring the cell size. The sum of all areas for all flooded pixels is equal to the planimetric area covered. The process is repeated for each elevation interval. There is an approximate 54% greater amount of area in 1858 than 1969 which occurs primarily above the HHWMT line, therefore is most likely associated with dyking of salt marsh (Figure 4.12). This will then essentially act as a 'wall' forcing a more rapid increase in area for each increment of elevation in subsequent years (Figure 4.12). Examination of the 2005 curve shows that under the LLWLT level, for every increment of elevation, there is a comparatively larger planimetric area which represents the deeper channel in those areas. Interestingly, the LLWLT mark appears to be a pivot point above which there is comparatively smaller planimetric area for each increase in elevation when compared to both 1969 and 1858 (Figure 4.12). This is likely due to the presence of intertidal sand bodies and growth of mudflats along the Avon River.
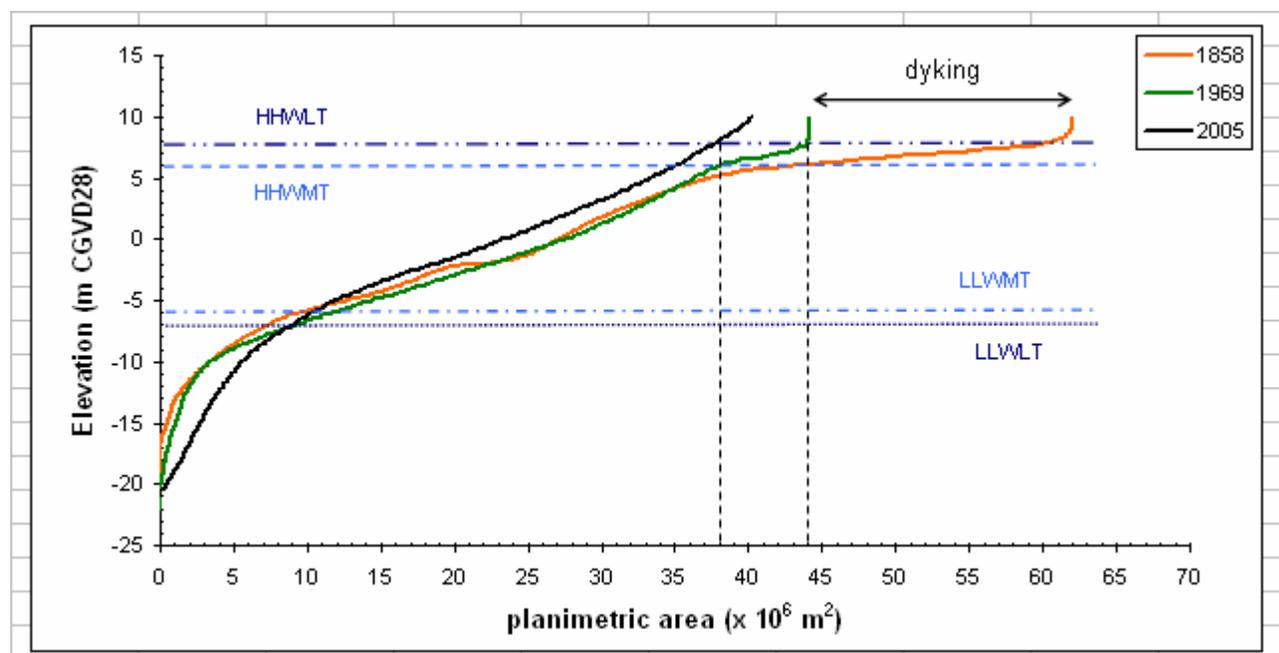
Figure 4.12: Comparison of hypsometric curves with change in planimetric area associated with change in elevation for the 1858, 1969 and 2005.

Figures 4.13 to 4.29 depict the change in intertidal geomorphology (as viewed on aerial photographs) and marsh habitat since 1858. ASTER and IKONOS satellite imagery are also included to help track the location of the main intertidal features. Survey posts as well as modern dykes and roads are included on all figures for references. The most notable change in salt marsh area occurred between 1858 and 1944 when extensive salt marshes were dyked for agriculture (Fig 4.13). These would become the future MMRA marsh bodies: Tregothic marsh (NS68), Armstrong marsh (NS75), Elderkin marsh (NS14), and Newport Town marsh (NS27). From 1944 to 1955, there was a large expansion of marsh habitat along both the Avon (west bank) and St. Croix (north bank) Rivers (Fig. 4.14). If measured as a straight line distance from 1944 along Line 6 (post 2.5), there was approximately 295 m of marsh growth on the Avon River and 80 m of growth along Line 3 (post TA) on the St. Croix. Very little change was observed elsewhere, except some loss of salt marsh due to dyking. Marsh area decreased from 1955 to 1964 along the river edge with erosion (~35 m) initiated along the western shore near post 2.5, likely associated with increased bank erosion from the developing channel evident in Figure 4.15. However, during this period a number of dykes were constructed along the western shore which cut off areas of marsh from tidal flow (Fig 4.15).

From 1964 to 1973, the erosion trends along the western bank of the Avon River continued, and new erosion was initiated on the north shore of the St. Croix River between Lines 1 and 2 (Fig 4.16). However, the southern bank of the St. Croix along the same lines saw about 16 m of new marsh growth. The main river thalweg is quite visible on the air photograph along the north shore of the St. Croix, swinging over to the western shore of the Avon River, joining with flows coming down the Avon through the Windsor tide gate. A mudbank becomes evident along the eastern edge near post SA/2A. The mudflat adjacent to the causeway continues to grow in size although there is still a defined channel running along the causeway itself. The mudbank observed in the 1973 air photo has facilitated the expansion of approximately 60 m of marsh vegetation by 1992 (Fig 4.17) when compared to the 1964 levels.
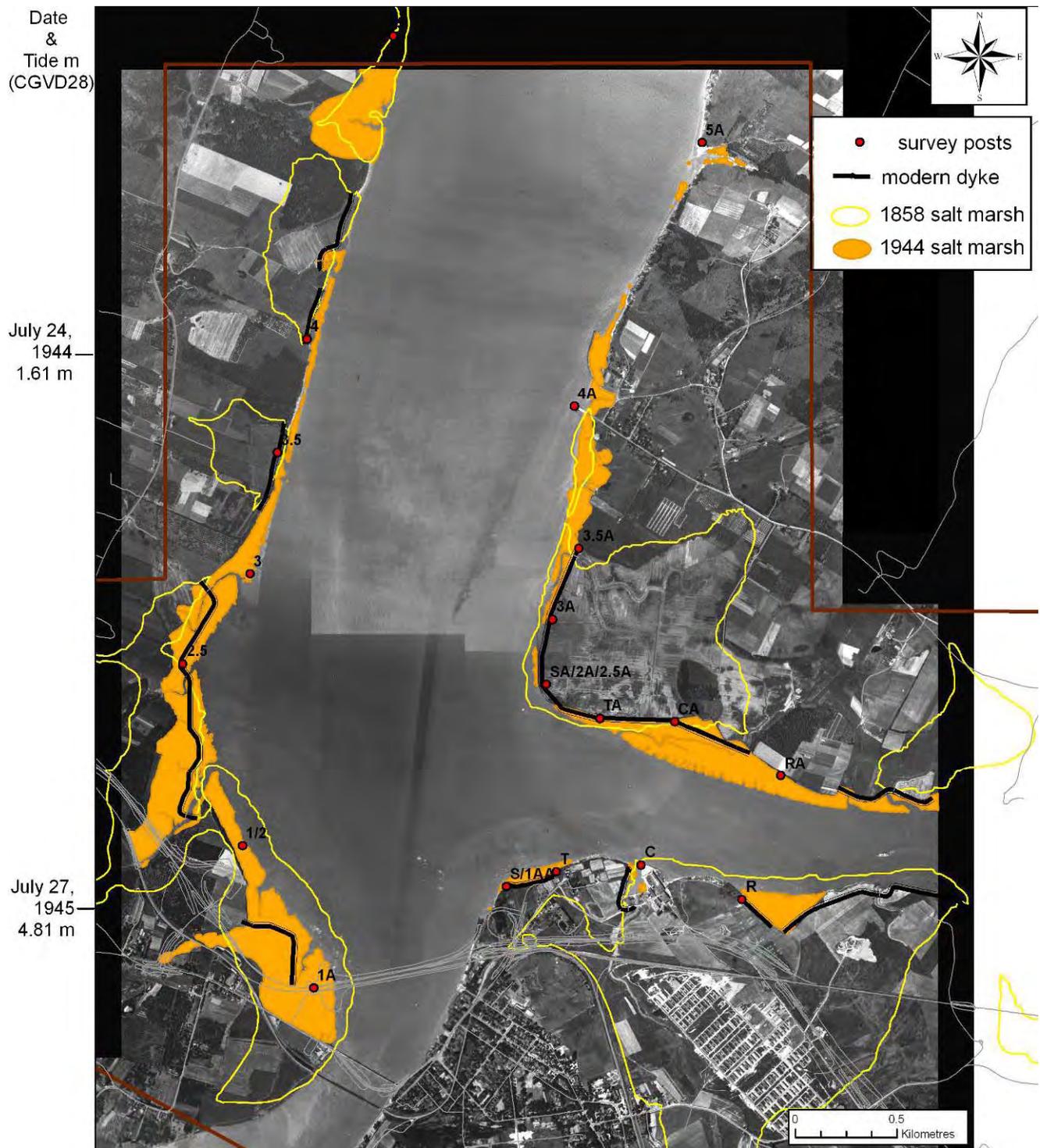
Figure 4.13: Digitized marsh polygons from 1858 and 1944 overlain on a 1944 aerial photograph. Tide level is just below level of the marsh. Note significant change in marsh area due to dyking. Dyke lines(post 1950-1960s) and roads represent present day for reference.
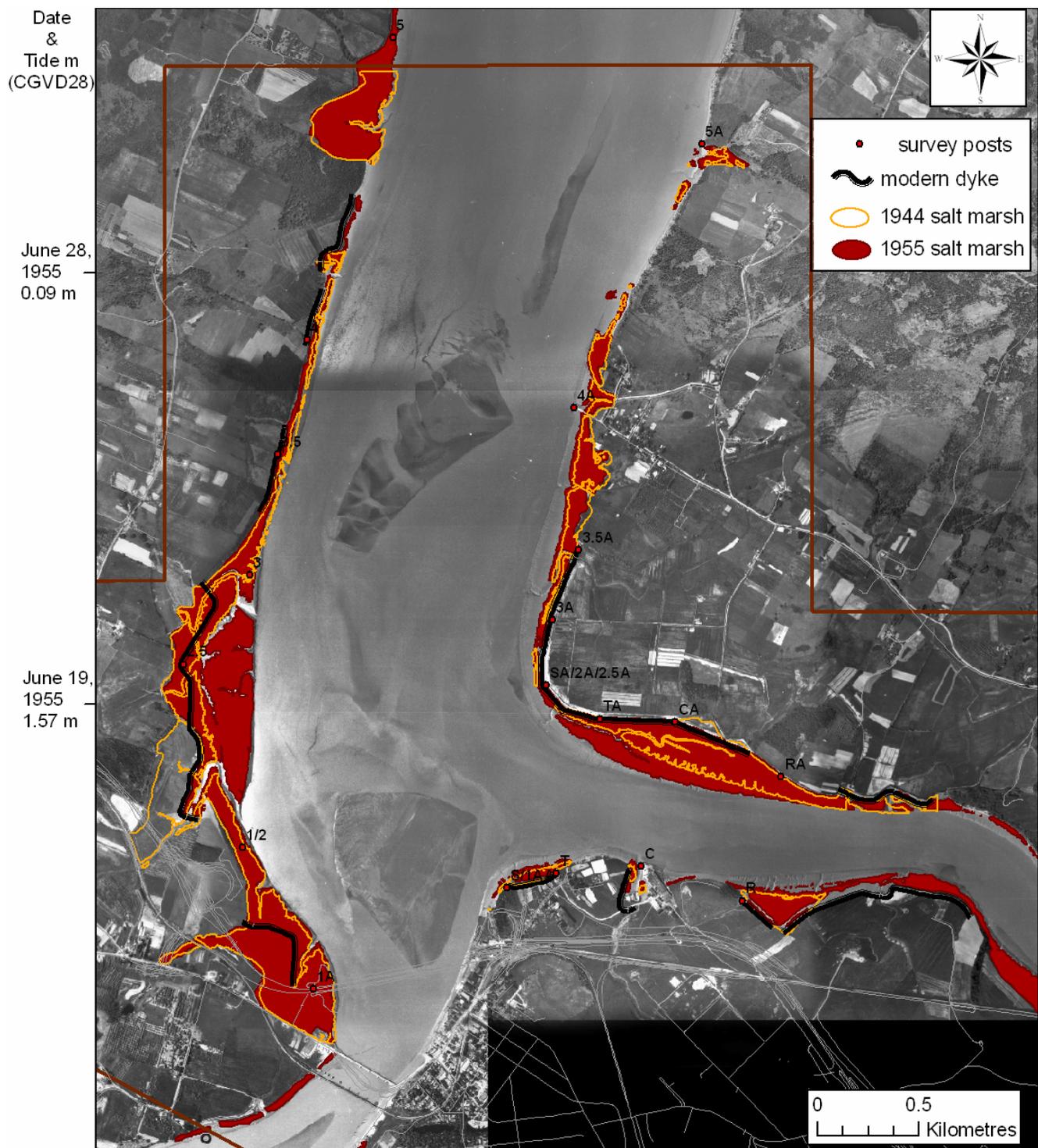
Figure 4.14: Digitized marsh polygons from 1944 to 1955 overlain on a 1955 aerial photograph. Note expansion of marsh particularly on the west bank of the Avon River near post 2.5 Dyke lines(post 1950-1960s) and roads represent present day for reference.
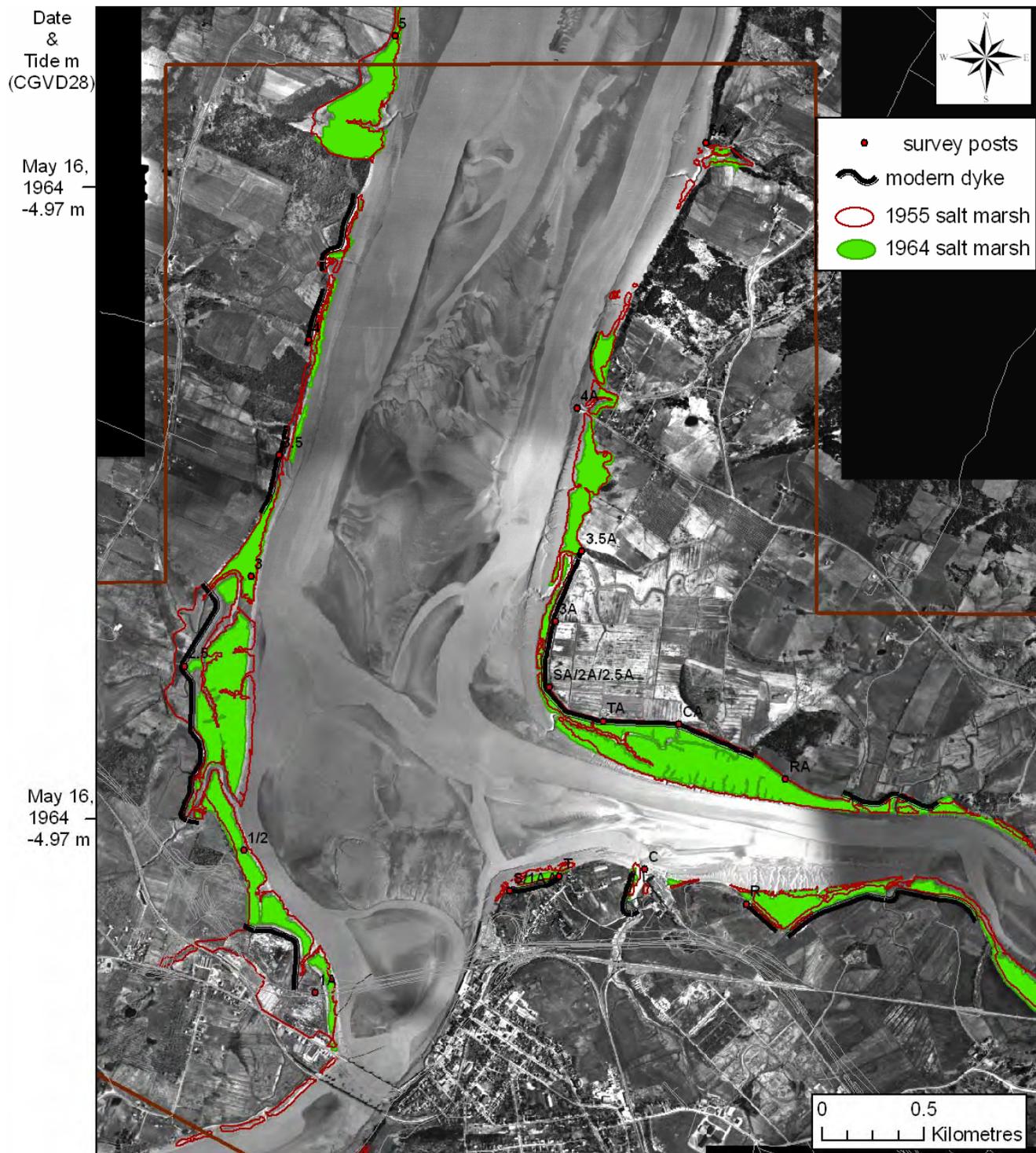
Figure 4.15: Digitized marsh polygons from 1955 to 1964 overlain on a 1964 aerial photograph. Note relative stability of marsh vegetation with some erosion initiated near post 3 and some loss of marsh through dyking along south west shore. Dyke lines (post 1950-1960s) and roads represent present day for reference.
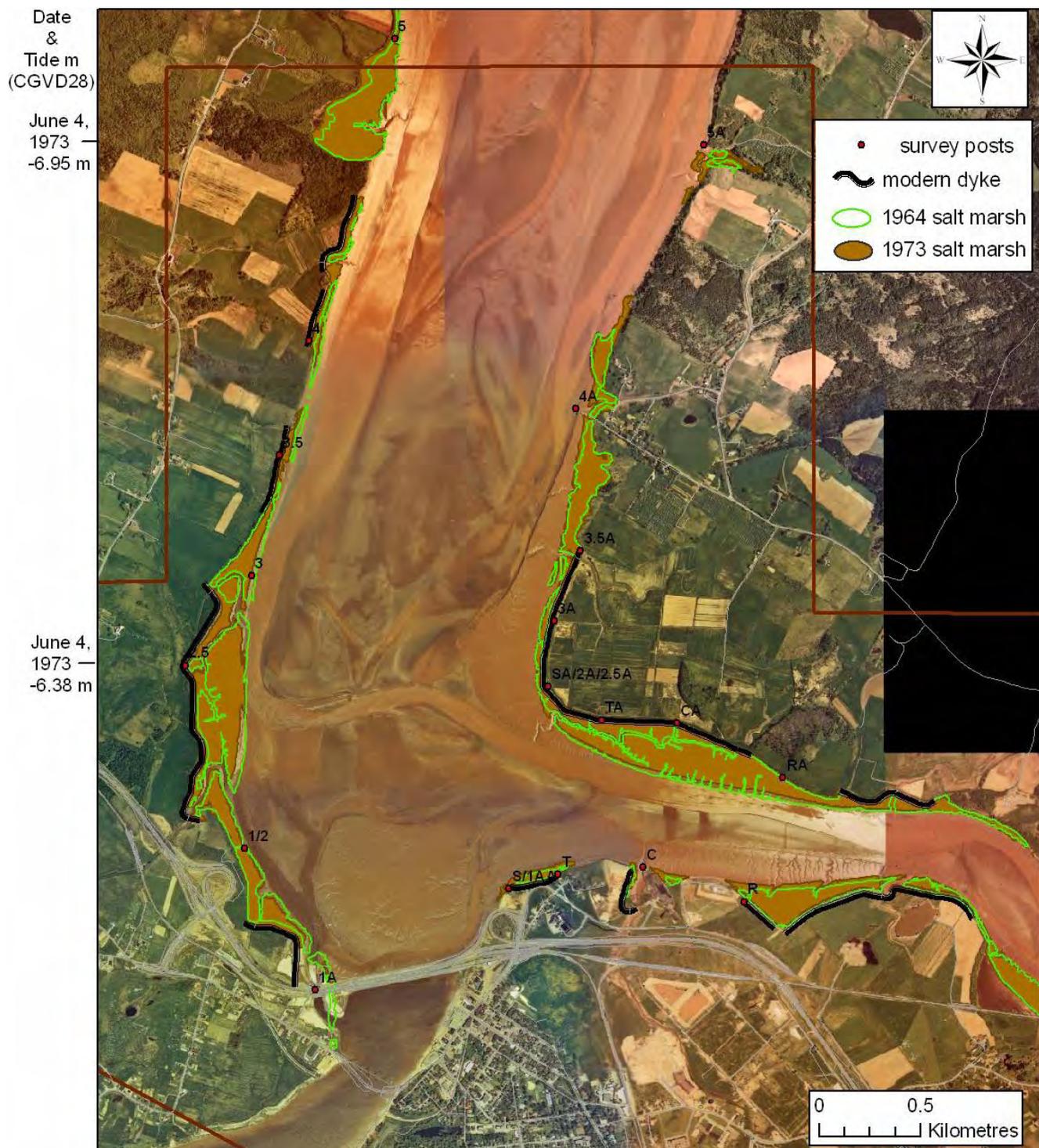
Figure 4.16: Digitized marsh polygons from 1964 to 1973 overlain on a 1973 aerial photograph. Note relative stability of marsh vegetation with some erosion initiated near post 3 and expansion of mudflat adjacent to the causeway. Dyke lines and roads represent present day for reference.
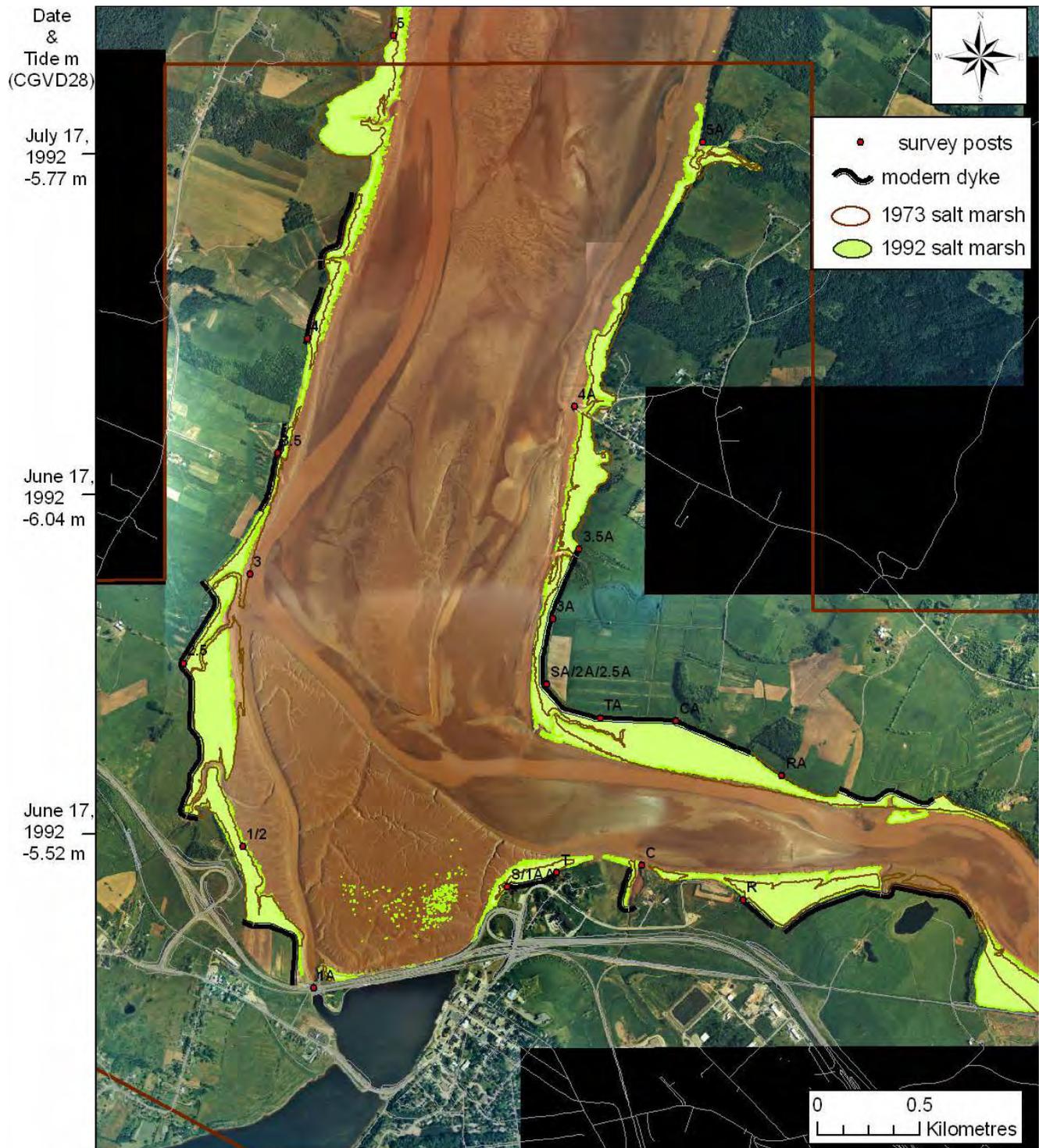
Figure 4.17: Digitized marsh polygons from 1973 to 1992 overlain on a 1992 aerial photograph. Note accelerated erosion along west bank near post 3 and 2.5, accelerated mudflat development and new channel thalweg position. Dyke lines and roads represent present day for reference.

Figure 4.18: 1999 Landsat 7 bands 6,4,3 false color composite illustrating position of main channels and intertidal bedforms. Resolution of satellite is 28.5 m.
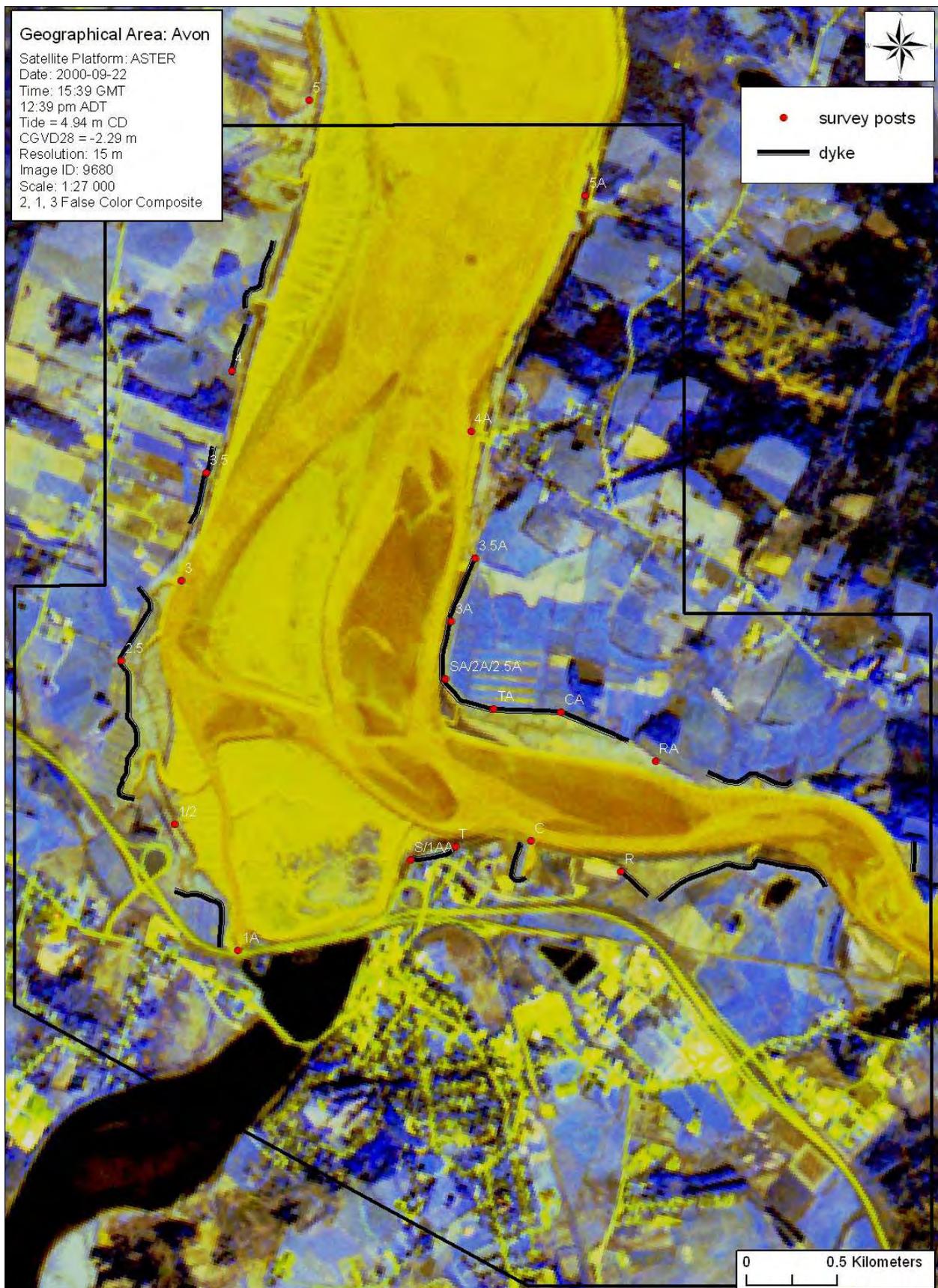
Figure 4.19: ASTER Satellite illustrating position of main channels and intertidal bedforms on Sept 22, 2000. Resolution of satellite is 15 m. Note vegetation on mudflat downstream of causeway.
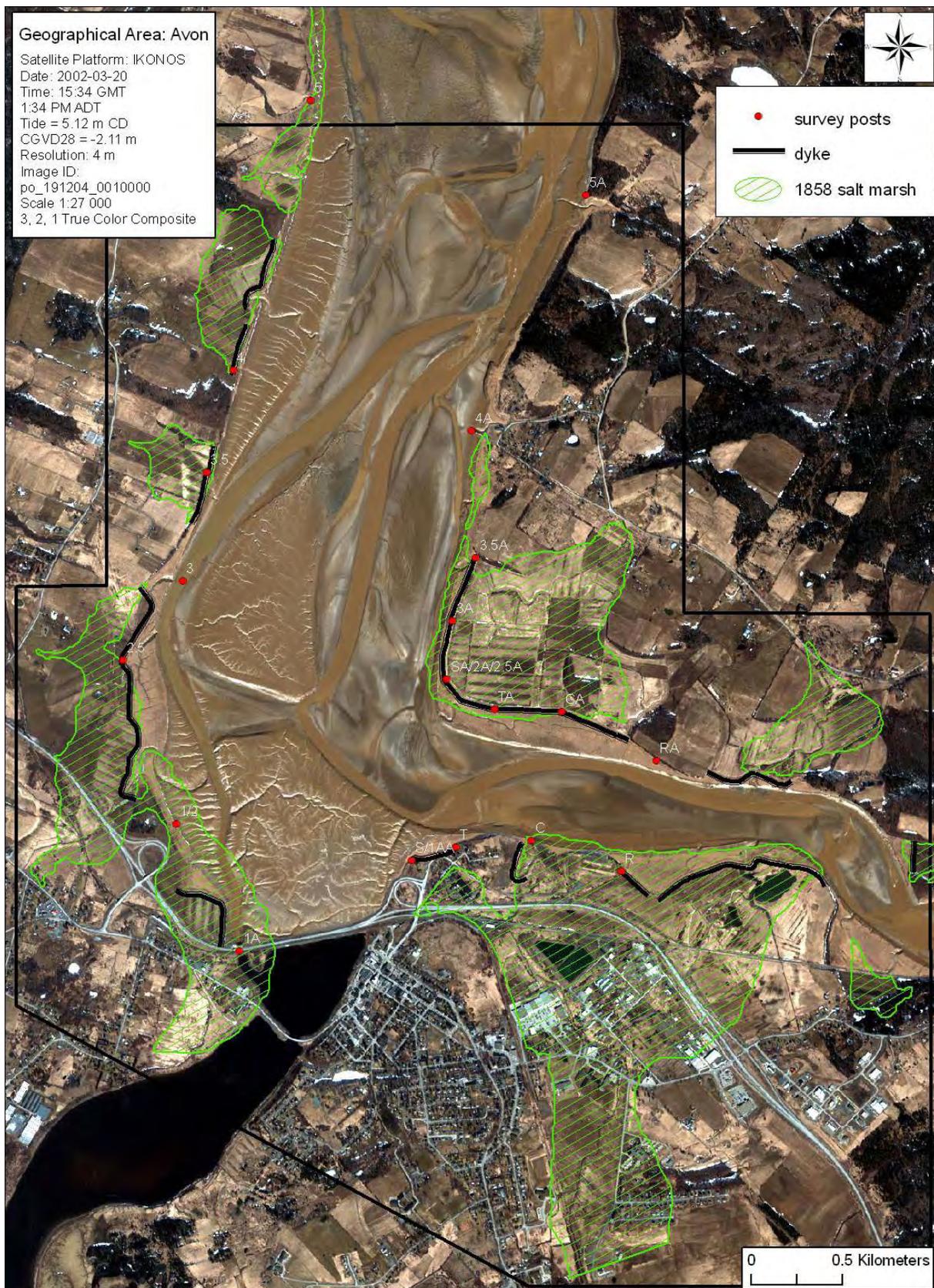
Figure 4.20: Multispectral IKONOS satellite image illustrating position of main channels and intertidal bedforms on March 20, 2002. Resolution of satellite is 4 m. Location of 1858 marsh provided for reference. No vegetation is visible on Windsor mudflat/salt marsh since it is too early in the growing season and most of the previous year's growth would be dead and/or sheared off therefore would not contain chorophyll which could be detected by the satellite.
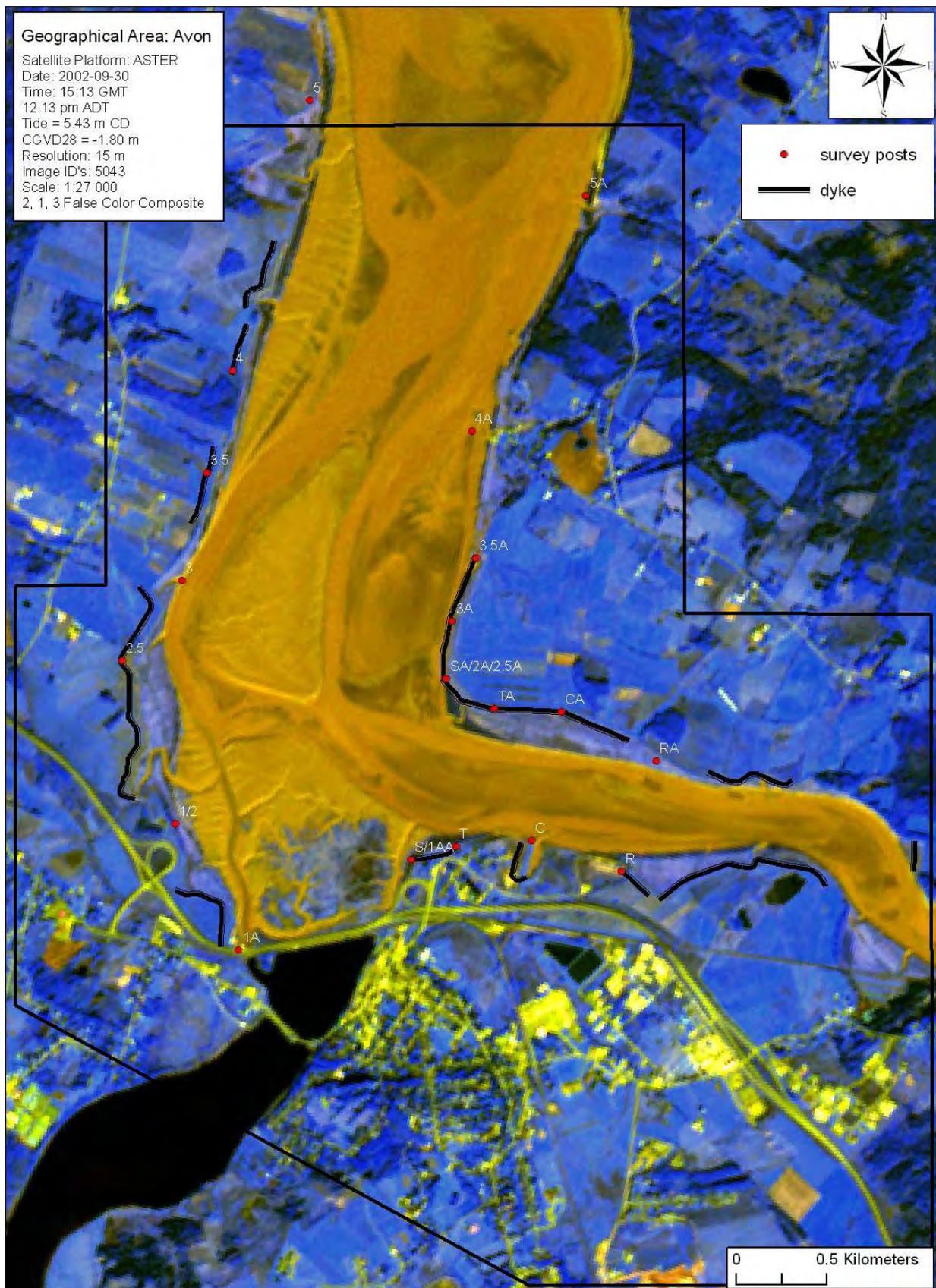
Figure 4.21: ASTER satellite image illustrating position of main channels and intertidal bedforms on Sept 30, 2002. Resolution of satellite is 15 m. Note expansive vegetation downstream of causeway.
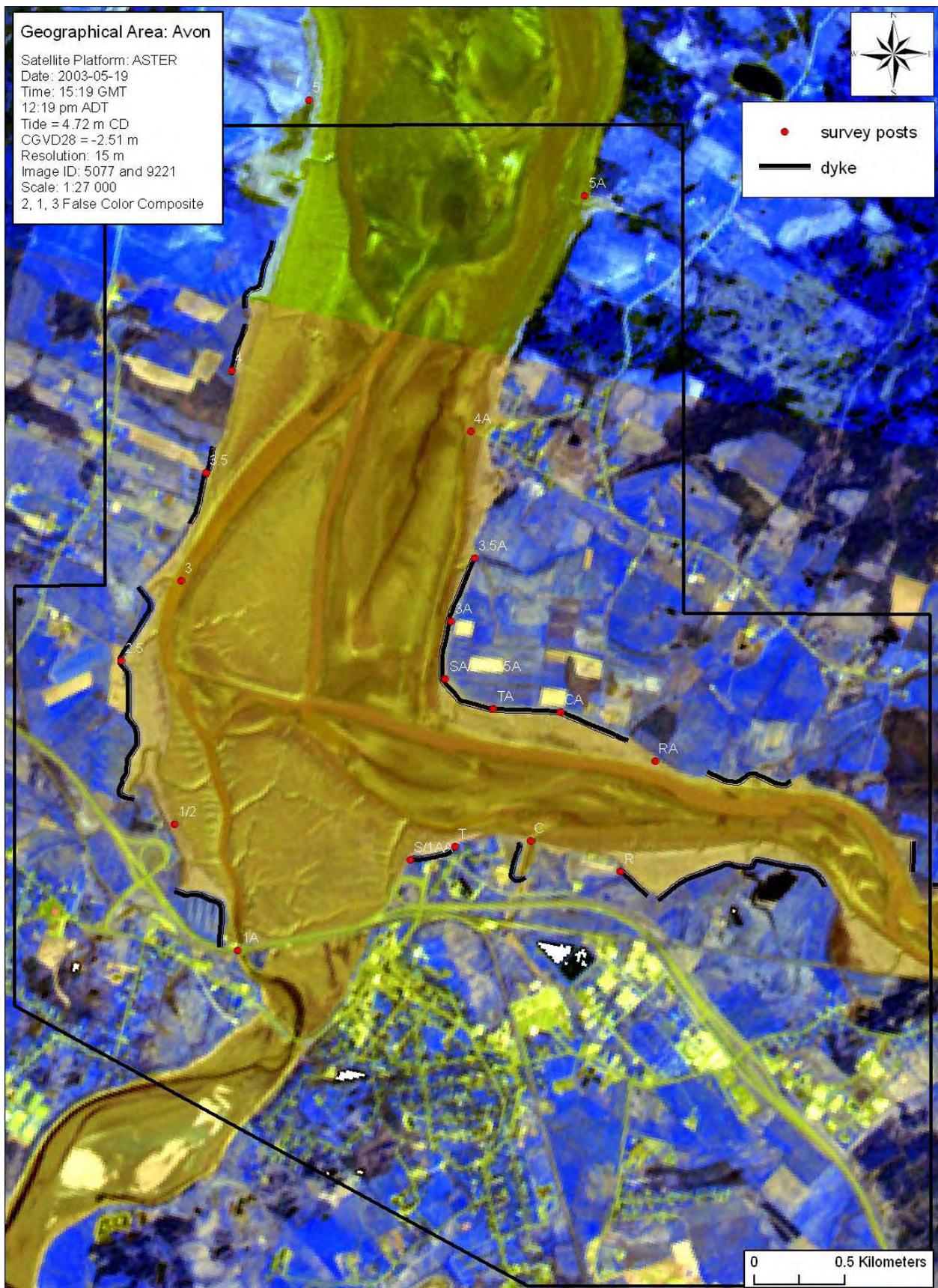
Figure 4.22: ASTER satellite image illustrating position of main channels and intertidal bedforms on May 19, 2003. Resolution of satellite is 15 m.
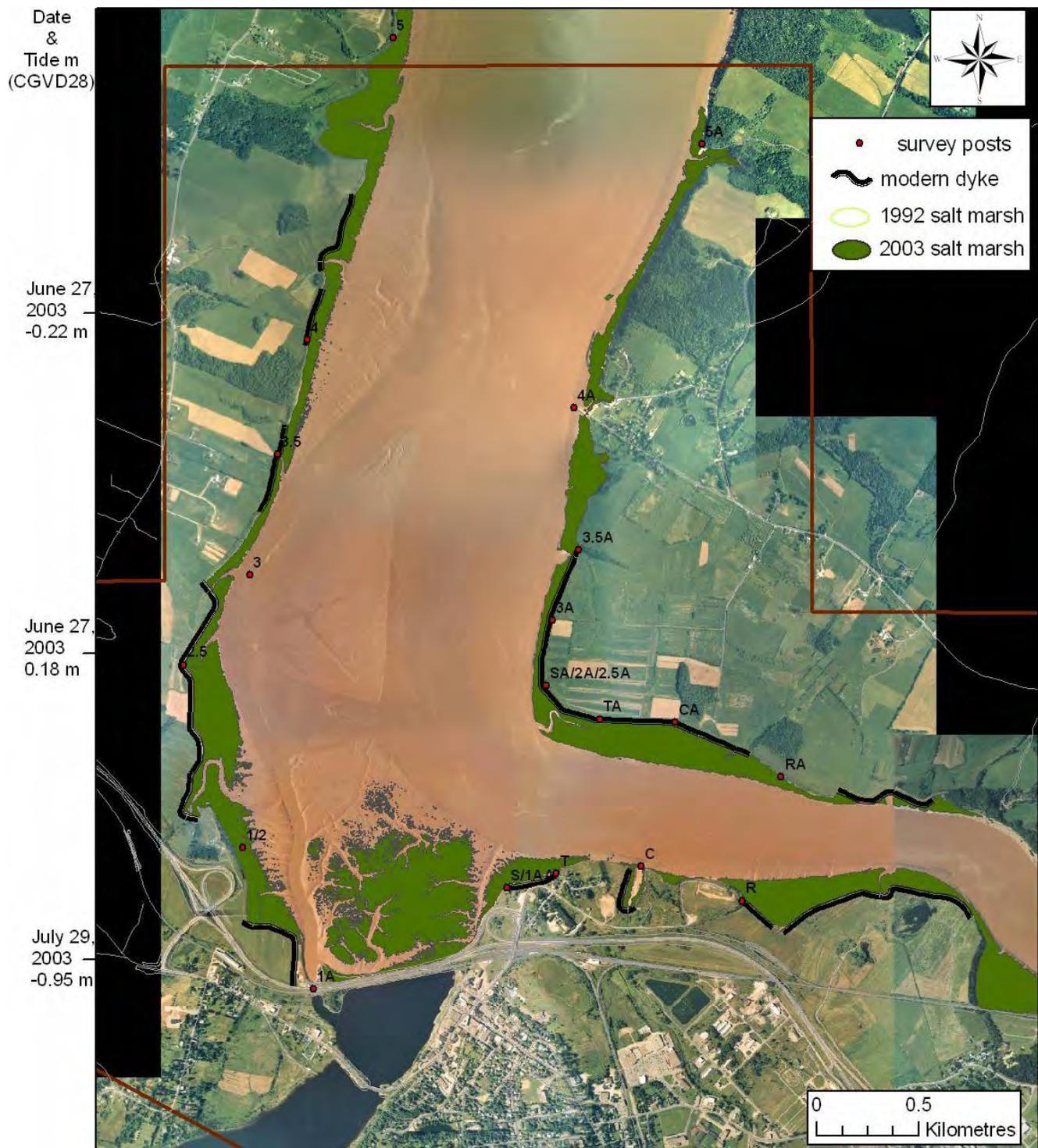
Figure 4.23: Digitized salt marsh polygons for 1992 and 2003 overlain on a 2003 aerial photograph. Note extensive erosion, near the west side of line 3 and colonization of mudflat adjacent to the causeway. Dyke lines and roads represent modern day.
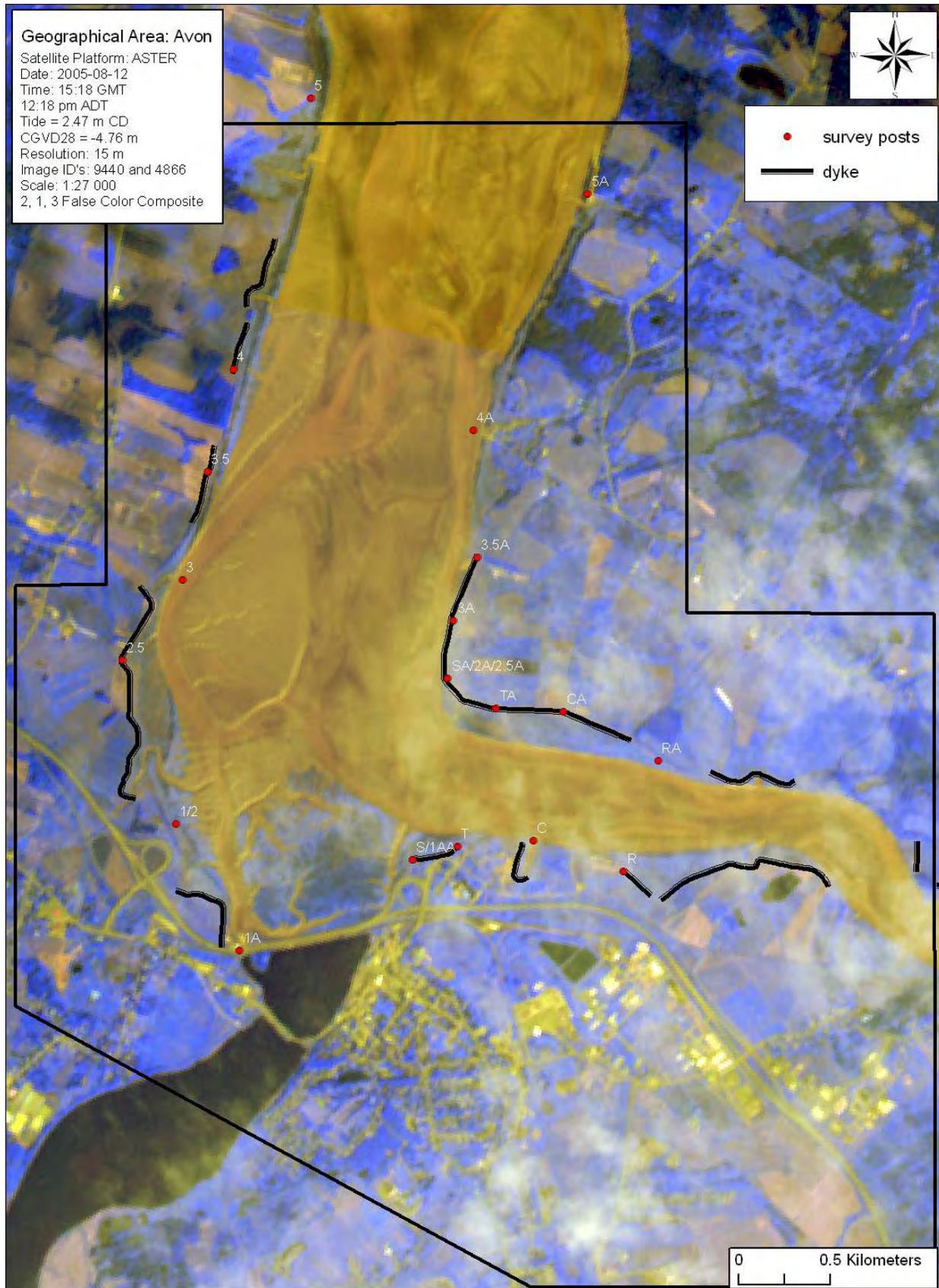
Figure 4.24: ASTER satellite image illustrating position of main channels and intertidal bedforms on July 12, 2005. Resolution of satellite is 15 m. Note exapansion of marsh on western bank of tidal gate channel near Post ½ and erosion on eastern side at posts 2.5a, 3A and 3.5 A.
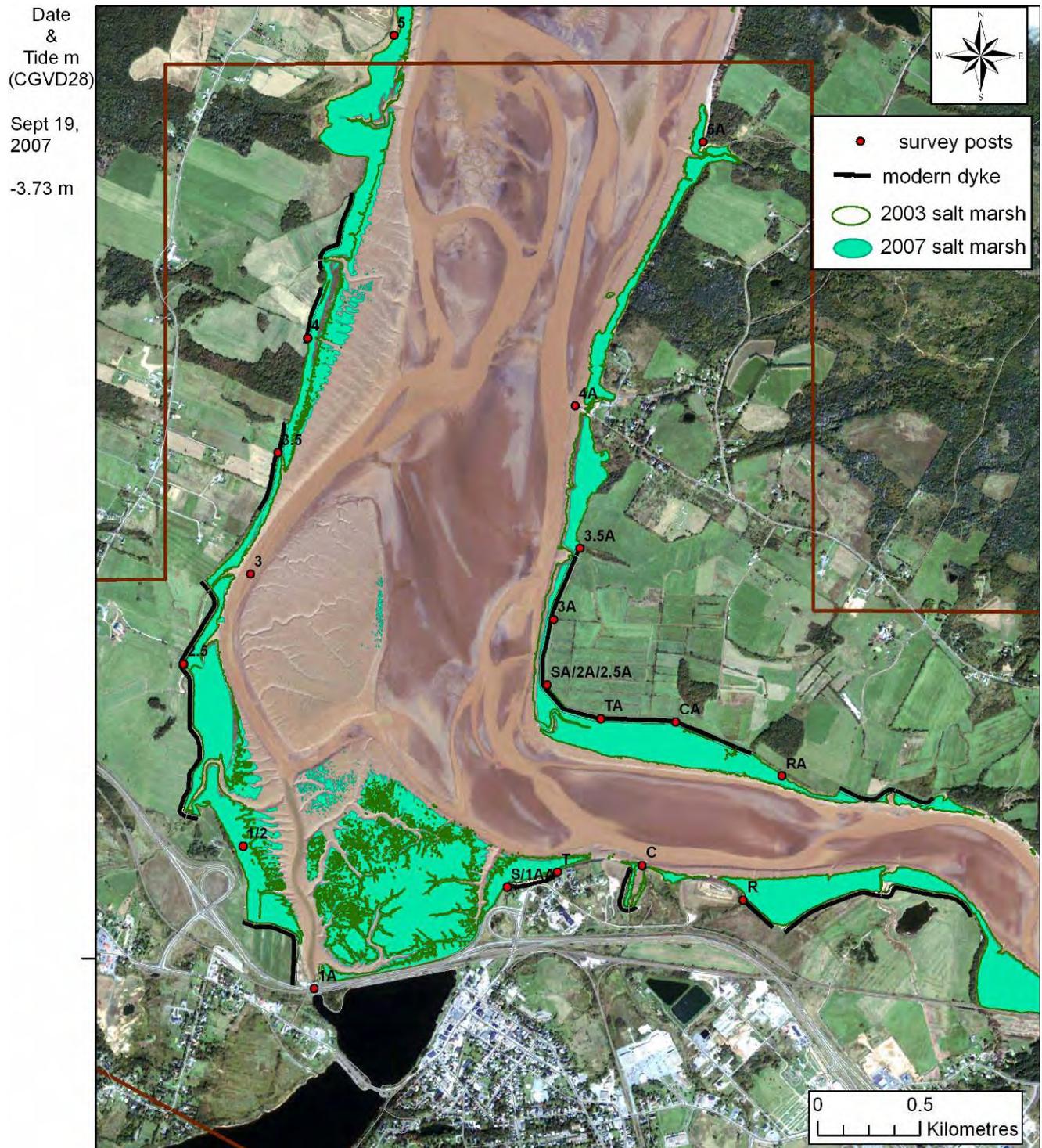
Figure 4.25: IKONOS satellite image illustrating position of main channels and intertidal bedforms on Sept 19, 2007. Resolution of multispectral image is 4 m. Note exapansion of marsh downstream of causeway to cover entire potential mudflat area for deposition.

Figure 4.26: Digitized marsh polygons in 1964 at low tide overlain on a 1964 aerial photograph just south of Hantsport.

Figure 4.27: Digitized marsh polygons in 1973 at low tide overlain on a 1973 aerial photograph just south of Hantsport.

Figure 4.28: Digitized marsh polygons in 1992 at low tide overlain on a 1992 aerial photograph just south of Hantsport.

Figure 4.29: Landsat 7 bands 6,4,3 false color composite illustrating position of main channels and intertidal bedforms at low spring tide. Note position of sand wave near Hantsport.
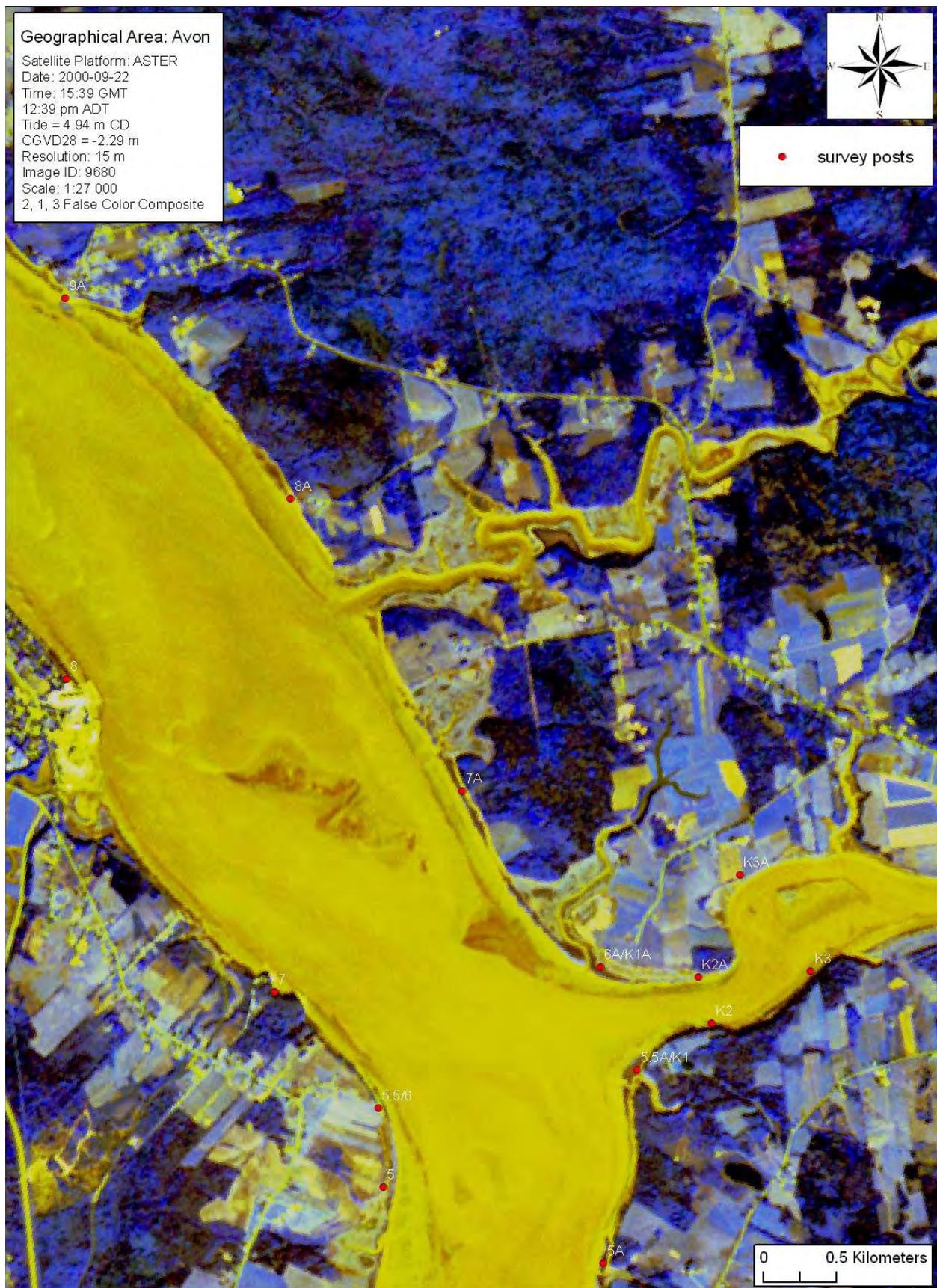
Figure 4.30: ASTER satellite image on Sept 22,2000 near Hantsport.

Figure 4.31: Multispectral IKONOS image illustrating sand bodies near Hantsport and Kennetcook River on March 20, 2002..
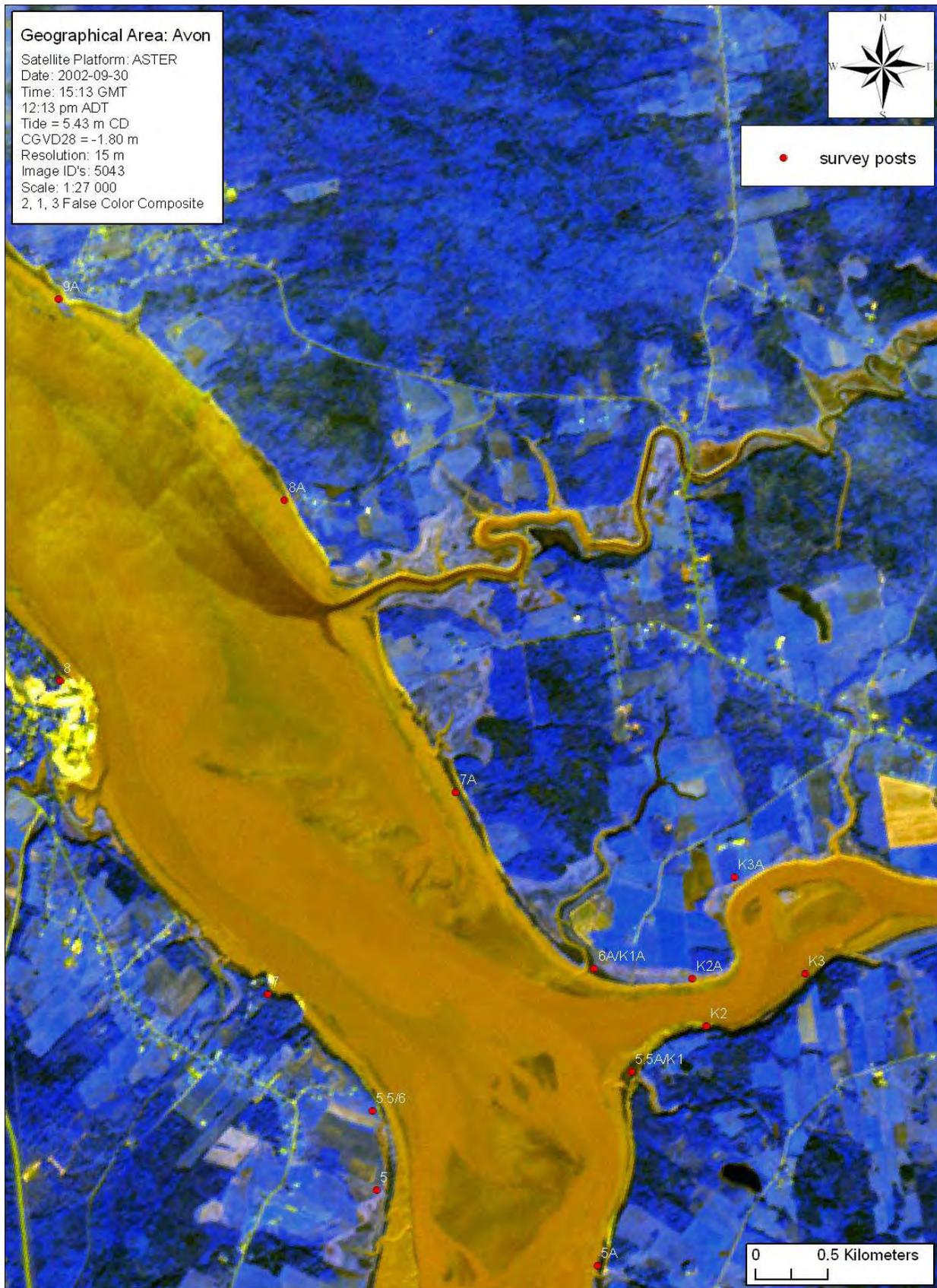
Figure 4.32: ASTER Satellite image illustrating intertidal bedforms on Sept 30, 2002.
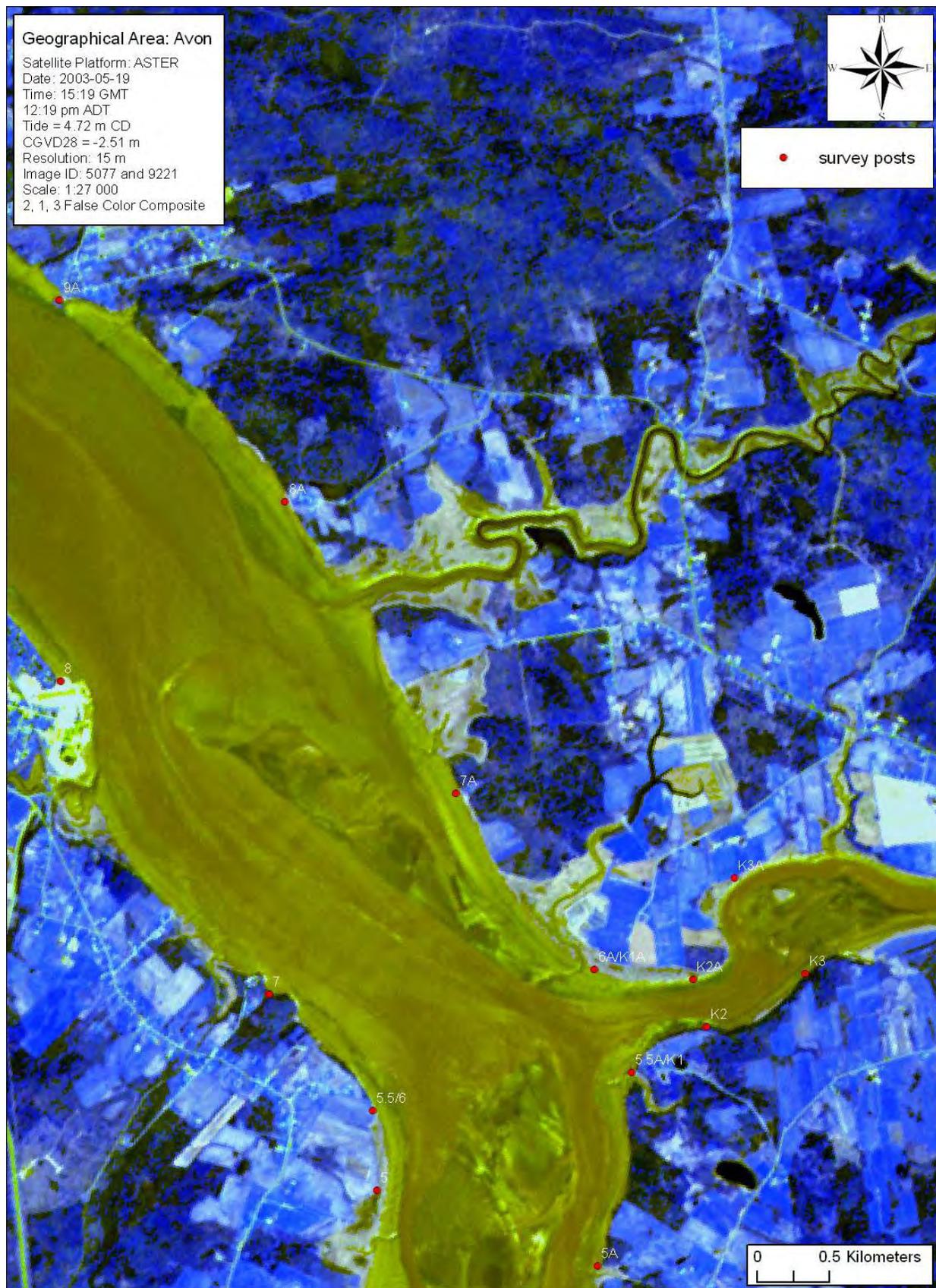
Figure 4.33: ASTER Satellite image illustrating intertidal beforms on May 19, 2003

Figure 4.34: Digitized marsh polyons in 2003 near Hantsport and Kennetcook River. Tide is just below level of low marsh.
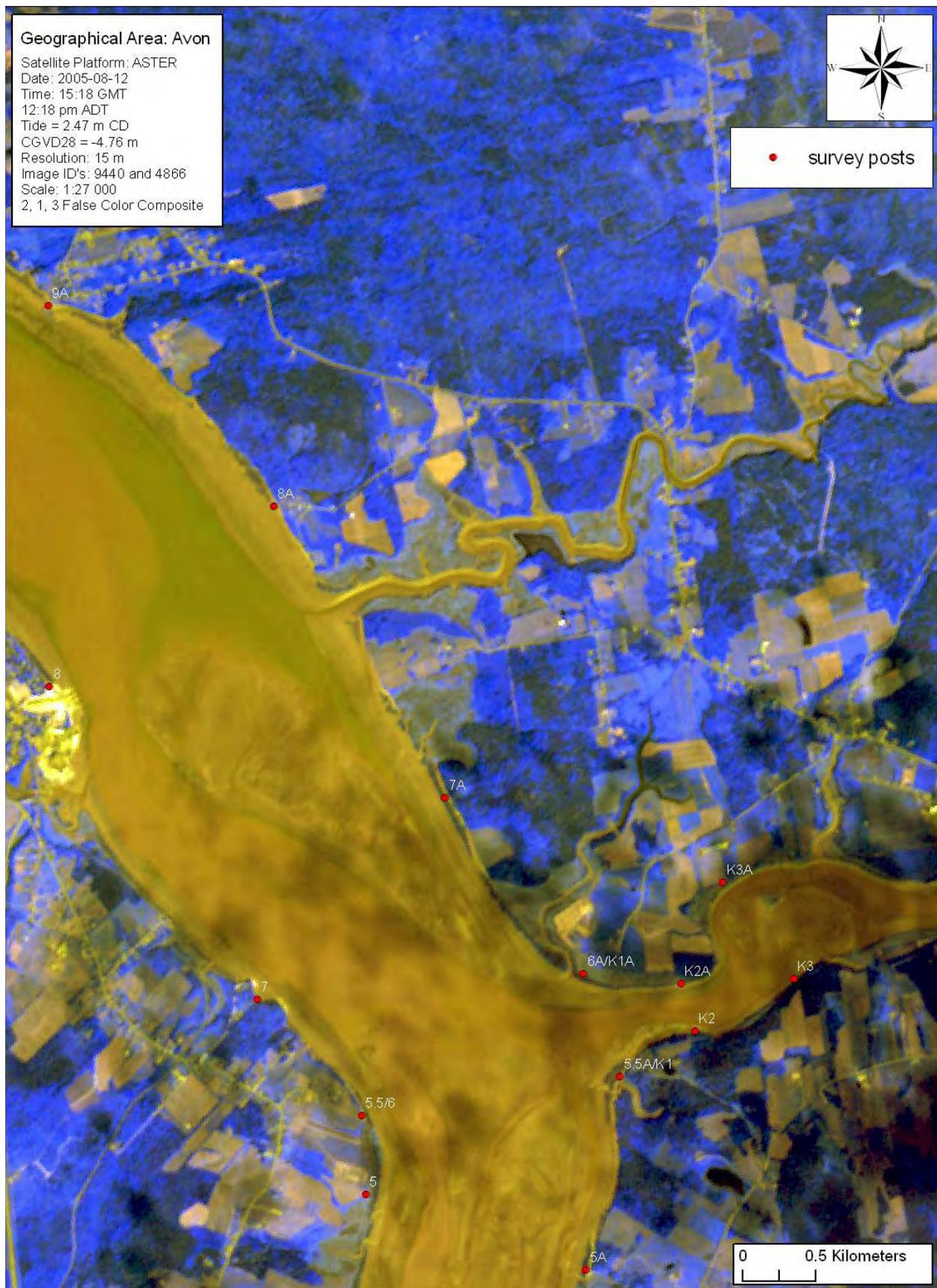
Figure 4.35:ASTER satellite image on July 12, 2005 illustrating large permanence of sand body near Hantsport.
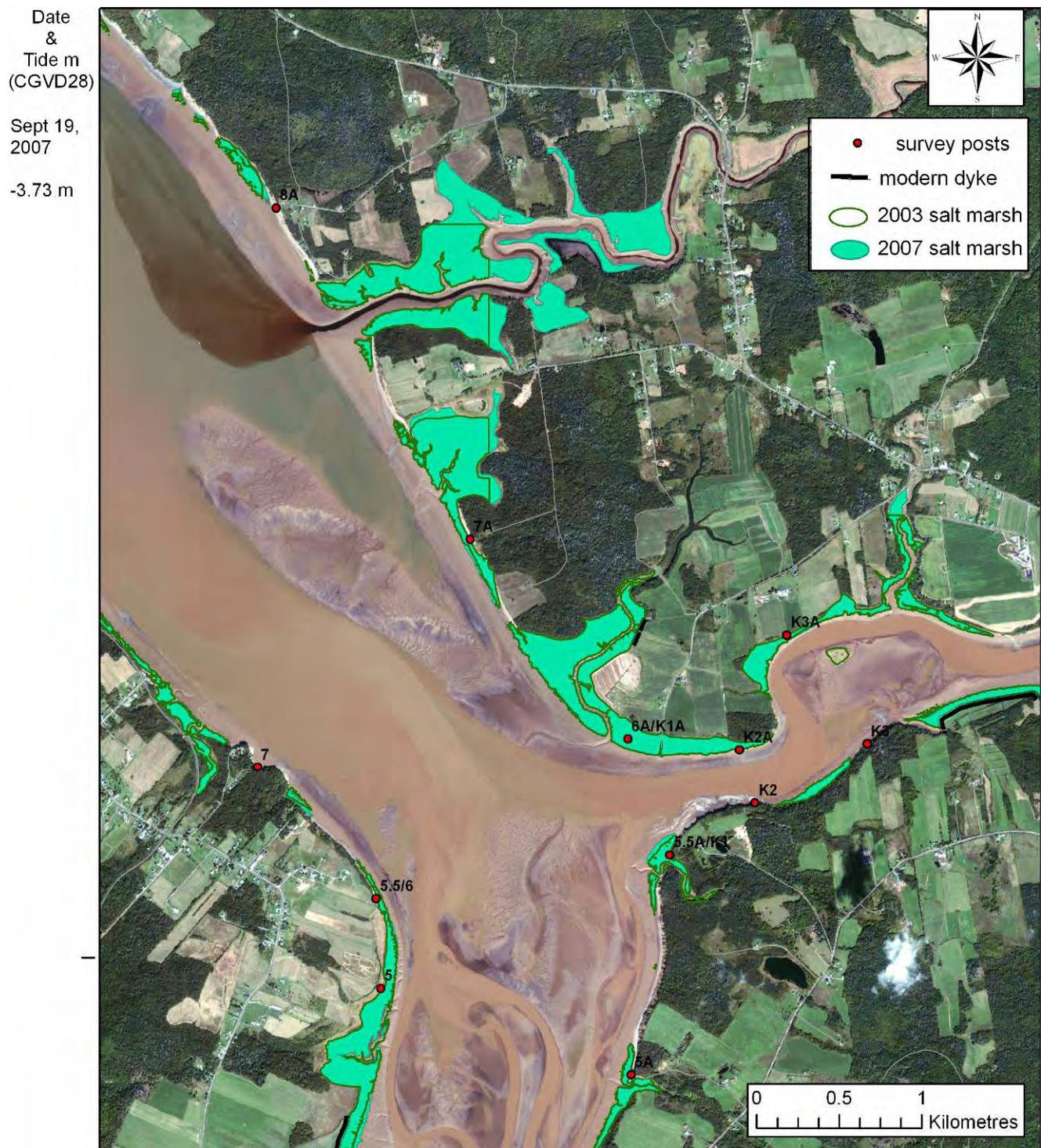
Figure 4.36:Multispectral IKONOS satellite image on Sept 19, 2007 illustrating large permanence of sand body near Hantsport. In addition, a potential plume of tanins is visible draining from the Cogmagun river. Field visits on Sept 21 indicate that tanins draining from marsh soils are the likely cause of this plume.

The St. Croix River thalweg continues to meander towards the northern bank of the river, causing 30 m of marsh loss since 1964. Approximately 65 m of new marsh has established on the south shore since 1964. Extensive erosion is still ongoing along the western bank and the limit of influence of the shifting channel has shifted further downstream (Fig 4.17). The mudflat deposit adjacent to the causeway has now considerably increased in size and elongated into almost a triangular form oriented downstream. A very defined and narrow channel from the tide gate is visible with accumulation along the western edge near post 1 / 2 (Fig 4.17). The causeway channel and tidal creek closest to the Windsor Tourist Bureau has infilled considerably. New marsh grass is visible on the mudflat surface.
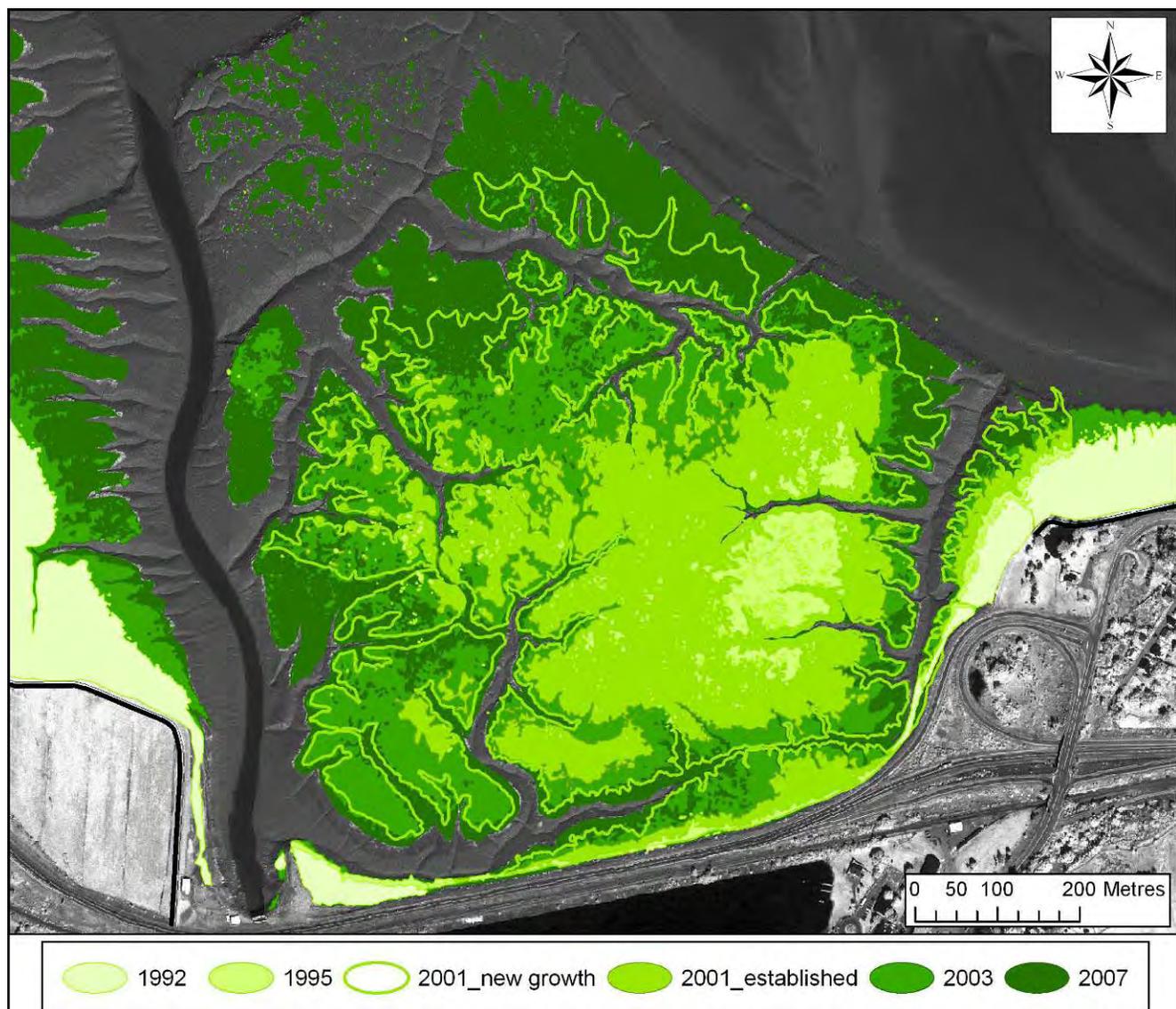
Figure 4.37: Comparison of Townsend, 2001 marsh GPS survey conducted in the fall of 2001 distinguishing between established spartina alterniflora (e.g. mature) and juvenile s. alt. Note expansion and coalescence within juvenile boundaries from 2001. In addition note relative stability of position of the tidal creek channels. Surperimposed over IKONOS panchromatic satellite image collected on September 19, 2007.

The most noticeable change between 1992 and 2003, particularly when compared with the earlier years (Fig 4.21, 4.22), is the extensive growth of marsh vegetation by the Windsor Causway (refer to van Proosdij and Townsend, 2006 for a detailed account and mechanisms of colonization by *Spartina alterniflora*) (Fig 4.37). Additional marsh growth is visible along the south shore of the St. Croix, and erosion continues along the western edge, threatening the dyke along that section (pers comm. K. Carroll, 2005) as the thalweg continues to shift towards the west. The edge of the dyke and foreshore have been armoured in the area. The mudflat area near post 1/ 2 now shows evidence of marsh colonization (Fig 4.22). In addition, the mudflat at the north western section of the Windsor marsh (Fig 4.37) that was not colonized in 2003 now has a healthy *Spartina alterniflora* population (Figure 4.38). By September 2007, the majority of the original mudflat surface had been colonized by *S. alterniflora* and the tidal channel parallel to the causeway has been almost completely infilled, particularly along the eastern edge.

Figure 4.38: New colonies of Spartina alterniflora on mudflat to the north west of the original Windsor marsh. Photo by D. van Proosdij August 2006.

4.3   Intertidal Sedimentary Features

As mentioned previously, prior to the construction of the causeway there was already an existing body of sand just upstream of the confluence of the St. Croix and Avon River (Figure 2.25, 4.15) in 1964. The size of this sand/mud body grew from 0.72 km^2 to 4.43 km^2 by 1973, three years after the causeway was completed .   By 1992, the mudflat developed a new lobe, extending towards the western bank, adding a net total of 5.77 km^2 to the mudflat area. However, the original mudflat area decreased by 1.36 km^2 due to bank erosion from the St. Croix River.
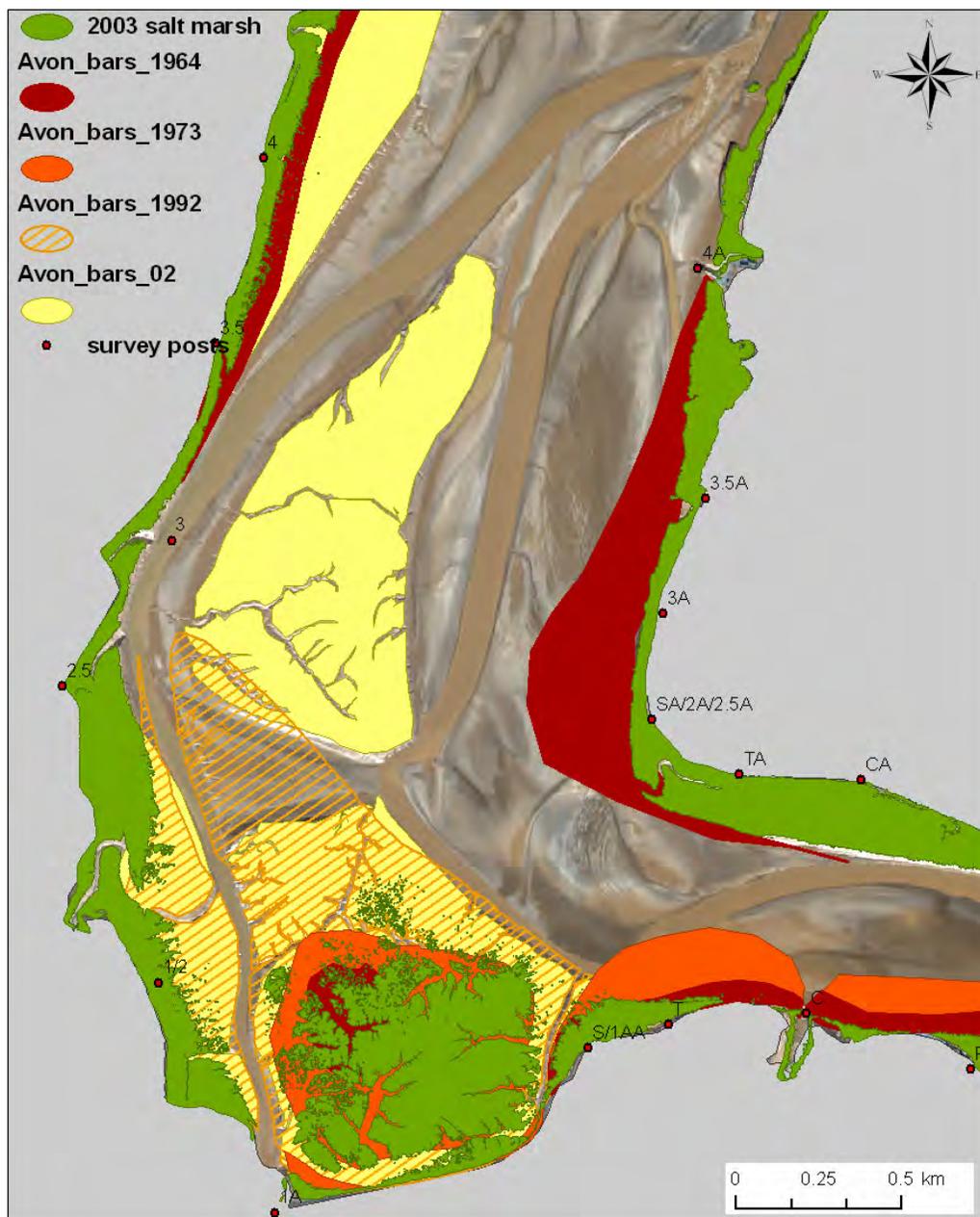
Figure 4.39: Growth of emergent intertidal features 1964 to 2002. The outline of intertidal flats were digitized if they would be exposed during neap tides. Polygons overlain over 2002 multispectral IKONOS image.
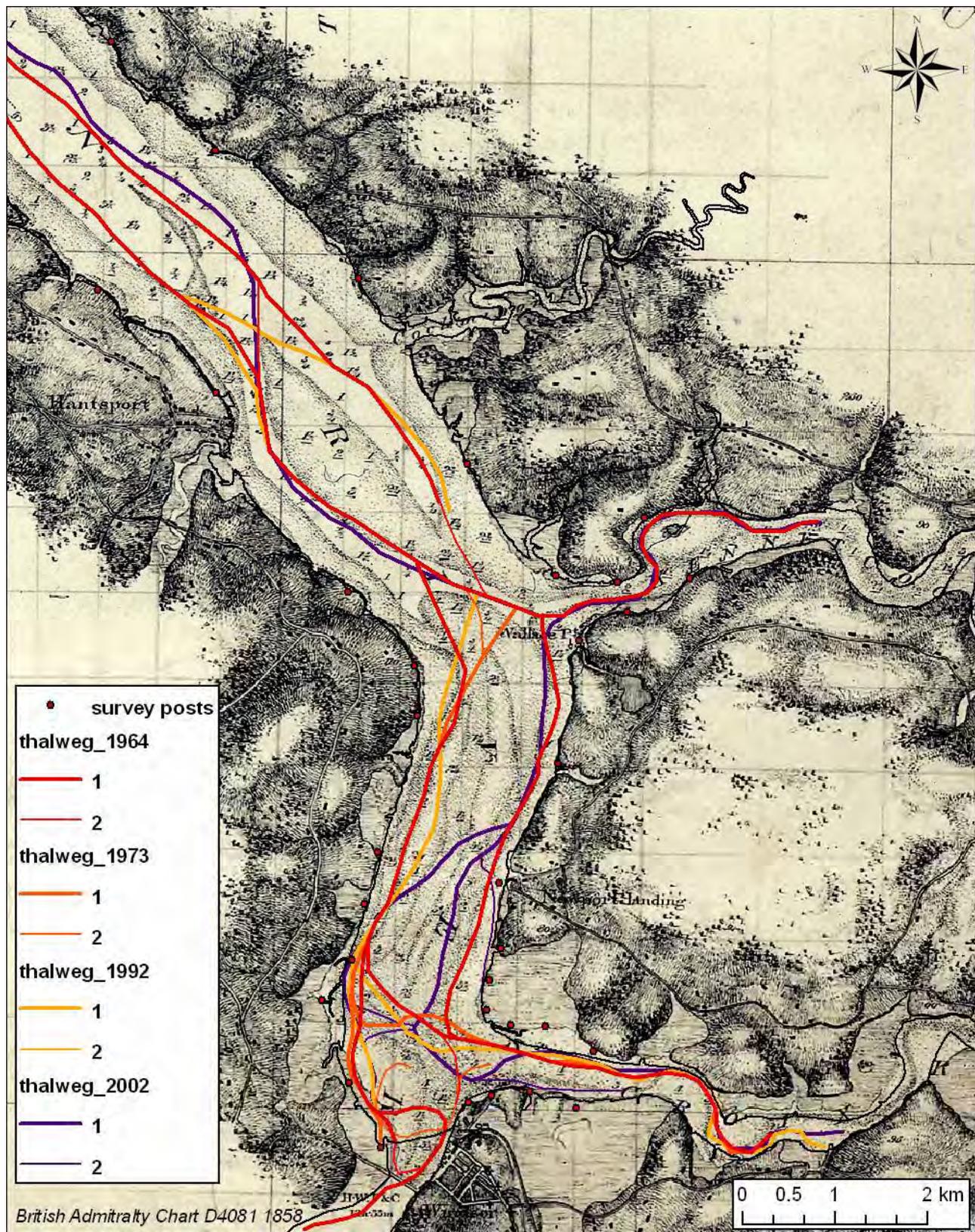
Figure 4.40: Change in the position of the main tidal channel thalwegs. Secondary channels are only operational for part of the tide. Positions digitized from aerial photographs and overlain on the 1858 British Admiralty Chart D4801.

After 1992, the main channel exiting the St. Croix shifted position and cut across the lobe, bissecting it and began to eroded the western shore of the Avon River.   This resulted in a net loss of 2.16 km^2 of mudflat area by 2002. However, some of this material likely fed the development of the Newport bar which covered 6.17 km^2 (Figure 4.37) by 2002.   Further downstream, there are the main sand bodies reported by Lambiase (1980) in the central portion of the river and mudflat development along the western shore south of Mitchener Point.   The Shad Bar (or Hantsport Bar) (Figures 4.25 – 4.34) is a relatively permanent feature, potentially resulting from a bedrock core which diverts flow to either side of this sand body (Figure 4.38). Position of the tidal channels downstream of Line 9 have been quite stable since 1858 (Figure 4.38) with minimal lateral migration. This has likely assisted in maintaining the position of the central sand bodies.   Closer to the causeway however, there has been a marked shift in the position of the main channel, contributing to cycles of erosion and progradation of mudflat and marsh bodies (Figure 4.38). It appears that the main channel exiting the St. Croix river is behaving similarly to a garden hose, directing the force of the water in whichever direction the outlet (or nozzle) is facing and will move back and forth if the main body of the hose (or channel) is not constrained.

Apart from the obvious mudflats (Figures 4.38 & 4.40e), there also three primary bedform features that can be identified within the study area. These include: 1) megaripples with wave lengths between 8 m (Fig 4.40a) to 2-5 m (Fig 4.40c) with sinuous crests oriented normal to the dominant currents; 2) sand waves with wavelengths between 30-75 m (increasing in wavelength upstream) with superimposed megaripples with wavelengths between 12-14 m (Fig 4.40b); and 3) small ripples with wavelengths of 0.05 to 0.1 m which were observed in the field on the sand bodies (with some silt) in Figures 4.40d and 4.41, although these are not clearly visible on the image given their very small size.

What appears to be some form of a point bar is developing near the mouth of the St. Croix river, shaped by the main channel of the St. Croix. The layers of deposition are clearly visible (Fig 4.40f) and this feature is likely reinforcing the current orientation of the channel, as well as the erosion of the mudflat and marsh on the opposite shore.   However, this feature is located relatively low within the tidal frame therefore its impact is restricted to the lower tides levels.

Figure 4.41: Ripples on sand flats on Sept 21, 2007
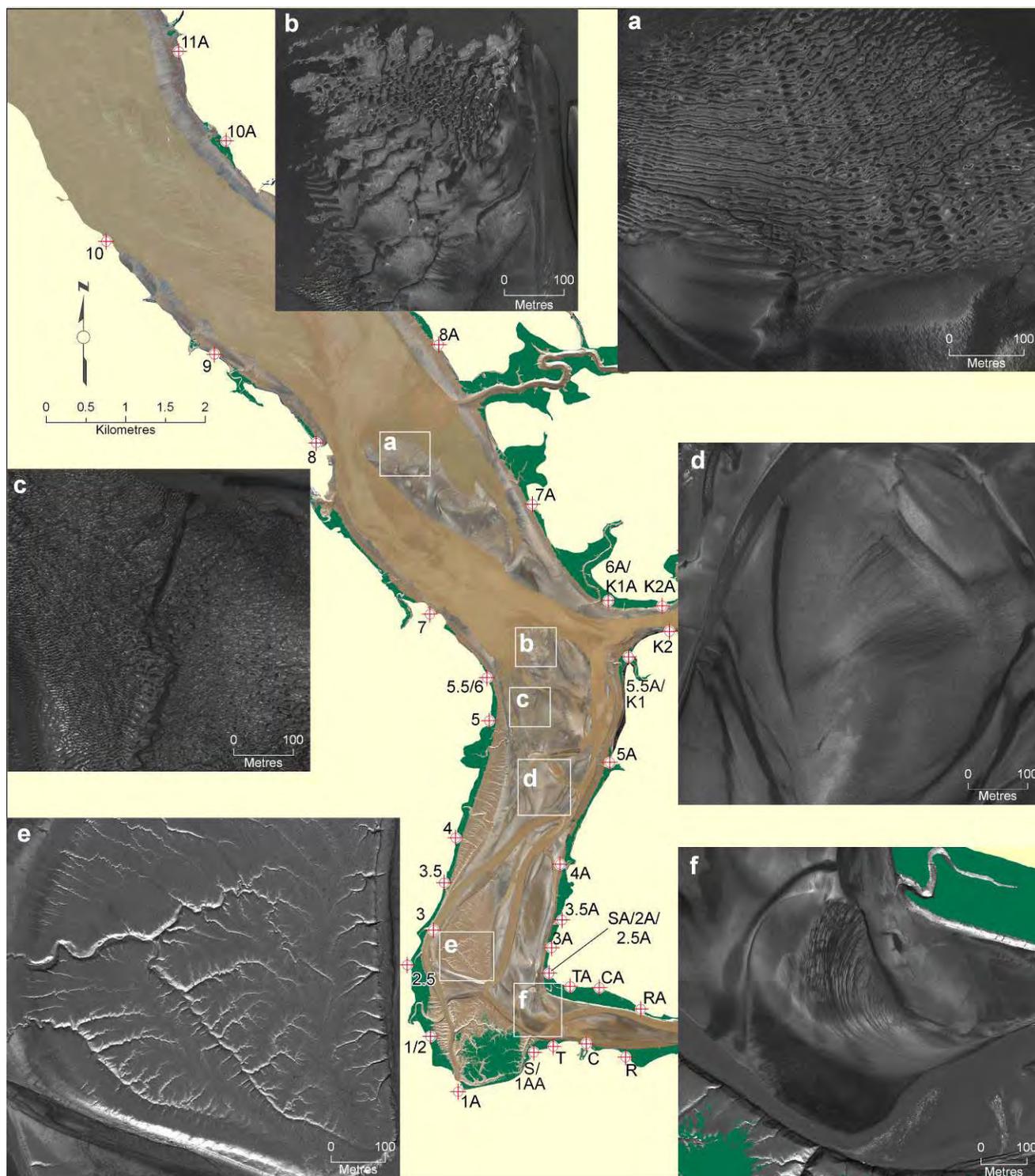
Figure 4.22: Type of intertidal features found within the Avon River estuary. Interpreted from IKONOS panchromatic 0.86 m resolution image in ArcGIS 9.1. Features depicted include: a) sand waves with megaripples on Shad bar (also known as Hantsport Bar); b) megaripples; c) bi-directional ripples; d) bi-directional ripples covered with thin veneer of fines e) mudflat and f) sand wave with superimposed unidirectional ripples.

5.0   DISCUSSION

The influence of the construction of barriers across tidal rivers and estuaries on the sediment dynamics and ecosystem processes in their surrounding areas has been well documented in many tidal systems (e.g. Owen and Odd, 1972; Bray et al., 1982; Wolanski et al., 2001 and Tonis et al., 2002). However, discerning the extent of the changes caused by these large scale structures from natural ecosystem changes such as fluctuations in metereological conditions (e.g. storms), sea level rise, and thalweg position can be a challenge.

The overall equilibrium state of an estuary results from a balance of sedimentological, hydrological, and biological forces. If some boundary condition is changed, then the system will adjust to a new state of equilibrium. However, rivers and estuaries do not respond to engineering works in the same manner (Kestner, 1966). In a river, engineering structures that cause a decrease in the cross sectional profile may result in a change in the local geometry of the river. In general, there is a local increase in velocities which will produce bed scour and therefore serve to increase the reduced cross sectional area again. This will have repercussions on the upstream and downstream sections until the regime of the river is readjusted to the new conditions (Kestner, 1966). However, a river's characteristic discharge will not change unless large amounts of water are stored upstream (e.g. reservoir or lake) of the constriction (Bray et al., 1980). In contrast, the discharge in an estuary varies throughout the flood and ebb of the tide. Its magnitude depends on the range and direction of the tide and on the size of the estuary itself (Kestner, 1966). Therefore, an engineering structure such as a dyke that reduces the extent of tidal flooding, or a structure that decreases the cross sectional area of a channel, or the closure of a section of an estuary, will, as a consequence, change the magnitude of the characteristic tidal discharge (Kestner, 1966). The decrease in tidal discharge will in turn decrease the velocity and transportation capacities of the tidal waters causing sedimentation. If this occurs an equilibrium form will develop, which is an expression of the dynamic equilibirum between erosional and depositional processes (Williams et al., 2002). This equilibrium form may be driven to a new state by the construction of coastal defense works such as dykes, or large scale damming projects. There may be a shift in channel position (e.g. Elias and van de Spek, 2006) or form, but the overall cross sectional areas do not change. The time to reach this new equilibrium state will vary, ranging from less than 10 years (e.g. Tonis et al., 2002) to more than 100 years (e.g. Kragtwijk et al., 2004). Recent studies indicate that large width to depth changes are necessary to jump from one equilibrium state to another

(Toffolon and Crossato, 2007). In the Eastern Scheldt Estuary in the Netherlands, the tidal area was reduced by 22%, which induced a redistribution in habitat and species but did not change the overall function of the estuarine food web (Smaal and Neinhuis, 1992).

Re-examination of the historical data and expanding the temporal scope of the analysis still supports the conclusions presented in van Proosdij et al., 2006, with some modifications. Within the first 1500 m of the Windsor causeway there has been a significant decrease in cross sectional area due to excess sedimentation. This supports previous research in the Avon system (e.g. Amos, 1977; Turk et al., 1980) and elsewhere (e.g. Allen, 2000; Schwimmaer and Pizzuto, 2000; Shi et al., 1995). However, the direct impacts of the causeway can only be attributed to changes within the first 1000 to 2000 m of the Windsor causeway and not the 20 km originally proposed by Amos, 1977. There is however, approximately a 10% decrease in cross sectional area recorded at around 4 km downstream of the causeway. This change in cross sectional area over time, although statistically significant, is low (when compared with seasonal variations) despite very visible changes in the intertidal geomorphology. The formation of intertidal bars (e.g., Newport bar – Daborn et al., 2003a,b and Daborn and Brylinski, 2004) is balanced by lateral erosion of the marsh bank, mostly along the western edge between 1.1 and 2.2 km from the causeway. The bank erosion is less noticable to casual observers, and this can lead to overestimates of sedimentation. In addition, the magnitude of change in elevation of the channel bed will vary depending on the timing of the survey. Seasonal differences in cross sectional area between surveys may be just as large as differences over many years. If data from 1858 to 2006 are examined, a trend of increasing cross sectional area over time was recorded 20 km downstream. Combined, this results in a decrease in the tidal prism by only 7%. Change in the bathymetry and overall morphology further downstream is more likely to be associated with changes in the position of the main river thalweg, as has been suggested by researchers in other estuaries around the world (e.g. Allen, 1996; Pringle, 1995; Pye, 1995 and Shi et al., 1995). The St. Croix and Kennetcook Rivers, and lesser extent the Cogmagun River, have likely played a key role in moderating the impacts of the causeway construction by both preventing the massive build up of sediment and the decreased hydraulic capacity recorded in the Petitcodiac River (Bray et al., 1982; Locke et al., 2002). In addition, the formation of large intertidal features in a macrotidal system such as the Avon will in turn cause an acceleration of flow during intermediate stages of the tide, when the bars become emergent and water is channeled between the shore and bar (Lambiase, 1980). The higher velocities at this time will serve to maintain and potentially deepen the main channel thalweg and cause bank erosion on the outer edge of the meander bend. This material will then be available for deposition on

the inner bed, as evidenced near Line 5.

The basic assumption is that a homogenous estuary will be in a state of equilibrium when no long term changes in cross section take place (Bray et al., 1982). In a study of the Petitcodiac River in New Brunswick, Bray et al (1982) used the value of an estuary constant '*a*' (Eq 1) to determine whether a channel section has adjusted to a new equilibrium (Figure 5.1). This constant incorporates the effect of hypsometry of the estuary. The current speed required to

Figure 5.1: Variation in parameter 'a' with distance from pre-causeway head of tide (modified from Bray et al, 1982)

change the water surface level by a fixed amount in a set period of time is affected by the cross sectional area and volume of water that must move through the cross section. Therefore, in a macrotidal system where there is a very large change in tidal prism, maximum current speeds should occur when relatively large volumes of water must pass through relatively small cross sections; this condition is met when the water surface level is slightly lower than the tops of the intertidal sediment bodies (Lambiase, 1980; Darymple et al., 1990). This will occur primarily in the upper reaches of the estuary. The value of '*a*' was derived for a cross section 4.7 km downstream of the Petitcodiac causeway (25 km from the head of the tide) in 1981. This value (indicated by the red point in Figure 5.1) is close to the value of 'a' for the pre-causeway channel at a point located 4.7 km from the head of the tide, suggesting that the channel form had essentially shifted downstream.

This value was computed for the Avon system (Figure 4.10) and compared to pre and post causeway values for '*a*'. With the exception of the section of marsh close to the causeway itself, there is minimal variation in the position of the curve. Pre and post causeway values for '*a*' are almost identical approximately 11 km from the head of the estuary or 7.2 km downstream of the causeway. This point coincides with what Bray et al (1982) describe as the pivot point between riverine and estuarine processes. Interestingly, in the pre causeway condition of the Petitcodiac River, this point was located about 10 km upstream of its causeway (Bray et al., 1982), whereas in the Avon system, this point was

located approximately 7.2 km downstream of the future causeway. The primary drivers on channel form may be either fluvial in nature or reflect the ebb dominance of the system. Therefore, one of the main differences between the response of the Petitcodiac River and the Avon River to causeway construction is due to the number of rivers that drain into the estuary. No rivers join the Petitcodiac until close to its mouth whereas the Avon has both the St. Croix and the Kennetcook rivers. These two rivers account for 67% of the drainage area of the Avon watershed basin. The St. Croix alone contributes 40%.

Further differences include the sediment composition and suspended sediment concentrations. The Avon system is primarily sand and silt with minimal fluid mud (suspended concentration of fine sediments $> 4,000$ mg·l^{-1}) due to the flushing of the tide gate and freshwater inflow from the St. Croix and Kennetcook rivers. In contrast, the Petitcodiac system has an excess of fluid mud which alters the hydrodynamics of the system, further inducing sedimentation. In addition, the smaller size of the Avon system relative to the Petitcodiac and the operation of the tide gates are two other potential factors. At the Windsor tide gates, there is a total average of 665 x 10^6 m^3 per year of freshwater that passes through the gates, with highest amounts in May (NSDA, 2006). Coupled with freshwater discharge through the St. Croix, this may contribute to the seasonal variability in bed elevation. In the Spring, river discharge erodes silt deposited during the Summer and early Fall when the river flows are greatly reduced. Consequently, river bottoms may accrete or erode by as much as 2 m. (Desplanque and Mossman, 2004). This seasonal cyclicity in bed elevation has been observed (as much as 2 m in places) over many years by NSDA personnel and is supported by a recent study in the Salmon River (Crewe, 2004).

Cycles of progradation and retreat in marsh habitat were recorded along the Avon and St. Croix Rivers, and have been documented on a number of marsh and intertidal systems (e.g. Cumberland Basin - Ollerhead et al. in press; Cobequid Bay - Baker and van Proosdij, 2004; United Kingdom - van der Wal and Pye, 2004; Cox et al., 2003; Pringle, 1995). These changes appear to be a response primarily to shifts in the main channel thalweg, however, additional forcing functions such as wind and wave climate (Fan et al., 2006; van der Wal and Pye, 2004; Cox et al., 2003; Allen and Duffy, 1998; Pye, 1995; Allen, 1989), sediment supply (Allen, 2000; Gordon et al, 1985), sea level (van der Wal and Pye, 2004; French and Burningham, 2003; van der wal and Pye, 2003; Vos and van Kesteren, 2000; Allen, 2000; Allen, 1989), and human activities such as dredging (French and Burningham, 2003; Cox et al., 2003) or dyke construction and shoreline armouring practices (Hood, 2004) remain to be examined. Preliminary results indicate that, similar to other systems in the UK, salt marshes will

develop rapidly in front of newly dyked land and will cause a general decrease in the width of the channel. Salt marshes also have the potential to decrease the tidal prism, as was observed in this study. From 1858 to 1969 there was a decrease in the tidal prism by approximately 7%, which is equal to the volume of tidal prism that was directly cut off by the construction of the causeway.

Salt marshes and mudflats represent systems delicately balanced between hydrodynamic forces and ecological, sedimentological, and morphological responses. Changes in the elevation of the intertidal habitat within the tidal frame or changes in edge morphology will induce changes in tidal prism, hydrodynamic forces, vegetation community structure, rates of sedimentation, and dissipation (marsh platform) or amplification (cliff) of wave energy. These factors will influence the morphology of the intertidal feature. This area has provided an ideal environment for the colonization of an extensive and productive salt marsh habitat (Daborn et al., 2003a,b; van Proosdij and Townsend, 2006). This vegetation is expanding at an exponential rate

Figure 5.2: Windsor mudflat and Saint Mary's University weatherhawk Meteorological station viewed from the Tide Gate in August 2006.

(37%) (Townsend, 2002) and is rapidly colonizing all available space (Fig 5.2). Comparison of the 2001 GPS field survey of juvenile *Spartina alterniflora* (sparse, representing new shoots in 2001) conducted by Townsend (2002) with the 2003 marsh polygons digitized from aerial photographs supports the mechanism of colonization by rhizome expansion as mature marsh vegetation is now contained with the 2001 survey boundary. However, growth does appear to be limited in certain areas, such as along the edge of the deeper tidal creek channels and on the northern mudflat/marsh edge which is heavily scoured by ice during the winter months (van Proosdij, 2005). Currently the elevation of the marsh surface is close to the level of the HHWMT and accretion rates will decrease as the surface is flooded by fewer and fewer tides. This will likely permit other intertidal bodies to expand as more sediments are available for deposition and similar mechanisms of marsh growth are also currently being observed on the Newport Bar and the banks for the St. Croix and Avon rivers.

6.0   CONCLUSIONS

The purpose of this research was to investigate the spatial and temporal variability in intertidal morphodynamics of the Avon River Estuary and assess the resilience of the system to the influence of tidal barrier construction. As previous research has indicated, the intertidal geomorphology of the Avon River Estuary has been impacted by the construction of the Windsor causeway. However, the magnitude of this impact is much less than originally postulated in the 1970s. Many of the changes might also be associated with natural fluctuations in the position of the main tidal channel thalweg. Expanding the temporal scope of the research to include almost a 150 year period has revealed that, despite significant changes in anthropogenic modifications to the estuary, the Avon River estuary is a resilient system which may be considered to be in an equilibrium state over most of its reach. This equilibrium state, however, is not necessarily the same one which existed in 1858. Key findings of the research are presented below:

- Over time, the St. Croix River has increased its cross sectional area by approximately 9% from 1971 to 2006, mostly through deepening of the main channel with some marsh loss on the northern shore. Seasonal variability in bed elevation ($\pm$ 1.5m) and cross sectional area ranged from 2.8 to 17%.   The wetted perimeter remains constant suggesting that although the form of the river channel is changing, primarily due to a shift in the main channel thalweg from the south shore to north shore of the river, the hydraulic capacity of the system has not changed. Although the width of the St. Croix river has decreased since 1858 due to marsh growth on the foreshore of dykes, the width to depth ratio indicates that the system has responded by deepening its channel.

- The most significant changes in cross sectional area and sedimentation were recorded along lines 1A_DS_1A1AA and 1_DS_11AA immediately downstream of the Windsor causeway. This decrease in cross sectional area (measured from HHWLT) ranged from 75% to 54% along the two lines from 1970 to 2006 as a layer of sediment between 5.8 to 6.5 m deep accumulated downstream of the causeway.

- This significant accumulation of sediment has occurred at the site of an intertidal bar which was present before the construction of the Windsor causeway, and evidence suggests that it was also present in 1858. The location of this bar was likely bounded by the convergence of the Avon and St. Croix Rivers.

- The extensive salt marsh which has evolved adjacent to the causeway marsh and mudflat surface is now near the limit of the HHWMT level, and rates of sedimentation on the marsh surface will decrease due to decreased innundation frequency.   An increase in the high marsh (*Spartina patens*) community is anticipated.

- The tidal channel parallel to the causeway should continue to infill, and the eastern end will likely be completely vegetated within the next few years.

- An approximate 24% (±2.5) decrease in cross sectional area was recorded 1000 m downstream of the causeway at Line 5 from 1969 to 2006, however, there is no change in wetted perimeter and w/d or D/d ratios.

- Evidence is presented to support seasonal cycles of changes in bed elevation by as much as 2 m, which exceed the differences recorded between 1858-1969 and 2005/2006 in some locations. Seasonality and meteorological conditions (e.g. rainfall and runoff) can exert a strong influence on the interpretation and comparison of survey data. In addition, the resolution of sampling points and employing spatial interpolation techniques can influence the interpretation of change in the tidal prism.

- By Line 7 (1.8 km downstream of causeway), a new intertidal bar (Newport Bar) has developed since 1969, with between 2.9 to 7.1 m of sediment accumulation. However, 150 m (1500 m^2) of marsh has eroded from the western shore (Line 7) since 1955. The resultant cross sectional area in 2006 is only 13% (±4) smaller than in 1969 despite the very visible bar formation. The river profile is compensating by decreasing the depth of its main channel, and it is currently close to 1858 base levels.

- The mudflat and expanding salt marsh that has developed on the western shore of Line 9 (3 km downstream of the causeway) has decreased the cross sectional area by about 14%.

However, there is also an observed seasonal variability of 8%. The bed of the channel has lowered by 3.5 m and is close to 1858 levels.

- From Line 11 (5 km from the causeway) to Line 15 there is negligiable change in intertidal cross sectional area since 1858. Beyond this point, downstream of the Kennetcook river, there is a slight (2%) increase in cross sectional area since 1969 and a 2-6 % increase since 1858. Most of this has occurred through channel deepening.

- The tidal prism decrease of 7.3% from 1858 to 1969 is likely associated with dyking, and an additional 7.2% from construction of the causeway.

- Despite this decrease in the tidal prism, the Avon River estuary appears to have adjusted to a new equilibrium state through channel deepening, particularly in the St. Croix and Kennetcook Rivers. Freshwater discharge through the Windsor tide gate is also assisting in maintaining this form.

- The shape of the channel curve's width versus distance from the head of the Avon River did not vary between 1858 and 2006.

- Measures of channel form (e.g. width to depth ratio (w/d) and max to mean depth ratio (D/d)) clearly demonstrate that there is a significant shift in channel form approximately 1-2 km from the causeway. This suggests that the direct influence of the causeway may be limited to the first 2000 m. Beyond this point, the w/d and D/d pattern of change with distance vary only minorly between 1969, 1970, and 2005/2006. Accretional and erosional changes in the Avon River beyond this point may be due more to natural processes such as shifts in the main river thalweg and re-distribution of sediment.

- After the first 1000 m, the Avon River is joined by the St. Croix, and then further downstream by the Kennetcook. Both likely play a key role in flushing the system and maintaining predominance of sand and silt rather than a build up of fluid mud.

- The Avon river is dominated by sand transport with accumulation of finer material, mostly silts, near the causeway and along the western shore. No fluid mud was observed in this study

however given the high suspended sediment concentrations may be present in the tide gate channel when the gates are closed.   This is completely different from the Petitcodiac river where fluid mud processes drive sediment transport.

- Cycles of erosion and accretion of mudflat and marsh habitat were shown to be strongly influenced by the position of the thalweg of the main tidal channel.   While the eroded material does have the potential to subsequently 'feed' any new bar formation, this has yet to be emprically tested.   However, this cyclicity in marsh habitat is similar in rate and pattern to studies elsewhere (e.g. UK and Cumberland Basin, NB).

- In general, there is an overall decrease in marsh area from 1858 to 1964 with the exception of 1955. Over the following decade, the percentage of marsh area (as a proportion of the tidal prism) remains constant at around 11 % and begins to increase slightly in 1992. By 2007, the proportion of the Avon River study area covered by salt marsh vegetation had exceeded 1955 levels, though it did not exceed the 1858 levels.

- Overall there was an 87% loss of salt marsh from 1858 to 1955 (including upstream of the causeway) and an additional 14% loss from 1955 to 1964. It is estimated that 11% of marsh loss was due to 'natural causes' and 89% was due to dyking. However, this value should be interpreted with caution due to the poor reliability of the 1858 upstream data.   The proportion of marsh lost between 1955 and the construction of the causeway has been more than compensated for by the growth of new marsh downstream of the causeway and along the western shore.

- The risk to the causeway from storm surges or wave effects is low due to the presence of the salt marsh which acts as a natural form of coastal defense. However, with the approach of the Saros Tides in 2012-2013, the risk will increase and should be assessed further. Additionally, there is a greater risk to the causeway from freshwater flooding, depending on the timing of the storm relative to the tide.

REFERENCES

Ackers, P. 1988. Alluvial channel hydraulics. *Journal of Hydrology,* 100: 177-204.

Allen, J.R.L. 1989. Evolution of salt-marsh cliffs in muddy and sandy systems: a qualitative comparison of British west-coast estuaries. *Earth Surface Processes and Landforms* 14: 85-92.

Allen, J.R.L. 1996. Shoreline movement and vertical textural patterns in salt marsh deposits: implications of a simple model for flow and sedimentation over tidal marshes. *Proceedings of the Geologists Association* 107: 15-23.

Allen, J.R.L. 2000. Morphodynamics of Holocene saltmarshes: a review sketch from the Atlantic and Southern North Sea coasts of Europe. *Quaternary Science Reviews* 19: 1155-1231.

Allen, J.P. ; Sauzay, G. and P. Castaing. 1976. Transport and deposition of suspended sediment in the Gironde Estuary, France. In Wiley (ed) *Estuarine Processes* volume II. Academic Press, p. 63-81.

Allen, J.R.L. and M.J. Duffy. 1998. Medium-term sedimentation on high intertidal mudflats and salt marshes in the Severn Estuary, SW Britain: the role of wind and tide. *Marine Geology* 150: 1-27.

Amos, C.L. 1977. Effects of tidal power structures on sediment transport and loading in the Bay of Fundy-Gulf of Maine System. In Daborn (ed) *Fundy Tidal Power and the Environment:* Proceedings of a workshop on Environmental Implications of Fundy Tidal Power held at Wolfville, NS, Nov 4-5, 1976. Acadia University Institute Publication #28 p. 233-253.

Amos, C.L. and D.C. Mosher. 1985. Erosion and deposition of fine-grained sediments from the Bay of Fundy. *Sedimentology* 32:815-832.

Baker, G. and D. van Proosdij. 2004. Historical change in salt marsh habitat surrounding Cobequid bay, Nova Scotia: examing change with the aid of aerial photographs. Proceedings of the 6th Bay of Fundy Workshop, Annapolis Royal. Environment Canada – Atlantic Region, Occasional Report. 7 pp.

Bowron, T. and A. Fitzpatrick. 2001. Assessment of tidal restrictions along Hant's County's highway 215: opportunities and recommendations for salt marsh restoration. *Marine Issues Committee Special Publication* #9, 48 pp.

Bray, D.I.; DeMerchant, D.P. and D.L. Sullivan. 1982. Some hydrotechnical problems relating to the construction of a causeway in the estuary of the Petitcodiac River, New Brunswick. *Canadian Journal of Civil Engineering* 9: 296-307.

Cox, R.; Wadsworth, R.A. and A.G. Thomson. 2003. Long-Term changes in Salt Marsh extent affected by channel deepening in a modified estuary. *Continental Shelf Research* 23: 1833-1846.

Cronin, L.E.; Pritchard, D.W.; Koo, T.S.Y.l and Lotrich, V. 1977. Effects of the enlargement of the Chesapeake and Deleware Canal. In M. Wiley (ed) *Estuarine Processes, Volume 2*, Academic Press, New York, 18-32.

Daborn, G.R. and M. Brylinsky. 2004. Fish population studies of the Avon estuary, Pesaquid Lake and lower Avon River 2003. Report prepared for Nova Scotia Department of Transportation. Acadia Centre for Estuarine Research Publication No. 76. 153 pp. http://www.gov.ns.ca/tran/publications/publication.asp

Daborn, G.R., Brylinsky, M. and D. van Proosdij. 2003. Ecological Studies of the Windsor Causeway and Pesaquid Lake, 2002. Report prepared for Nova Scotia Department of Transportation Contract # 02-00026.

Acadia Centre for Estuarine Research Publication No. 69. 111 pp
http://www.gov.ns.ca/tran/publications/publication.asp

Daborn, G.R.; van Proosdij, D**.** and M. Brylinsky. 2003. Environmental Implications of Expanding the Windsor Causeway. Report prepared for Nova Scotia Department of Transportation Contract # 02-00026. Acadia Centre for Estuarine Research Publication No. 72. 15 pp
http://www.gov.ns.ca/tran/publications/publication.asp

Dalrymple, R.W. 1984. Morphology and internal structures of sandwaves in the Bay of Fundy. *Sedimentology* 31: 365-382.

Dalrymple, R.W.; Knight, R.J.; Zaitlin, B.A.; and Middleton, G.V. 1990. Dynamics and facies model of a macrotidal sand-bar complex, Cobequid Bay – Salmon River Estuary (Bay of Fundy). *Sedimentology* 37: 577-612.

Desplanque, C. and Mossman 2004. Tides and their seminal impact on the geology, geography, history, and socioeconomics of the Bay of Fundy, eastern Canada. *Atlantic Geology* 40 (1): 1-130.

Crewe, B. 2004. Characterization of sediment in the Salmon River Estuary. Unpublished Msc Dalhousie University and the Nova Scotia Agricultural College, Truro, N.S. 126 pp.

Fan, D.; Y. Guo, P. Wang and J.Z. Shi. 2006. Cross-shore variations in morphodynamic processes of an open-coast mudflat in the Changjiang Delta, China: with an emphasis on storm impacts. *Continental Shelf Research* 26: 517-538.

Forrester, W.D. 1983. *Canadian Tidal Manual.* Canadian Hydrographic Service. 138 pp.

French, P.W. 2001. Coastal Defences: Processes, problems, and solutions. Routledge, London.

French, J.R. and H. Burningham. 2003. Tidal Marsh Sedimentation Versus Sea-level Rise: A Southeast England Estuarine Perspective. *Proceedings of the International Conference on Coastal Sediments 2003*. CD-ROM Published by World Scientific Publishing Corp. and East Meets West Productions, Corpus Christi, Texas USA. ISBN 981-238-422-7. 14pp.

French, J.R.; Benson, T.; and Burningham, H. 2005. Morphodynamics and sediment flux in the Blyth Estuary, Suffolk, UK: Conceptual modelling and high resolution monitoring. In D.M . Fitzgerald and J. Knight (eds) *Morphodynamics and sedimentary evolution of estuaries*, Springer, 143-171.

French, J.R. and Clifford, N.J. 2000. Hydrodynamic modelling as a basis for explaining estuarine environmental dynamics: some computational and methodological issues. *Hydrological Processes* 14: 2089-2108.

Friedrichs, C.T. and Perry J.E. 2001. Tidal Salt Marsh Morphodynamics: A Synthesis. *Journal of Coastal Research* 27: 7-37.

Gordon, D.C. Jr. and P.J. Cranford. 1994. Export of organic matter from macro tidal salt marshes in the upper Bay of Fundy, Canada. In W.J. Mitsch (ed.) *Global Wetlands: Old World and New*. Elsevier, NY, pp. 257-264.

Gordon, D.C.,Jr.; Cranford, P.J. and C. Desplanque. 1985. Observations on the ecological important of salt marshes in the Cumberland Basin, a macrotidal estuary in the Bay of Fundy. *Estuarine, Coastal and Shelf Science* 20:205-217.

Hood, G.W. 2004. Indirect environmental effects of dikes on estuarine tidal channels: thinking outside of the dike for habitat restoration and monitoring. *Estuaries* 27(2): 273-282.

Hutchinson, M.F. 1989. A new procedure for gridding elevation and stream line data with automatic removal of spurious pits. Journal of Hydrology 106: 211-232.

Isaacman, L.A. 2005. Historic examination of the changes in diadromous fish populations and potential anthropogenic stressors in the Avon River watershed, Nova Scotia. Unpublished Master of Environmental Studies thesis, Dalhousie University, Halifax, Nova Scotia. 122 pp.

Jacques, Whitford and Associated Limited. 2002. Geotechnical Investigation Proposed Twinning of Highway 101 Avon River Causeway Windsor, NS. Report to the Nova Scotia Department of Public Works Project No. NSD16062-13.

Ke, X. and Collins, M. 2002. Saltmashes in the West Solent (southern England): their morphodynamics and evolution. In T. Healy, Y. Wang and J.A. Healy (eds) *Muddy Coasts of the World: Processes, Deposits and Function*, Elsevier Science B.V. 411-440.

Kestner, F.J.T. 1966. The Effects of Engineering Works on Tidal Estuaries. In Thorn (ed) *River Engineering and Water Conservation Works*, Butterworths, London. 226-238.

Knigton, D. 1984. *Fluvial Forms and Processes.* Routledge, Chapman and Hall, Inc. New York. 218 pp.

Kragtwijk, N.G.; Zitman, T.J.; Stive, M.J.F.; and Wang, Z.B. 2004. Morphological response of tidal basins to human interventions. *Coastal Engineering* 51: 207-221.

Locke, A; Hanson, J.M; Klassen, G.J.; Richardson, S.M. and C. I. Aube. 2003. The damming of the Petitcodiac River: species, populations and habitats lost. Northeastern Naturalist, 10(1):39-54.

Maritime Marshland Rehabilitation Administration (MMRA). 1966. Seventeenth annual report on activities under the Maritime Marshland Rehabilitation Act for the fiscal year ended March 31, 1966. 29 pp.

Möller, I and T. Spencer. 2002. Wave dissipation over macro-tidal saltmarshes: effects of marsh edge topography and vegetation change. *Journal of Coastal Research* SI 36: 506-521.

Myrick, R.M. and Leopold, L.B. 1963. Hydraulic Geometry of a small tidal estuary. *USGS Professional Paper 411-B.* U.S. Government Printing Office, Washington, DC. 18 pp.

Nichols, F.H.; Cloern, J.E.; Luoma, S.N.; and Peterson, D. H. 1986. The Modification of an Estuary. *Science* 231: 567-573.

Nova Scotia Department of Agriculture and Marketing (NSDAM). 1987. *Maritime Dykelands: the 350 Year Struggle.* Department of Government Services Publishing Division, 110 pp.

Niles, E. 2001. Review of the Petitcodiac River Causeway and Fish Passage Issues. Report prepared for Minister of Fisheries and Oceans Canada.

Ollerhead, J.; Davidson-Arnott, R.G.D. and A. Scott. In press. Cycles of salt marsh extension and contraction, Cumberland Basin, Bay of Fundy, Canada. In *Geomorphologia Littoral I Quaternari: Homenarge el Professor V.M. Rossello I Verger.* E. Sanjaume (ed).

Ollerhead, J.; van Proosdij, D. and R.G. D Davidson-Arnott. 1999. Ice as a Mechanism for Contributing Sediments to the Surface of a Macro-tidal Saltmarsh, Bay of Fundy. Proceedings of the Canadian Coastal Conference, CCSEA, 345-359.

Owen, M.W. and N.V.M. Odd. 1972. A mathematical model of the effect of a tidal barrier on siltation in an estuary. In Gray and Gashius (eds) *Tidal Power:* Proceedings of an International Conference on the utilization of tidal power, May 24-29, 1970 in Halifax, NS. Plenum Press, New York-London p. 457-485.

Perillo, G.M.E.; Drapeau, G.; Piccolo, M.C.; and Chaouq, N. 1993. Tidal circulation pattern on a tidal flat, Minas Basin, Canada. *Marine Geology* 112: 219-236.

Prandle, D. 2006. Dynamical controls on estuarine bathymetry: Assessment against UK database. *Estuarine, Coastal and Shelf Science* 68: 282-288.

Pringle, A.W., 1995. Erosion of a cyclic saltmarsh in Morecambe Bay, North-west England. *Earth Surface Processes and Landforms* 20: 387-405.

Pye, K. 1995. Controls on long-term saltmarsh accretion and erosion in the Wash, eastern England. *Journal of Coastal Research* 11(2): 337-356.

Robinson, S., van Proosdij, D. and H. Kolstee. 2004. Change in dykeland practices in agricultural salt marshes in Cobequid Bay, Bay of Fundy. Proceedings of the 6th Bay of Fundy Ecosystem Partnership Conference, Annapolis Royal, NS. Environment Canada – Atlantic Region, Occasional Report. 9 pp.

Schwimmer, R.A. and Pizzuto, J.E. 2000. A model for the evolution of marsh shorelines. *Journal of Sedimentary Research* 70(5): 1026-1035.

Shi, Z.; Lamb, H.F. and R.L. Collin. 1995. Geomorphic change of saltmarsh tidal creek networks in the Dyfi Estuary, Wales. *Marine Geology* 128: 73-83.

Slagle, A.L.; Ryan, W.B.F.; Carbotte, S.M.; Bell, R.; Nitsche, F.O.; and Kenna, T. 2006. Late-stage estuary infilling controlled by limited accommodation space in the Hudson River. *Marine Geology* 232: 181-202.

Smaal, A.C. and Nienhuis, P.H. 1992. The Eastern Scheldt (the Netherlands), from an estuary to a tidal bay: a review of responses at the ecosystem level. *Netherlands Journal of Sea Research* 30:161-173.

Sucsy, P.V.; Pearce, B.R.; and Panchang, V.G. 1993. Comparison of two- and three-dimensional model simulation of the effect of a tidal barrier on the Gulf of Maine tides. *Journal of Physical Oceanography* 23: 1231-1248.

Swift, D.J.P.; McMullen, R.M.; and Lyall, A.K. 1967. A Tidal Delta with an Ebb-Flood Channel System in the Minas Basin, Bay of Fundy: Preliminary Report. *Maritime Sediments* 3: 12-16.

Swift, D.J.P.; Pelletier, B.R.; Lyall, A.K.; and Miller, J.A. 1973. Quaternary Sedimentation in the Bay of Fundy. *Geology Survey of Canada: Earth Science Symposium on Offshore Eastern Canada* Paper 71-12: 113-151

Tang, Y.M. and Grimshaw, R. 2003. The effects of barriers on the tidal range in estuaries. *Estuarine, Costal and Shelf Science* 58: 57-66.

Tang, Y.M. and Grimshaw, R. 2002. The effect of a barrier on tidally forced flow in a density-stratified estuary. *Continental Shelf Research* 22: 2035-2044.

Thomas, C.G.; Spearman, J.R.; and Turnbull, M.J. 2002. Historical morphological change in the Mersey Estuary. *Continental Shelf Research* 22:1775-1794.

Toffolon, M. and Crosato, A. 2007. Developing macroscale indicators for estuarine morphology: The case of the Scheldt Estuary. *Journal of Coastal Research* 23 (1): 195-212.

Tonis, I.E.; Stam, J.M.T. and J. van de Graaf. 2002. Morphological changes of the Haringvliet estuary after closure in 1970. *Coastal Engineering* 44: 191-203.

Townsend, S. 2002. Spatial analysis of *Spartina alterniflora* colonization on the Avon River mudflats, Bay of Fundy, following causeway construction. Unpublished Honours B.A. thesis, Saint Mary's University Department of Geography, 108 pp.

Turk, T.R; Risk, M.J.; Hirtle, R.W.M. and R.Y. Yeo. 1980. Sedimentological and biological changes in the Windsor mudflat, an area of inducted siltation. *Canadian Journal of Fisheries and Aquatic Science* 37: 1387-1397.

Uncles, R.J. 2002. Estuarine Physical Processes Research: Some Recent Studies and Progress. *Estuarine, Coastal and Shelf Science* 55: 829-856.

US Army Corps of Engineers. 2002. *Engineering and Design: Hydrographic Surveying.* USACE Publication # EM1110-2-1003.

Van der Wal, D. and K. Pye. 2004. Patterns, rates and possible causes of erosion in Greater Thames Area (UK). *Geomorphology* 61:373-391.

Van der Wal, D., and K. Pye. 2003. The use of historical bathymetric charts in a GIS to assess morphological change in estuaries. *The Geographical Journal* 169 (1): 21-31.

van Proosdij, D. 2005. Monitoring Seasonal Changes in Surface Elevation in Intertidal Environments near the Windsor Causeway. Final report prepared for the Nova Scotia Department of Transportation 22 pp. http://www.gov.ns.ca/tran/publications/publication.asp

van Proosdij, D. and P. Horne. 2006. Development of a series of historical digital mosaics depicting change in intertidal habitat in the Minas Basin. Final report prepared for the Gulf of Maine Council and Bay of Fundy Ecosystem Partnership. 26 pp.

van Proosdij, D. and S., Townsend. 2006. Spatial and Temporal Patterns of Salt Marsh Colonization Following Causeway Construction in the Bay of Fundy. *Journal of Coastal Research*, SI 39 (Proceedings of the 8th International Coastal Symposium):1858-1862, Itajaí, SC – Brazil, 2004 ISSN 0749-0208

van Proosdij, D.; Bambrick.J and G. Baker. 2006. Spatial and Temporal Variations in the Intertidal Geomorphology of the Avon River Estuary. Final report prepared for Nova Scotia Department of Transportation and Public Works 73pp. http://www.gov.ns.ca/tran/publications/publication.asp

van Proosdij, D.; Ollerhead, J. and R.G.D. Davidson-Arnott. 2006. Seasonal and Annual Variations in the Sediment Mass Balance of a Macro-tidal Salt Marsh. *Marine Geology* 225: 103-127.

van Proosdij, D**.**, Daborn., G.R. and M. Brylinsky. 2004. Environmental Implications of Expanding the Windsor Causeway (Part Two): Comparison of 4 and 6 Lane Options. Report prepared for Nova Scotia Department of Transportation Contract # 02-00026. Acadia Centre for Estuarine Research Publication No. 75. 17 pp.

van Zoost, J.R. 1969. The ecology and waterfowl utilization of the John Lusby National Wildflie Area. Msc Thesis, Acadia University. 183 p.

Vos, P. C. and W.P. van Kesteren. 2000. The long-term evolution of intertidal mudflats in the northen Netherlands during the Holocene; natural and anthropogenic processes. *Continental Shelf Research* 20: 1687-1710.

Wells, P. 1999. Environmental Impacts of Barriers on Rivers Entering the Bay of Fundy. Report of an ad hoc Environment Canada Working Group. Technical Report Series Number 334, Canadian Wildlife Service, Ottawa, ON. 43 p.

Williams, P.B.; Orr, M.K.; and Garrity, N.J. 2002. Hydraulic Geometry: A Geomorphic Design Tool for Tidal Marsh Channel Evolution in Wetland Restoration Projects *Restoration Ecology* 10(3): 577–590.

Wilkens,J. and R. Mayerle. 2005. Morphodynamic response to natural and anthropogenic influences in the Dithmarschen Bight. *Kurste* 69:311-337.

Wolanski, E.; Moore, K.; Spagnol, S.; N D'Adamo and C. Pattiaratchi. 2001. Rapid, human-induced siltation of the macro-tidal Ord Estuary, Western Australia. *Estuarine, Coastal and Shelf Science* 53:717-732.

APPENDIX A

A.1   Kentville Meteorological Charts

Figure A.1:   Kentville meteorological data. Station located at 45º4.2'N, 64 º 28.8'W.   Data for these graphs were obtained from Environment Canada's 'Canadian Climate Data' website, WMO ID 7167. Survey dates are indicated with arrows.
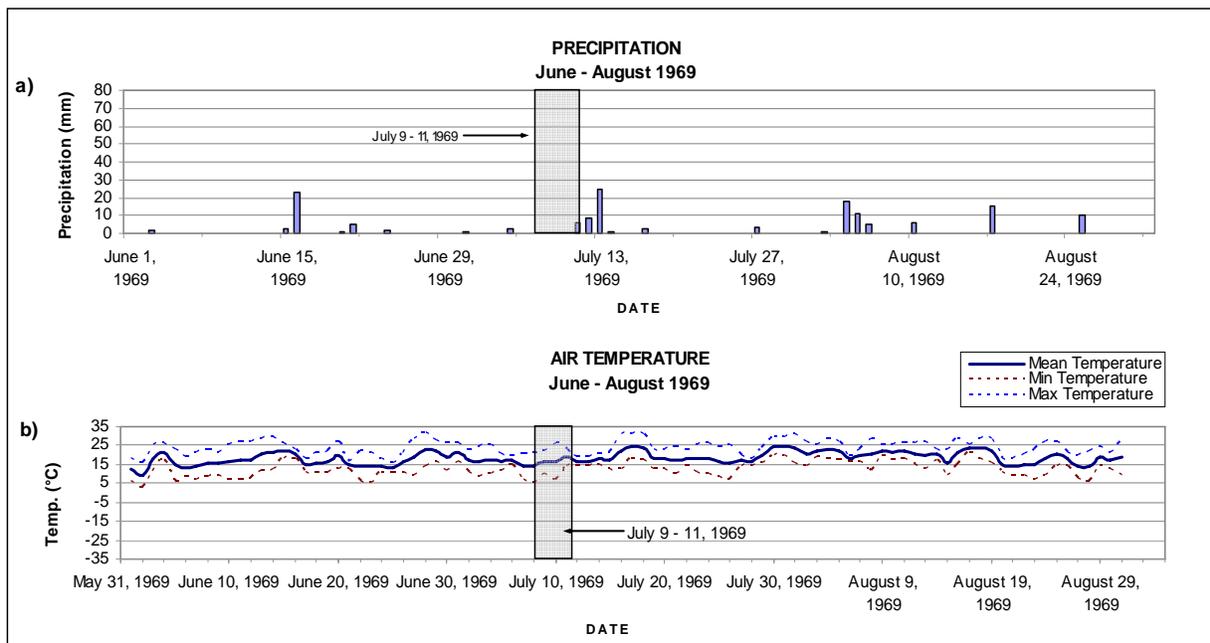
a) Precipitation from June 1st - August 31st, 1969. b) Air temperature from June 1st - August 31st, 1969.
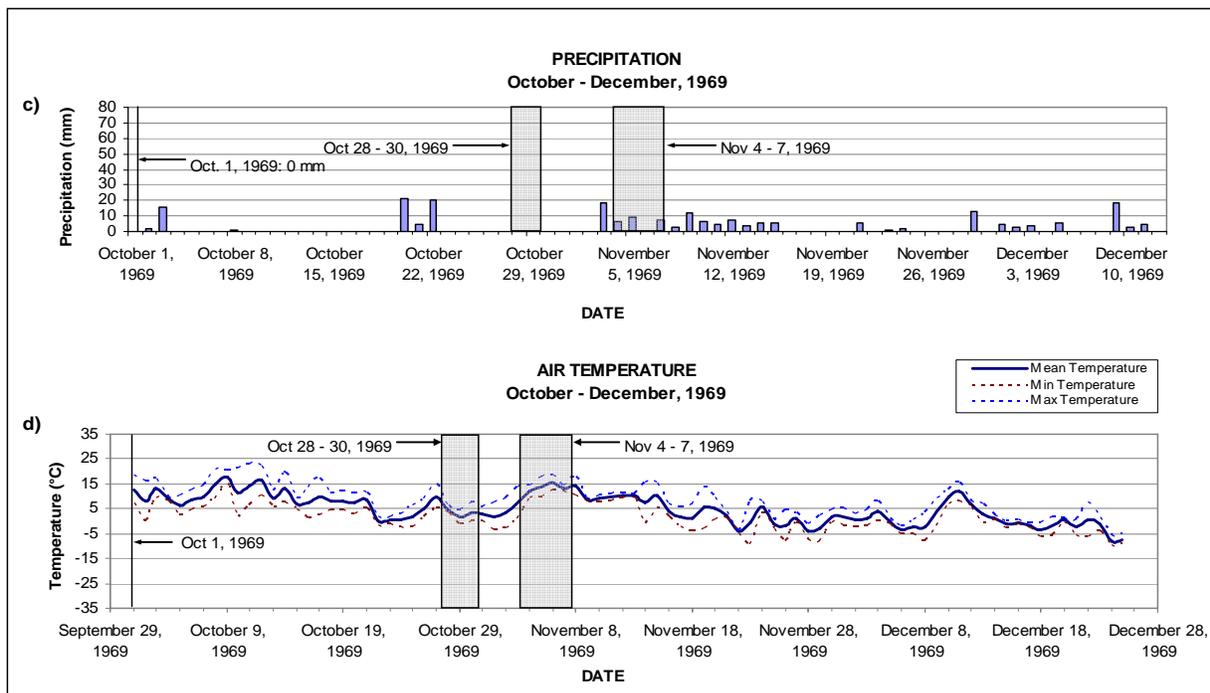
c) Precipitation from October 1st - December 15th, 1969.   d) Air temperature from October 1st - December 28th, 1969.

e)

PRECIPITATION
April - June, 1970

f)

AIR TEMPERATURE
April - June, 1970
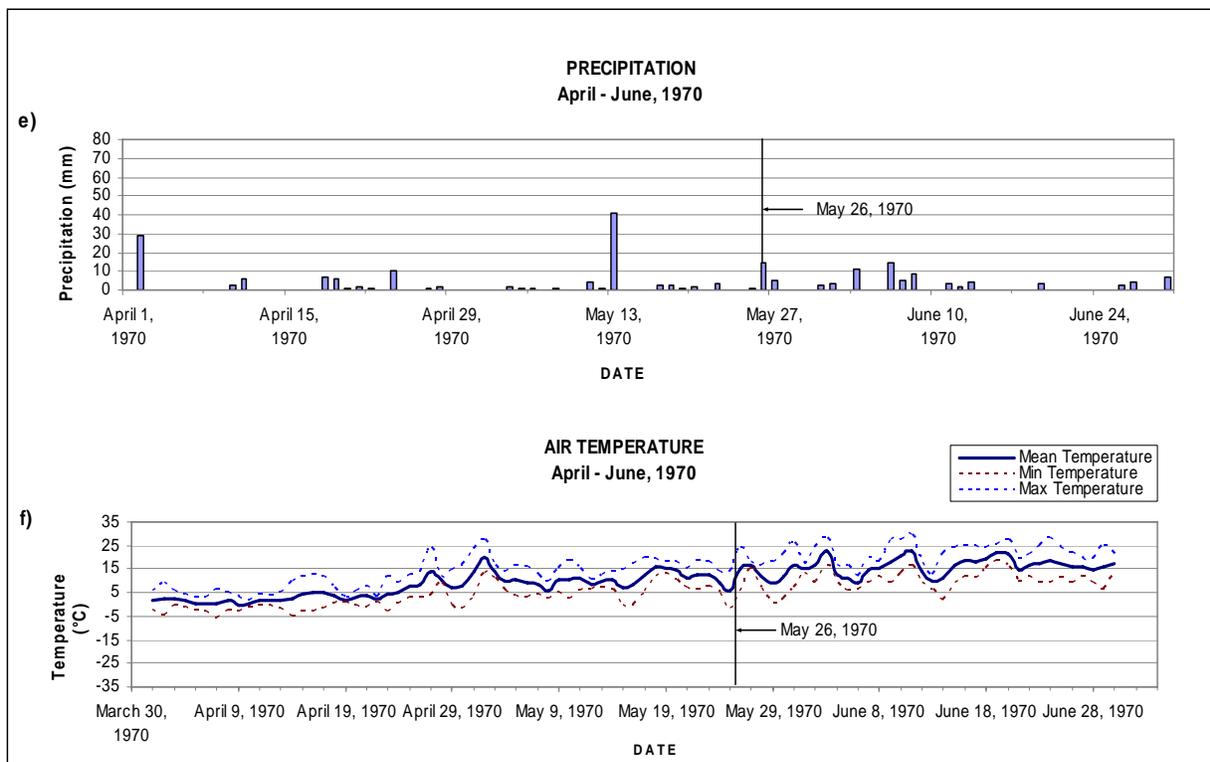
e)Precipitation from April 1st - June 30th, 1970.   *f) Air temperature from April 1st - June 30th, 1970.*

g)

PRECIPITATION
October - December, 1970

h)

AIR TEMPERATURE
October - December, 1970
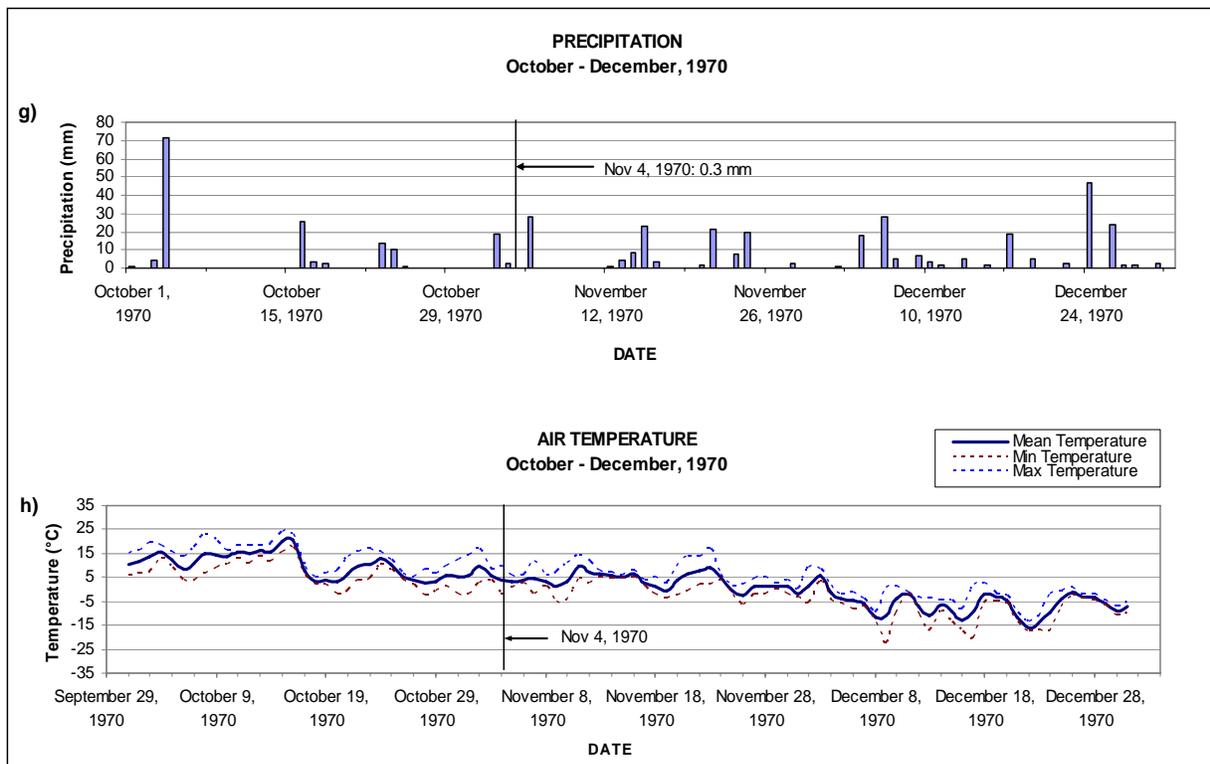
g) Precipitation from October 1st - December 31st, 1970.   *h)Air temperature from October 1st - December 31st, 1970*
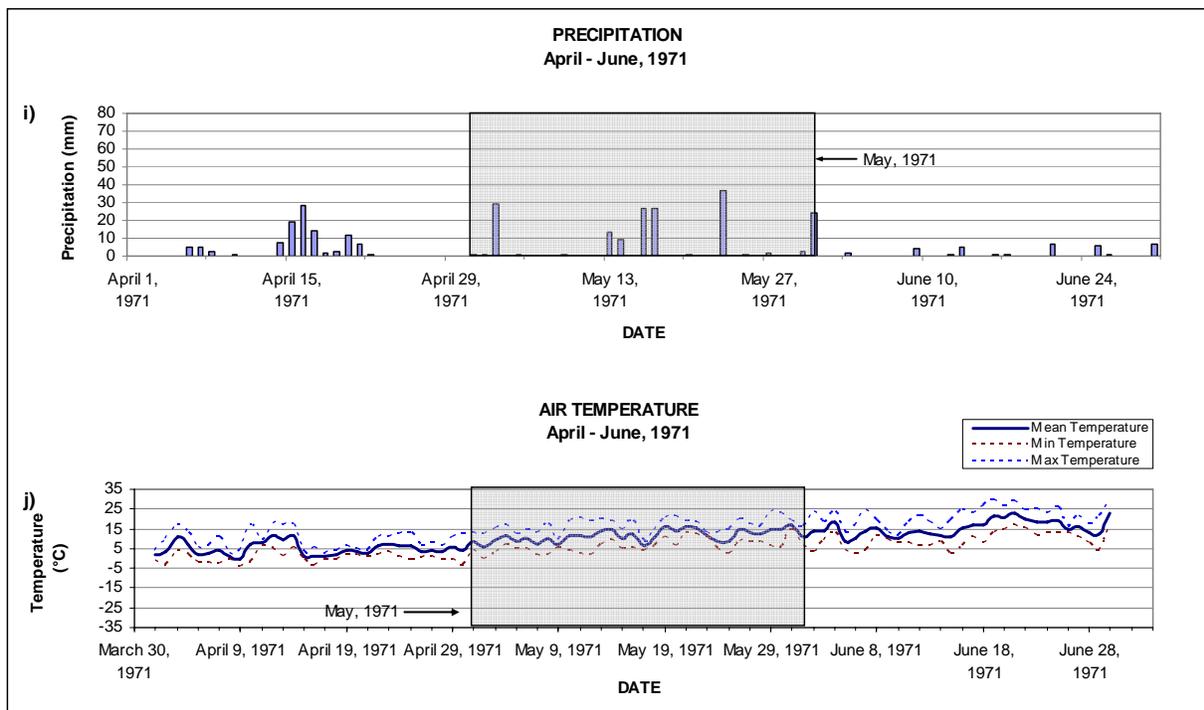
i) Precipitation from April 1st - June 30th, 1971.   *j) Air temperature from April 1st - June 30th, 1971.*
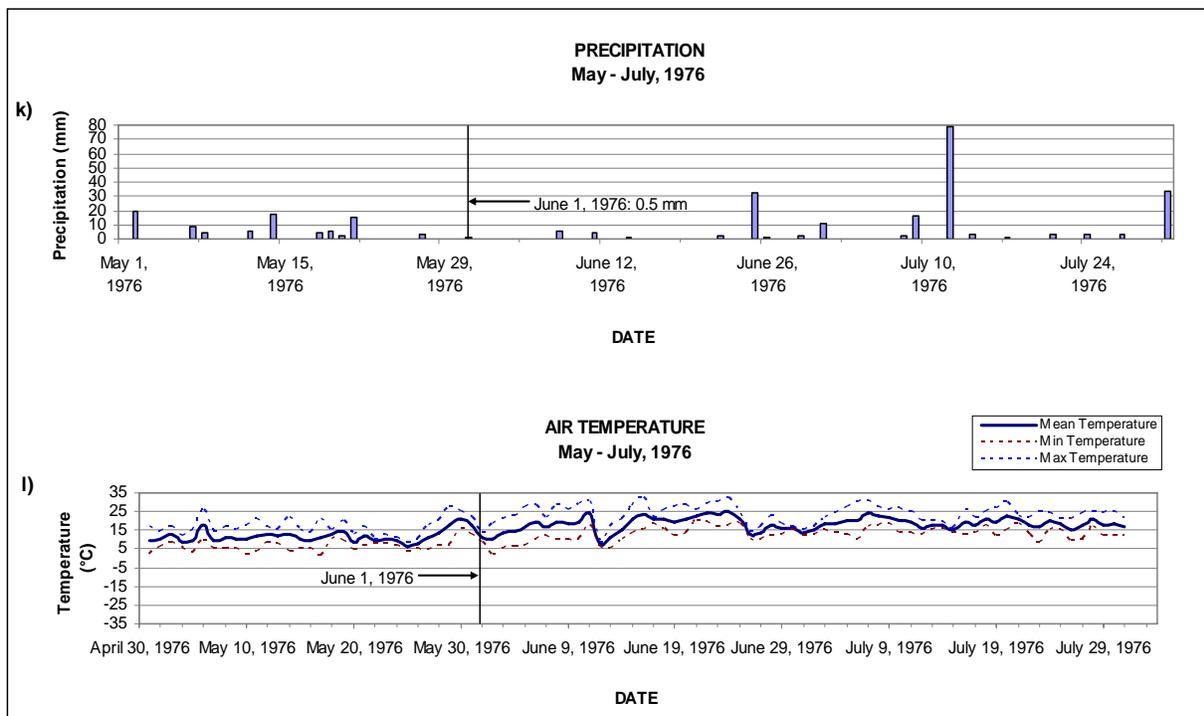
k) Precipitation from May 1st - July 31st, 1976. l) Air temperature from May 1st - July 31st, 1976.
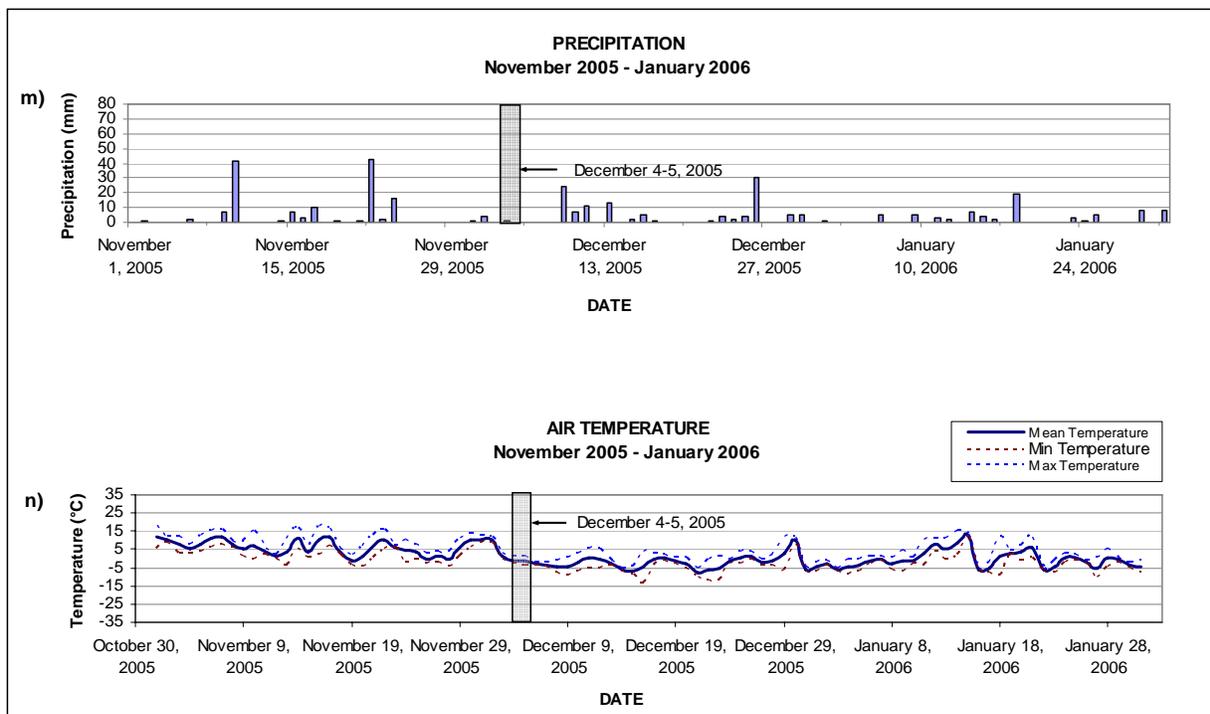
m) Precipitation from November 1st 2005 - January 31st, 2006.   *n) Air temperature from November 1st, 2005 - January 31st, 2006.*
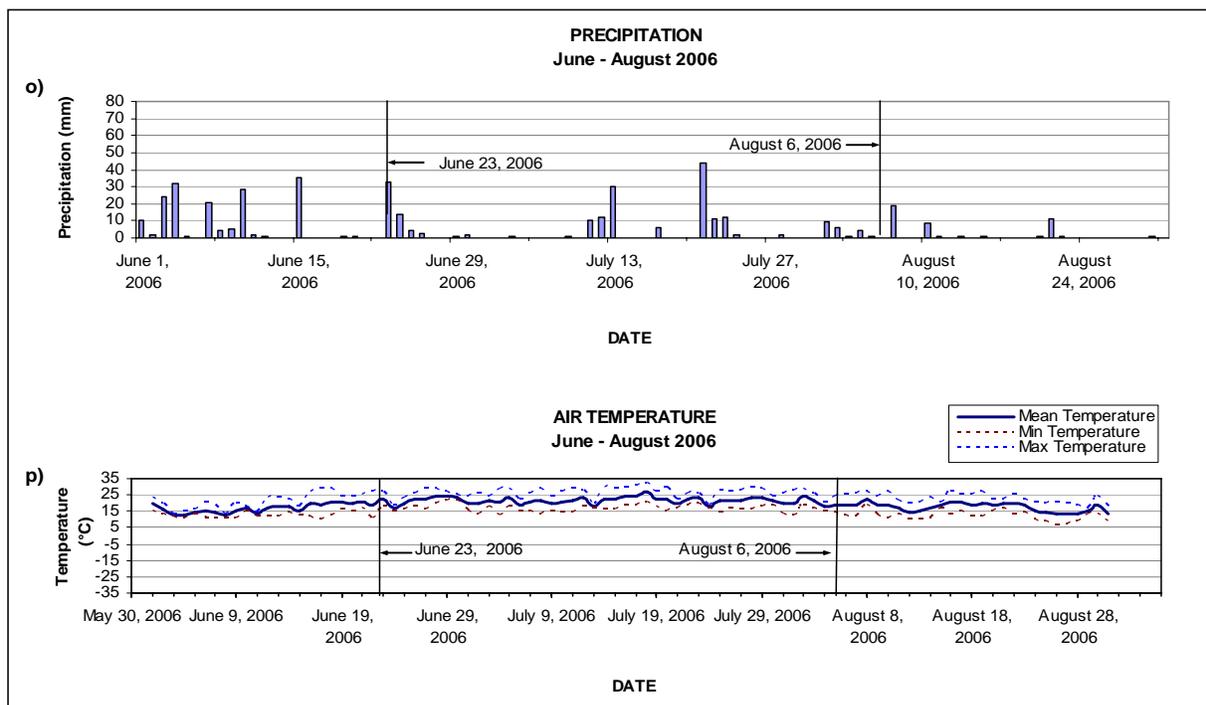
o) Precipitation from June 1st - August 31st, 2006. p) Air temperature from June 1st - August 31st, 2006.

A.2   Windsor Meteorological Charts

Figure A.2:   Windsor meteorological data were recorded at the Weatherhawk^{tm} meteorological station (44.99 N, -64.15 W) illustrated in Figure 5.2. Survey dates are indicated with arrows
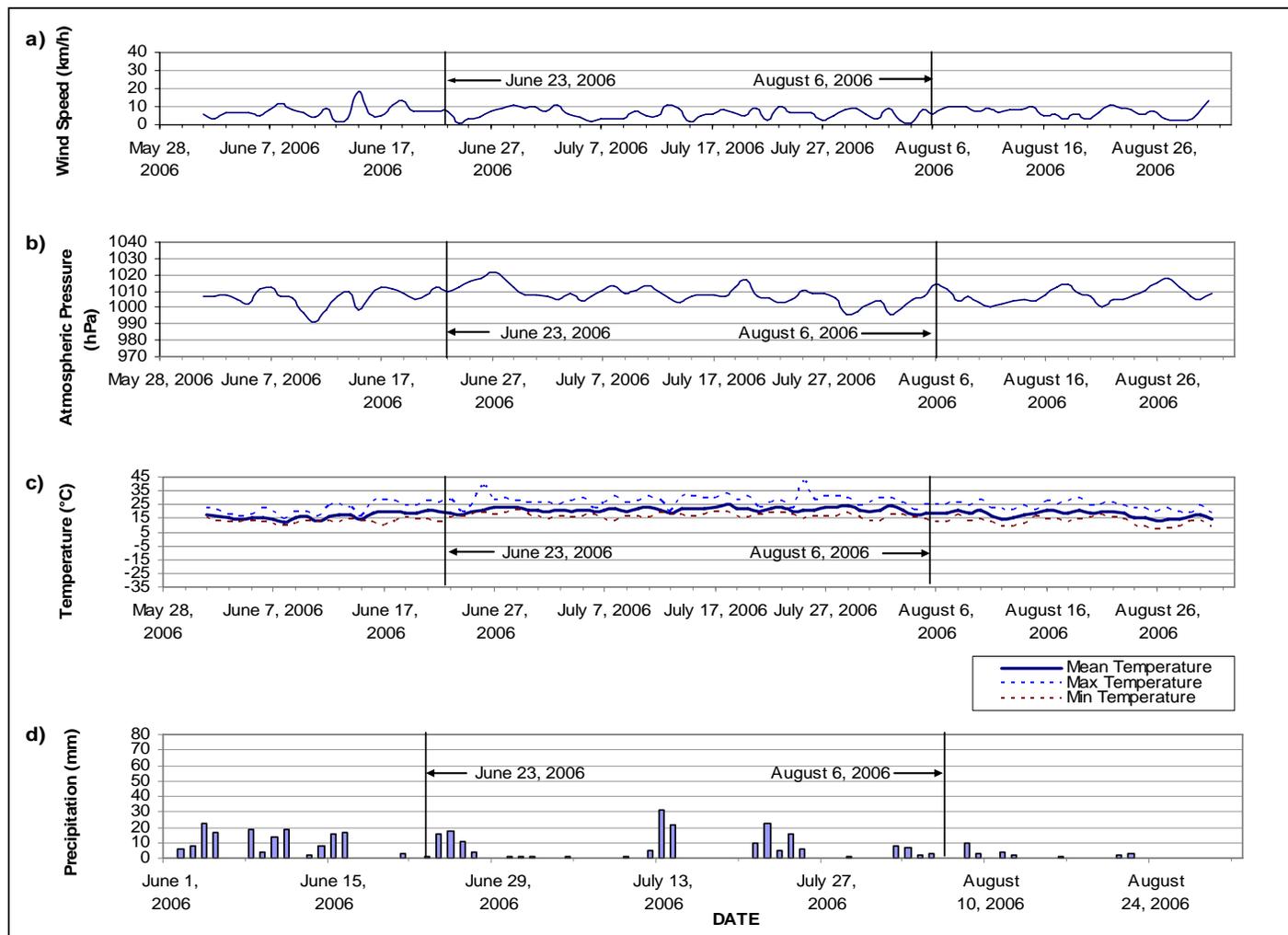
a) Mean daily wind speed from June 1st - August 31st, 2006. b) Mean daily atmospheric pressure from June 1st - August 31st, 2006.   c) Mean daily temperature, minimum temperature, and maximum temperature from June 1st - August 31st, 2006. d) Total daily precipitation from June 1st - August 31st, 2006.
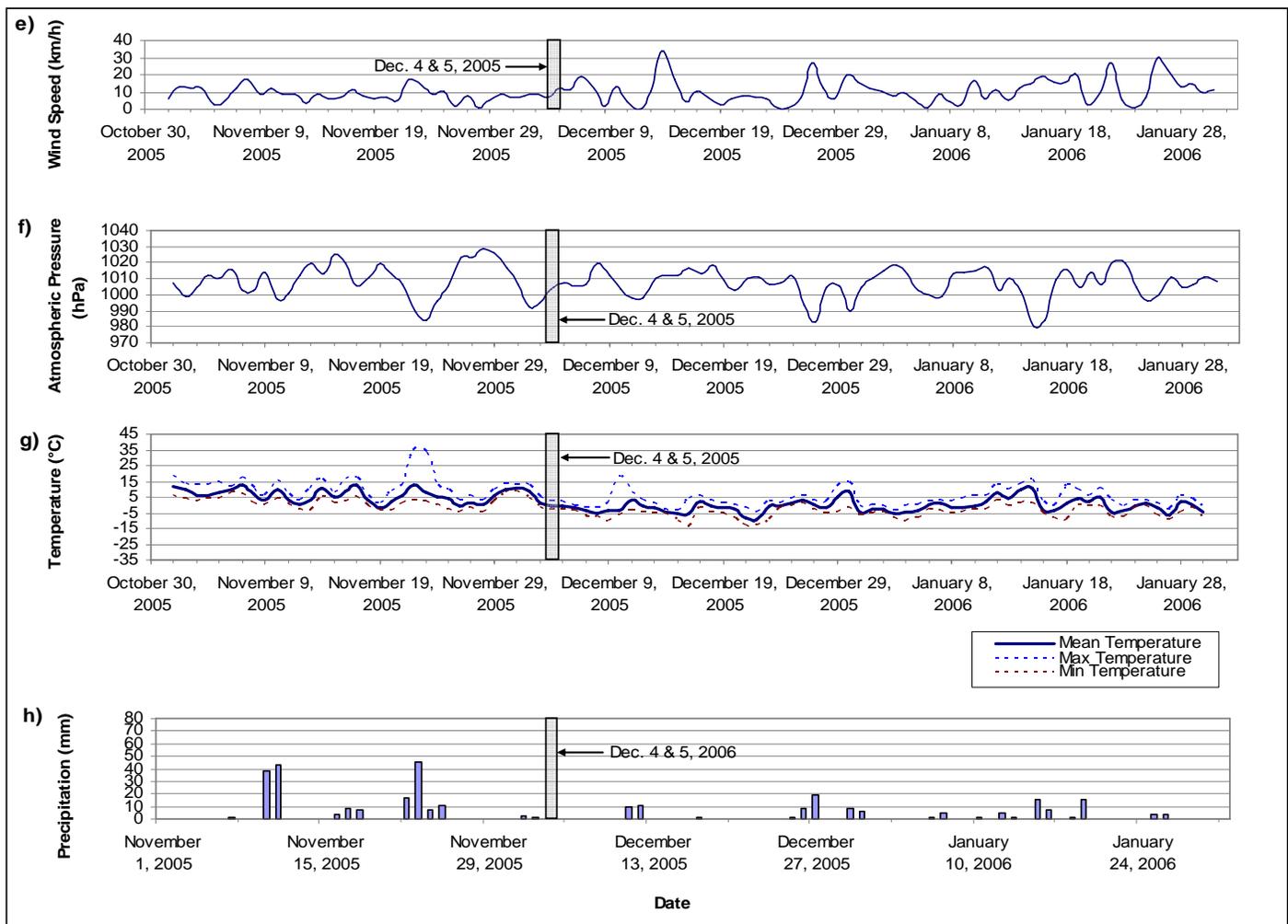
e) Mean daily wind speed from November 1st 2005 – January 31ˢᵗ, 2006. f) Mean daily atmospheric pressure from November 1st 2005 – January 31ˢᵗ, 2006.   g) Mean daily temperature, minimum temperature, and maximum temperature from November 1st 2005 – January 31ˢᵗ, 2006. h) Total daily precipitation from November 1st 2005 – January 31ˢᵗ, 2006.

A.3   Windsor Tide Data

Figure A.3:   Graphs of observed tide height and predicted tide height. Observed tide height was recorded at the Weatherhawk[tm] meteorological station (44.99 N, -64.15 W), and predicted tide height was obtained using Tides and Weather[tm] software
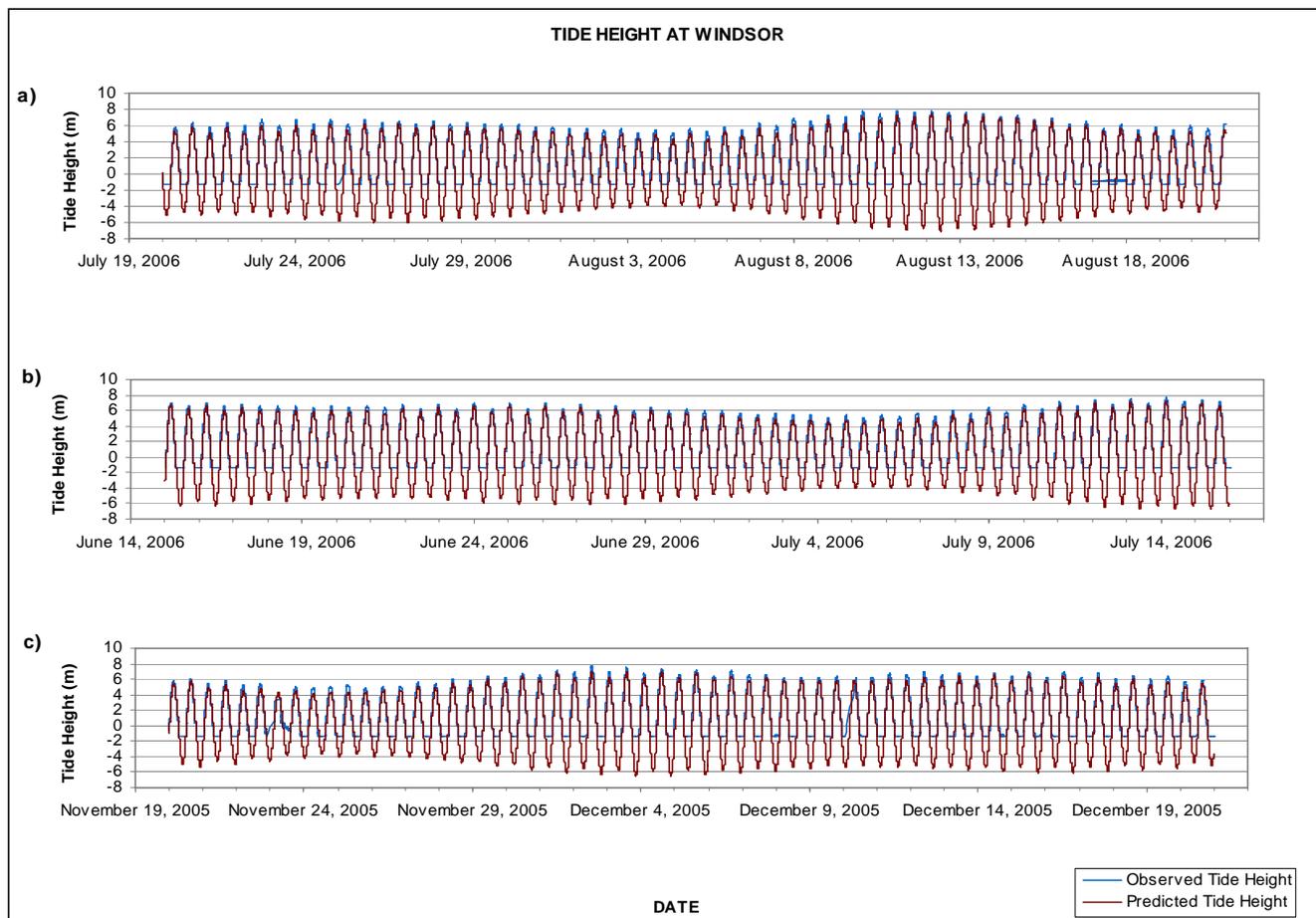
a) Tide data from July 20th – August 20th, 2006 for survey date August 6th, 2006. b) Tide data from June 15th – July 15th, 2006 for survey date June 23, 2006. c) Tide data from November 20th – December 20th, 2005 for survey dates December 4 -5, 2005.

A.4 Windsor Wind Charts

Figure A.4:   *Wind rose diagrams for Windsor, Nova Scotia. Data for these graphs were recorded at the Weatherhawk[tm] meteorological station (44.99 N, -64.15 W).*
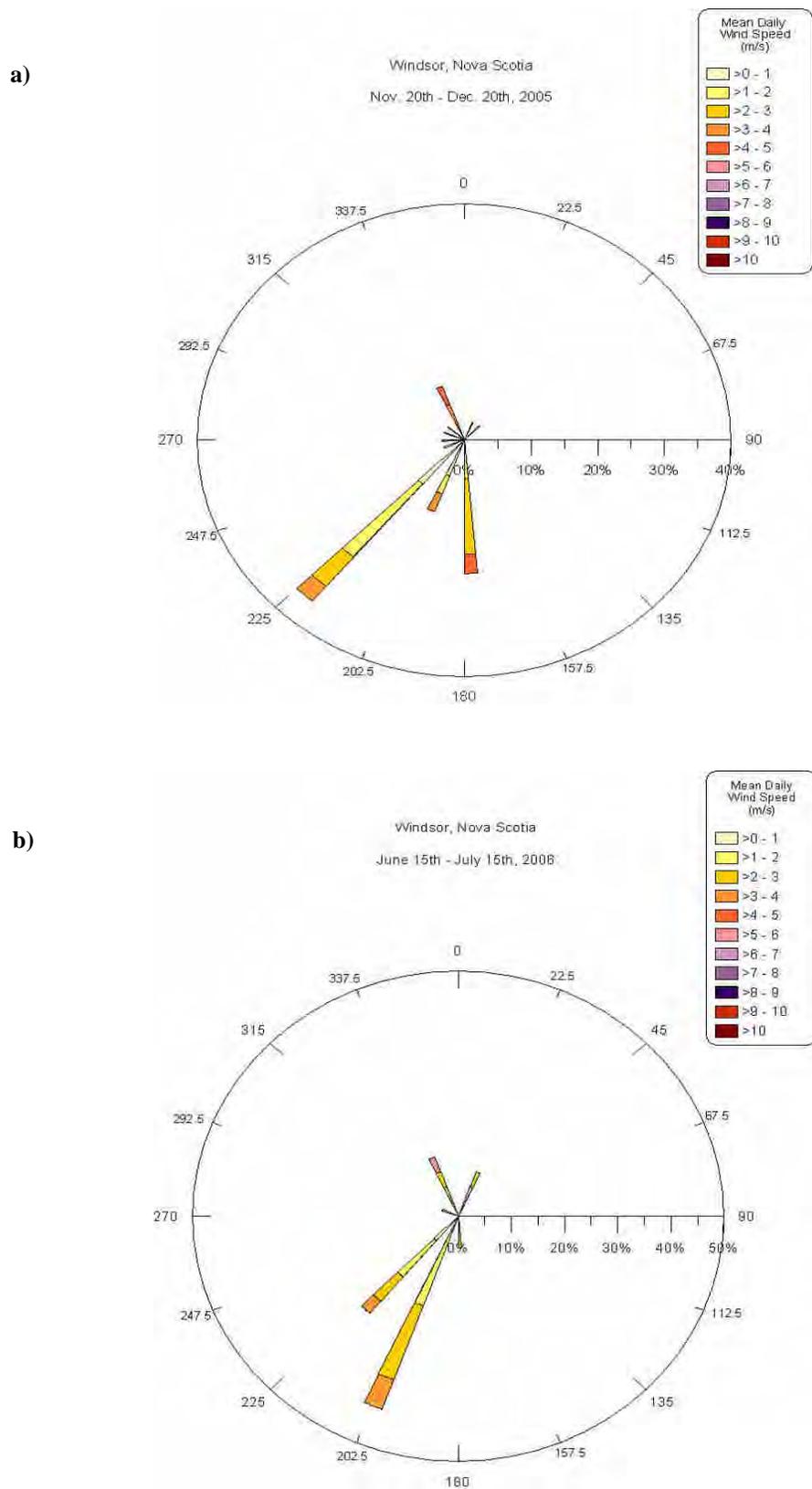
c)
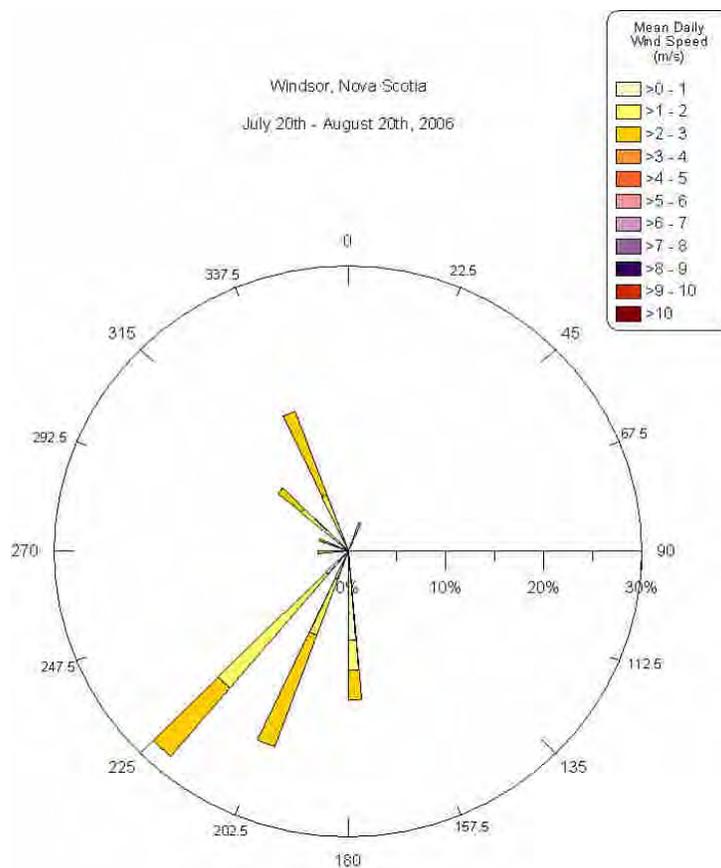
a) Wind data from November 20th – December 20th, 2005 for survey dates December 4-5, 2005. b) Wind data from June 15th – July 15th, 2006 for survey date June 23rd, 2006. c) Wind data from July 20th – August 20th, 2006 for survey date August 6th, 2006.

A.5   Normalized Precipitation Graphs

Figure A.5:   Normalized precipitation graphs.
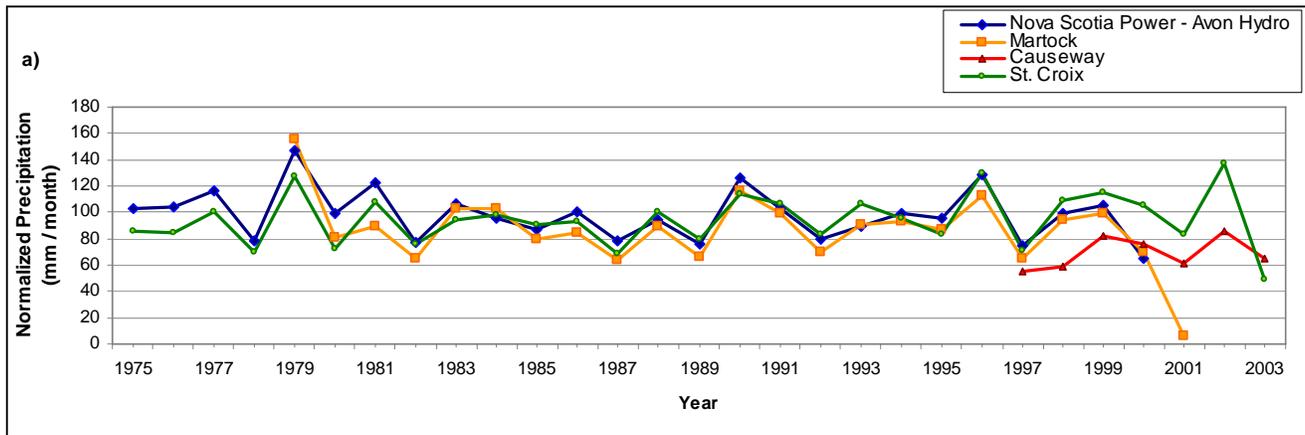
a) Normalized precipitation line graph for Nova Scotia Power Avon Hydro, Martock, Causeway, and St. Croix from 1975 – 2003.
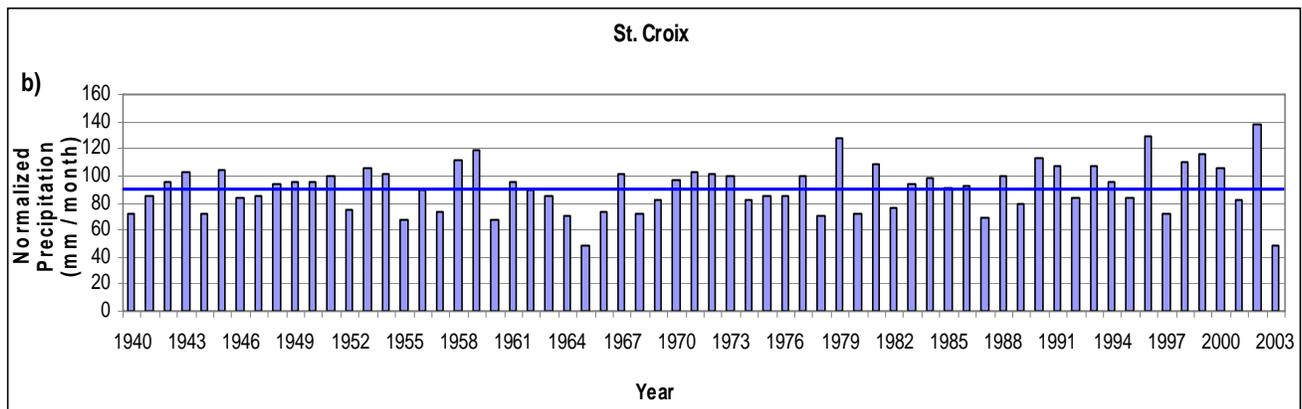
b) Normalized precipitation bar graph for St. Croix from 1940 – 2003. Blue line indicates the average normalized precipitation value of 91.1 mm/month.

APPENDIX B

Calculation of Tide Water Levels for Aerial Photo Mosaics

		From Air Photography Report				From Mosaic		Calculated			Tidal Data		
Roll #	Date	Photo #	to Photo #	Start (GMT)	End (GMT)	Photo # Start	Photo # End	Start (ADT)	End (ADT)	Average (ADT)	Tide in Feet (CD)	Conversion to Metres	Tide (CGVD28)
03301	27-Jun-03	1	181	11:45	12:18	15	16	8:47	8:47	8:47	23	7.0104	-0.2196
03302	27-Jun-03	1	150	12:37	13:08	14	17	9:39	9:40	9:40	24.3	7.40664	0.17664
02202	27-Jul-03	1	150	12:37	13:08	22	26	9:41	9:42	9:41	3	0.9144	-6.3156
03308	8-Jul-03	1	85	12:08	12:23	25	25	9:12	9:12	9:12	3.6	1.09728	-6.13272
03308	8-Jul-03	86	150	12:29	12:41	93	99	9:30	9:31	9:30	42	12.8016	5.5716
03308	8-Jul-03	151	208	12:45	12:55	164	171	9:47	9:48	9:47	40.3	12.28344	5.05344
03316	31-Jul-03	1	195	12:54	13:36	16	17	9:57	9:57	9:57	3.7	1.12776	-6.10224
03316	31-Jul-03	1	195	12:54	13:36	27	27	9:59	9:59	9:59	14.3	4.35864	-2.87136
03317	29-Jul-03	1	62	20:13	20:25	15	19	17:15	17:16	17:16	20.6	6.27888	-0.95112
03317	29-Jul-03	1	62	20:13	20:25	24	24	17:17	17:17	17:17	20.6	6.27888	-0.95112
03318	15-Aug-03	1	106	12:17	12:37	31	31	9:22	9:22	9:22	3.5	1.0668	-6.1632
02307	12-Jul-02	122	146	13:21	13:28	146	146	10:28	10:28	10:28	5.5	1.6764	-5.5536
02307	13-Jul-02	149	181	11:41	11:44	180	180	8:43	8:43	8:43	8.9	2.71272	-4.51728
02307	13-Jul-02	182	189	11:48	11:50	183	189	8:48	8:50	8:49	8.9	2.71272	-4.51728
02308	13-Jul-02	39	80	12:37	12:41	75	79	9:40	9:40	9:40	2.9	0.88392	-6.34608
02308	13-Jul-02	88	115	13:07	13:10	114	114	10:09	10:09	10:09	1.7	0.51816	-6.71184
02308	13-Jul-02	116	165	13:22	13:26	153	165	10:25	10:26	10:25	2	0.6096	-6.6204
02309	15-Jul-02	1	18	12:25	12:27	3	18	9:25	9:27	9:26	14.6	4.45008	-2.77992
02322	8-Aug-02	70	142	12:37	12:42	116	142	9:40	9:42	9:41	13.8	4.20624	-3.02376
02322	8-Aug-02	143	175	13:06	13:09	175	175	10:09	10:09	10:09	18.8	5.73024	-1.49976
02327	12-Aug-02	88	114	19:57	20:01	114	114	17:01	17:01	17:01	46.5	14.1732	6.9432
02329	1-Sep-02	99	146	18:41	18:47	144	146	15:46	15:47	15:46	12.2	3.71856	-3.51144
02329	1-Sep-02	147	203	18:50	18:57	190	200	15:55	15:56	15:56	14.1	4.29768	-2.93232
92300	17-Jun-92	1	222	11:25	12:08	87	97	8:41	8:43	8:42	5.6	1.70688	-5.52312
92301	17-Jun-92	28	217	12:40	13:21	62	62	9:47	9:47	9:47	3.9	1.18872	-6.04128
92302	18-Jun-92	1	122	11:25	11:52	43	59	8:34	8:37	8:36	10	3.048	-4.182
92303	18-Jun-92	1	127	12:40	13:07	46	63	9:49	9:53	9:51	4.4	1.34112	-5.88888
92303	18-Jun-92	128	220	13:11	13:32	172	211	10:21	10:29	10:25	5	1.524	-5.706
92316	24-Jun-92	1	63	17:43	17:55	48	63	14:52	14:55	14:53	10.2	3.10896	-4.12104
92316	24-Jun-92	64	92	18:14	18:22	88	92	15:20	15:22	15:21	11.6	3.53568	-3.69432
92317	27-Jun-92	56	161	11:48	12:18	96	137	8:59	9:11	9:05	32.7	9.96696	2.73696
92343	17-Jul-92	86	130	12:05	12:17	97	107	9:08	9:10	9:09	5.3	1.61544	-5.61456
92344	17-Jul-92	1	52	12:35	12:45	22	28	9:39	9:40	9:39	4.8	1.46304	-5.76696
92363	6-Aug-92	1	216	13:33	14:11	87	95	10:48	10:49	10:48	20.2	6.15696	-1.07304
92379	22-Aug-92	63	109	16:14	16:26	63	73	13:14	13:16	13:15	12.1	3.68808	-3.54192
92389	13-Sep-92	1	122	12:36	13:01	61	63	9:48	9:48	9:48	10.1	3.07848	-4.15152
NSA30670	4-Jun-73	99	145	15:03	15:20	136	136	12:16	12:16	12:16	15.9	4.84632	-2.38368
NSA30670	4-Jun-73	146	178	15:23	15:31	155	155	12:25	12:25	12:25	15.9	4.84632	-2.38368
NSA30671	5-Jun-73	1	24	12:38	12:45	1	1	9:38	9:38	9:38	4.5	1.3716	-5.8584
NSA30676	4-Jun-73	1	46	12:54	13:01	6	12	9:54	9:55	9:55	0.9	0.27432	-6.95568
NSA30676	4-Jun-73	47	91	13:10	13:26	83	89	10:23	10:25	10:24	1	0.3048	-6.9252
NSA30676	4-Jun-73	92	134	13:28	13:39	94	94	10:28	10:28	10:28	1	0.3048	-6.9252
NSA30676	4-Jun-73	135	178	13:41	13:58	178	178	10:58	10:58	10:58	2.8	0.85344	-6.37656
NSA30893	5-Sep-73	1	40	12:43	12:58	10	10	9:46	9:46	9:46	7.8	2.37744	-4.85256
NSA30893	5-Sep-73	118	132	13:43	13:47	121	121	10:43	10:43	10:43	2.3	0.70104	-6.52896
18352	16-May-64	7	74	14:32	15:02	73	74	12:01	12:02	12:01	3.2	0.97536	-6.25464
18352	16-May-64	75	139	15:08	15:26	75	76	12:08	12:08	12:08	3.2	0.97536	-6.25464
18352	16-May-64	140	206	15:55	16:05	205	205	13:04	13:04	13:04	9.4	2.86512	-4.36488
18354	16-May-64	199	253	11:58	12:13	207	209	9:00	9:00	9:00	15.9	4.84632	-2.38368

A18357	16-May-64	1	73	12:25	12:56	62	65	9:51	9:52	9:51	7.4	2.25552	-4.97448
A18357	16-May-64	74	142	13:01	13:21	81	86	10:03	10:04	10:03	7.4	2.25552	-4.97448
A18357	16-May-64	143	213	13:25	13:54	202	216	10:49	10:55	10:52	2.6	0.79248	-6.43752
A18357	16-May-64	214	271	14:00	14:17	210	214	10:58	11:00	10:59	2.6	0.79248	-6.43752
A18407	9-Jun-64	181	260	19:49	20:16	248	248	17:11	17:11	17:11	16	4.8768	-2.3532
A18439	28-Jun-64	1	48	12:55	13:11	44	48	10:09	10:11	10:10	5.1	1.55448	-5.67552
A18439	28-Jun-64	49	82	13:15	13:25	49	51	10:15	10:15	10:15	5	1.524	-5.706
A18599	29-Aug-64	18	22	13:55	13:57	21	21	10:56	10:56	10:56	9.4	2.86512	-4.36488
A18599	29-Aug-64	23	34	14:03	14:07	33	33	11:06	11:06	11:06	9.4	2.86512	-4.36488
A14713	28-Jun-55	80	93	11:57	12:02	88	90	11:00	11:00	11:00	24	7.3152	0.0852
A14662	19-Jun-55	13	80	16:05	16:18	69	72	15:15	15:16	15:16	28.9	8.80872	1.57872
A14662	19-Jun-55	81	150	16:33	16:48	92	93	15:35	15:35	15:35	28.9	8.80872	1.57872
A14714	30-Jun-55	34	52	11:18	11:35	50	50	10:33	10:33	10:33	38.2	11.64336	4.41336
A8646	24-Jul-45	68	94	10:59	11:06	82	84	10:02	10:03	10:03	20	6.096	-1.134
A8648	24-Jul-45	33	99	11:52	12:12	45	46	10:55	10:55	10:55	29	8.8392	1.6092
A8725	27-Jul-45	1	93	15:09	15:26	12	14	14:11	14:11	14:11	39.5	12.0396	4.8096
A8725	27-Jul-45	1	93	15:09	15:26	80	80	14:23	14:23	14:23	39.5	12.0396	4.8096
A8727	27-Jul-44	1	102	15:56	16:23	18	19	15:00	15:00	15:00	17.7	5.39496	-1.83504
A8728	27-Jul-44	69	111	16:54	17:03	104	104	16:01	16:01	16:01	26	7.9248	0.6948

NOTE: 1955 and 1944 air photo film reports are in AST!